

**NOVEL BUILDING BLOCKS FOR MOLECULAR  
IMPRINTING: PYRIDINE-BASED BINDING  
MONOMERS AND BIO-RENEWABLE CROSS-  
LINKERS**

**STEFANIA LETTIERI**

A thesis submitted in partial fulfilment of the requirements of  
the University of Kent and the University of Greenwich for the  
Degree of Doctor of Philosophy

November 2015

# DECLARATION

I certify that this degree has not been accepted in substance for any degree, and is not concurrently being submitted for any degree other than of Doctor of Philosophy being studied at the Universities of Greenwich and Kent. I also declare that this work is the result of my own investigations except where otherwise identified by references and that I have not plagiarised the work of others.

Candidate: Stefania Lettieri

Signed: .....

Supervisor: Dr Andrew J. Hall

Signed: .....

Date: 30/11/2015

## ACKNOWLEDGEMENTS

*To my dearest family and friends, to my supervisor, to my colleagues and to all the people I had the pleasure to meet and share moments with during this journey...thanks.*

Firstly I would like to thank *Dr Andrew J. Hall* for being my mentor during these years. He gave me the opportunity to start this journey and guided me through my PhD. Special thanks go to *Dr Panagiotis Manesiotis* which I consider not only a mentor, but also a friend. Thank you for your kindness and laughs during the time spent in Belfast.

Great thanks go to my family: *mum & dad, Elisa, Ivan, Elli, Tatiana, Eri, Barons and Arnie*. You were always present during those years regardless the distance. Past and present memories make me keep going. Ivan, thanks for being supporting and always understanding me. Love you all.

Thanks to *Carmen, Evelina, Anna and Francesca*, my little Italy. I spent great time with you during these years and it wouldn't be the same without you. *Carmen*, you are my partner in crime, scientifically speaking, and a good friend.

Thanks to the coolest lab, *Giorgia, Filip and Colin*. You are the best colleagues a person can ask for. *Giorgia*, thank you for cheering me up, making me laugh, and most importantly, having a drink, or two, with me in the darkest moment. *Filip*, you are so special. Your attention to details, your kindness and passion for life (and Canada) reveal the amazing person you are. *Colin* I consider you the pioneer of this lab. We became good colleague during those years but most importantly good friend. There are no words that can explain my gratitude.

*Killian, Diana, Rob, Ben, Mus, Stuart and Stratos*, thank you for the laugh, the time spent together inside and outside the University and the friendship. Each of you gives me a reason to love this place and make my time in Medway special.

Thanks Vladimir and Alison to be supportive of my research and good mentors to look at.

Thank you Mark, your kindness and friendship make me love this job. Thanks to all the staff at Greenwich and Kent that help me to achieve my goals.

I won't forget any of you, and I will be always grateful for your help and support.

## ABSTRACT

Molecular imprinting refers to the creation of synthetic materials with built-in memory for a selected target (atom, ion, molecule, complex or a molecular, ionic or macromolecular assembly, including micro-organisms) used as a template to direct the synthesis of the material, a Molecularly Imprinted Polymer (MIP). Here we would like to report on the development of Molecularly Imprinted Polymers (MIPs) for the recognition of molecules of biological/pharmaceutical interest such as biotin and barbiturates using a series of pyridine-based binding monomers which contain hydrogen bonding arrays complementary to their particular targets.

MIPs are already widely used for the creation of artificial receptors that will be less expensive, more stable and far more easily reusable compared to their natural counterparts. However there remains plenty of room for improvement in the affinity and selectivity exhibited by MIPs. The common use of commercially available monomers, such as methacrylic acid, is a limitation in the imprinting process. The design of new functional monomers for stoichiometric non-covalent molecular imprinting can enhance the selectivity and specificity of the MIP towards a specific target by decreasing the level of non-specific binding in the polymer, which is generally caused by the use of an excess of functional monomer in the pre-polymerisation mixture.

Bio-renewable cross-linkers were also synthesised from isomannide, isosorbide and 2,5-bis(hydroxymethyl)furan as a greener and bio-sustainable alternative to ethylene glycol dimethacrylate (EGDMA) in the Molecular Imprinting technology. Herein we will report on the preparation of novel MIPs selective towards uridine prepared using BAAPy as the functional monomer, 2',3',5'-tri-O-acetyluridine (TAU) as the dummy template and three acrylate- and methacrylate-based bio-sustainable crosslinking monomers prepared by esterification of isosorbide (1,4:3,6-dianhydrosorbitol), isomannide (1,4:3,6-dianhydromannitol) and 2,5-bis(hydroxymethyl)furan.

The selectivity, specificity and capacity of the reported polymers towards their imprinted templates and similar analytes were evaluated through chromatography and rebinding studies.

# CONTENTS

<b>CHAPTER 1</b> .....	<b>1</b>
<b>1.1 INTRODUCTION</b> .....	<b>2</b>
<b>1.2 THE ORIGINS</b> .....	<b>3</b>
<b>1.2.1 Application of silica MIP</b> .....	<b>4</b>
<b>1.2.2 A new era</b> .....	<b>5</b>
<b>1.3 TYPES OF POLYMERISATION</b> .....	<b>6</b>
<b>1.3.1 Free radical addition polymerisation</b> .....	<b>6</b>
<b>1.3.2 Step-growth polymerisation</b> .....	<b>8</b>
<b>1.3.3 Ionic polymerisation</b> .....	<b>9</b>
<b>1.3.4 Copolymerisation</b> .....	<b>11</b>
<b>1.4 METHODS OF MOLECULAR IMPRINTING</b> .....	<b>12</b>
<b>1.4.1 Covalent</b> .....	<b>12</b>
<b>1.4.2 Semi-covalent</b> .....	<b>13</b>
<b>1.4.3 Non-covalent approach</b> .....	<b>14</b>
<b>1.4.4 Stoichiometric non covalent imprinting</b> .....	<b>17</b>
<b>1.4.5 Metal ion mediated imprinting</b> .....	<b>17</b>
<b>1.5 FACTORS INFLUENCING THE DESIGN OF MIPs</b> .....	<b>18</b>
<b>1.5.1 The functional monomer</b> .....	<b>18</b>

1.5.2 The template .....	20
1.5.3 The crosslinker .....	21
1.5.4 The solvent .....	22
1.5.5 The initiator .....	23
<b>1.6 MORPHOLOGY .....</b>	<b>24</b>
1.6.1 “Bulk”: crushed monoliths .....	24
1.6.2 Beads .....	26
1.6.3 Thin films .....	28
1.6.5 Membranes .....	28
1.6.6 Nanostructured MIPs .....	29
1.6.7 Conclusion.....	29
<b>1.7 APPLICATIONS.....</b>	<b>30</b>
1.7.1 HPLC .....	30
1.7.2 Molecularly Imprinted solid phase extraction (MISPE).....	31
1.7.3 Process scale purification.....	31
1.7.4 Pseudo-immunoassays .....	32
1.7.5 Chemical sensors.....	34
1.7.6 Synthesis and catalysis.....	35
1.7.7 Therapeutic applications .....	36
<b>1.8 CONCLUSION (AIM OF THE PROJECT) .....</b>	<b>36</b>
1.8.1 Can we create hosts closer to nature? .....	37
1.8.2 Hydrogen bonds .....	38

<b>CHAPTER 2.....</b>	<b>40</b>
<b>2.1 MATERIALS.....</b>	<b>41</b>
<b>2.2 INSTRUMENTATION .....</b>	<b>41</b>
<b>2.3 METHOD .....</b>	<b>42</b>
<b>2.3.1 Molecular Imprinting Protocol .....</b>	<b>42</b>
<b>2.3.2 Chromatographic evaluation.....</b>	<b>43</b>
<b>2.3.5 Job plot.....</b>	<b>48</b>
<b>2.3.6 <sup>1</sup>NMR Titrations .....</b>	<b>49</b>
<b>CHAPTER 3.....</b>	<b>50</b>
<b>3.1 INTRODUCTION .....</b>	<b>51</b>
<b>3.1.1 Barbiturates: discovery &amp; decline .....</b>	<b>51</b>
<b>3.1.2 Barbiturate abuse, dependence and death .....</b>	<b>52</b>
<b>3.1.3 Recognition of barbiturates using MIP technology .....</b>	<b>53</b>
<b>3.1.4 Hamilton cleft.....</b>	<b>53</b>
<b>3.2     EXPERIMENTAL.....</b>	<b>58</b>
<b>3.2.1 Synthesis of Monomer 1.....</b>	<b>59</b>
<b>3.2.2 Synthesis of Monomer 2.....</b>	<b>60</b>
<b>3.2.3 Synthesis of Monomer 3.....</b>	<b>63</b>
<b>3.2.4 Synthesis of Monomer 4.....</b>	<b>66</b>
<b>3.2.5 Synthesis of Monomer 5.....</b>	<b>69</b>
<b>3.2.5 Synthesis of Pentobarbital – MIP1/NIP1 .....</b>	<b>71</b>
<b>3.3     RESULTS AND DISCUSSION .....</b>	<b>72</b>

3.3.1	Job plot .....	72
3.3.2	<sup>1</sup> NMR titrations.....	72
3.3.3	Chromatographic evaluation .....	78
3.3.4	Equilibrium Rebinding Experiments .....	81
3.3.5	MISPE .....	83
3.4	CONCLUSIONS .....	85
<b>CHAPTER 4.....</b>		<b>87</b>
4.1	INTRODUCTION .....	88
4.1.1	Biotin.....	89
4.1.2	Application for Avidin- and Streptavidin-Biotin probes .....	89
4.1.3	Mimicking biotin natural receptors .....	90
4.2	EXPERIMENTAL .....	92
4.2.1	Synthesis of 2-amino-5-vinyl-pyridine (20.) .....	92
4.2.2	Synthesis of 1,3-bis[[5-vinylpyrid-2-yl)amido]carbonyl]5-tert-butyl- benzene (monomer 6) .....	93
4.2.3	Polymer synthesis.....	97
4.3	RESULTS AND DISCUSSION .....	98
4.3.1	Job Plot .....	98
4.3.2	<sup>1</sup> NMR titrations.....	98
4.3.3	Chromatographic evaluation.....	100
4.3.4	Equilibrium rebinding experiments .....	105
4.3.5	MISPE .....	106



4.4	CONCLUSIONS .....	107
<b>CHAPTER 5.....</b>		<b>110</b>
5.1	INTRODUCTION .....	111
5.1.1	The imide structural motif.....	111
5.1.2	Enhancing the properties of BAAPy? .....	113
5.2	EXPERIMENTAL .....	116
5.2.1	Synthesis of 2,6- <i>bis</i> (acrylamido)pyridine (monomer 7) .....	117
5.2.2	Synthesis of 4-(3-methyl-butoxy)-2,6- <i>bis</i> (acrylamido)pyridine (monomer 8) .....	117
5.2.3	Synthesis of 4-Bromo-2,6- <i>bis</i> (acrylamido)pyridine (monomer 9).....	119
5.2.4	Synthesis of 4-Chloro-2,6- <i>bis</i> (acrylamido)pyridine (monomer 10) .....	120
5.2.5	Synthesis of 4-Cyano-2,6- <i>bis</i> (acrylamido)pyridine (monomer 11) .....	121
5.2.6	Synthesis of 4- Piperidino-2,6- <i>bis</i> (acrylamido)pyridine (monomer 12) ...	122
5.2.7	Synthesis of monomer 12 intermediate .....	123
5.3	RESULTS AND DISCUSSION.....	124
5.3.1	Job plot.....	124
5.3.2	<sup>1</sup> NMR titrations.....	125
5.3.3	Inductive and mesomeric effects of substituents .....	128
5.3.3.1	The substituent effect .....	132
5.3.4	Synthesis and overall yields .....	134
5.4	CONCLUSIONS .....	135
<b>CHAPTER 6.....</b>		<b>137</b>

<b>6.1 INTRODUCTION</b> .....	138
<b>6.1.1 Uridine and Pseudouridine</b> .....	139
<b>6.1.2 Colorectal cancer (CRC)</b> .....	140
<b>6.1.3 Dummy templates</b> .....	140
<b>6.1.4 The functional monomers</b> .....	141
<b>6.2 EXPERIMENTAL</b> .....	143
<b>6.2.1 Synthesis of 2',3',4'-Tri-<i>O</i>-acetylpsseudouridine<sup>94</sup></b> .....	143
<b>6.2.2 Synthesis of 2',3',4'-Tri-<i>O</i>-propionyluridine<sup>94</sup></b> .....	144
<b>6.2.3 Synthesis of 2',3',4'-Tri-<i>O</i>-butyryluridine<sup>94</sup></b> .....	144
<b>6.2.4 Polymer formulations</b> .....	145
<b>6.3 RESULTS AND DISCUSSION</b> .....	147
<b>6.3.1 Job plot</b> .....	147
<b>6.3.2 <sup>1</sup>H NMR titration</b> .....	148
<b>6.3.3 MIPs/NIPs evaluation</b> .....	151
<b>6.4 CONCLUSIONS</b> .....	156
<b>CHAPTER 7</b> .....	<b>157</b>
<b>7.1 INTRODUCTION</b> .....	158
<b>7.1.1 The role of the Cross-linker</b> .....	158
<b>7.1.2 Biomass as renewable resources</b> .....	160
<b>7.1.2 Isomannide, isosorbide and isoidide</b> .....	162
<b>7.1.3 2,5-Bis(hydroxymethyl)furan</b> .....	163
<b>7.2 EXPERIMENTAL</b> .....	165

7.2.1 Synthesis of 2,5- <i>bis</i> (hydroxymethyl)furan [BHF] <sup>142</sup> .....	165
7.2.2 Synthesis of 2,5- <i>bis</i> (hydroxymethyl)furan-diacrylate (CM-6) .....	166
7.2.3 Synthesis of isomannide-dimethacrylate (CM-5) <sup>143</sup> .....	166
7.2.4 Synthesis of isosorbide-dimethacrylate (CM-4) .....	167
7.2.5 Polymer formulations .....	167
<b>7.3 RESULTS AND DISCUSSION</b> .....	<b>168</b>
7.3.1 Synthesis.....	168
7.3.2 Chromatographic evaluation.....	170
7.3.3 Equilibrium rebinding.....	176
<b>7.4 CONCLUSIONS</b> .....	<b>178</b>
<b>CHAPTER 8</b> .....	<b>180</b>

# TABLES

<b>Table 1:</b> Effect of the substituent on choice of initiator. <sup>12</sup> .....	7
<b>Table 2:</b> Solubility parameters, Hydrogen Bond capacity and refractive indices of solvents used for preparing MIPs. <sup>38</sup> .....	23
<b>Table 3:</b> List of free radical initiators generally used in Molecular Imprinting. <sup>38</sup> .....	24
<b>Table 4:</b> A comparison between natural antibodies and molecularly imprinted polymers <sup>66</sup> . .....	33
<b>Table 5:</b> Key features and performances of antibody- and MIP-based assays <sup>66</sup> . .....	34
<b>Table 6:</b> Strength of Several Noncovalent Forces <sup>92</sup> . * <5 per surface area. ....	38
<b>Table 7:</b> Barbiturates currently employed and their therapeutic application. <sup>98</sup> .....	51
<b>Table 8:</b> <i>Monomer M1-template/analyte binding constants value. <math>K_a</math> (<math>M^{-1}</math>) (association constant) and <math>\Delta\delta_{max}</math> (maximum change in the chemical shift) were calculated by fitting data to a 1:1 binding isotherm using OriginPro 8.5.1.</i> .....	73
<b>Table 9:</b> <i>Association constants of monomer 1 with Phenobarbital.</i> .....	75
<b>Table 10:</b> <i>Association constants of monomer 2 with Phenobarbital.</i> .....	76
<b>Table 11:</b> <i>Selectivity and specificity of template/analytes on MIP1 and NIP1 in 1% TFA/acetonitrile (v/v) as mobile phase. Selectivity <math>\alpha(1)=k_1'/k_z'</math>; 1=Pentobarbital, z=structurally related analyte. For analytes with a negative <math>k'</math>, a fixed value of <math>k'=0.1</math> was used. <sup>a</sup> SD (standard deviation, n=3). <sup>b</sup> RSD (relative standard deviation)=(SD/x) *100, x= mean value.</i> .....	79
<b>Table 12:</b> <i>Binding constants (<math>k_a</math>) and number of sites (<math>N</math>) of MIP1 and NIP1.</i> .....	82
<b>Table 13:</b> <i>Monomer 6-templates binding constants value.</i> .....	99
<b>Table 14:</b> <i>Selectivity and specificity of template/analytes on MIP2 and NIP2 in 1% acetic acid/acetonitrile (v/v) as mobile phase. <sup>a</sup> SD (standard deviation, n=3). <sup>b</sup> RSD (relative standard deviation)=(SD/x) *100, x= mean value.</i> .....	102
<b>Table 15:</b> <i>Binding constant (<math>k_a</math>) and number of sites (<math>N</math>) of MIP2 and NIP2.</i> .....	106

<b>Table 16:</b> Binding constants for association of monomers 7-11 with Tegafur. $K_a$ ( $M^{-1}$ ) (association constant) and $\Delta\delta_{max}$ (maximum change in the chemical shift) were calculated using OriginPro 8.5.1. ....	126
<b>Table 17:</b> Experimental association constants for monomers 7-12 and para-substituent constants ( $\sigma$ ) from the Hammett Equation <sup>128</sup> . $K_a(R)$ = association constant 4-substituted BAAPY. $K_a(H)$ = association constant BAAPy. ....	130
<b>Table 18:</b> Predicted $pK_a$ values for the ring nitrogen in monomers 7-12. $pK_a$ calculated at <a href="https://epoch.uky.edu/ace/public/pKa.jsp">https://epoch.uky.edu/ace/public/pKa.jsp</a> ).....	131
<b>Table 19:</b> Total yield of monomer 7-12.....	134
<b>Table 20:</b> Formulations of imprinted and non-imprinted polymers. ....	146
<b>Table 21:</b> Monomer 1,6 and 7 – Tegafur complexes binding constants value.....	148
<b>Table 22:</b> <i>Selectivity and specificity of template/analytes on MIPs and NIPs imprinted with TA<math>\psi</math> in 1% acetic acid/acetonitrile (v/v) as mobile phase. <sup>a</sup> SD (standard deviation, n=3). <sup>b</sup> RSD (relative standard deviation)=(SD/x) *100, x= mean value. * Elution time &gt; 40 min, N/D (non-determinate). ....</i>	153
<b>Table 23:</b> MIPs 4-6 and NIPs 4-6 formulation.....	167
<b>Table 24:</b> Selectivity and specificity of template/analytes on imprinted polymers MIP 4, MIP 5, MIP 6 and control polymers NIP 4, NIP 5, NIP 6 in 1% acetic acid/acetonitrile (v/v) as mobile phase. SD (standard deviation, n=3). <sup>b</sup> RSD (relative standard deviation)=(SD/x) *100, x= mean value. ....	172
<b>Table 25:</b> Selectivity and specificity of template/analytes on imprinted polymers MIP 4, MIP 5, MIP 6 and control polymers NIP 4, NIP 5, NIP 6 in 100% water as mobile phase. <sup>a</sup> SD (standard deviation, n=3). <sup>b</sup> RSD (relative standard deviation)=(SD/x) *100, x= mean value. ....	176
<b>Table 26:</b> Binding constants ( $k_a$ ) and number of sites (N) of MIPs 4-6 and NIPs 4-6. ...	178

# FIGURES

<b>Figure 1:</b> MIP formation scheme. Three synthetic steps involved in the imprinting process: 1. A self-association step whereby the template and certain “functional” monomers form a complex; 2. The host-guest complex is incorporated into a polymer scaffold by polymerisation in the presence of cross-linking monomers and an adequate solvent/porogen; 3. Removal of the template from the matrix to reveal binding sites having the correct shape, size and functional group complementarity to recognise the template and related molecules. ....	2
<b>Figure 2:</b> Template removal from the MIP particles to reveal binding cavities with functionality and shape complementary to the template or a template analogue. ....	3
<b>Figure 3:</b> Number of papers published annually in the field of molecular imprinting between 1931 and 2003 <sup>11</sup> .....	5
<b>Figure 4:</b> Typical Step-Growth Polymerization Reactions <sup>12</sup> .....	9
<b>Figure 5:</b> Four different ways in which the initiation of an ionic polymerisation can occur. The monomer can gain or lose an electron to produce an ion or radical ion which becomes the chain carrier. ....	9
<b>Figure 6:</b> <i>Probable initiator mechanism in two-step process. Step one is the rapid formation of a <math>\pi</math>-complex and step two is a slow intramolecular rearrangement</i> <sup>12</sup> . ....	10
<b>Figure 7:</b> Heterocycles that can be polymerised also anionically <sup>12</sup> . ....	11
<b>Figure 8:</b> Covalent imprinting by Wulff 1982 <sup>14</sup> . ....	13
<b>Figure 9:</b> Semi-covalent Imprinting of cholesterol using the sacrificial spacer method (Whitcombe et al. 1995 <sup>18</sup> ). ....	14
<b>Figure 10:</b> Commercially available acidic, basic and neutral functional monomers. ....	16
<b>Figure 11:</b> <i>Factors affecting the recognition properties of MIPs related to the monomer-template assemblies</i> <sup>25</sup> . ....	19
<b>Figure 12:</b> Crosslinking monomers commonly used in molecular imprinting (EGDMA, MDA, DVB, TRIM, PETRA).....	21

<b>Figure 13:</b> Scheme of preparation of macroporous monolith using a thermal free radical polymerisation. The figure is modified from the Monolithic Materials book. <sup>40</sup> .....	25
<b>Figure 14:</b> Gulliver constrained by a multitude of weak “bonds”. Illustration by Ulrike Schramm in Jonathan Swift’s Gullivers Reisen; reprinted with permission from Überreuter Verlag, Vienna <sup>93</sup> . .....	39
<b>Figure 15:</b> Structures of analytes used for the chromatographic evaluation of polymers.	44
<b>Figure 16:</b> MISPE protocol scheme. ....	47
<b>Figure 17:</b> Job Plot samples preparation. Different molar ratios of monomer and template solution ( $x_r=1 - 0$ ) are prepared by mixing 1 mM solutions of the guest and the host in chloroform in NMR tubes. <sup>1</sup> H NMR spectra are then obtained and the change in chemical shift of the monomer protons involved in the interaction with the template determined. ...	48
<b>Figure 18:</b> Deaths from overdose of barbiturates in England and Wales during the period 1905-1960 (Registrar-General’s Statistical Review for England and Wales). <sup>98</sup> .....	52
<b>Figure 19:</b> Synthetic receptors with strong selectivity for barbiturates. The receptor design is based on two 2,6-diaminopyridine groups linked through an isophthalic acid spacer. a) Schematic of a barbiturate binding site <sup>28</sup> . b) Hamilton cleft example <sup>101</sup> .....	54
<b>Figure 20:</b> Intramolecular pre-organization of monomer 2 in a rigid cleft due to H-bonds interactions between the Nitrogen of the pyridine and the NH of the amido groups (blue dots). Host-guest repulsion (black arrow). ....	56
<b>Figure 21:</b> Hamilton-based functional monomers structures.....	57
<b>Figure 22:</b> Scheme of monomers 1-5 synthesis. <b>a.</b> H <sub>2</sub> SO <sub>4</sub> , MeOH or EtOH, reflux; <b>b.</b> K <sub>2</sub> CO <sub>3</sub> , CH <sub>3</sub> CN, Br-R <sub>1</sub> , reflux, 22hrs; <b>c.</b> NaOH 1N or LiOH·H <sub>2</sub> O; <b>d.</b> i) PCl <sub>5</sub> ; ii) MeOH; <b>e.</b> i) 50% aqueous solution piperidine, 175°C, 24hrs; ii) NaOH aqueous solution; <b>f.</b> i) SOCl <sub>2</sub> , 100°C, 4h; ii) THF, 2,6-diaminopyridine, 0°C →RT, overnight; <b>g.</b> THF or DCM, TEA, CH <sub>2</sub> =CHCOCl, N <sub>2</sub> , 0°C →RT, overnight. ....	58
<b>Figure 23:</b> Job Plot of monomer 1 with Pentobarbital, Phenobarbital, TAU and TAψ. The monomer interacts with the analytes in a 1:1 stoichiometric complex. The experiments were	

made in CDCl <sub>3</sub> using 5mM monomer and template concentration solution. X <sub>r</sub> = molar fraction Δδ = chemical shift change. ....	72
<b>Figure 24:</b> Binding Isotherms of monomer 1 and 2 – templates complexes obtained by <sup>1</sup> H NMR titrations studies. ....	73
<b>Figure 25:</b> Binding Isotherms of monomer 1– barbiturates complexes obtained by <sup>1</sup> H NMR titrations studies. ....	74
<b>Figure 26:</b> <sup>1</sup> H NMR titrations spectrums. Red and black arrows = 1 <sup>st</sup> NH of M1, green arrows = 2 <sup>nd</sup> NH of M1, blue arrows = CH isophthaloyl 2-H. (a) Monomer 1 with Pentobarbital (0.1mM in CDCl <sub>3</sub> ), (b) Monomer 1 with Phenobarbital (0.1mM in CDCl <sub>3</sub> ), (c) Monomer 1 with 2',3',4'-Tri-O-acetyluridine (1mM in CDCl <sub>3</sub> ), (d) Barbiturate cleft with 2',3',4'-Tri-O- acetylpseudouridine (1mM in CDCl <sub>3</sub> ). ....	77
<b>Figure 27:</b> <sup>1</sup> H NMR titration (1mM in CD <sub>3</sub> CN) of Monomer1 with Phenobarbital (f). Red arrow = 1st NH of M1, blue arrow = 2nd NH of M1. ....	78
<b>Figure 28:</b> Chromatographic evaluation of MIP1 and NIP1 using 1% TFA/acetonitrile (v/v) as eluent. [*] means greater than, based on a run of 1 hour. a) Complete graph showing k' and IF for the all tested analytes. b) Close up of the graph reporting k' and IF of all analytes except for barbiturates. ....	80
<b>Figure 29:</b> Binding isotherms obtained with equilibrium rebinding experiments of MIP1 and NIP1 in acetonitrile. 0-10 mM concentration range of Pentobarbital were used. All experiments were repeated in triplicate. The [Pentobarbital] <sub>free</sub> in the supernatant was evaluated with HPLC (Wavelength: 240 nm, Flow rate: 1 mL/min, Injection: 5μL, RSD % < 21, N=3). ....	82
<b>Figure 30:</b> Percentage of phenobarbital eluted in each step (load, wash and elution) through MIP1 and the control polymer (NIP1). ....	84
<b>Figure 31:</b> Biotin structure .....	89
<b>Figure 32:</b> Synthetic receptor for biotin previously reported by Claramunt group <sup>108</sup> . ....	91



<b>Figure 33:</b> <i>Biotin-monomer 6 complex formation. The two molecules interact with a total of four H-bonds.</i> .....	91
<b>Figure 34:</b> <i>Job Plot of monomer 6 with Biotin-OMe. The monomer interact with the analytes in a 1:1 stoichiometric complex. The experiment was made in CDCl<sub>3</sub> using 5mM monomer and template concentration solution. X<sub>r</sub> = molar fraction Δδ = chemical shift change.</i> .....	98
<b>Figure 35:</b> <i><sup>1</sup>H NMR titration binding isotherms of monomer 6 with different templates. The experiments were performed in chloroform or acetonitrile using 1mM solution of the monomer except for the monomer 6-phenobarbital titration where a 0.5mM solution of Phenobarbital (the “host”) was added an increasing concentration of monomer 6.</i> .....	100
<b>Figure 36:</b> <i>Chromatographic evaluation of the Biotin-MIP and NIP using 100% acetonitrile (a) and 1% acetic acid/acetonitrile (v/v) (b) as eluent. [*] means greater than, based on a run of 1 hour.</i> .....	104
<b>Figure 37:</b> <i>Binding isotherms obtained with equilibrium rebinding experiments of MIP2 and NIP2 in acetonitrile. 0-10mM concentration range of Biotin-nitrophenylester were used. The [Biotin-nitrophenylester]<sub>free</sub> in the supernatants was evaluated with HPLC (Wavelength: 275 nm, Flow rate: 1mL/min, Injection: 5μL, RSD % &lt; 16, N=3).</i> .....	105
<b>Figure 38:</b> <i>Percentage of Biotin eluted in each step (load, wash and elution) through the MIP2 and NIP2.</i> .....	107
<b>Figure 39:</b> <i>Highly schematic representation of a thin layer Imprinted Polymer for the binding of biotinylated macromolecules.</i> .....	109
<b>Figure 40:</b> <i>Structures of molecules previously imprinted using BAAPy as the functional monomer. The recognition part of the compounds is the imide moiety. Hydrogen bond donors are in red, while hydrogen bond acceptors are in blue.</i> .....	111
<b>Figure 41:</b> <i>BAAPy-template H-bonds interactions.</i> .....	112
<b>Figure 42:</b> <i>2,4-bis(acrylamido)-6-piperidinopyrimidine and 1-benzyluracil complex previously reported by Manesiotis<sup>123</sup>.</i> .....	113

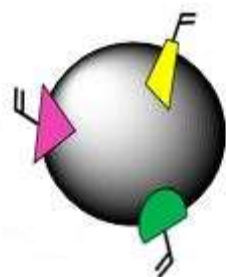
<b>Figure 43:</b> <i>Modified scheme showing modes of 2,4-bis(acrylamido)-6-piperidinopyrimidine incorporation in the imprinting of 1-benzyluracil (BU)<sup>123</sup>.</i> .....	114
<b>Figure 44:</b> Novel 4-substituted BAAPy functional monomers. Six different groups in four-position (red). Hydrogen-bond donor (pink) and hydrogen-bond acceptor (blue).....	115
<b>Figure 45:</b> <i>Scheme of monomers 7-12 synthesis. a. i) PBr<sub>5</sub>, 130°C, 4h; ii) MeOH, 0°C; b. EtOH, H<sub>2</sub>SO<sub>4</sub>, 7 h, reflux; c. NH<sub>3</sub> 7N in MeOH, 3h, RT; d. KOH 5M, Br<sub>2</sub>, 90°C, 5h; e. i) 50% aqueous solution piperidine, 175°C, 24 h; ii) CuCN, DMF, sealed tube, 190°C, 3h; f. THF or DCM, TEA, CH<sub>2</sub>=CHCOCl, N<sub>2</sub>, 0°C →RT, overnight.</i> .....	116
<b>Figure 46:</b> Job plot experiments of Tegafur with monomer 8 and 10. ....	125
<b>Figure 47:</b> <i>4-substituted 2,6-bis(acrylamido)pyridines - Tegafur complex. The D-A-D motif of the functional monomer binds the complementary A-D-A motif of Tegafur with three H-bonds.</i> .....	126
<b>Figure 48:</b> <i>Binding isotherms of monomers 7, 8, 9, 10, 11 and 12 with Tegafur obtained by <sup>1</sup>H NMR titrations studies.</i> .....	127
<b>Figure 49:</b> <i>Binding isotherms for monomers 7, 9, 10 and 11 with Tegafur obtained by <sup>1</sup>H NMR titrations studies.</i> .....	128
<b>Figure 50:</b> <i>Selected resonance structures of pyridine substituted with electron donating (blue) and electron withdrawing (red) substituent<sup>127</sup>.</i> .....	129
<b>Figure 51:</b> The Hammett Equation <sup>128</sup> .....	130
<b>Figure 52:</b> Correlation between $\sigma$ (para-substituent constants $\sigma$ from the Hammett Equation) and the association constants of monomer 7-12. The Para substituents constants $\sigma$ were plotted with $\log k_{aR}/k_{aH}$ ( $R^2=0.97$ ). $k_{aR}$ = association constant of 4-substituted BAAPY. $k_{aH}$ = association constant of BAAPY. $\sigma = -(pK_a - pK_a(H))$ .....	131
<b>Figure 53:</b> Chemical structure of the esters of Uridine and Pseudouridine. ....	141
<b>Figure 54:</b> Pseudouridine and uridine hydrogen bond donator (in red) and hydrogen bond acceptor (in blue). ....	142
<b>Figure 55:</b> Functional monomers used for the imprinting of pseudouridine. ....	143

<b>Figure 56:</b> Potential 1:2 binding ration of Pseudouridine with monomer 7. ....	147
<b>Figure 57:</b> Job Plot of monomer 7 with Pseudouridine. ....	147
<b>Figure 58:</b> <i>Primary positive hydrogen-bonded interactions (blue and pink) and secondary electrostatic repulsive interactions (red arrow): a) monomer 6 with four positive interactions and five negative interactions; b) monomer 7 with three positive interactions and four negative interactions; c) monomer 1 with five positive interactions and seven negative interactions. ....</i>	149
<b>Figure 59:</b> <sup>1</sup> H NMR titration of BAAPy with 2',3',4'-Tri-O-acetylpsudouridine .....	150
<b>Figure 60:</b> <sup>1</sup> H NMR titration of monomer 1 with 2',3',4'-Tri-O-acetylpsudouridine ..	150
<b>Figure 61:</b> <sup>1</sup> H NMR titration of monomer 6 with 2',3',4'-Tri-O-acetylpsudouridine ..	151
<b>Figure 62:</b> <i>MISPE experiment for MIP 8 (a) and NIP 8 (b). Percentage of analytes eluted in each step (load, wash and elution) through the MIP and the control polymer (NIP). Uridine, 5-methyl-uridine (5-MeU), 5-fluoro-uracil (5-FU) and pseudouridine were used as analytes. Experimental data obtained from Aleksandra Krstulja. ....</i>	155
<b>Figure 63:</b> <i>CL-6. 2,5-Bis(hydroxymethyl)furan-diacrylate; CL-5. isomannide-dimethacrylate; CL-4. isosorbide-dimethacrylate. ....</i>	159
<b>Figure 64:</b> <i>BAAPy and 2',3',4'-tri-O-acetyluridine interaction in the pre-polymerization mixture. Three hydrogen bonds are shared between host (DAD) and guest (ADA). ....</i>	159
<b>Figure 65:</b> <i>MIP5 preparation scheme. ....</i>	160
<b>Figure 66:</b> <i>Main biomass components<sup>141</sup> .....</i>	161
<b>Figure 67:</b> <i>The structures of isomannide, isosorbide and isoidide. ....</i>	162
<b>Figure 68:</b> <i>The preparation of isosorbide and isomannide from cereals starch. ....</i>	162
<b>Figure 69:</b> <i>L-idose structure. ....</i>	163
<b>Figure 70:</b> <i>Products obtained from the treatment of lignocellulose obtained from biomass<sup>141</sup>. ....</i>	163
<b>Figure 71:</b> <i>Products obtained from the treatment of lignocellulose obtained from biomass<sup>141</sup>. ....</i>	164

<b>Figure 72:</b> Cross-linkers reaction scheme. a) i. HMF, THF and NaBH <sub>4</sub> , 0 °C, ii. HCl 2N, 0 °C; b) BHF, TEA, DCM, CH <sub>2</sub> =CHCOCl, 0°C→RT, N <sub>2</sub> ; c) Isomannide, NaOH 5M, CH <sub>2</sub> =C(CH <sub>3</sub> )COCl, 0°C→RT; d) Isosorbide, NaOH 5M, CH <sub>2</sub> =C(CH <sub>3</sub> )COCl, 0 °C→RT.	165
<b>Figure 73:</b> MAACl's impurity (3) <sup>144</sup>	168
<b>Figure 74:</b> a) <sup>1</sup> H NMR of MAACl's impurities <sup>144</sup> ; b) <sup>1</sup> H NMR of bis(hydroxymethyl)furan-dimethacrylate showing the MAACl impurity 3 presents in the upfield area (red box).	169
<b>Figure 75:</b> Chromatographic evaluation of MIP 4-6 and NIP 4-6 using 1% acetic acid/acetonitrile (v/v) as eluent. K' = retention factor.	170
<b>Figure 76:</b> Selectivity (α) of the target and related nucleoside for MIPs 4-6 and NIPs 4-6 in 1% acetic acid/acetonitrile (v/v).	171
<b>Figure 77:</b> Uridine structure with a three hydrogen bond donors on the β-D-ribofuranose (blue). Crosslinker CM-5 with two hydrogen bond acceptors (red).	173
<b>Figure 78:</b> anhydroerythritol-dimethacrylate (P7) and 1,4:3,6-dianhydro-D-sorbitol-dimethacrylate (P6) structure previously reported by Wulff <sup>36b</sup> .	174
<b>Figure 79:</b> Retention factor (k') of the target and related nucleoside for MIPs 4-6 and NIPs 4-6 in 100% water.	175
<b>Figure 80:</b> Binding isotherms obtained with equilibrium rebinding experiments of MIPs 4-6 and NIPs 4-6 in acetonitrile. The [TAU] <sub>free</sub> in the supernatant was evaluated with HPLC (Wavelength: 260 nm, Flow rate: 1mL/min, Injection: 5μL, RSD % < 21, N=3).	177

# CHAPTER 1

## *MOLECULARLY IMPRINTED POLYMERS (MIPs)*



## 1.1 INTRODUCTION

Molecularly Imprinted Polymers (MIPs) are extraordinary materials that have been described as “artificial receptors” or “plastic antibodies”. The reason why this definition has been used is because the whole idea around MIPs was to create smart materials that can bind with high affinity and selectivity to a specific entity (atom, ion, molecule, complex or a molecular, ionic or macromolecular assembly, including micro-organisms) just as a natural receptor will do with its ligand.

What is a Molecularly Imprinted Polymer? A MIP is a synthetic material with built-in memory for a selected target, which is generally used to direct the synthesis of this material, i.e. MIPs are prepared via templated synthesis (Figure 1).

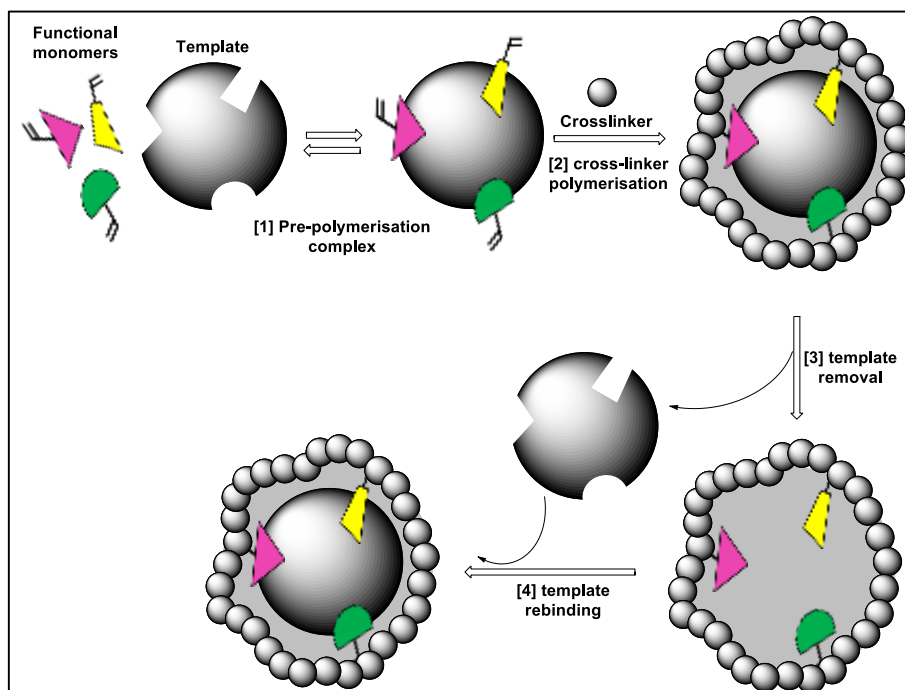


**Figure 1:** MIP formation scheme. Three synthetic steps involved in the imprinting process: *1. A self-association step whereby the template and certain “functional” monomers form a complex; 2. The host-guest complex is incorporated into a polymer scaffold by polymerisation in the presence of cross-linking monomers and an adequate solvent/porogen; 3. Removal of the template from the matrix to reveal binding sites having the correct shape, size and functional group complementarity to recognise the template and related molecules.*

Post-polymerisation removal of the template species reveals binding cavities complementary to the template (or closely analogous species) in terms of functionality and three-dimensional shape and size (Figure 2).

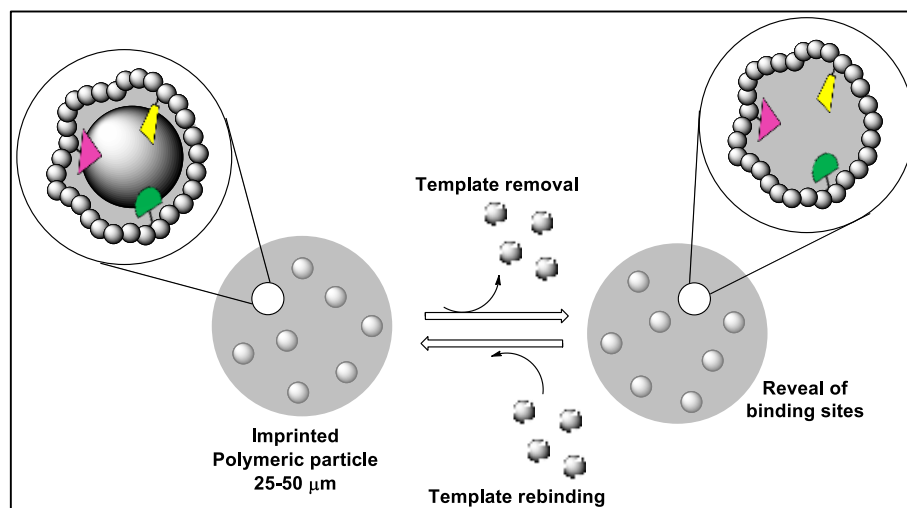


**Figure 2:** *Template removal from the MIP particles to reveal binding cavities with functionality and shape complementary to the template or a template analogue.*

## 1.2 THE ORIGINS

Molecularly imprinted polymers (MIPs), as we know them today, can be traced back to 1972, when Wulff<sup>1</sup> and Klotz<sup>2</sup> independently applied the use of organic polymers in the imprinting process.

However, the basic idea dates back to 1931, when a Soviet chemist, Polyakov<sup>3</sup>, reported the presence of memory for different additives (benzene, toluene or xylene) in silica gels which were dried in the presence of a particular additive. This is the first example of a material whose surface is directly affected by a template (the additive in this case) resulting in an increased affinity towards the additive in question. Unfortunately, Polyakov's work went largely unnoticed until more recent times.

A few years later, in 1949, Dickey<sup>4</sup>, a senior student from Pauling's lab, published the first example of molecular imprinting in silica where sodium silicate was polymerised in the presence of different dyes (methyl-, ethyl-, *n*-propyl- and *n*-butyl orange). The final imprinted silicas showed a preference in the binding for the dye

used during polymerisation. In his work, Dickey used a procedure based on Pauling's theory<sup>5</sup> on the formation of antibodies reported in 1942. Pauling suggested that the antigen was involved in the change of conformation of the antibody from the primary structure, identical in all antibodies, giving a high selectivity to the antibody itself.

More studies on the imprinting of silica using different dyes were reported by Haldeman and Emmett<sup>6</sup>; they were the first to mention the word "footprints" for this process and to propose the theory that the interactions between the dye and the silica were due to hydrogen and van der Waals' bonding. This theory was proposed by Dickey<sup>7</sup> in the same year.

Historically, Polyakov and Dickey are the fathers of imprinting, but Dickey's method, where the template is present in the pre-polymerisation mixture before the formation of the silica matrix, is closer to the modern technology.

### **1.2.1 Application of silica MIP**

Soon, several practical purposes for this field arose and some of these applications were certainly ahead of their time and are still in use nowadays. In the early 1950s, imprinted silica was used in chromatography<sup>8</sup> as a stationary phase, for separation techniques and for thin layer chromatography.

Molecular Imprinting was also employed in 1957<sup>9</sup> to determinate the structure of an organic molecule (e.g. cinchona alkaloids, morphine and atropine analogues) and then to obtain a specific catalysis in a synthetic reaction.

To conclude with the history of molecular imprinting in silica, one of the most avant-garde papers at the beginning of this era is that reporting the first examples of "bacteria-imprinted" silica<sup>10</sup>. This imprinted silica was found to promote the growth of the templated bacterial species better than non-imprinted silica, silica imprinted with another bacteria or sand.

Molecular imprinting in silica soon faced a decline, probably due to the limited range of functionalities that can be used on a silica-based material and the poor stability and reproducibility of imprinted silica.



### 1.2.2 A new era

Even with the introduction of molecular imprinting in organic polymer in 1972 made independently by Wulff<sup>1</sup> and Klotz<sup>2</sup>, this field needed to wait until the 1990s to finally see an upsurge in interest from the scientific community.

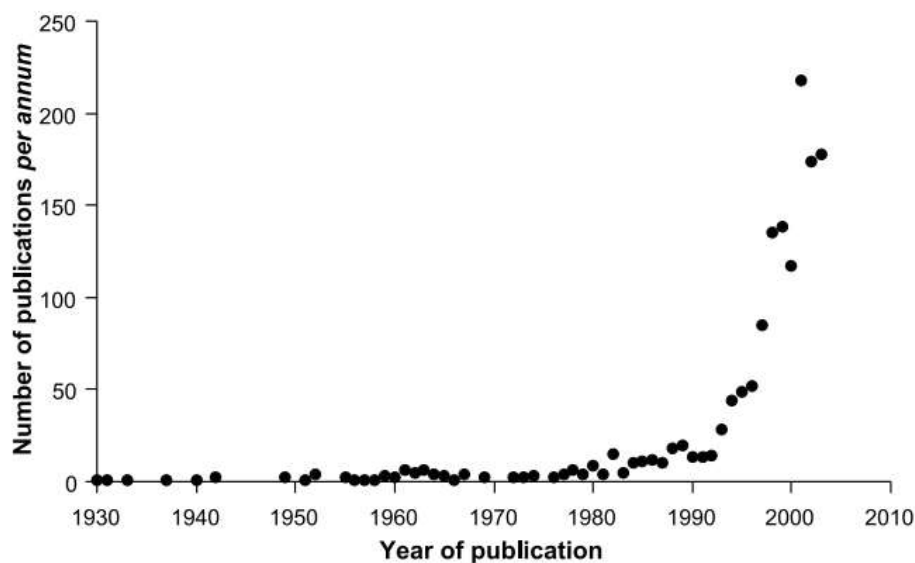


**Figure 3:** Number of papers published annually in the field of molecular imprinting between 1931 and 2003<sup>11</sup>

Each year the number of publications in this field increases, showing a huge interest on this topic from the scientific community. This is most likely due to the fact that MIPs are smart materials with a huge potential and plenty of room for improvement.

The number of fields in which MIPs can be applied is constantly increasing. Further, the imprinting technique can create easily polymers with a high affinity for the target or a target-like compound and having a great stability against mechanical stresses, high temperatures and intense radiation. They are also resistant to treatment with acid, base or metal ions and stable to a wide range of solvents; they are also autoclave compatible. Imprinted polymers can also be reused many times without loss of their memory and they have high storage endurance. It must also be

mentioned that they are a cheaper alternative to sensors or other techniques already available for the recognition of several chemical species in food, water or urine, for instance. Finally, and perhaps most importantly, they are a less expensive alternative to biological assays. All these advantages lead to the increasing interest in this field from the scientific community and from the industrial sector in recent years.

### 1.3 TYPES OF POLYMERISATION

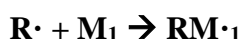
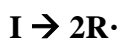
The classical subdivision of polymers was introduced in 1929 by Carothers, who proposed to classify these materials as either *condensation* or *addition* polymers based on the fact that the polymeric reaction was based on elimination, or not, of a small molecule, such as water, at each step. This classification has since changed and now the definition of a polymer is based on the description of its *chain growth mechanism*.

#### 1.3.1 Free radical addition polymerisation

Long chain polymers are easily obtained using vinyl monomers with a general structure  $\text{CH}_2=\text{CR}_1\text{R}_2$ . The polymerisation is structured in three different stages: (i) *Initiation*, (ii) *Propagation* and (iii) *Termination*.

##### (i) *Initiation*

During the initiation process an active centre is created. This is then responsible for carrying on the chain's formation.



Three different categories of initiator can be used: free radical, cationic and anionic initiators. The choice between them depends on the  $\text{R}_1$  and  $\text{R}_2$  groups in the monomers, but *free radicals* are the most used due to their neutral nature (Table 1)

**Table 1:** Effect of the substituent on choice of initiator. <sup>12</sup>

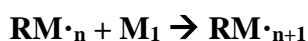
Monomer	Initiator		
	Free Radical	Anionic	Cationic
Ethylene, $H_2C=CH_2$	+	-	+
1,1'-Diarylethylene, $H_2C=CR_1R_2$	-	-	+
Vinyl ethers, $H_2C=CHOR$	-	-	+
Vinyl halides, $H_2C=CH(Hal)$	+	-	-
Vinyl esters, $H_2C=CHOCOR$	+	-	-
Methacrylic esters $H_2C=C(CH_3)COOR$	+	+	-
Acrylonitrile, $H_2C=CHCN$	+	+	-
Styrene, $H_2C=CHPh$	+	+	+
1,3-Butadiene, $H_2C=CH-CH=CH_2$	+	+	+

“A free radical is an atomic or molecular species whose normal bonding system has been modified such that an unpaired electron remains associated with the new structure. The radical is capable of reacting with an olefinic monomer to generate a chain carrier which can retain its activity long enough to propagate a macromolecular chain under the appropriate conditions”<sup>12</sup>.

An initiator can be activated by *thermal decomposition* (organic peroxides or azo compounds), *photolysis* (metal iodides, metal alkyls and azo compounds), *redox reactions* (e.g. ferrous ion and hydrogen peroxide produces hydroxyl radicals), *persulfates* and *ionizing radiation*.

### (ii) Propagation

The propagation process is the chain growth stage. The chain carrier formed by the reaction of the free radical with the monomer, rapidly produces a linear polymer.



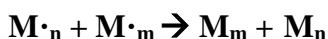
**(iii) Termination**

Termination of the free radical polymerisation can occur in three different ways.

a) *Termination by combination*, where mutual annihilation of two radicals occurs to form a paired electron bond. This process can be generically explained by the following equation:



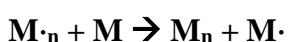
b) *Termination by disproportionation*, where two radicals form two new molecules through a reaction that transfers a hydrogen atom.



c) *A combination of both disproportionation and combination reactions.*

**1.3.1.1 Chain Transfer**

During a free radical polymerisation, the chain growth can be terminated by a chain transfer of the growing polymer to a monomer, a solvent, a polymer, a free-radical or a chain transfer agent. During this event, a new free radical species is also created, which usually no longer reactive and can terminate the polymerisation. An example is the iniferter polymerisation, where the iniferter is a species that acts as initiator, transfer agent, and terminator in a controlled free radical polymerisation.



**1.3.2 Step-growth polymerisation**

The step-growth or chain-growth processes involved the formation of a linear chain by intermolecular condensation or addition of the reactive groups in bi-functional monomers. There are two major types of step-growth polymerisation:

*Type 1:* two polyfunctional monomers are involved in the polymerisation process, and each one has only one type or reactive functional group. These polymerisations follow the  $\mathbf{A-A} + \mathbf{B-B} \rightarrow \mathbf{-(A-AB-B)-}$  scheme, where A and B are the functional groups.

Type 2: the monomer involved in the polymerisation contains more than one type of functionality, such as a hydroxyacid (HO-R-COOH), represented as A-B, where the reaction is  $nA-B \rightarrow -(AB)_n-$ .

Important polymers formed via a step-growth process are showed in Figure 4.

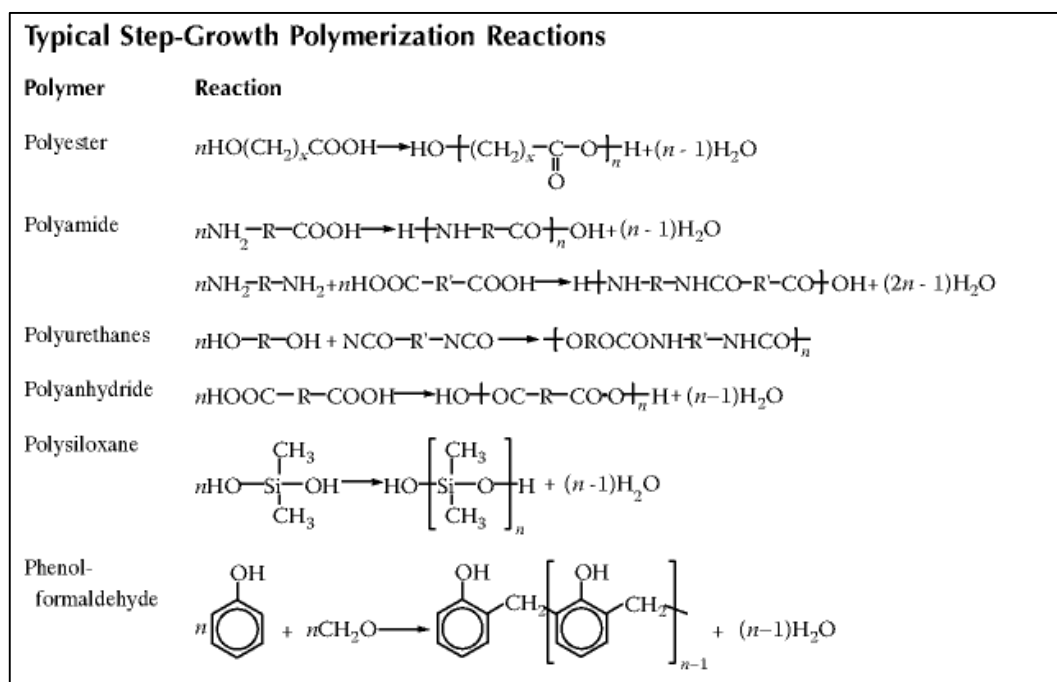


Figure 4: Typical Step-Growth Polymerization Reactions <sup>12</sup>

### 1.3.3 Ionic polymerisation

Ionic polymerisation is an addition polymerisation where the initiator is an ion, which may be either an anion or a cation.

1.  $M + I^+ \rightarrow MI^+$       Cationic
2.  $M + I^- \rightarrow MI^-$       Anionic
3.  $M + e^- \rightarrow \cdot M^-$       Anionic
4.  $M - e^- \rightarrow \cdot M^+$       Cationic (charge transfer)

Figure 5: Four different ways in which the initiation of an ionic polymerisation can occur. The monomer can gain or lose an electron to produce an ion or radical ion which becomes the chain carrier.

a) *Cationic polymerisation.* In ionic polymerisations there are also 3 steps: initiation, propagation and termination. The most common cationic initiators are strong Lewis acids  $\text{MX}_n$ , but they need a co-catalyst SH to act as a proton donor.

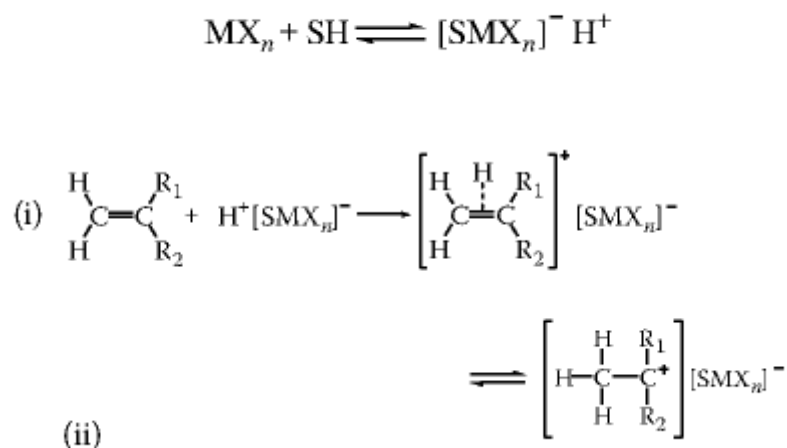


**Figure 6:** Probable initiator mechanism in two-step process. Step one is the rapid formation of a  $\pi$ -complex and step two is a slow intramolecular rearrangement<sup>12</sup>.

The propagation is carried out by the repeated addition of monomer in a head-to-tail manner to the carbonium ion. The termination can take place in two ways: by unimolecular rearrangement of the ion pair or through a bimolecular transfer reaction with a monomer.

b) *Cationic ring opening polymerisation.* Cationic initiators can also be used to form linear polymers starting from cyclic monomers such as lactones, cyclic amines and cyclic ethers (Figure 7). Cyclic monomers undergo ring-opening reactions to relieve the ring strain. Also macrocycles can undergo ring-opening polymerisation due to entropic driven forces<sup>13</sup>.

Heterocycles That Can Be Polymerized Cationically

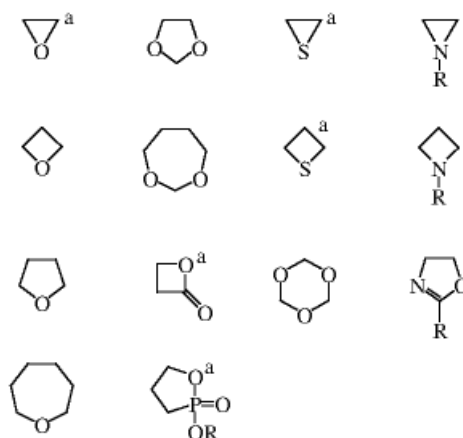


Figure 7: Heterocycles that can be polymerised also anionically<sup>12</sup>.

c) Anionic polymerisation; the polymerisation of monomers with an electronegative group can be initiated by two different mechanisms. The first requires the formation of a carbanion due to an ionic molecule capable of adding the anion to the vinyl double bond. In the second mechanism there is a direct transfer of an electron from a donor to a monomer to form a radical anion.

### 1.3.4 Copolymerisation

A copolymerisation is the synthesis of polymeric chains containing more than one monomer. The different monomers, e.g. A and B, can be incorporated in the polymer using either free radical or ionic initiation.

Five important types of co-polymeric structures exist:

- a) *Random copolymers* occur when monomers A and B enter in the chain with a random propagation (e.g.  $-(ABBAAAABBBBBBABABB)-$ ).
- b) *Alternating copolymers* are obtained by a controlled polymerization of two monomers in an equimolar quantities (e.g.  $-(ABABABABA)-$ ).
- c) *Block copolymers* are polymers that contain long sequences of one monomer joined to another long sequence of another monomer.

d) *Graft copolymers* are branched polymers obtained by the addition of polymeric chains to the main chain of another homopolymer.

e) *Stereoblock copolymers* are polymers formed by one monomer where the distinguishing feature is the tacticity.

## 1.4 METHODS OF MOLECULAR IMPRINTING

### 1.4.1 Covalent

In covalent imprinting, the template is attached covalently to the monomer or a polymerisable group. After polymerisation the template is cleaved from the polymers and only functionalities able to covalently re-bind the template are left in the binding cavity. This approach is advantageous for several reasons: the solvent used during the imprinting (which is a key factor in the non-covalent approach) can be decided based on the template/monomers solubility as the strength of the interactions in the pre-polymerisation mixture is irrelevant, given that the covalent bond should allow the location of the functional groups involved in the interaction in the right position in the polymeric matrix. Also, a covalent approach should reduce the non-specific cavities problem, which is often found in the non-covalent approach; the imprinted cavities should, in theory, be homogeneous as only the template-monomer complex should allow the formation of a binding site in the MIP. Unfortunately only a limited number of functional groups (e.g. alcohols, aldehydes, ketones amines and carboxylic acids) can be imprinted with this approach, as the covalent bonds that can be used in this field need to be completely reversible under certain conditions. Wulff and co-workers have been studying covalent imprinting since 1972 and one of the most common covalent approaches uses boronate esters for the imprinting of template with a pairs of hydroxyl groups (1,2- and 1,3-diol functionality). In a 1982 paper, Wulff used as the template a phenyl- $\alpha$ -D-mannopyranoside<sup>14</sup> which was linked to polymerisable functionalities by two diester linkages between the template and two 4-vinylbenzeneboronic acid units.



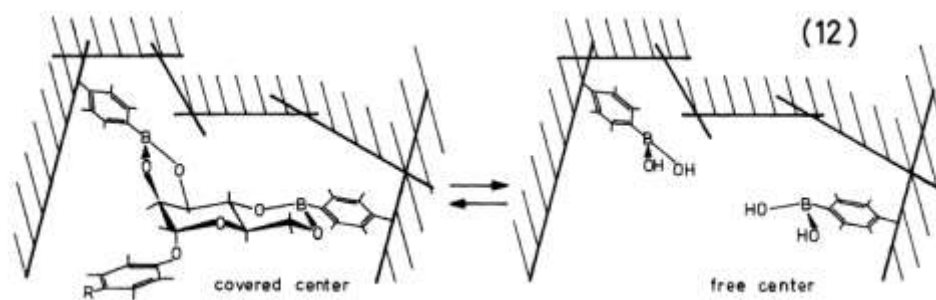


**Figure 8:** Covalent imprinting by Wulff 1982<sup>14</sup>

A recent example of covalent imprinting is the preparation of water soluble protein-like nanoparticles for the recognition of amines<sup>15</sup>. Using covalent imprinting, it was possible to introduce for each nanoparticle one binding site with the right size and shape of the template. Mendes *et al.*<sup>16</sup> also reported on the imprinting of glycoproteins using a covalent templating approach, where an acrylamide-appended boronic acid was used to covalently bind the saccharide motif of the glycoprotein.

#### 1.4.2 Semi-covalent

The semi-covalent approach combines the advantages of covalent and non-covalent imprinting. The idea was introduced by Wulff<sup>1</sup> when his group imprinted glyceric acid using boronic acid and 4-vinylaniline. In the rebinding process the template was re-capture through a covalent boronate ester bond and an ion pair bond with the amine group of 4-vinylaniline. The real first semi-covalent imprinting examples was introduced by Sellergren and Andersson,<sup>17</sup> with the imprinting of p-aminophenylalanine ethyl ester.

Another example of semi-covalent imprint is the *sacrificial spacer* method: the polymer is imprinted using a covalent approach, but after the removal of a “spacer” which covalently links the template to the monomer, the re-binding of the template by the MIP is driven by non-covalent forces (as in the non-covalent imprinting). The method was introduced by Whitcombe *et al.*<sup>18</sup> in 1995 to imprint cholesterol

(Figure 9) where after the cleavage of the template and the spacer, a phenolic residue was left in the recognition site. A similar approach can be used to introduce other functionalities as amino, carboxyl or hydroxyl in the recognition site.

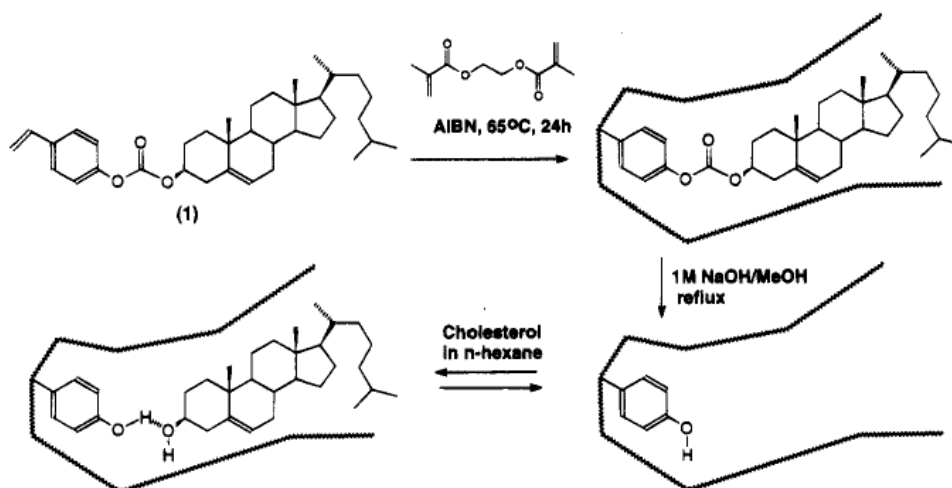


**Figure 9:** Semi-covalent Imprinting of cholesterol using the sacrificial spacer method (Whitcombe et al. 1995<sup>18</sup>).

Recently the Takeuchi group reported the synthesis of a MIP for the recognition of proteins using a semi-covalent imprinting approach<sup>19</sup>. The protein binding sites were prepared by copolymerization of the acrylated protein with 6-monoacryloyl-trehalose and 6,6'-diacryloyl-trehalose as a hydrophilic co-monomer and crosslinker, respectively, followed by enzymatic decomposition of the grafted protein with pepsin to reveal the protein-imprinted cavities.

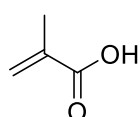
### 1.4.3 Non-covalent approach

The non-covalent approach was introduced by the group of Mosbach in 1981.<sup>20</sup> It is the most widely used due to its simplicity and the large number of template structures, containing a hydrogen bond- or proton-accepting functional group, that can be imprinted. This method is apparently straightforward as it is based on three simple synthetic steps: **1**) interaction between template and functional monomers prior to polymerisation (pre-polymerisation complex); **2**) free-radical

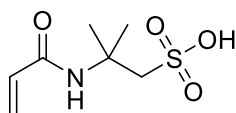
polymerisation in the presence of a crosslinker; **3**) removal of the template from the material to reveal binding cavities complementary to the template or a template analogue. The binding between the template and the functional monomers occurs through non-covalent forces, such as H-bonding, ion-pairing and dipole-dipole interactions, which are the same used to recognise the guest in the imprinted polymer.

The most common functional monomer used is Methacrylic acid, but a wide range of commercially available acidic, basic or neutral functional monomers (Figure 10) have been employed successfully in the preparation of non-covalent imprinted polymer.

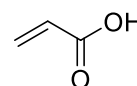
Acid functional monomers:



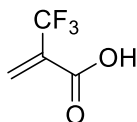
Methacrylic acid  
(MAA)



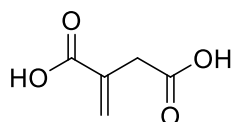
Acrylamidomethylpropane  
sulfonic acid  
(AMPSA)



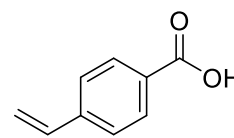
Acrylic acid  
(AA)



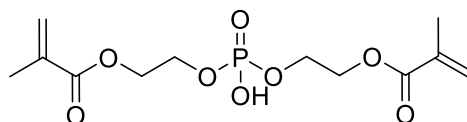
Trifluoromethyl acrylic acid  
(TFM)



Itaconic acid  
(ITA)

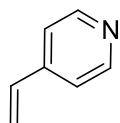


p-Vinylbenzoic acid  
(PVB)

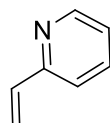


2-(methacryloyloxy)ethyl phosphate

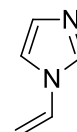
Basic functional monomers:



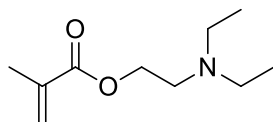
4-vinylpyridine  
(4-VP)



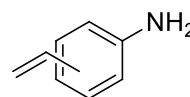
2-vinylpyridine  
(2-VP)



1-vinylimidazole

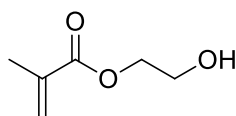


N,N-diethyl-2-aminoethylmethacrylate  
(DEAEMA)

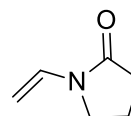


Aminostyrene

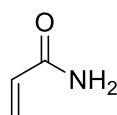
Neutral functional monomers:



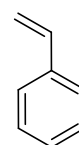
2-hydroxyethylmethacrylate



N-vinylpyrrolidone



Acrylamide  
(AMM)



Styrene

**Figure 10:** Commercially available acidic, basic and neutral functional monomers.

Nonetheless there are few drawbacks to this method: compared to covalent imprinting, in the non-covalent method it is necessary to use a solvent that doesn't interfere with the non-covalent interactions between host and guest in the complexation stage, as these are the main interactions that drive the imprinting. Also, the binding strength between template and functional monomer needs to be

adequate in order to have a host-guest complex in the pre-polymerisation mixture that can lead to imprinted binding sites. It is therefore understandable that with this method it is more difficult to obtain a homogeneous distribution of imprinting binding cavities than when using covalent imprinting, as the use of an excess of functional monomer or a weak pre-polymerisation interaction between the two molecules can generate weakly or non-specific cavities in the polymeric matrix.

On the other hand, there are techniques that can be used to predict the intermolecular interactions and the binding constants of the complexes present in the pre-polymerization mixture, such as molecular modelling or IR, UV-vis and <sup>1</sup>H NMR titrations<sup>21</sup>. Other important factors to consider are the use of the right template, functional monomer(s) and solvent(s).

#### **1.4.4 Stoichiometric non covalent imprinting**

When non-covalent imprinting was introduced, one of the drawbacks was the necessity to use an excess of the functional monomer due to the low binding constants between the monomers used and the templates studied. The result is that non-specific cavities are formed in the macroporous polymer, decreasing the specificity and selectivity. Stoichiometric non-covalent imprinting uses instead a stoichiometric amount of template and functional monomer, as in the covalent method. However, in order to use a monomer in a stoichiometric amount, the association constant of the host-guest complex needs to be in a range of  $5 \cdot 10^2$ - $10^7$  M<sup>-1</sup>.<sup>22</sup>

Usually multiple hydrogen bonds between template and monomers are used in order to create a stable complex which will result in the incorporation of functionality only in the imprinted cavities.

#### **1.4.5 Metal ion mediated imprinting**

Metal ions have the ability to bind several functional groups by accepting electrons from the heteroatoms of ligands. Depending on the metal and the ligand, this interaction can vary from weak to extremely strong. Metal-ligand coordination is vital in Nature and this technique can be applied to imprint biologically important

molecules. The advantages of metal ion coordination are the directional nature and the fast rebinding kinetics. Also these interactions are not affected by the solvent, meaning that this method can also work well in aqueous media. The imprinting is also stoichiometric, avoiding the formation of non-specific binding sites.

Fujii *et al.*<sup>23</sup> were the first to report this method using this technique for the imprinting of amino acids. Recently, a metal-ion-mediated complex-imprinted-polymer-coated solid-phase microextraction (SPME) fibre was reported, using Cu(II) as the ion, for the separation of thiabendazole (TBZ) from citrus and soil samples<sup>24</sup>. The recognition and enrichment properties of the novel SPME were improved compared to polymers that rely on hydrogen bonding interactions.

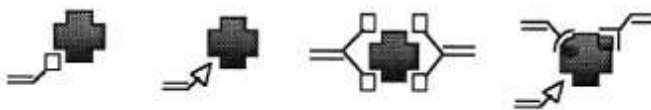
## 1.5 FACTORS INFLUENCING THE DESIGN OF MIPs

Engineering and studying the pre-polymerisation complex is now possible in non-covalent imprinting. It has become routine to analyse different aspects of the polymerisation mixture, from the functional monomer to the solvent, in order to make better MIPs and avoid all the negative aspects that can affect the final product, e.g. low specificity, high number of non-specific binding cavities, etc. Here I will refer mostly to non-covalent imprinting, in particular using a “bulk” polymerisation.

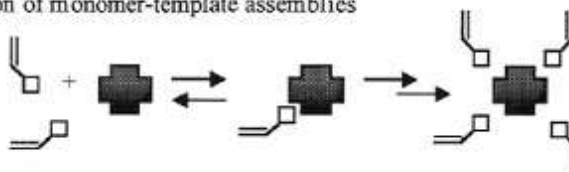
### 1.5.1 The functional monomer

The functional monomer is possibly the most important factor influencing the success of the imprinted polymer. As mentioned before, it is vital that the strength and positioning of the template-functional monomer in the pre-polymerisation mixture are ideal to introduce and fix the functionality only in the specific binding cavities. In Figure 11 are shown the factors that can affect the recognition properties of the imprinted sites.

## • Choice of the functional monomer



## • Stabilisation of monomer-template assemblies



## • Template size and shape



## • Monomer-template conformational rigidity



**Figure 11:** Factors affecting the recognition properties of MIPs related to the monomer-template assemblies<sup>25</sup>.

With the use of commercially-available monomers, it is more difficult to achieve this aim for two reasons. Firstly, the strength of the interaction is not always great enough and, as the result, the functional monomer is used in excess to make sure all the template is engaged in a complex with the monomer. This can lead to the formation of non-specific binding cavities. Secondly, a perfect fit between the template and monomer, using a limited range of functionalities, is not always possible. This evident problem has challenged few groups to develop novel functional monomers that can bind to template functionalities more strongly and attract the molecule to the correct position. An early example are the *N,N'*-distributed *p*-vinylbenzamidines introduced by Wulff<sup>26</sup> for the recognition of chiral carboxylic acids. The novel monomer gave high fidelity sites and allowed efficient recognition, even in aqueous media. The inspiration for the synthesis of novel functional monomers for molecular imprinting came also from supramolecular chemistry. Takeuchi<sup>27</sup> reported the synthesis of 2,6-*bis*(acrylamido)pyridine (BAAPy) for the imprinting of barbiturates, basing the approach on the well-known

Hamilton cleft<sup>28</sup> motif. Cyclodextrins have also been used for the imprinting of cholesterol<sup>29</sup>. Further examples of tailor-made functional monomers are: 2-acrylamidopyridine<sup>30</sup>, a series of methacrylamide-based functional monomers<sup>31</sup>, a *bis*-amide-based functional monomer<sup>32</sup> and a *bis*-urea-based functional monomer.<sup>33</sup> Fluorescent monomers have also been created.<sup>34</sup>

The criteria for the design of the monomer are the presence of a polymerisable group close to the hydrogen-bonding receptor site, a directed hydrogen-bonding interaction and an easy synthetic access.

### 1.5.2 The template

Not all molecules are perfectly suitable candidates to be imprinted, due to their size, functionality and other characteristics. In recent years the imprinting of macromolecules, such as bacteria or proteins, has increased due to a huge improvements in the field. Nonetheless, the imprinting of fairly small molecules is still easier and more common.

Also, the common use of only commercially-available functional monomers creates an obstacle to imprint every sort of template; this problem has been tackled with the development of novel functional monomers and I will discuss later the underlying positive effect brought by tailor-made monomers.

The chosen molecule for the imprinting process is a key factor in the design of the ideal conditions to create a better-performing MIP. A dummy template is a molecule similar to the target molecule, which has the same functionality that is complementary to the functional monomer and a similar size. Usually, a dummy template is used when the original target molecule has solubility problems, is toxic or explosive, or simply too expensive. A successful example of dummy template imprinting was the use of riboflavin<sup>35</sup> esters for the imprinting of riboflavin, as the target molecules was not soluble in chloroform, a better solvent in terms of facilitating the hydrogen-bonds (H-bonds) interaction between template and functional monomer.



### 1.5.3 The crosslinker

The crosslinker plays a huge role in the imprinting process. Most MIPs are porous organic materials which need to have the right balance of rigidity and flexibility in order to have a balance between selectivity towards the imprinted molecule and quick re-binding kinetics. Usually, the crosslinker is added to the polymerisation mixture in a high excess compared to the functional monomer to avoid the functionality in the binding cavities to be too flexible and, as a result, less specific toward the target. On the other hand, if the amount of crosslinker is too high, the obtained polymer will have a weak flexibility which won't allow a fast removal and re-uptake of the template during equilibrium rebinding or chromatography, making the polymer less useful.

In Figure 12 are shown the crosslinkers that are usually used in imprinting; the most common is EGDMA.

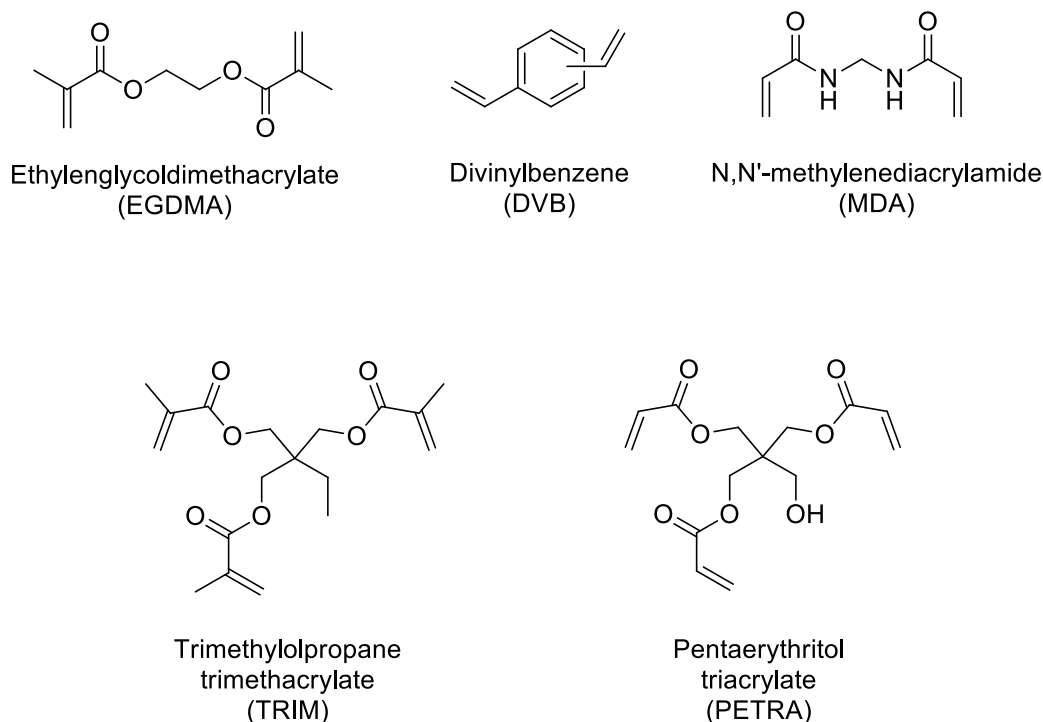


**Figure 12:** Crosslinking monomers commonly used in molecular imprinting (EGDMA, MDA, DVB, TRIM, PETRA)

The selectivity is particularly influenced by the amount of crosslinker used in the MIP. Studies by Wulff<sup>36</sup> have shown that no selectivity is observed if only 10% of crosslinking is used. Instead, the use of between 50% and 66% of EGDMA can hugely increase the selectivity. In this study, it was shown that EGDMA was the best crosslinker in terms of selectivity, as it gives the right swellability, splitting percentage (template removal) and inner surface area, providing a good balance in terms of rigidity and flexibility.

#### **1.5.4 The solvent**

The solvent has an impact on both the recognition behaviour and the morphology of the MIP. The solvent can influence the porosity and, therefore, the binding kinetics and the selectivity towards the template. A good porogen drives the polymerisation towards the formation of a porous material where the template can freely move inside to gain access to the binding cavities. The amount of solvent/porogen usually used in “bulk” polymerisation is between 0.29-1.76mL/g, with 1.2-1.4 mL/g being the optimum quantity<sup>37</sup>.

Also the polarity of the solvent used in non-covalent imprinting needs to be considered. As mentioned before, when H-bonds are the driving force creating the imprinted sites, it is not possible to use just any solvent, as polar solvents can interfere with the template-functional monomer complex formation and strength. Poor recognition behaviour in non-covalent imprinting can be caused by the use of a polar solvent. Considering the solubility of the template and monomer, a solvent with low to medium polarity (chloroform, acetonitrile, tetrahydrofuran) can be used and the template, if only soluble in a polar solvent, can be modified to decrease its polarity (dummy template) (Table 2).

**Table 2:** Solubility parameters, Hydrogen Bond capacity and refractive indices of solvents used for preparing MIPs.<sup>38</sup>

SOLUBILITY PARAMETERS, HYDROGEN BOND CAPACITY AND REFRACTIVE INDICES OF SOLVENTS USED FOR PREPARING MIPs

Solvent	$\delta_d$	$\delta_p$	$\delta_h$	$\delta$ (MPa) <sup>0.5</sup>	H-bond	$n_D$
MeCN	15.3	18.0	6.1	24.6	P	1.34
THF	16.8	5.7	8.0	19.4	M	1.41
CHCl <sub>3</sub>	17.8	3.1	5.7	19.0	P	1.45
C <sub>6</sub> H <sub>6</sub>	18.4	0	2.0	18.6	P	1.50
DMF	17.4	13.7	11.3	24.8	M	1.43
CH <sub>2</sub> Cl <sub>2</sub>	18.2	6.3	6.1	20.3	P	1.42
<i>i</i> -propanol	15.8	6.1	16.4	23.5	S	1.38
HOAc	14.5	8.0	13.5	21.3	S	1.37
MeOH	15.1	12.3	29.3	29.7	S	—
Toluene	18.0	1.4	2.0	18.6	P	—
H <sub>2</sub> O	15.5	16.0	42.4	47.9	S	—
Cyclohexane	16.8	0	0.2	16.8	P	—

The solubility parameter  $\delta$  has been divided into one dispersive term  $\delta_d$ , one polar term  $\delta_p$  and one hydrogen bonding term  $\delta_h$ . H-bond is a measure of the hydrogen bonding capacity of the solvent in terms of both donor and acceptor ability: P = poor, M = moderate and S = strong.  $n_D$  = refractive index.

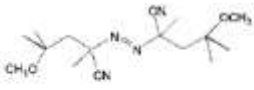
Nonetheless, in covalent imprinting or when a template with lower polarity is used, where the interaction is mainly driven by hydrophobic forces, a more competitive solvent may be used (such as water).

### 1.5.5 The initiator

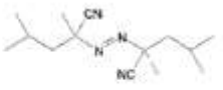
Commonly used free radical initiators are azo-initiators such as 2-2'azo-bisobutyronitrile (AIBN), activated either by photochemical homolysis below room temperature or thermochemically at 60 °C or higher, or 2-2'azo-bis-(2,4-dimethyl-valeronitrile) (ABDV) and 2-2'azo-bis-(4-methoxy-2,4-dimethyl-valeronitrile) which are thermally activated at 40 °C and 30 °C, respectively. In Table 3 is shown a list of normally used initiators.

**Table 3:** List of free radical initiators generally used in Molecular Imprinting.<sup>38</sup>

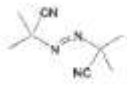
Type	Initiator	Initiation temperature	Reference to MIPs
Peroxide:	RC(O)OO(O)CR: R=ethyl	110 - 130 °C [10]	-
	R= benzoyl	40 - 70 °C	-
Persulphate:	R = tert-butyl	100 - 120 °C	-
	S <sub>2</sub> O <sub>8</sub> <sup>2-</sup>	90 °C [21]	Acrylamide MIPs [56]
Azo:	V-70 <sup>a</sup>	30 °C <sup>a</sup>	For use of V-68 see [14]
	ABDV (V-65) <sup>b</sup>	50 °C <sup>a</sup>	[12, 14, 46]
	AIBN (V-60) <sup>b</sup>	65 °C <sup>a</sup>	[52]
Ionizing radiation	γ-rays	15 °C	[80]



V70



ABDV



AIBN

Studies to compare the selectivity and retention behaviour on MIPs prepared at low and high temperatures has been done, but apparently only a change in chromatographic retention has been noticed with polymers synthesised at lower temperature exhibiting a longer retention time<sup>25</sup>. The suggestion is that the morphology of the polymers changes based on the polymerisation temperature, making the binding sites more or less accessible.

## 1.6 MORPHOLOGY

Different types of polymerisation have been developed in order to change the physical morphology of imprinted materials and to obtain materials that can perform better; what still needs to be achieved is a homogeneous distribution of binding sites, saturation capacities and easy to access imprinted cavities, to name a few. Below are described a series of morphologies and techniques applied in imprinting.

### 1.6.1 “Bulk”: crushed monoliths

MIPs are commonly prepared by “bulk” polymerisation. The obtained monoliths are then crushed to obtain smaller particles, for example in the range of 25-36 μm to be used for chromatographic application or a bigger size, 36-63 μm, to be used

for SPE applications<sup>39</sup>. Nonetheless, this morphology is not ideal for chromatographic separation as the particles display poor efficiencies in this mode. First of all, the shape of the particles is not homogeneous, as they been crushed and sieved leading to “rock-like” particles. Also, for chromatographic applications, particle sizes of 3-10  $\mu\text{m}$  are ideal. This morphology is still widely used as it is a simple and straightforward method which can give a quick idea as to the performance of the polymer before working on the morphology; it is still efficient for MISPE application.

Ideally, all the particles will have a spherical shape and a narrow size distribution, which can be obtained with imprinted beads or nanoparticles.

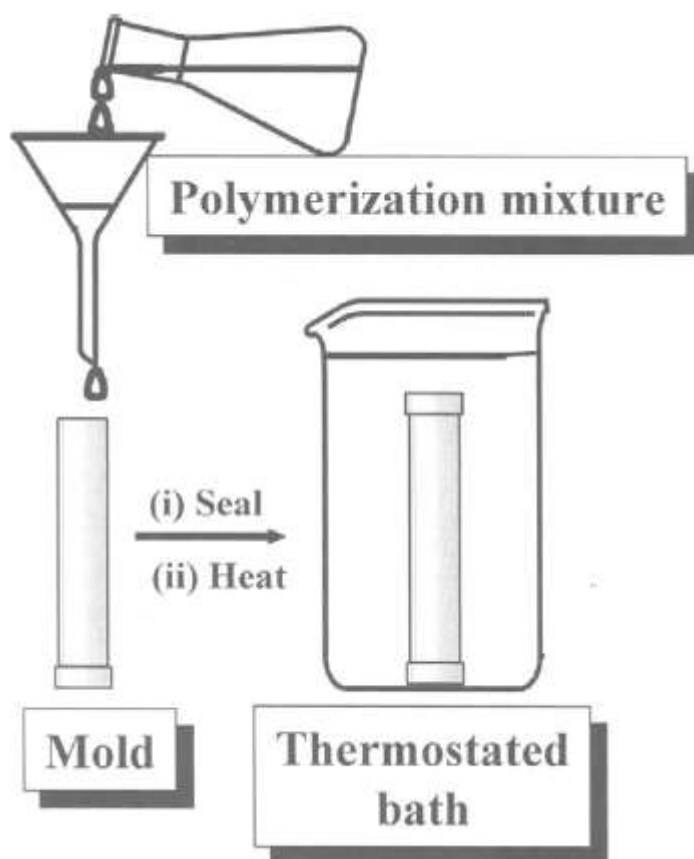


**Figure 13:** Scheme of preparation of macroporous monolith using a thermal free radical polymerisation. The figure is modified from the *Monolithic Materials* book.<sup>40</sup>

The polymeric block obtained by “bulk” polymerisation is crushed, manually or mechanically, and then sieved. This leads to the formation of irregularly shaped

particles. It is acceptable for a research laboratory quantity and aim, where the purpose is to test the polymer. However the process won't be productive if it needs to be scaled-up industrially. Also, some results obtained in HPLC can be compromised by the particle shape and size and can create high back pressures during use.

### 1.6.2 Beads

Beaded polymers have been investigated to obtain particles showing higher efficiencies in separation science, with a spherical shape and a monodispersed size distribution being of major importance for efficiency in application where the polymer is used as a chromatographic stationary phase. Beads are superior to "bulk" monolith particles in terms of shape and size distribution. They are usually prepared by suspension or emulsion polymerisation techniques, which lead to micron-sized MIPs. Such methods generally give quantitative yields of MIP, a better efficiency in chromatographic techniques, with better flow rates and lower back pressures, problems usually present by "bulk" MIPs.

There are several techniques in place to prepare beads but it is really important to consider the nature of the template-monomer interaction before applying them to a particular imprinting situation. For example, if the interaction is based on H-bonds, perhaps the use of competitive polar solvent is not ideal, but the same solvent can be used in covalent imprinting where the complex is strong. Also to take in consideration is the partitioning of the polymerisation component in the two phases in the suspension or emulsion polymerisation.

Here is a list of techniques for making imprinted polymer beads<sup>41</sup>:

I) *Bulk - in bead pores* (may fill the pores or just coat the surfaces of the pores in both inorganic (silica) and organic (trimethylol propane trimethacrylate – TRIM) beads. This leads to better particle shape and better chromatographic packing. The drawback is the yield (5-40%), limited by the space occupied by the original bead structure.

IIa) *Suspension - in water*. This technique produces spherical beads with differing levels of size polydispersity. The technique leads to highly reproducible results, the

possibility of large scale preparation and high quality beads. One of the disadvantages is that the water is incompatible with most non-covalent imprinting procedures, so is only used for covalent imprinting and metal chelate-based processes. An example of beads prepared with this technique are the cholesterol imprinted beaded polymers reported Whitcombe,<sup>42</sup> which were made using a sacrificial spacer technique. Usually in this technique, emulsion suspension is formed by mixing the imprinting mixture with 4-10 volumes of water containing a suspension stabilizer. Organic droplets are formed in the water and the size of the beads is determined by the droplet size. It is also possible to use a water-in-oil suspension by choosing different surfactants and apolar solvents as the dispersing phase.

IIb) *Suspension – in perfluorocarbon*. The beads obtained are spherical, of good quality and polydisperse in size. The solvent does not interfere with the imprinting process. Liquid fluorocarbons are immiscible with most of the organic compounds, providing the opportunity to imprint using a non-covalent approach, but can give issues with the stabilisation of the suspension. In this technique, a special surfactant needs to be used and there is less literature than in the oil-in-water suspension-water method.

III) *Non-aqueous dispersion*. During this polymerisation random aggregates or precipitates can be formed depending on solvents used, but stabilisers are present and size monodispersity can be obtained. Many dispersion polymerisation experiments have been reported using styrene- and acrylate-based monomers<sup>43</sup>. With the right conditions, spherical and monodisperse particles can be obtained, with a size range of 2 – 6  $\mu\text{m}$ . Precipitation polymerisation is a dispersion technique generally used to make imprinted beads. With this method the pre-polymerisation mixture is firstly dissolved in a large quantity of solvent, which is purged with inert gas to remove oxygen, and then heated to start the polymerisation while gentle agitating the solution (e.g. with a roller). The particles are then recovered by filtration or centrifugation and washed to remove the template.

IV) *Two-stage swelling*. This technique is more complex, but monodisperse beads can be obtained that give an excellent packing. Unfortunately, the aqueous emulsion compromises some imprinting processes. In this technique a “seed” latex is first

produced by emulsifier-free polymerisation. The seed particles are then swollen in a micro-emulsion made of free radical initiator, a solvent, water and a stabilizer. The seed particles in the emulsion are stirred until the emulsion droplets are absorbed into the seeds. The swollen particles are then added to a second dispersion containing functional monomers, cross-linkers, porogenic solvent and template. After several hours the temperature is increased to start the polymerisation. The usual particle size is 5  $\mu\text{m}$ , but 100  $\mu\text{m}$  particles can be also produced.

V) *Aerosol polymerisation* can result in polydisperse spherical beads, but there are only few imprinting examples. In this method, as we have the polymerisation of droplets of the imprinting mixture as aerosols, there is no need for large amounts of solvent that can interfere with the imprinting process or surfactant. Nonetheless, this technique limited with respect to the monomers and functionality that can be imprinted and need to be explored further.

VI) *Surface rearrangement of latex* (latex obtained from seeded emulsion polymerisation) can result in near-monodisperse beads. However, this technique was demonstrated only for metal ions.

### 1.6.3 Thin films

Imprinting in layers or thin film can be applied in sensor or in liquid chromatography as these polymers show improved mass transfer properties. They can be prepared by grafting techniques, where the polymerisation occurs only on a thin surface. Sometimes, the problem with imprinted sensors is the weak signal produced by the binding event, but this problem can be overcome by using a suitable signal transducer, e.g. quartz crystal microbalance, electrochemical detection.

### 1.6.5 Membranes

Imprinted membrane can find their application in environmental and industrial separations and purification. The membrane can selectively block the passage of the imprinted molecules or create an active transport or gate effect for the template<sup>39</sup>. The imprinted membrane can be produced using a one-step imprinting



method, combining the phase inversion technique used for the production of microporous membrane with imprinting, or by using a supporting membrane which is then grafted to generate the imprinting or MIP particles can be attached to it. An example are organic solvent nanofiltration (OSN) membranes prepared by a phase inversion molecular imprinting technique using aminopyrimidine as the template<sup>44</sup>.

### 1.6.6 Nanostructured MIPs

Shea<sup>45</sup> has reported on the synthesis of melittin-imprinted nanoparticles (NPs) using *precipitation polymerisation* using acrylamides as monomers. The conditions were mild, in order to avoid the protein denaturation, and a 10-100 nm monomodal distribution of NPs in aqueous solution using a small amount of surfactant were obtained. Later, his group reported again the preparation of protein-size imprinted nanoparticles with high affinity towards melittin tested on mice<sup>46</sup>. This example shows how Molecularly Imprinted Nanoparticles (MINPs) can be useful for drug-like application of the imprinting technique. The right shape, size and morphology can create new horizons for this field of study.

Other examples of MINPs are those synthesised by the group of Takeuchi to be used as the recognition element in Surface Plasmon Resonance (SPR) sensing of Bisphenol A<sup>47</sup>. The NPs were prepared by seed polymerisation, with the seed NPs synthesised via *emulsion-free seed polymerisation*. Water-soluble MINPs<sup>15</sup> were recently reported where surface cross-linked micelles (SCMs) were used. The micelles solubilise the hydrophobic methacrylate in water.

In general, micro-emulsion polymerisation, inverse micro-emulsion polymerisation, or precipitation polymerisation can be used for the preparation of MINPs.

### 1.6.7 Conclusion

In conclusion, the use of different types of morphology in imprinting are developing very quickly, in order to have MIPs with better properties, allowing for wider use in commercially applications. Further, the techniques used to imprint large molecules, such as bacteria and protein, are to be noted. Some examples are *gel*

*imprinting*, where the degree of crosslinking is minimum in order to create a soft matrix and a pore size network large enough to the protein to move freely in the polymer, and *surface imprinting* where the template, a protein for instance, is confined between a monomer rich and monomer-poor phases to obtain after polymerisation the binding sites external to the polymeric material making it easy to remove and re-bind the protein. Another way is to immobilise the protein on a surface, expose the surface to a polymerisation mixture and, after polymerisation, remove the template. All these methods are 2D approaches that can lead only to the recognition of a site of the template, decreasing the number of functionalities involved in the recognition process. 3D protein imprinting is surely more efficient<sup>48</sup> as is *epitope and fragment imprinting*<sup>49</sup>, where the template is a substructure or epitope of a larger or inaccessible target.

## 1.7 APPLICATIONS

The molecular imprinting approach has been applied in different scientific disciplines due to its versatility and the seemingly infinite number of synthetic receptors that can be created with this technique. The creativity that the scientific community can experience with MIPs makes them a great and multi-faceted method to apply in different research projects. Some of the areas that will be discussed in this chapter are just at the beginning of their studies and hold great potential for the future.

### 1.7.1 HPLC

MIPs have been employed as a stationary phase in liquid chromatography since the beginning, when only silica matrices were used. Since then, the use of MIPs in this application has evolved, and there have been examples of separations of *carbohydrates*<sup>50</sup>, *amino acids and derivatives*<sup>21a, 51</sup>, *peptides*<sup>52</sup> and *proteins*<sup>51a, 53</sup>. Also *biochemicals, drugs and biologically active compounds* have been used as targets to develop different stationary phases; for example, an enantioselective chromatographic stationary phase selective for the NSAIDs naproxen,<sup>54</sup> ketoprofen and ibuprofen<sup>55</sup> has been developed. The development in the use of imprinted

materials in chromatographic techniques relies on the development of more efficient, mono-disperse and spherical particles, as mentioned before. An example are microspheres prepared by precipitation polymerisation for the separation from a complex media of caffeic acid using high-performance liquid chromatography<sup>56</sup>.

### **1.7.2 Molecularly Imprinted solid phase extraction (MISPE)**

Molecularly Imprinted Solid Phase Extraction (MISPE) is one of the applications that has seen enormous growth in the last years. The robustness and the affordability of the technique combine to provide a highly sensitive and selective analytical method, making MISPE one of the fields where MIPs have been most successful. To name some examples, we have the development of MISPE for the biomarker 4-(methylnitrosamino)-1-(3-pyridyl)-1-butanol (NNAL), an indicator of tobacco exposure found in urine samples<sup>57</sup>, the extraction of caffeine on a caffeine-MIP<sup>58</sup> from beverages and spiked human plasma and of triazine pesticides from ground water, soil and corn<sup>59</sup>. It must also be mentioned the use of MISPE in other fields, such as lipidomics, which is the study of lipids in biological samples that play a critical role in cellular functionality. The imprinting technique was used for the biological sample enrichments that subsequently led to the discovery and characterisation of several phosphate-monoester lipids not previously reported<sup>60</sup>.

### **1.7.3 Process scale purification**

The demand for more efficient and selective but also affordable purification techniques has increased in the past years. For instance, in the pharmaceutical industry, the use of such techniques could speed up the purification process in drug synthesis. Also the food industry can gain advantages from better methods to pre-treat raw materials or to process foodstuffs in order to remove specific agents to preserve it longer or to give to it a better flavour<sup>61</sup>.

Nowadays, environmental and health preservation have become increasingly important; the need to purify water and air from pollutants that can lead to adverse health problems has been an issue for governments. MIPs can offer a solution to these problems by binding pollutants at low concentration with a high selectivity<sup>62</sup>.

#### 1.7.4 Pseudo-immunoassays

MIPs have also found a huge interest as the replacement of biological receptors, such as antibodies, in immunoassays. Their potential relies on the advantageous characteristics of MIPs compared to their biological counterparts; they are more stable and easier to store, they can be used to both aqueous and non-aqueous assays and they don't have the need to involve laboratory animals for production.

On the other hand, one limitation is the need for a template molecule for each MIP's preparation, while antibodies can be cloned; however, this can be alleviated by recycling the template after the MIP synthesis. Reducing the polyclonality of MIPs is another disadvantage, which is still a matter of intense study.

The MIP-based assay can be prepared with the "*Radio-Ligand Displacement*" technique, which is carried out using  $^3\text{H}$ -labelled version of the drug. As an alternative, "*Displacement assays with optical detection*" can be used, employing both chromophore- and fluorophore-labelled template analogues. The first example of the latter technique was reported by the group of Karube<sup>63</sup>. Also, displacement of electro-active analogues using electrochemical detection<sup>64</sup> and assays employing chemiluminescent detection<sup>65</sup> were reported.

More studies need to be conducted in order to obtain better antibody-like polymers to be used in immunoassays. In the following table are listed the main characteristics of natural and artificial antibodies and the different performances of antibody- and MIP-based assays.

**Table 4:** A comparison between natural antibodies and molecularly imprinted polymers<sup>66</sup>.

	Natural antibodies	Molecularly imprinted polymers
low-mass molecules (< 5000 Da) as immunogen / template	yes, but necessity of a covalent linker between the immunogenic carrier protein and the low-mass antigen could affect the binding selectivity of resulting antibodies	yes, with exception for poorly functionalized or very low-mass molecules. Difficult for very polar templates
high-mass molecules (>5000 Da) as immunogen / template	yes	yes, but with marked experimental difficulties for large proteins (difficult template release, poor selectivity)
binding mechanism	well known	known, but some aspects under debate
binding affinity spectrum	discrete and narrow for monoclonal antibodies, continuous and broad for polyclonal antibodies	discrete and narrow for covalent imprinting, continuous and broad for non-covalent imprinting
mean affinity constant	frequently above $10^9 \text{ M}^{-1}$	rarely exceeds $10^7 \text{ M}^{-1}$ for bulk-imprinted polymers
binding site density	low, $\mu\text{M}$	high, mmol/g
binding kinetics	fast association, slow dissociation	slow association and dissociation
binding selectivity	high, fine tuning for monoclonals feasible. Difficult to be obtained for classes of ligands	high, fine tuning difficult when non-covalent approach is used
reproducibility	limited from batch-to-batch	very high
non-specific binding	negligible	depending from experimental conditions, rarely negligible
resistance to extreme experimental conditions (pH, cold, heat, sonication, organic solvents, denaturing agents)	no	yes
resistance to biological agents	no	yes (can be autoclaved)
needs of a solid phase as support	yes, this frequently involves the use of complex covalent coupling reactions	no, the polymer itself can be the support
reuse	very difficult	yes
cost for single batch	low for polyclonals, medium to high for monoclonals	very low (except for expensive templates)
commercial availability	high, frequently produced on demand	limited
in-house feasibility	no, a stabularium, trained people and a dedicated laboratory (monoclonals only) are necessary	yes, simple to make, with exceptions for advanced polymerization methods or mimic template approaches
health risks	not significant	sub-micrometric particles can be dangerous if inhaled. Some polymerization reagents (acrylamide, styrene, vinylpyridine) are toxic
literature	very large	very large and rapidly growing
state of the art	mature	in continuous evolution

**Table 5:** Key features and performances of antibody- and MIP-based assays<sup>66</sup>.

	antibody-based	MIP-based
low-mass analytes	yes	yes
high-mass analytes	yes	yes, but with marked experimental difficulties for large proteins
assay selectivity	high, fine tuning feasible	high, but fine tuning can be difficult
assay sensitivity	very high (up to pg/ml)	high (up to ng/ml)
non-specific tracer binding	negligible	depending from experimental conditions, rarely negligible
sample pretreatment	very limited	very limited
reproducibility	high	high
robustness	moderate	moderate
speed of execution	fast	fast
complexity of execution	moderate	moderate
automatization	yes	possible
reusability	no	dubious
cost for single analysis	low	low
in-house feasibility	yes	yes
commercial availability	yes	no
literature	very large	limited
state of the art	mature	in evolution

### 1.7.5 Chemical sensors

Due to the high selectivity and specificity of molecularly imprinted materials, MIPs can be integrated in sensors as the recognition element. Some of the devices that have been used since the beginning are the *Quartz-crystal microbalance-based sensing devices* (QCM).

Some successful examples have been applied to real-life problems, e.g. MIP-QCM sensors for the monitoring of engine-oil degradation<sup>67</sup> and the content of poly-aromatic hydrocarbons in water.<sup>68</sup> Even though most of the applications involve the recognition of analytes in liquid phase, some examples of detection in the gas phase were also reported.<sup>69</sup> New strategies have been explored to manipulate the morphology of the imprinted material to create more accessible binding sites and favour the scale-up production of these materials, as for Imprinted Polymer films selective towards Bupivacaine prepared on gold-coated quartz.<sup>70</sup>

*Fluorescent-based sensing devices* are also one of the most used and offer a great possibility to create an effective chemo-sensor for detection of sub-micromolar concentrations. The fluorescent signalling of the binding events can be introduced by including a fluorescent moiety in the functional monomer, as in the detection of

carbohydrates by integrating an anthracene-boronic acid conjugate monomer into a MIPs<sup>71</sup>, or incorporating a fluorescent reporter group into the binding site.<sup>72</sup> Another way is the use of compounds with an inherent fluorescence as functional monomers in the imprinting process.<sup>73</sup>

Other techniques that have been explored are: *surface plasmon resonance spectroscopy (SPR)*<sup>74</sup>, *electrochemical techniques*,<sup>64a, 75</sup> *field effect transistors (FETs)*,<sup>76</sup> *optical sensors, luminescence techniques*,<sup>77</sup> *spectroscopic techniques*<sup>78</sup> and *surface-enhanced Raman scattering*.<sup>79</sup>

### 1.7.6 Synthesis and catalysis

The use of MIPs with enzyme-like properties is possible, but more studies need to be done on this topic, as imprinted materials still cannot compete with enzymes in terms of stereo-chemical selectivity, reaction diversity, rate enhancement and turnover. Nevertheless, there are a number of different examples of MIPs that can mimic enzymes applied in synthesis and catalysis.

MIPs have been employed in chemical synthesis giving the opportunity to perform reactions with increase selectivity towards a particular enantiomeric form. The first report was from Damen and Neckers.<sup>80</sup> These groups created a kind of “microreactor” with the capacity to induce enantiomeric selectivity of the reaction through the orientation of the reacting group within the binding cavities. In other cases, a particularly well-characterized inhibitor of an enzyme was imprinted to obtain a “reactor” to create novel inhibitors of the same enzyme.<sup>81</sup> Catalysis of a Diels-Alder cycloaddition reaction between 1,3-butadiene carbamic acid benzyl ester and N,N-dimethyl acrylamide using an Imprinted Polymer was also reported,<sup>82</sup> where transition state analogues of the final products were used as the template during the imprinting process. Another examples of catalysis of C-C bond formation have been reported, where a class II aldolase mimic was developed to promote the condensation between camphor and benzaldehyde to yield 3-benzylidenecamphor.<sup>83</sup> Catalysis using imprinted polymers can be divided in two major classes. The first type of artificial catalyst is a sort of metallo-enzyme; the selected catalyst is transformed in a polymerisable form and is then complexed with a suitable template (e.g. the reaction substrate or the transition-state analogue).

Some examples include the regioselective hydrogenation of ketones<sup>84</sup> and MIP catalysts for the Suzuki coupling reaction.<sup>85</sup> The second type of catalyst is closer to the real structure of an enzyme, as it is created by incorporating the key features of the active site into the binding site of the MIP.

### 1.7.7 Therapeutic applications

Huge potential for molecular imprinting lies on the area of drug delivery. In particular “intelligent drug release” can be envisaged, whereby MIPs can be employed as a vehicle to carry and release the drugs in a predictable way in response to a specific stimuli; further, “magic bullet” drug targeting, where a drug conjugated to a targeting vector is released or in some cases internalized with its vector into the cell when the MIP binds to its target on the surface of a cell, is another way for imprinted materials to be used drug delivery.

Controlled delivery of norfloxacin in the treatment of ocular infection<sup>86</sup> or a pH-responsive drug delivery system for the proton pump inhibitor omeprazole have been reported.<sup>87</sup>

Also, the idea of using imprinted material to synthesize materials with drug-like properties has arisen. Examples of MIPs as drugs *per se* are include molecularly imprinted micro-gels capable of inhibiting the enzyme trypsin<sup>88</sup> and MIP nanoparticles capable of binding to the peptide toxin melittin present in the bee venom;<sup>46</sup> the latter is the first example of a MIP tested in the bloodstream of a living animal. Further, a cholesterol-selective MIP was developed for use as an oral adsorbent<sup>89</sup> and imprinted bile acid sequestrants.<sup>90</sup> MIPs have also been used for bio-purification, such as the case of a biocompatible membrane imprinted with uric acid for blood purification.<sup>91</sup>

## 1.8 CONCLUSION (AIM OF THE PROJECT)

In this thesis I will report the synthesis of pyridine-based novel functional monomers for the imprinting of molecules of pharmaceutical and biological interest. My main focus was on preparing building blocks for stoichiometric non-covalent imprinting, the advantages of which I have listed previously. To reiterate,



these include the reduction in the number of non-specific binding cavities in the final polymer and fast removal and rebinding kinetics of the template from the imprinted sites

### **1.8.1 Can we create hosts closer to nature?**

Nature is the most amazing example to look at if one wants to find perfect receptors. Biological macromolecules, such as antibodies and enzymes, benefit from a variety of functional groups, ideally placed or manoeuvred to participate in the recognition and catalysis mechanism, making them more versatile and selective towards a huge number of compounds.

In molecular imprinting scientist are trying to create artificial receptors as they will be relatively inexpensive, more stable and more readily reusable compared to the natural ones. Of course, the binding affinity and selectivity still need to be improved. The common use of commercially-available monomers (Figure 10), such as methacrylic acid, can cause a limitation in the number of targets that can be imprinted, and the decrease of the receptor's selectivity. The latter problem may originate by the use of an excess of functional monomer during the imprinting process, leading to an increased number of not selective binding cavities in the polymeric matrix and making the MIP less specific. As mentioned before, it is vital in the design of an imprinted polymer that the template-functional monomer complex is strong and stable during the polymerisation process. Without a strong engagement of the template with the monomer, it will be difficult to create imprinted cavities inside the matrix.

The overall aim of this research is to create tailored, engineered functional monomers to be used in stoichiometric non-covalent imprinting. The stoichiometric imprinting can allow us to approach a monodisperse population of binding cavities by creating a 1:1 monomer-template engagement creating, ideally, a final polymer having only specific binding cavities. This goal can be reached by designing and creating hosts selective for specific templates with a certain number of H-bonds complementary to the molecule to be imprinted. The inspiration for this approach derives from supramolecular chemistry, and a great example is certainly the Hamilton cleft,<sup>28</sup> which was created for the binding of barbiturates.

### 1.8.2 Hydrogen bonds

As mentioned before, the forces responsible for the template-monomer interaction first and the recognition of the template in the imprinted polymers later, are relatively weak non-covalent interactions, such as hydrogen-bonds, ion-pairing, dipole-dipole interactions and van der Waals' forces. Of particular interest is the hydrogen bond interaction, which is a major component in Host-Guest (H-G) complex formation.

**Table 6:** *Strength of Several Noncovalent Forces*<sup>92</sup>. \* <5 per surface area.

type of interaction or bonding	strength (kJ mol <sup>-1</sup> )
covalent bond	100–400
Coulomb	250
hydrogen bond	10–65
ion–dipole	50–200
dipole–dipole	5–50
cation– $\pi$	5–80
$\pi$ – $\pi$	0–50
van der Waals forces	<5 *
hydrophobic effects	difficult to assess
metal–ligand	0–400

*“...Hydrogen bonds are like human beings in the sense that they exhibit typical group-like behaviour. As an individual they are feeble, easy to break, and sometimes hard to detect. However, when acting together they become stronger and lean on each other. This phenomenon, which in scientific terms is called cooperativity, is based on the fact that 1+1 is more than 2...”*<sup>93</sup> (Figure 14)



**Figure 14:** *Gulliver constrained by a multitude of weak “bonds”. Illustration by Ulrike Schramm in Jonathan Swift’s Gullivers Reisen; reprinted with permission from Überreuter Verlag, Vienna<sup>93</sup>.*

Taking inspiration from this definition of hydrogen bonds, our aim to introduce in our novel functional monomers a certain number of hydrogen bonds that can lead to host-guest complex with a high binding strength becomes understandable. As we used hydrogen-bonding as the driving force for our MIP creation, the solvent used also became an important factor to consider in the design process. As mentioned before, polar solvents can reduce or completely destroy this sort of interaction between the template and the monomer, so an apolar solvent, generally chloroform, was utilised.

# CHAPTER 2

## *MATERIALS & METHODS*

## 2.1 MATERIALS

All solvents and reagents were used without any further purification except for ethylene glycol dimethacrylate (EGDMA), which was freed from inhibitor and purified before use as follows: EGDMA was washed sequentially with 10 % aqueous NaOH and brine, then dried over MgSO<sub>4</sub>. After filtration, EGDMA was distilled under reduced pressure and stored at -20°C prior to use. 5-*tert*-butylisophthalic acid, chelidamic acid, tegafur, 5-methyluridine (5-MeU) and uracil were purchased from Tokyo Chemical Industries (TCI) (Oxford, UK). Pseudouridine ( $\psi$ ), Uridine, 2',3',4'-tri-*O*-acetyluridine (TAU), D-(+)-biotin, pentobarbital, phenobarbital, isomannide and 2-hydroxymethylfurfural were purchased from Carbosynth (Compton, UK). Deuterated chloroform and dimethyl sulfoxide (DMSO) were purchased from Goss Scientific. 2-acetamido-5-vinylpyridine was donated by Pfizer (Groton, USA). Piperidine, dipropylamine and *N*-(3-Dimethylaminopropyl)-*N'*-ethylcarbodiimide hydrochloride (EDC) were purchased from Alfa Aesar. 7N methanolic ammonia solution was purchased from Acros Organic. Azo-*bis*-dimethylvaleronitrile (ABDV) was received from DuPont BV (Netherlands). All the other reagents and solvent were purchased from Sigma Aldrich (Gillingham, UK). 2',3',4'-tri-*O*-propionyl uridine (TPU), 2',3',4'-tri-*O*-butyryl uridine (TBU) and 2',3',4'-tri-*O*-acetylpsseudouridine (TA $\psi$ ) were prepared from Uridine or Pseudouridine and the appropriate acid anhydride using a literature method<sup>94</sup> and the synthesis of TPU and TBU was previously reported<sup>95</sup>. 2,6-bis(acrylamido)pyridine (BAAPy) was prepared as reported previously<sup>96</sup>. MERCK silica gel 60, 230-400 mesh ASTM was used for column chromatography. Thin-layer chromatography (TLC) was performed on aluminium-backed plates MERCK silica gel 60 or on aluminium-backed plates aluminum oxide (Fluka Analytiks)F254.

## 2.2 INSTRUMENTATION

Melting points were determined using a STUART melting point apparatus and are uncorrected. Infrared spectra were recorded on a Perkin Elmer Spectrum One FT-IR Spectrometer. <sup>1</sup>H NMR and <sup>13</sup>C NMR spectra were obtained on a JEOL ECA,

400 MHz FT NMR Spectrometer or a JEOL ECA, 500 MHz FT NMR Spectrometer. Chemical shifts are reported in ppm on the  $\delta$  scale relative to TMS as internal standard or to the solvent signal used. Coupling constants are given in Hz.  $^1\text{H}$  NMR titration experiments in Belfast were performed on a Bruker Ultrashield™ 400 PLUS NMR spectrometer.  $^1\text{H}$  NMR titration experiments for the BAAPy series were obtained on a JEOL ECX, 400 MHz NMR spectrometer. Mass Spectra were obtained on a Finnigan AQA single quadrupole instrument. Chromathographic evaluation of MIPs and non-Imprinted Polymers (NIPs) was performed on an Agilent 1100 series HPLC, using empty chromatography columns (Restek, 50mmX4.6mmX1/4"OD) and a reverse phase column (Kinetex® 5 $\mu\text{m}$  C18 100 Å, LC Column 150 × 4.6 mm)

## 2.3 METHOD

### 2.3.1 Molecular Imprinting Protocol

All imprinted polymers were prepared using a molar ratio of *template/functional monomer/cross-linker* of 1:1:20 and using ABDV as the initiator and chloroform as the solvent/porogen. The control, non-imprinted polymers (NIPs) were prepared in an identical fashion but in the absence of the template.

The template, functional monomer, cross-linking monomer and ABDV (1% w/w total monomers) were dissolved in chloroform ( $\text{CHCl}_3$ ) and then introduced to a borosilicate polymerisation tube. The solution was cooled on ice and degassed for 10 min with dinitrogen in order to remove dissolved oxygen. The tube was then sealed using a flame. The polymerisation was initiated by placing the sealed tubes in a water bath set at 50 °C. Polymerisation was allowed to continue for a period of 24 hours at this temperature, after which the tubes were removed from the water bath, broken with a hammer and the monolithic polymers recovered. The resulting monoliths were lightly crushed to give smaller particles, which were then extracted with methanol using a Soxhlet apparatus over a period of 24 hours to remove the template from the polymeric matrix and reveal the imprinted binding cavities.

The methanol extracts were evaporated to dryness and weighed; they were then analysed by  $^1\text{H}$  NMR to identify the composition of the extract. The washed polymer particles were then crushed and sieved, with and the size fraction 25-50  $\mu\text{m}$  collected for further use. These particles were then subjected to sedimentation in methanol to remove fine particles prior to further use. For all polymers, particles of the desired size were obtained in a yield of 50-60%.

### 2.3.2 Chromatographic evaluation

The polymers were evaluated by HPLC in order to determine the retention factor on the imprinted polymers of the template used, template analogues and non-related compounds (Figure 15). Polymer particles (25–50  $\mu\text{m}$ , 200 mg dry weight) were slurry packed under gravity into stainless steel HPLC columns (50 mm x 4.6 mm), using an acetonitrile suspension of particles. The columns were then connected to the HPLC and acetonitrile was continuously passed through the column at a flow rate of 5mL/min until the signal from injection of acetone (void volume marker) was acceptable (sharp and symmetrical peak).

Before starting the analysis, each column was washed with a polar solution (1% acetic acid/acetonitrile v/v) to make sure the polymers were template free, and then washed again with acetonitrile or the eluent used for the analysis. Prior to analysis, 5mM stock solutions of the analytes were prepared in deionised water, or in acetonitrile and diluted in water or acetonitrile to give 1 mM solutions. HPLC analyses were performed by injecting 5  $\mu\text{L}$  of these 1 mM analyte solutions at 25  $^\circ\text{C}$ , using a flow rate of 1 mL/min. The elution profiles were recorded at different wavelengths (245, 260 and 275 nm) depending on the analytes under study. The retention factors ( $k'$ ) for each analyte were calculated as  $k' = (t_R - t_0)/t_0$ , where  $t_0$  is the retention time of the void marker (acetone) and  $t_R$  is the retention time of the analyte. Imprinting factors (IF) were calculated using the formula  $\text{IF} = k'(\text{MIP})/k'(\text{NIP})$ . The selectivity ( $\alpha$ ) of the polymers were calculated as  $\alpha(1) = k'_1/k'_z$  where “1” is the template used for the imprinting and “z” a structurally related analyte.

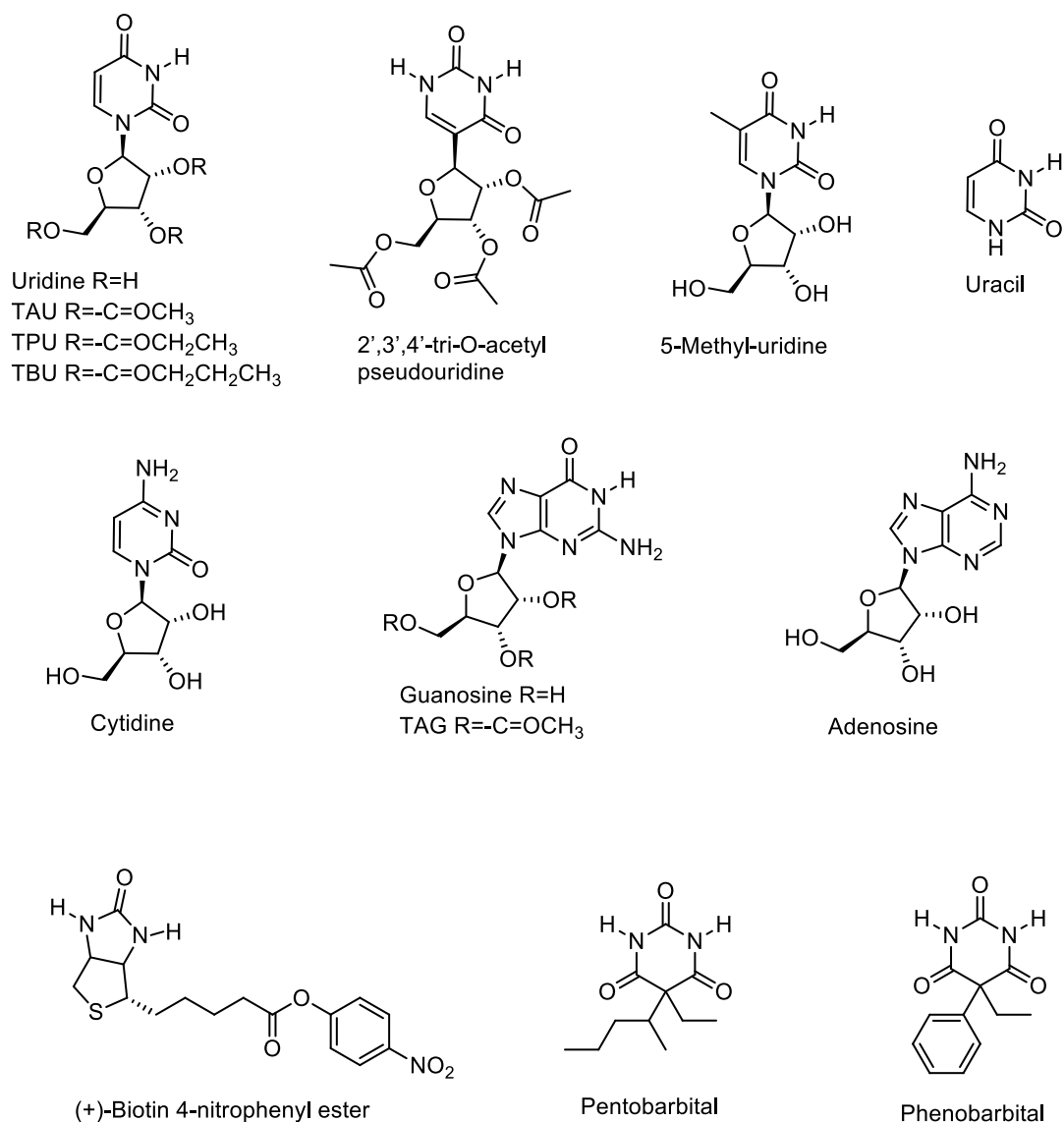


**Figure 15:** Structures of analytes used for the chromatographic evaluation of polymers.

### 2.3.3 Equilibrium rebinding experiments

Equilibrium binding experiments were performed on the MIPs and NIPs to evaluate the affinity of the polymers towards their respective template. The saturation capacity and association constant for the binding sites are obtained by means of this experiment. The imprinting process introduces the formation of binding sites with different fidelities in the terms of selectivity and affinity. The heterogeneity of binding sites formed during the imprinting process decreases the number of useful binding sites in the polymeric matrix. Equilibrium rebinding can give information



about the saturation capacity (site density) of the polymer and the binding constant related to this site.

Heterogeneous and homogeneous binding site formation depends mostly by the type of imprinting and the strength of the host-guest complex. Usually, in covalent imprinting where no excess of either template or functional monomer is needed in the pre-polymerisation mixture and, regardless solvent or other conditions, the complex is stable, a homogeneous set of binding cavities can be obtained as potentially all monomer will lead to an imprinted cavity formation. Conversely, in non-covalent imprinting, where the functional monomer is often used in excess to reach an 100% complexation of the template in solution, and depending of chosen polymerisation condition this complex is weak, different type of sites are formed, specific and not, with high or low affinity. We used a stoichiometric non-imprinting method, which potentially can lead to a single type of binding cavity. This is the reason why the experimental data obtained by equilibrium rebinding experiments were fitted with a Langmuir type adsorption model, where the adsorbent is assumed to contain only one type of site.<sup>25</sup> This system is defined ideal. This isotherm depends on two parameters:  $q_{s1}$  which is the saturation capacity (or number of sites, site density) and the binding constant  $b_1$  which is related to  $k_a$  (association constant).<sup>25</sup> By fitting the data obtained by the rebinding experiments to this model, the number of binding sites present in the polymer and their average  $k_a$  is obtained.

$$q = \frac{a_1 C}{1 + b_1 C} \quad (1)$$

$$q_{s1} = a_1 / b_1 \quad (2)$$

$$k_a = b_1 \cdot M_w \quad (3)$$

**Equation 1:** Langmuir adsorption isotherm equation (1).  $q_{s1}$  = saturation capacity,  $b_1$  = binding constant,  $k_a$  = association constant and  $M_w$  = molecular weight of the adsorbate.

When the assumption of homogeneous binding sites in the polymer cannot be made other models can be used, e.g. the bi- and tri-Langmuir models (equation 4) where the assumption is that two or three different site classes are present in the adsorbent and the Freundlich model (equation 5,  $a$  and  $n$  are numerical parameters) which assumes that no saturation capacity is present, but the adsorbent has a continuous distribution of binding sites with different binding energies<sup>25</sup>.

$$q = \frac{a_1 C}{1+b_1 C} + \frac{a_2 C}{1+b_2 C} \quad (4)$$

$$q = aC^{1/n} \quad (5)$$

**Equation 2:** Bi- and tri-Langmuir model (equation 4) and Freundlich model (equation 5,  $a$  and  $n$  are numerical parameters)

*Protocol:*

To 10 mg of polymer particles (25–50  $\mu\text{m}$ , 10 mg dry weight) was added 1mL of template solution in acetonitrile or 1% acetic acid/acetonitrile (v/v) at different concentrations (0 – 10 mM) in HPLC vials. The vials were left at room temperature overnight over a period of 25 hours. After 25 hours, the supernatant was examined using HPLC with UV detection at different wavelength based on the analytes, usually 245, 260 and 275 nm, to obtain the concentration of free template in the supernatant in each vial. The experimental data were fitted to the mono-Langmuir model, using the Origin Pro 8.5.1 software, to obtain an adsorption isotherm and calculate number of sites and related binding constants. The Langmuir model was chosen as the one that provided the best fit to the binding isotherm data obtained ( $R^2 > 0.98$ ).

### 2.3.4 Molecularly Imprinted solid phase (MISPE)

Imprinted and non-imprinted particles (100 mg) were packed into polypropylene cartridges with 20  $\mu\text{m}$  porous polyethylene frits. The optimised MISPE protocol consisted of conditioning the cartridge with water prior to loading 1 mL of a 0.1 mM water solution of template, washing with 1 mL of acetonitrile and finally eluting the template in the a cartridge with 1 mL solution of 1% acetic acid in methanol. The cartridge was then washed three times with 1 mL of 1% acetic acid in methanol, to ensure complete template elution, and four times with water to wash out any remaining acidic methanol solution prior to repeating the experiment. The loading, washing and elution process was performed using a general MISPE apparatus or by gravitation, with the vacuum in the apparatus was created using a water pump. The flow rate was maintained constant at 1 mL/min. The collected fractions were transferred to HPLC vials to be analysed by HPLC. The eluent used for the HPLC was AcOH:H<sub>2</sub>O/60:40 or 100% acetonitrile (CH<sub>3</sub>CN) and the detection was made using a wavelength of 220-240 nm or 270 nm and the column used was a reverse phase column (Kinetex® 5 $\mu\text{m}$  C18 100 Å, LC Column 150  $\times$  4.6 mm) . Each experiment was performed in duplicate or triplicate.

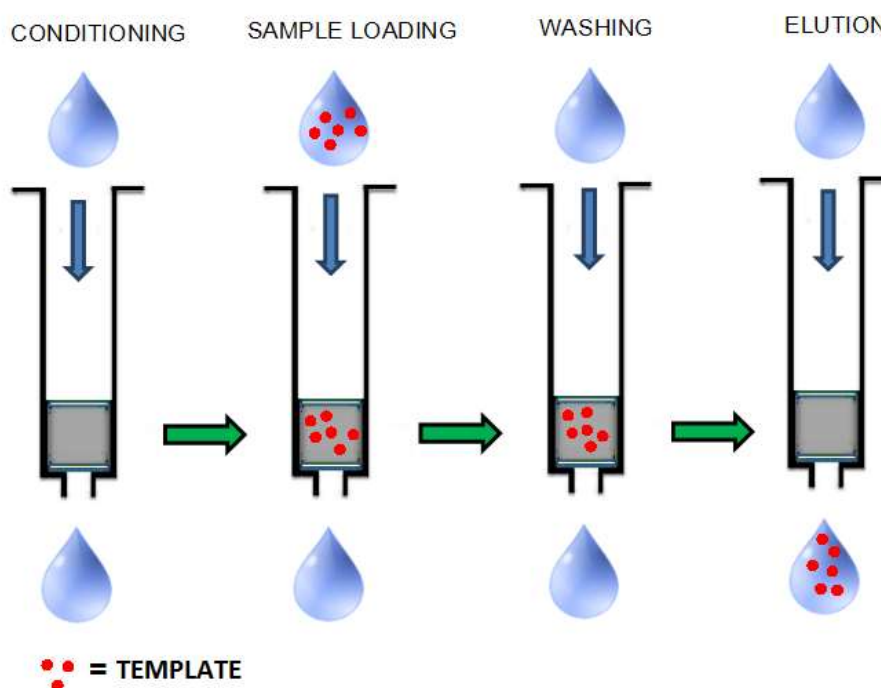


**Figure 16:** MISPE protocol scheme.

### 2.3.5 Job plot

A Job plot is a spectrophotometric experiment which gives information about the molar ratio of host and guest interacting in solution. In the Job plot, solutions of host and guest with different molar ratios are prepared and then analysed by  $^1\text{H}$  NMR in order to calculate the  $\Delta\delta$  of proton involved in the binding event.

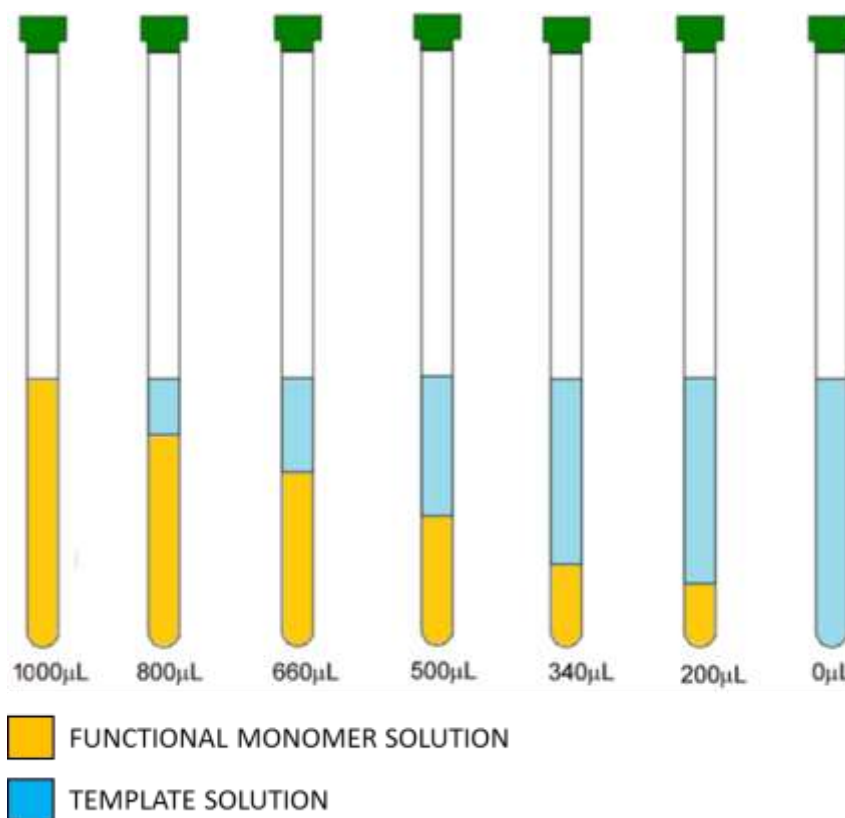


**Figure 17:** Job Plot samples preparation. Different molar ratios of monomer and template solution ( $x_r=1 - 0$ ) are prepared by mixing 1 mM solutions of the guest and the host in chloroform in NMR tubes.  $^1\text{H}$  NMR spectra are then obtained and the change in chemical shift of the monomer protons involved in the interaction with the template determined.

In general, 1 or 5 mM solution of host and guest were prepared in deuterated chloroform ( $\text{CDCl}_3$ ). Then 7 different samples with an  $x_r$  of 1 to 0 were prepared by mixing the solutions of monomer and guest. A chemical shift ( $\delta$ ) of the amido proton in the functional monomers was determined. The product  $x_r \cdot \Delta\delta$  is then plotted against the molar ratio to obtain a curve.

$$x_r = \frac{x_{host}}{x_{guest}}$$

where  $x_r$  is the molar ratio between of host and guest. When the maximum value of  $x_r \cdot \Delta\delta$  is at a molar ratio of 0.5, we are in the presence of a 1:1 binding event.

### 2.3.6 <sup>1</sup>H NMR Titrations

<sup>1</sup>H NMR titration<sup>97</sup> is a well-known technique applied to determine the association constant between two interacting species. <sup>1</sup>H NMR titration studies were performed in order to determine the binding constant ( $K_a$ ) between the novel functional monomers and the templates and other species.

All the NMR titrations were performed in CDCl<sub>3</sub> or CD<sub>3</sub>CN at 25°C. To a 0.1 or 1 mM monomer solution an increasing amount of guest was added. The interaction between the host and the guest induces a shift in the host and guest protons involved in the binding event. We have followed the  $\Delta\delta$  of the proton in the monomer amido functionality, which is then plotted against the concentration of free guest and the curve produced non-linearly fitted to the 1:1 binding isotherm, which is described by equation 1, using *OriginPro 8.5.1*.

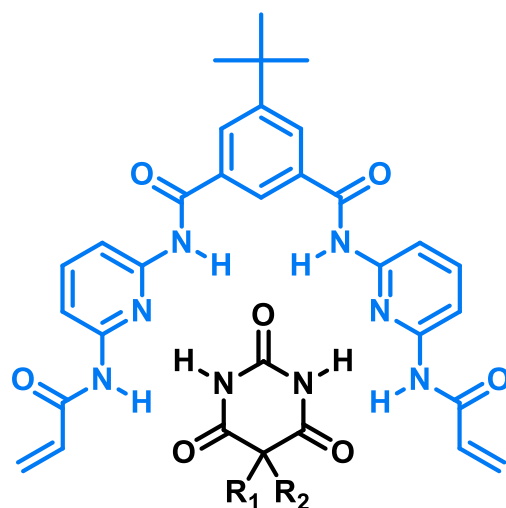
$$\Delta\delta = \frac{K_a [Guest]_{free}}{1 + K_a [Guest]_{free}} \cdot \Delta\delta_{max}$$

**Equation 3:** Langmuir equation for <sup>1</sup>H NMR titration studies.

In *equation 3*,  $K_a$  (M<sup>-1</sup>) refers to the binding strength between the monomer and the template. The  $\Delta\delta_{max}$  is the maximum chemical shift calculated which refers to the plateau of the binding curve, when the monomer is totally complexed with the target. During the titration, it is not always possible to reach saturation (plateau) and this is correlated to the strength of the host-guest interaction. The stronger the interaction, saturation is observed at lower guest concentrations.

# CHAPTER 3

## *MOLECULARLY IMPRINTED POLYMER SELECTIVE TOWARDS BARBITURATES*



## 3.1 INTRODUCTION

### 3.1.1 Barbiturates: discovery & decline

Barbiturates are a class of drugs with hypnotic, sedative and anxiolytic effects. They were discovered at the beginning of the 20<sup>th</sup> century, thanks to the previous synthesis of malonylurea by Adolf von Baeyer in 1864. After that, more than 2500 barbiturates were synthesised, although only around 50 were employed clinically. After their clinical introduction in 1904 and their widespread use worldwide due to their positive effect in the cure of epilepsy in reducing the strength and the frequency of seizures, and their use as sedative, hypnotic and anaesthetic drugs, their decline started in the 1960s due to the acceptance that they led to dependency and the increased number of death linked to their use. While their use in medicine has largely been supplanted by benzodiazepines, which have a lower potential for lethal overdose, barbiturates are still used in the treatment of insomnia, epilepsy and as an inducer of general anaesthesia. In Table 7 are shown those barbiturates that are still in clinical use.

**Table 7:** *Barbiturates currently employed and their therapeutic application.*<sup>98</sup>

Barbiturate	Routes of administration	Therapeutic uses
Amobarbital	Oral, IM, IV	Insomnia Preoperative sedation Emergency management of seizures
Aprobarbital	Oral	Insomnia
Butobarbital	Oral	Insomnia Preoperative sedation
Mephobarbital	Oral	Epilepsy Daytime sedation
Methohexital	IV	Induction/maintenance of anesthesia
Pentobarbital	Oral, rectal, IM, IV	Insomnia Preoperative sedation Emergency management of seizures
Phenobarbital	Oral, IM, IV	Epilepsy Status epilepticus Daytime sedation
Primidone	Oral	Epilepsy
Secobarbital	Oral, rectal, IM, IV	Insomnia Preoperative sedation Emergency management of seizures
Thiopental	Rectal, IV	Induction/maintenance of anesthesia Preoperative sedation Emergency management of seizures

Adapted from Charney et al (2001).  
Abbreviations: IM, intramuscular; IV, intravenous.

### 3.1.2 Barbiturate abuse, dependence and death

The dependence caused by barbiturates was described since the beginning in medical literature from the time that they were first used, but no evidence was available until the 1950s. Barbiturates can give real withdrawal syndrome if consumed in doses 4-6 times higher than the recommended one. Their abuse can then lead to death: patients become tolerant to the effect, hence they consume higher dosage of the drug which has a respiratory depressant effect which can cause death.<sup>99</sup>

In the 1950-60s the number of deaths caused by barbiturate misuse, either accidental or suicidal, increased enormously (Figure 18) causing the regulation of this class of drugs through prescription and the eventual decline in their use.

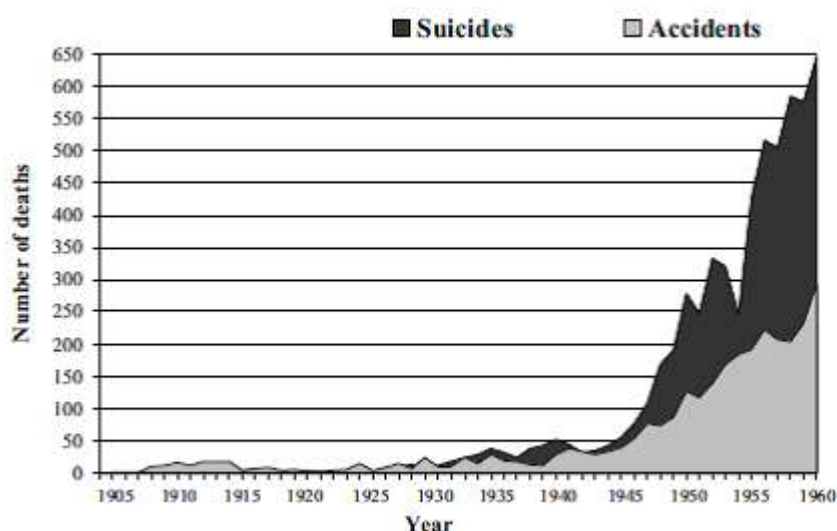


**Figure 18:** Deaths from overdose of barbiturates in England and Wales during the period 1905-1960 (Registrar-General's Statistical Review for England and Wales).<sup>98</sup>

Some addicts use barbiturates in combination with other drugs of abuse or to alleviate the adverse or withdrawal effects of illicit drug abuse. Abusers can develop a tolerance to these drugs up to a daily dose of 2000-2500 mg, but few people can take more than this quantity, which can cause a fatal overdose. The overdose can be caused on purpose by people attempting suicide or by accident: due to the



hypnotic and sedative effect of this drug, some people forget that have they already taken their daily dose, causing the daily intake to become double or more.<sup>99</sup>

### 3.1.3 Recognition of barbiturates using MIP technology

Barbiturate abuse is a common issue, especially amongst the teenage population, people suffering from depression and those with suicidal tendencies. Ready identification of barbiturates in urine can prove vital as overdose can cause coma or even death.

Molecularly imprinted polymers selective for barbiturates can have different applications: A) *Sensor* - the MIP can be the recognition part in sensors to promptly recognize small quantities of these drugs in urine or plasma; B) *MISPE* (molecularly imprinted solid-phase extraction) for sample enrichment before the evaluation of barbiturates in urine, especially if we consider that abused barbiturates often appear in complex mixtures with other illicit drugs and excipients, which can cause complication in the determination of barbiturates by HPLC and MS in forensic laboratories<sup>100</sup>. C) A *drug* capable of binding barbiturates in the bloodstream after an overdose, similar to the melittin-imprinted nanoparticles of Shea *et al.*<sup>46</sup>

### 3.1.4 Hamilton cleft

Hamilton developed a series of macrocyclic artificial receptors for barbiturates<sup>28, 101</sup> (Figure 19): the hydrogen bonding core of barbiturate was complexed by two 2,6-diaminopyridine units linked through two different spacers. He used an isophthaloyl group as one of the spacers to provide the necessary organization and rigidity to form the hexadentate binding site which will allow the host-guest complexation in solution. As a second spacer a diphenylmethane derivative was tested, in order to have also the interaction of the 5,5-ethyl groups of barbital and enhance the strength of host-guest interaction. He successfully managed to bind this class of drugs with such receptors with a  $10^5$ - $10^6$  M<sup>-1</sup> affinity (in chloroform).

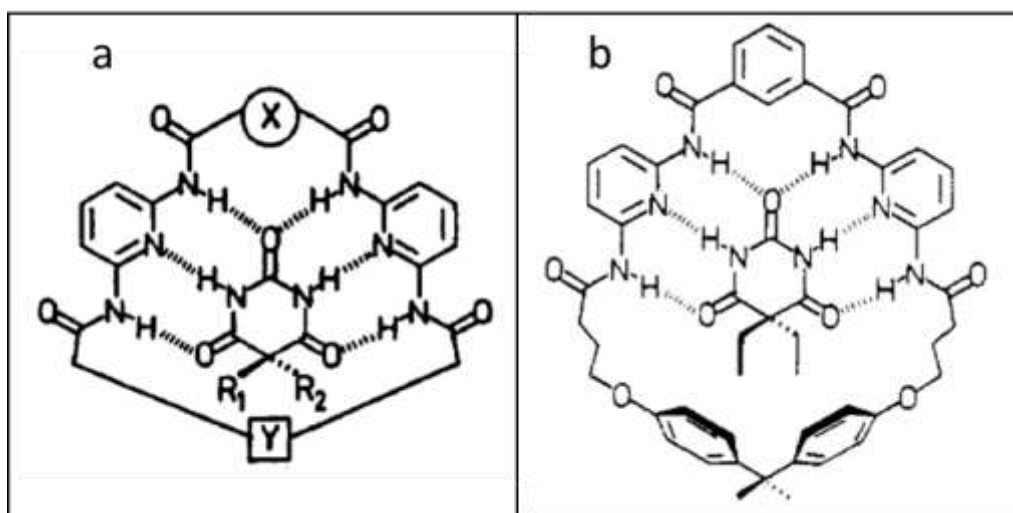


**Figure 19:** Synthetic receptors with strong selectivity for barbiturates. The receptor design is based on two 2,6-diaminopyridine groups linked through an isophthalic acid spacer. a) Schematic of a barbiturate binding site<sup>28</sup>. b) Hamilton cleft example<sup>101</sup>.

Toshifumi Takeuchi<sup>27</sup> used this idea to develop a reasonably simple functional monomer, a 2,6-bis(acrylamido)pyridine (BAAPy), to be used for the binding of nucleotide bases and barbiturates in particular. Takeuchi first compared two different MIP protocols using either methacrylic acid (MAA) or BAAPy, respectively, as functional monomers for the recognition of nucleobase-like compounds, such as uracil, demonstrating the superior capacity factors of polymers prepared with the novel functional monomer. BAAPy was then used for the stoichiometric imprinting of alloxan using EDGMA as the cross-linker. The alloxan-MIP showed recognition behaviour for barbiturates, as they are structurally similar to the template. Later, more studies were performed by the Takeuchi group for the imprinting of barbiturates.<sup>102</sup> BAAPy is a great monomer, but it is a simplification Hamilton's clefts and NMR titration studies of our monomers have shown binding constants of almost  $10^5 \text{ M}^{-1}$  for this type of cleft, while BAAPy can reach only values of  $10^2 - 10^3 \text{ M}^{-1}$ , making the Hamilton cleft far superior.

The Hamilton cleft creates a strong complex between template and functional monomer in the pre-polymerisation mixture that can potentially lead to the incorporation of all monomer molecules inside the imprinted binding cavities, creating a more specific MIP. In our work we designed and synthesized five

Hamilton-inspired functional monomers (monomers 1-5, Figure 21). The general structure of two 2,6-diaminopyridine groups linked through a spacer) was kept from the original Hamilton's cleft, as we needed the rigidity and organisation of the monomer to be able to share six H-bonds with the host molecule. However a second spacer wasn't necessary for our design, and two polymerisable functionalities were needed to allow the incorporation of the monomer in the polymeric matrix, hence the formation of binding cavities in the MIP.

A general Hamilton cleft, monomer A, was synthesized previously by A. J. Hall. Unfortunately it was never used due to its poor solubility in organic solvents, such as chloroform and acetonitrile. Only a  $^1\text{H}$  NMR titration was performed on the monomer, showing that it had good potential in molecular imprinting. In order to bypass the solubility issue, we have introduced functionality in position 5 of the spacer (e.g. alkoxy groups and tert-butyl group). The 5- tert-butyl-benzene was chosen as spacer in monomer 1 (Figure 21) as the tert-butyl group can increase the solubility of the monomer in organic solvents. Also monomer 1 can be synthesised in two synthetic steps using 5-tert-butylisophthalic acid as starting material, which is inexpensive and commercially available. 5-(3-methylbutoxy)-benzene (monomer 3) and 5-(2-ethylhexyloxy)-benzene (monomer 4) were also used as spacer in order to improve the cleft's solubility. The different size of the alkyl chain can affect the solubility of the monomer in a polar solvent and the electron-donating property of the alkoxy group can have a negative/positive effect on the H-bond strength of donor and acceptor by decreasing the acidity or increasing the basicity respectively. 4-(3-methyl-butoxy)-pyridine (monomer 2) and 4-piperidine-pyridine (monomer 5) were used as spacer in order to have both rigidity of the cleft and a pre-organisation of the latter in solution previous to the interaction with the guest. The pyridine nitrogen can create two H-bonds interaction with the cleft's arms which pre-organise the monomer in the right tri-dimensional geometry which can fit the ligand (Figure 20). The alkoxy functionality has also electron-donating properties, as mentioned before, which can increase the pyridine N basicity, enhancing its H-bond acceptor strength. Although the pyridine ring has a positive effect in pre-organising the monomer in the space, it has also a negative effect in repulsing the carbonyl oxygen of barbiturates due to primary electrostatic negative interaction (Figure 20).

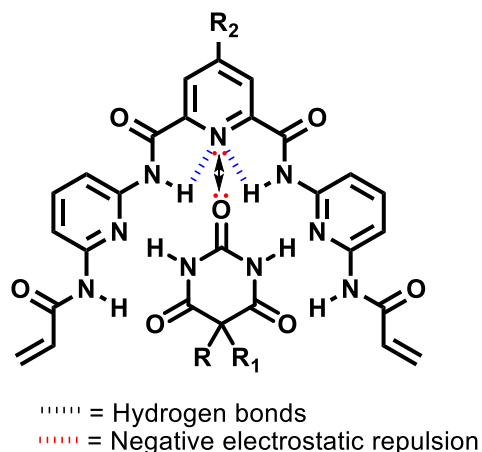


**Figure 20:** Intramolecular pre-organization of monomer 2 in a rigid cleft due to H-bonds interactions between the Nitrogen of the pyridine and the NH of the amido groups (blue dots). Host-guest repulsion (black arrow).

Unfortunately none of the monomers have great solubility in organic solvents, but the presence of the template in the pre-polymerisation mixture leads to creation of a soluble complex. The novel clefts binding constants were then calculated by means of  $^1\text{H}$  NMR titration studies in chloroform and the binding constant calculated were of the order of  $1,000 - 90,000 \text{ M}^{-1}$ .

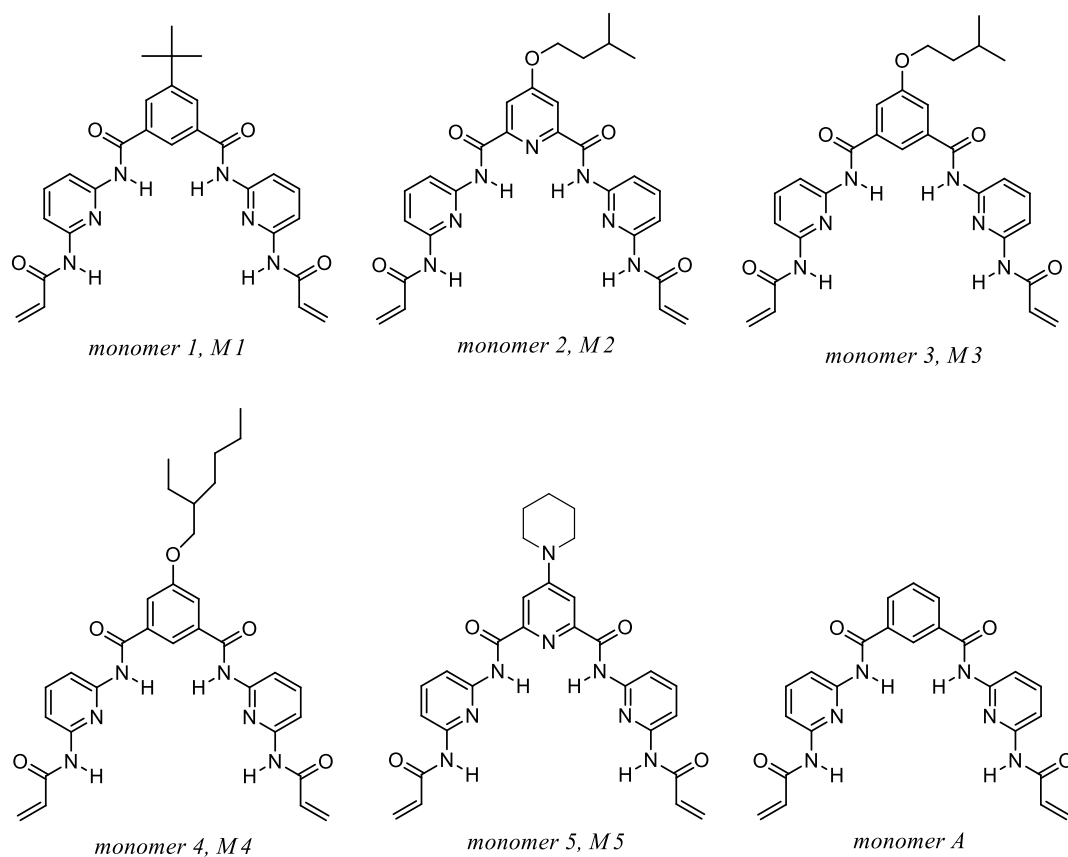


**Figure 21:** Hamilton-based functional monomers structures.

M1 was used for the imprinting of barbiturates due to its favourable characteristics: it may be prepared by a two-step reaction, from inexpensive starting materials, it has reasonable solubility in chloroform in the presence of the template and complexes barbiturates with a binding constant of almost  $10^5 \text{ M}^{-1}$ .

In this chapter, we will report on the synthesis and characterisation of these novel clefts as functional monomers for the imprinting of barbiturates and on the preparation of an anti-pentobarbital MIP showing strong selectivity and affinity towards the template and analogues.

### 3.2 EXPERIMENTAL

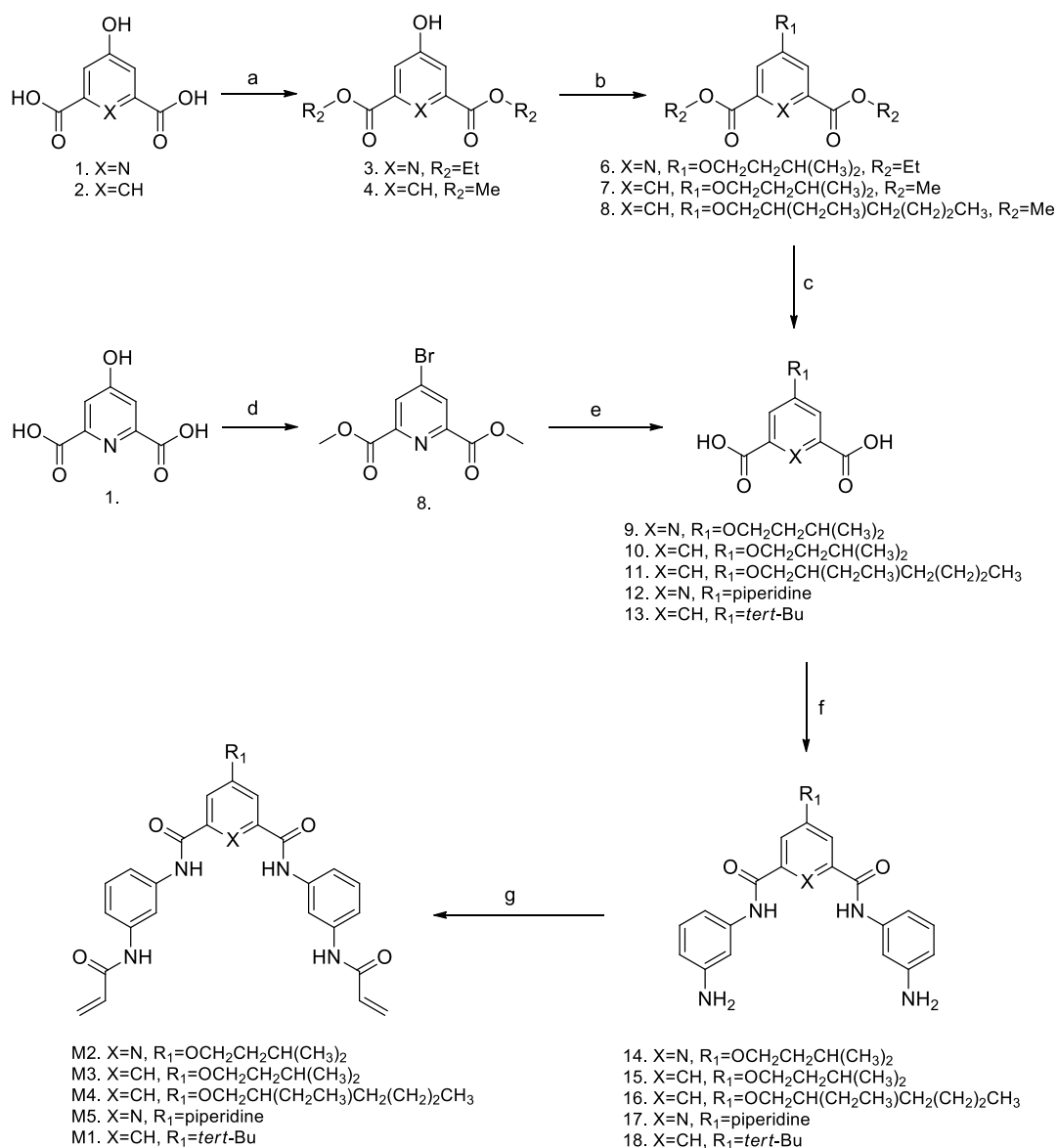


**Figure 22:** Scheme of monomers 1-5 synthesis. **a.** H<sub>2</sub>SO<sub>4</sub>, MeOH or EtOH, reflux; **b.** K<sub>2</sub>CO<sub>3</sub>, CH<sub>3</sub>CN, Br-R<sub>1</sub>, reflux, 22hrs; **c.** NaOH 1N or LiOH·H<sub>2</sub>O; **d.** i) PCl<sub>5</sub>; ii) MeOH; **e.** i) 50% aqueous solution piperidine, 175°C, 24hrs; ii) NaOH aqueous solution; **f.** i) SOCl<sub>2</sub>, 100°C, 4h; ii) THF, 2,6-diaminopyridine, 0°C →RT, overnight; **g.** THF or DCM, TEA, CH<sub>2</sub>=CHCOCl, N<sub>2</sub>, 0°C →RT, overnight.

### 3.2.1 Synthesis of Monomer 1

*1,3-bis[[6-amino-2-yl)amido]carbonyl]5- tert-butyl-benzene (18)*. 5-tert-butylisophthalic acid (**13**, 3 g, 0.0135 mol, 1eq, FW=222.24) was refluxed with 20 mL of SOCl<sub>2</sub> for 4 h. The solvent was then evaporated to obtain the corresponding diacid chloride, which was dissolved in 20 mL of dry THF and added dropwise to a solution of 2,6-diaminopyridine (14.73 g, 0.135 mol, 10 eq, FW=109.13) and triethylamine (TEA) (3.76 mL, 2.73 g, 0.027 mol, FW= 101.19, d=0.726) in anhydrous THF (220 mL) at 0°C and under dinitrogen atmosphere. The reaction mixture was stirred at room temperature overnight. The next day the solvent was evaporated and the crude product washed with water. The sticky solid was filtered, dissolved in hot ethyl acetate and filtered again. The filtrate was evaporated to obtain a brown solid, which was then purified with a chromatographic column using silica gel as the stationary phase and ethyl acetate as the eluent. The first fraction coming out of the column was the desired intermediate (light brown solid, 88%). **<sup>1</sup>H NMR (400 MHz, DMSO-*d*<sub>6</sub>)**: δ 1.372 (s, 9H, tert-butyl-CH<sub>3</sub>), 5.796 (s, 4H, NH<sub>2</sub>), 6.29 (dd, <sup>2</sup>J = 0.8 Hz, <sup>3</sup>J = 8 Hz, 2H, Py-CH<sub>2</sub>[H-5]), 7.41 (dd, <sup>2</sup>J = 0.8 Hz, <sup>3</sup>J = 8 Hz, 2H, Py-CH<sub>2</sub>[H-3]), 7.45 (t, <sup>3</sup>J = 7.6 Hz, 2H, Py-CH<sub>2</sub>[H-4]), 8.11 (d, <sup>3</sup>J = 1.2 Hz, 2H, Ph-CH-4 and 6), 8.33 (s, 1H, Ph-CH-2), 10.292 (s, 2H, NH) ppm. **<sup>13</sup>C NMR (400 MHz, DMSO-*d*<sub>6</sub>)**: δ 31.507 (tert-butyl-CH<sub>3</sub>), 35.384 (tert-butyl-C), 102.401 (Py-CH<sub>2</sub>[C-5]), 104.642 and 139.565 (Py-CH<sub>2</sub>[C-3 and C-4]), 124.86 (Ph-C-2), 128.576 (Ph-C-4 and 6), 134.694, 150.982, 151.945, 159.156, and 165.717 ppm. **MS [M-H<sup>+</sup>]**: 403.49. **HRMS (ESI-TOF) m/z**: [M+H]<sup>+</sup> Calcd for C<sub>22</sub>H<sub>25</sub>N<sub>6</sub>O<sub>2</sub>H 405.46; Found 405.203. **IR**: 1526.6, 1614.9, 1697.4, 2965.1, 3317.4, 3450.2 cm<sup>-1</sup>. **M.p.**: 99-104 °C.

*1,3-bis[[6-bisacrylamid-2-yl)amido]carbonyl]5- tert-butyl-benzene (monomer 1, M1)*. To a solution of **18** (3.5g, 8.65 mmol, FW=404.46, 1 eq) and triethylamine (3.61 mL, 2.62 g, 25.95 mmol, FW= 101.19, d=0.726, 3 eq) in anhydrous THF (180 mL), 1.75 mL of acryloyl chloride (1.95 g, 21.62 mmol, FW=90.51, d=1.114, 2.5 eq) in 20 mL of THF was added slowly at 0°C and under dinitrogen atmosphere. The reaction mixture was stirred at room temperature overnight. The next day the precipitate was filtered off and the solvent evaporated. The residue was washed with water and a saturated solution of sodium bicarbonate (NaHCO<sub>3</sub>). The solid was then sonicated in 100 mL of DCM. **Monomer 1** was obtained as a white solid

in a 52% yield (2.3g). **<sup>1</sup>H NMR (400 MHz, DMSO-*d*<sub>6</sub>)**: δ 1.41 (s, 9H, tert-butyl-CH<sub>3</sub>), 5.80 (dd, <sup>2</sup>J = 2 Hz, <sup>3</sup>J=12 Hz, 2H, CH<sub>cis</sub>=), 6.33 (dd, <sup>2</sup>J = 1.6 Hz, <sup>3</sup>J=20 Hz, 2H, CH<sub>trans</sub>=), 6.67 (dd, <sup>3</sup>J<sub>cis</sub>= 10.4 Hz, <sup>3</sup>J<sub>trans</sub>= 16. Hz, 2H, -CH=), 7.87 (m, <sup>3</sup>J =8 Hz, 4H, Py-CH<sub>2</sub>[H-3 and H-4]), 7.95(m, <sup>3</sup>J =4 Hz, 2H, Py-CH<sub>2</sub>[H-5]), 8.21 (d, <sup>3</sup>J =1.6 Hz, 2H, Ph-CH-4 and 6), 8.382 (s, 1H, Ph-CH-2), 10.458 (s, 2H, NH-C<sup>6</sup>), 10.593 (s, 2H, NH-C<sup>2</sup>) ppm. **<sup>13</sup>C NMR (400 MHz, DMSO-*d*<sub>6</sub>)**: δ 31.50 (tert-butyl-CH<sub>3</sub>), 35.510 (tert-butyl-C), 110.778 (Py-CH<sub>2</sub>[C-5]), 111.586 and 140.707 (Py-CH<sub>2</sub>[C-3 and C-4]), 125.747 (Ph-C-2), 128.439 (CH<sub>2</sub>=), 128.67 (Ph-C-4 and 6), 132.089 (-CH=), 134.655, 150.897, 151.035, 152.060, 164.298 and 166.076 ppm. **MS** [M+H<sup>+</sup>]: 513. **HRMS** (ESI-TOF) m/z: [M+H]<sup>+</sup> Calcd for C<sub>28</sub>H<sub>29</sub>N<sub>6</sub>O<sub>4</sub>H 513.56; Found 513.224. **IR**: 977.6, 1638.9, 1691.6, 2962, 3277.5 cm<sup>-1</sup>. **M.p.**: 223-229 °C.

### 3.2.2 Synthesis of Monomer 2

*Diethyl 4-hydroxy-2,6-pyridinedicarboxylate (3)*<sup>103</sup>. Chelidamic acid (**1**, 5 g, 27.3 mmol) was suspended in absolute ethanol (100 mL) and sulfuric acid (100 drops) was carefully added at room temperature with vigorous stirring. The yellow mixture was refluxed for 4 hours and then the solvent was evaporated. Water (100 mL) was then added to the residue and the mixture freeze-dried. The viscous residue was neutralized with a saturated solution of NaHCO<sub>3</sub> (75 mL) and the pH raised to 8. The aqueous solution was then extracted with DCM (1 ×200 mL + 3 × 100 mL). The organic phase was dried with MgSO<sub>4</sub>, filtered and then evaporated to give **3** as a white solid upon standing at room temperature (4.43g, 66.8%). **<sup>1</sup>H NMR** (400 MHz, DMSO-*d*<sub>6</sub>): δ 1.33 (t, <sup>3</sup>J =6.8Hz, 6H, -CH<sub>3</sub>) 4.34(q, <sup>3</sup>J =7.2Hz, 4H, -OCH<sub>2</sub>-), 7.56 (s, 2H, CH-Ar) ppm. **<sup>13</sup>C NMR** (400 MHz, DMSO-*d*<sub>6</sub>): δ 14.65 (-CH<sub>3</sub>), 61.96 (-CH<sub>2</sub>-), 115.77 (CH-Ar), 150.11 (-C-OH), 164.82 (C=O), 166.55 (C-Ar) ppm. **MS** [M+H<sup>+</sup>]: 240.2. **IR**: 1229, 1721, 2984 cm<sup>-1</sup>. **M.p.**: 121-126 °C.

*Diethyl 4-(3-methyl-butoxy)-2,6-pyridinedicarboxylate (6)*<sup>104</sup>. Diethyl 4-hydroxy-2,6-pyridinedicarboxylate (**3**, 10 g, 0.042 mol) was solubilized in 200 mL of acetonitrile at room temperature. 1-Bromo-2-methylbutane (0.060 mol, d=1.26, FW=151.04, 9.06 g, 7.19 mL) and potassium carbonate (K<sub>2</sub>CO<sub>3</sub>) (FW=138.206, 10 g, 0.072 mol) were then added and the solution refluxed for 22h. The reaction mixture was left to cool, then filtered to remove K<sub>2</sub>CO<sub>3</sub>. The solvent was evaporated



to obtain a dark yellow oil. The product was then purified by chromatographic column using diethyl ether as eluent and silica gel as stationary phase. A pale yellow oil was obtained (12.32g, 94.8%). **<sup>1</sup>H NMR** (400MHz, CDCl<sub>3</sub>): δ 0.988 (d, <sup>3</sup>J =6.4 Hz, 6H, -CH-CH<sub>3</sub>), 1.46 (t, <sup>3</sup>J =6.8 Hz, 6H, -CH<sub>2</sub>-CH<sub>3</sub>), 1.74 (q, <sup>3</sup>J =6.4 Hz, 2H, -O-CH<sub>2</sub>-CH<sub>2</sub>-CH-), 1.85 (m, <sup>3</sup>J =6.8 Hz, 1H, -CH-), 4.18 (t, <sup>3</sup>J=6.4 Hz, 2H, -O-CH<sub>2</sub>-CH<sub>2</sub>-CH-), 4.48 (q, <sup>3</sup>J =6.8 Hz, 4H, -CH<sub>2</sub>-CH<sub>3</sub>), 7.68 (s, 2H, CH-Ar). **<sup>13</sup>C NMR** (400MHz, CDCl<sub>3</sub>): δ 14.22 (-CH<sub>2</sub>-CH<sub>3</sub>), 22.49 (-CH-CH<sub>3</sub>), 24.96 (-CH-), 37.41 (-O-CH<sub>2</sub>-CH<sub>2</sub>-CH-), 62.35 (-CH<sub>2</sub>-CH<sub>3</sub>), 67.47 (-O-CH<sub>2</sub>-CH<sub>2</sub>-CH-), 114.33 (CH-Ar), 150.15 (C-O), 164.80 (C=O), 167.02 (C=N). **MS** [M+H<sup>+</sup>]: 310.3(relative abundance=100%), 352.4 (35%), 394.4 (2%). **HRMS** (ESI-TOF) m/z: [M+H]<sup>+</sup> Calcd for C<sub>16</sub>H<sub>23</sub>NO<sub>5</sub>H 310.36; Found 310.1661. **IR**: 739, 1024, 1101, 1224, 1371, 1446, 1716, 2868, 2958 cm<sup>-1</sup>.

*2,6-bis[[6-amino-2-yl)amido]carbonyl]4-3-methyl-butoxy-pyridine* (**14**): i) Compound **6** (8 g, FW=309.36, 0.0258 mol) was stirred at room temperature for 2 days in 200 mL of 1N aqueous NaOH. 4M aqueous HCl was then added until the pH was equal to 2 and a white precipitate formed. The diacid (**10**) was filtered and washed with water (4.44g, 68%). ii) The diacid (**9**, 3 g, 0.0118 mol, 1 eq, FW=253.25) was refluxed with 20 mL of SOCl<sub>2</sub> for 4h. The solvent was then evaporated to obtain the correspondent diacid chloride. iii) Without any further purification, the diacid chloride was dissolved in 50 mL of dry THF and added dropwise to a solution of 2,6-diaminopyridine (12.92 g, 0.118 mol, 10 eq, FW=109.13) and TEA (3.29 mL, 2.38 g, 0.0236 mol, FW= 101.19, d=0.726) in anhydrous THF (200 mL) at 0°C and under a dinitrogen atmosphere. The reaction mixture was stirred at room temperature overnight. The next day, the precipitate was filtered off and the solvent was evaporated. The dark brown crude material was then washed with water and a saturated aqueous solution of NaHCO<sub>3</sub>. The solid was filtered and sonicated in 300 mL of MeOH and filtered to obtain pure monomer 2 intermediate (**14**) as a brownish light solid. From the methanol solution more **14** to crystallized over time (total yield = 3.44 g, 67%). **<sup>1</sup>H NMR** (400 MHz, DMSO-*d*<sub>6</sub>): δ 0.948 (d, <sup>3</sup>J=6 Hz, 6H, -CH-CH<sub>3</sub>), 1.69 (q, <sup>3</sup>J =6.8 Hz, 2H, -O-CH<sub>2</sub>-CH<sub>2</sub>-CH-), 1.80 (m, <sup>3</sup>J =6.8 Hz, 1H, -CH-), 4.29 (t, <sup>3</sup>J =6.4 Hz, 2H, -O-CH<sub>2</sub>-CH<sub>2</sub>-CH-), 5.926 (s, 4H, NH<sub>2</sub>), 6.30 (d, <sup>3</sup>J =8 Hz, 2H, Py-CH<sub>2</sub>[H-5]), 7.42 (d, <sup>3</sup>J =8 Hz, 2H, Py-CH<sub>2</sub>[H-3] ), 7.48 (t, <sup>3</sup>J =7.6 Hz, 2H, Py-CH<sub>2</sub>[H-4]), 7.786 (s, 2H, CH-Ar),

10.937 (s, 2H, NH) ppm.  $^{13}\text{C}$  NMR (400 MHz, DMSO- $d_6$ ):  $\delta$  22.956 (-CH-CH<sub>3</sub>), 25.126 (-CH-), 37.467 (-O-CH<sub>2</sub>-CH<sub>2</sub>-CH-), 67.851 (-O-CH<sub>2</sub>-CH<sub>2</sub>-CH-), 102.576 (Py-C3), 104.981 (Py-C5), 111.845 (CH-Ar), 139.667 (Py-C4), 150.105, 151.650, 159.268, 162.379 and 167.865 ppm. MS [M+H<sup>+</sup>]: 435.5 HRMS (ESI-TOF) m/z: [M+H]<sup>+</sup> Calcd for C<sub>22</sub>H<sub>25</sub>N<sub>7</sub>O<sub>3</sub>H 436.48; Found 436.2097. IR: 794, 1051, 1298, 1454, 1525, 1618, 1685, 2887, 3267, 3354, 3477 cm<sup>-1</sup>. M.p.: 289-290 °C.

*2,6-bis[[6-bisacrylamid-2-yl]amido]carbonyl]4-3-methyl-butoxy-pyridine* (monomer 2, **M2**). To a solution of **14** (3 g, 6.9 mmol, FW=435.48, 1 eq.) and triethylamine (2.88 mL, 2.09 g, 0.02 mol, FW= 101.19, d=0.726, 3 eq) in anhydrous THF (180 mL), 1.40 mL of acryloyl chloride (1.56 g, 0.017 mol, FW=90.51, d=1.114, 2.5 eq) in 20 mL of THF was added slowly at 0°C and under a dinitrogen atmosphere. The reaction mixture was stirred at room temperature overnight. The next day the precipitate was filtered off and the solvent evaporated. To the residue (yellow-orange) was added a saturated aqueous solution of NaHCO<sub>3</sub> and the precipitate was filtered and washed with water. The yellow solid was sonicated with DCM and the solid filtered. The monomer was obtained as a white solid (910 mg, 24%).  $^1\text{H}$  NMR (400 MHz, DMSO- $d_6$  and CDCl<sub>3</sub>):  $\delta$  0.97 (d,  $^3\text{J}$ =6.8 Hz, 6H, -CH-CH<sub>3</sub>), 1.72 (q,  $^3\text{J}$ =6.8 Hz, 2H, -O-CH<sub>2</sub>-CH<sub>2</sub>-CH-), 1.83 (m,  $^3\text{J}$ =6.4 Hz, 1H, -CH-), 4.31 (t,  $^3\text{J}$ =6.4 Hz, 2H, -O-CH<sub>2</sub>-CH<sub>2</sub>-CH-), 5.80 (dd,  $^2\text{J}$  = 2 Hz,  $^3\text{J}$ =8Hz, 2H, CH<sub>cis</sub>=), 6.36 (dd,  $^2\text{J}$  = 2 Hz,  $^3\text{J}$ =16 Hz, 2H, CH<sub>trans</sub>=), 6.61 (dd,  $^3\text{J}_{\text{cis}}$  = 10 Hz,  $^3\text{J}_{\text{trans}}$  = 16 Hz, 2H, -CH=), 7.856 (s, 2H, CH-Ar), 7.90 (d, 2H, Py-CH<sub>2</sub>[H-3]), 7.91 (s, 2H, Py-CH<sub>2</sub>[H-4]), 8.03 (m,  $^3\text{J}$  = 4 Hz, 2H, Py-CH<sub>2</sub>[H-5]), 10.388 (s, 2H, NH-C<sup>6</sup>), 10.959 (s, 2H, NH-C<sup>2</sup>) ppm.  $^{13}\text{C}$  NMR (400 MHz, DMSO- $d_6$  and CDCl<sub>3</sub>):  $\delta$  22.395 (-CH-CH<sub>3</sub>), 24.587 (-CH-), 36.964 (-O-CH<sub>2</sub>-CH<sub>2</sub>-CH-), 67.448 (-O-CH<sub>2</sub>-CH<sub>2</sub>-CH-), 110.319 (Py-CH<sub>2</sub>[C-5]), 110.480 and 140.459 (Py-CH<sub>2</sub>[C-3 and C-4]), 111.576 (CH-Ar), 127.786 (CH<sub>2</sub>=), 131.423 (-CH=), 149.370, 150.593, 150.661, 161.793, 163.677 and 167.651 ppm. MS [M+H<sup>+</sup>]: 543. HRMS (ESI-TOF) m/z: [M+H]<sup>+</sup> Calcd for C<sub>28</sub>H<sub>29</sub>N<sub>7</sub>O<sub>5</sub>H 544.57; Found 544.2308. IR: 796, 991, 1440, 1504, 1678, 2330, 2362, 2958, 3387, 3388 cm<sup>-1</sup>. M.p.: 220-224°C.

### 3.2.3 Synthesis of Monomer 3

*Dimethyl 5-hydroxyisophthalate*<sup>105</sup> (**4**) [from a modified procedure<sup>105</sup>]. 5-hydroxyisophthalic acid (**2**, 9.11 g, 50 mmol) was dissolved in methanol (100 mL) and concentrated H<sub>2</sub>SO<sub>4</sub> (5.90 mL, 11 mmol) was added. The reaction mixture was refluxed for 21h and then concentrated *in vacuo*. The crude product was obtained as a white solid, which was dissolved in 125 mL of ethyl acetate. The organic layer was extracted with a saturated aqueous solution of NaHCO<sub>3</sub> (2 x 75 mL) and brine (1 x 75 mL). The combined aqueous layers were then back-extracted with EtOAc (2 x 70 mL). The combined organic layers were dried over MgSO<sub>4</sub>, filtered and evaporated to obtain a white solid which was dried overnight at 50°C under vacuum (9g, 86%). <sup>1</sup>H NMR (400 MHz, DMSO-*d*<sub>6</sub>): δ 3.871 (s, 6H, -OCH<sub>3</sub>), 7.571 (t, <sup>3</sup>J = 1.6Hz, 2H, CH(4-6)-Ar), 7.946 (t, <sup>3</sup>J = 1.6Hz, 1H, CH(2)-Ar), 10.326 (s, 1H, Ar-OH) ppm. <sup>13</sup>C NMR (400 MHz, DMSO-*d*<sub>6</sub>): δ 52.987 (O-CH<sub>3</sub>), 120.60 (Ph-C-2), 120.83 (Ph-C-4 and 6), 131.956 (Ph-C-5), 158.476 (C=O), 165.962 (Ph-C-1 and 3) ppm. MS [M+H<sup>+</sup>]: 210.1. IR: 755, 991, 1096, 1243, 1428, 1597, 1700, 1794, 2963, 3357 cm<sup>-1</sup>. M.p. = 168-172 °C

*Dimethyl 5-(3-methylbutoxy) - isophthalate*<sup>105</sup> (**7**) [from a modified procedure<sup>105</sup>]. Dimethyl 5-hydroxyisophthalate (**4**, 8 g, 0.038 mol, FW= 210.18), 1-bromo-3-methylbutane (6.35 mL, 0.053 mol, 8 g, FW=151.04, d=1.26) and potassium carbonate (8.9 g, 0.0644 mol, FW= 138.206) were refluxed in CH<sub>3</sub>CN (100 mL) for 22h. The next day, the K<sub>2</sub>CO<sub>3</sub> was filtered off and the solvent evaporated. The yellow oil was purified by flash chromatography using diethyl ether as eluent and silica gel as stationary phase. **7** was obtained as a light yellow oil in quantitative yield. <sup>1</sup>H NMR (500MHz, CDCl<sub>3</sub>): δ 0.944 (d, <sup>3</sup>J = 6.5 Hz, 6H, -CH-CH<sub>3</sub>), 1.709 (q, <sup>3</sup>J = 7 Hz, 2H, -O-CH<sub>2</sub>-CH<sub>2</sub>-CH-), 1.859 (m, <sup>3</sup>J = 7 Hz, 1H, -CH-), 3.942 (s, 6H, -O-CH<sub>3</sub>), 4.06 (t, <sup>3</sup>J = 7 Hz, 2H, -O-CH<sub>2</sub>-CH<sub>2</sub>-CH-), 7.741 (d, <sup>3</sup>J = 1.5 Hz, 2H, CH(4,6)-Ar), 8.259 (t, <sup>3</sup>J = 1.5 Hz, 1H, CH(2)-Ar) ppm. <sup>13</sup>C NMR (500MHz, CDCl<sub>3</sub>): δ 22.62 (-CH(CH<sub>3</sub>)<sub>2</sub>), 25.09 (-CH-), 37.86 (-O-CH<sub>2</sub>-CH<sub>2</sub>-CH-), 52.44 (-O-CH<sub>3</sub>), 67.08 (-O-CH<sub>2</sub>-CH<sub>2</sub>-CH-), 119.88 (Ph-C-2), 122.81 (Ph-C-4 and 6), 131.76 (Ph-C-5), 159.29 (C=O), 166.28 (Ph-C-1 and 3) ppm. MS [M+CH<sub>3</sub>CN+H<sup>+</sup>] = 322. HRMS (ESI-TOF) m/z: [M+H]<sup>+</sup> Calcd for C<sub>15</sub>H<sub>20</sub>O<sub>5</sub>H 281.32; Found 281.1390. IR: 755, 9063, 1003, 1284, 1433, 1594, 1722, 2342, 2954 cm<sup>-1</sup>.

5-(3-methylbutoxy) – isophthalic acid (**10**). Dimethyl 5-(3-methylbutoxy) – isophthalate (**7**, MC-2, 10.2 g, 0.036 mol, FW=280.32) was stirred in 200 mL of 1N aqueous NaOH for 72 h at 60 °C. 4M aqueous HCl was then added until precipitation of a white solid occurred (pH=2-4). The solid was filtered and washed with water, then dried under vacuum for 48 h at 50°C (8.94g, 98%). **<sup>1</sup>H NMR** (400 MHz, DMSO-*d*<sub>6</sub>): δ 0.94 (d, <sup>3</sup>J =6.8 Hz, 6H, -CH-CH<sub>3</sub>), 1.65 (q, <sup>3</sup>J =6.8 Hz, 2H, -O-CH<sub>2</sub>-CH<sub>2</sub>-CH-), 1.80 (m, <sup>3</sup>J =6.8 Hz, 1H, -CH-), 4.10 (t, <sup>3</sup>J =6.4 Hz, 2H, -O-CH<sub>2</sub>-CH<sub>2</sub>-CH-), 7.64 (d, <sup>3</sup>J =1.2 Hz, 2H, CH(4-6)-Ar), 8.07 (t, 1H, <sup>3</sup>J =2 Hz, CH(2)-Ar) ppm. **<sup>13</sup>C NMR** (400 MHz, DMSO-*d*<sub>6</sub>): δ 22.992 (-CH(CH<sub>3</sub>)<sub>2</sub>), 25.149 (-CH-), 37.821 (-O-CH<sub>2</sub>-CH<sub>2</sub>-CH-), 67.134 (-O-CH<sub>2</sub>-CH<sub>2</sub>-CH-), 119.549 (Ph-C-2), 122.682 (Ph-C-4 and 6), 133.251 (Ph-C-5), 159.332 (C=O), 167.020 (Ph-C-1 and 3) ppm. **MS** [M-H<sup>+</sup>+2Na<sup>+</sup>] = 297. **HRMS** (ESI-TOF) m/z: [M+H]<sup>+</sup> Calcd for C<sub>13</sub>H<sub>16</sub>O<sub>5</sub>H 253.26; Found 253.1076. **IR**: 691, 906, 1057, 1273, 1463, 1594, 1688, 2557, 2874, 2960 cm<sup>-1</sup>. **M.p.** = 257-266 °C

*1,3-bis[[6-amino-2-yl]amido]carbonyl] 5-(3-methylbutoxy)-benzene* (**15**). i) 5-(3-methylbutoxy) isophthalic acid (**10**, 3.5 g, 0.0138 mol, 1 eq, FW=253.26) was refluxed with 25 mL of SOCl<sub>2</sub> for 4h. The solvent was then evaporated to obtain the corresponding diacid chloride, which was used without further purification. ii) To a cooled (ice bath) solution of 2,6-diaminopyridine (15.08 g, 0.138 mol, FW=109.13, 10 eq) and TEA (3.85 mL, 2.8 g, 0.03 mol, FW= 101.19, d=0.726) in anhydrous THF (200 mL), the crude 5-(3-methylbutoxy) isophthalic acid dichloride dissolved in THF (10mL) was added slowly under a dinitrogen atmosphere. The reaction mixture was stirred at room temperature overnight. The next day the solvent was evaporated and water (100 mL) added to the crude product (a brown sticky solid). A precipitate was formed which was filtered and washed with a saturated aqueous solution of NaHCO<sub>3</sub>. To the crude product was added 100 mL of EtOAc and the pale brown precipitate (**15**) was filtered (3.63g, 60%). **<sup>1</sup>H NMR** (400 MHz, DMSO-*d*<sub>6</sub>): δ 0.959 (d, <sup>3</sup>J=14 Hz, 6H, -CH-CH<sub>3</sub>), 1.662 (q, <sup>3</sup>J =6.8 Hz, 2H, -O-CH<sub>2</sub>-CH<sub>2</sub>-CH-), 1.824 (m, <sup>3</sup>J =6.4 Hz, 1H, -CH-), 4.145 (t, <sup>3</sup>J =6.4 Hz, 2H, -O-CH<sub>2</sub>-CH<sub>2</sub>-CH-), 5.799 (s, 4H, NH<sub>2</sub>), 6.277 (d, <sup>3</sup>J =7.2 Hz, 2H, Py-CH<sub>2</sub>[H-5]), 7.38 (d, <sup>3</sup>J =7.2 Hz, 2H, Py-CH<sub>2</sub>[H-3]), 7.442 (t, <sup>3</sup>J =7.6 Hz, 2H, Py-CH<sub>2</sub>[H-4]), 7.613 (d, <sup>3</sup>J =1.2 Hz, 2H, CH(4-6)-Ar), 8.106 (s, 1H, CH(2)-Ar), 10.055 (s, 2H, NH) ppm. **<sup>13</sup>C NMR** (400 MHz, DMSO-*d*<sub>6</sub>): δ 22.034 (-CH-CH<sub>3</sub>), 25.200 (-

CH-), 37.902 (-O-CH<sub>2</sub>-CH<sub>2</sub>-CH-), 67.104 (-O-CH<sub>2</sub>-CH<sub>2</sub>-CH-), 102.461 (Py-C3), 104.719 (Py-C5), 117.548 (Ph-C-2), 119.531 (Ph-C-4 and 6), 136.274 (Ph-C-5), 139.558 (Py-C4), 150.845 (C=O), 159.159 and 159.324 Py-C2-6), 165.127 (Ph-C-1 and 3) ppm. **MS** [M+H<sup>+</sup>] = 435. **HRMS** (ESI-TOF) m/z: [M+H]<sup>+</sup> Calcd for C<sub>13</sub>H<sub>16</sub>O<sub>5</sub>H 253.26; Found 253.1076. **IR**: 789, 1060, 1242, 1449, 1531, 1627, 2961, 3207, 3340 cm<sup>-1</sup>. **M.p.** = 112-114 °C

*1,3-bis[[6-bisacrylamid-2-yl]amido]carbonyl*                      *5-(3-methylbutoxy)-benzene*  
(*monomer 3, M3*). To a solution of **15** (1 g, 2.3 mmol, FW=434.49, 1 eq) and TEA (0.80 mL, 2.5 eq, 5.75 mmol, FW= 101.19, d=0.726, 0.58 g) in anhydrous THF (100 mL), acryloyl chloride (0.41 mL, 5 mmol, 2.2 eq, FW=90.51, d=1.114, 0.45 g) dissolved in 20 mL of THF was added dropwise at 0°C and under a N<sub>2</sub> atmosphere. The reaction mixture was left to react overnight at room temperature. The solvent was evaporated and the crude dissolved in DCM in order to precipitate the solid from 250 mL of petroleum ether (60-80). A light brown solid was obtained which was washed with water, a saturated aqueous solution of NaHCO<sub>3</sub> and petroleum ether (750 mg of crude). The solid was purified with a chromatographic column (dry column) using silica gel as stationary phase and PE: EtOAc [6:4] as eluent. The monomer was the first compound to elute from the column. The yield was very low, most likely due to the low quality of the acryloyl chloride used (62 mg, 5%). **<sup>1</sup>H NMR** (400 MHz, DMSO-*d*<sub>6</sub>): δ 0.975 (d, <sup>3</sup>J=6.8 Hz, 6H, -CH-CH<sub>3</sub>), 1.686 (q, <sup>3</sup>J = 6.8 Hz, 2H, -O-CH<sub>2</sub>-CH<sub>2</sub>-CH-), 1.828 (m, <sup>3</sup>J = 6.8 Hz, 1H, -CH-), 4.177 (t, <sup>3</sup>J = 6.4 Hz, 2H, -O-CH<sub>2</sub>-CH<sub>2</sub>-CH-), 5.799 (dd, <sup>2</sup>J = 2 Hz, <sup>3</sup>J=10.2 Hz, 2H, CH<sub>cis</sub>=), 6.325 (dd, <sup>2</sup>J = 2 Hz, <sup>3</sup>J=17.2 Hz, 2H, CH<sub>trans</sub>=), 6.667 (dd, <sup>3</sup>J<sub>cis</sub>=6.6 Hz, <sup>3</sup>J<sub>trans</sub>= 10.4 Hz, 2H, -CH=), 7.721 (d, <sup>3</sup>J = 1.2 Hz, 2H, Py-CH<sub>2</sub>[H-5]), 7.806 (d, <sup>3</sup>J = 8 Hz, 2H, Py-CH<sub>2</sub>[H-3]), 7.874 (t, <sup>3</sup>J = 8 Hz, 2H, Py-CH<sub>2</sub>[H-4]), 7.9435 (d, <sup>3</sup>J = 7.6 Hz, 2H, CH(4-6)-Ar), 8.119 (s, 1H, CH(2)-Ar), 10.430 (s, 2H, NH-C<sup>6</sup>), 10.519 (s, 2H, NH-C<sup>2</sup>) ppm. **<sup>13</sup>C NMR** (400 MHz, DMSO-*d*<sub>6</sub>): δ 23.05 (-CH-CH<sub>3</sub>), 25.23 (-CH-), 37.93 (-O-CH<sub>2</sub>-CH<sub>2</sub>-CH-), 67.24 (-O-CH<sub>2</sub>-CH<sub>2</sub>-CH-), 110.85 (Py-CH<sub>2</sub>[C-5]), 111.63 and 140.72 (Py-CH<sub>2</sub>[C-3 and C-4]), 117.72 (Ph-C-2), 120.33 (Ph-C-4 and 6), 128.46 (CH<sub>2</sub>=), 132.08 (-CH=), 136.16, 150.78, 151.04, 159.25, 164.30, 165.56 ppm. **MS** [M+H<sup>+</sup>] = 543. **HRMS** (ESI-TOF) m/z: [M+H]<sup>+</sup> Calcd for C<sub>23</sub>H<sub>26</sub>N<sub>6</sub>O<sub>3</sub>H 543.59; Found 543.2354. **IR**: 800, 979, 1061, 1240, 1448, 1507, 1582, 1670, 2347, 2956, 3276 cm<sup>-1</sup>. **M.p.** = 142-159 °C

### 3.2.4 Synthesis of Monomer 4

*Dimethyl 5-(2-Ethylhexyloxy) – isophthalate (8)*. *Dimethyl 5-hydroxyisophthalate (4*, SL-181, 5.5 g, 0.026 mol), 2-ethylhexylbromide (6.5 mL, 0.036 mol, 7 g, FW=193.13, d=1.086), and potassium carbonate (6.09 g, 0.044 mol, FW= 138.206) were refluxed in CH<sub>3</sub>CN (100 mL) for 22h. The next day, the K<sub>2</sub>CO<sub>3</sub> was filtered off and the solvent evaporated. The yellow oil was purified by flash chromatography using diethyl ether as eluent and silica gel as stationary phase. **8** was obtained as a transparent yellow oil in quantitative yield (5.41g). <sup>1</sup>H NMR (400 MHz, DMSO-*d*<sub>6</sub>): δ 0.94 – 0.84 (t and t, 6H, -CH<sub>2</sub>-CH<sub>3</sub>), 1.32 – 1.24 (m, 4H, -CH<sub>2</sub>-CH<sub>2</sub>-CH<sub>2</sub>-CH<sub>3</sub>), 1.54 – 1.32 (m, 4H, -CH-(CH<sub>2</sub>)<sub>2</sub>-), 1.78 – 1.60 (hept, <sup>3</sup>J = 6.0 Hz, 1H, -CH-), 3.90 (s, 6H, -OCH<sub>3</sub>), 3.98 – 3.91 (d, <sup>3</sup>J = 4 Hz, 2H, -O-CH<sub>2</sub>-CH-), 7.67 – 7.60 (d, <sup>3</sup>J = 4 Hz, 2H, CH(4-6)-Ar), 8.07 – 7.99 (t, 1H, <sup>3</sup>J = 0.6 Hz, CH(2)-Ar) ppm. <sup>13</sup>C NMR (400 MHz, DMSO-*d*<sub>6</sub>): δ 11.41 (-O-CH<sub>2</sub>-CH(CH<sub>2</sub>CH<sub>3</sub>)-CH<sub>2</sub>-CH<sub>2</sub>-CH<sub>2</sub>-CH<sub>3</sub>), 14.42 (-O-CH<sub>2</sub>-CH(CH<sub>2</sub>CH<sub>3</sub>)-CH<sub>2</sub>-CH<sub>2</sub>-CH<sub>2</sub>-CH<sub>3</sub>), 23.03 (-O-CH<sub>2</sub>-CH(CH<sub>2</sub>CH<sub>3</sub>)-CH<sub>2</sub>-CH<sub>2</sub>-CH<sub>2</sub>-CH<sub>3</sub>), 23.82 (-O-CH<sub>2</sub>-CH(CH<sub>2</sub>CH<sub>3</sub>)-CH<sub>2</sub>-CH<sub>2</sub>-CH<sub>2</sub>-CH<sub>3</sub>), 28.98 and 30.40 (-O-CH<sub>2</sub>-CH(CH<sub>2</sub>CH<sub>3</sub>)-CH<sub>2</sub>-CH<sub>2</sub>-CH<sub>2</sub>-CH<sub>3</sub>), 39.15 (-CH-), 53.00 (-O-CH<sub>3</sub>), 71.15 (-O-CH<sub>2</sub>-CH(CH<sub>2</sub>CH<sub>3</sub>)-CH<sub>2</sub>-CH<sub>2</sub>-CH<sub>2</sub>-CH<sub>3</sub>), 119.69 (Ph-C-2), 122.17 (Ph-C-4 and 6), 131.97 (Ph-C-5), 159.61 (C=O), 165.70 (Ph-C-1 and 3) ppm. HRMS (ESI-TOF) m/z: [M+H]<sup>+</sup> Calcd for C<sub>18</sub>H<sub>26</sub>O<sub>5</sub>H 323.40; Found 323.1860. IR: 721, 1041, 1114, 1236, 1334, 1433, 1722, 2360, 2862, 2922, 2956 cm<sup>-1</sup>.

*5-(2-Ethylhexyloxy) – isophthalic acid<sup>106</sup> (11)*. To a stirred solution of **8** (4.12 g, 0.0128 mol) in THF (71 mL), methanol (24 mL) and water (24 mL), lithium hydroxide monohydrate (LiOH.H<sub>2</sub>O, 1.43 g) was added. The mixture was stirred at room temperature overnight and the solvent was then removed. To the residue 100 mL of 1N aqueous HCl was added and a white precipitate was formed. The precipitate was washed with water and freeze-dried for 2 days to obtain the white di-acid **11** (3.84g, 98%). <sup>1</sup>H NMR (400 MHz, DMSO-*d*<sub>6</sub>): δ 0.911 (t and t, 6H, -CH<sub>2</sub>-CH<sub>3</sub>), 1.300 (m, 4H, -CH<sub>2</sub>-CH<sub>2</sub>-CH<sub>2</sub>-CH<sub>3</sub>), 1.422 (m, 4H, -CH-(CH<sub>2</sub>)<sub>2</sub>-), 1.706 (m, <sup>3</sup>J = 6 Hz, 1H, -CH-), 3.973 (d, <sup>3</sup>J = 6 Hz, 2H, -O-CH<sub>2</sub>-CH-), 7.641 (d, <sup>3</sup>J = 1.2 Hz, 2H, CH(4-6)-Ar), 8.065 (t, 1H, <sup>3</sup>J = 1.6 Hz, CH(2)-Ar) ppm. <sup>13</sup>C NMR (400 MHz, DMSO-*d*<sub>6</sub>): δ 11.487 (-O-CH<sub>2</sub>-CH(CH<sub>2</sub>CH<sub>3</sub>)-CH<sub>2</sub>-CH<sub>2</sub>-CH<sub>2</sub>-CH<sub>3</sub>), 14.502 (-O-CH<sub>2</sub>-CH(CH<sub>2</sub>CH<sub>3</sub>)-CH<sub>2</sub>-CH<sub>2</sub>-CH<sub>2</sub>-CH<sub>3</sub>), 23.052 (-O-CH<sub>2</sub>-

CH(CH<sub>2</sub>CH<sub>3</sub>)-CH<sub>2</sub>-CH<sub>2</sub>-CH<sub>2</sub>-CH<sub>3</sub>), 23.858 (-O-CH<sub>2</sub>-CH(CH<sub>2</sub>CH<sub>3</sub>)-CH<sub>2</sub>-CH<sub>2</sub>-CH<sub>2</sub>-CH<sub>3</sub>), 28.987 and 30.431 (-O-CH<sub>2</sub>-CH(CH<sub>2</sub>CH<sub>3</sub>)-CH<sub>2</sub>-CH<sub>2</sub>-CH<sub>2</sub>-CH<sub>3</sub>), 39.138 (-CH-), 71.135 (-O-CH<sub>2</sub>-CH(CH<sub>2</sub>CH<sub>3</sub>)-CH<sub>2</sub>-CH<sub>2</sub>-CH<sub>2</sub>-CH<sub>3</sub>), 119.592 (Ph-C-2), 122.674 (Ph-C-4 and 6), 133.203 (Ph-C-5), 159.547 (C=O), 166.996 (Ph-C-1 and 3) ppm. **MS** [M-H<sup>+</sup>] = 294.3. **HRMS** (ESI-TOF) m/z: [M+H]<sup>+</sup> Calcd for C<sub>16</sub>H<sub>22</sub>O<sub>5</sub>H 295.34; Found 295.1541. **IR**: 761, 912, 1051, 1269, 1382, 1462, 1708, 2362, 2852, 2920, 2960 cm<sup>-1</sup>. **M.p.** = 190-193°C.

*1,3-bis[[6-amino-2-yl]amido]carbonyl] 5-(2-Ethylhexyloxy)-benzene (16)*. i) 5-(2-Ethylhexyloxy) – isophthalic acid (**11**, 3 g, 0.0102 mol, 1 eq, FW=294.34) was refluxed with 30 mL of SOCl<sub>2</sub> for 4h. The solvent was then evaporated to obtain the corresponding diacid chloride (dark brown oil) which was used without further purification. ii) To a cooled (ice bath) solution of 2,6-diaminopyridine (11.13 g, 0.102 mol, FW=109.13, 10 eq) and TEA (2.843 mL, 2.064 g, 0.0204 mol, FW=101.19, d=0.726) in anhydrous THF (100 mL), 5-(2-ethylhexyloxy)isophthalic acid dichloride dissolved in 10 mL of THF was added slowly under a dinitrogen atmosphere. The reaction mixture was stirred at room temperature overnight. The next day, the solution was filtered remove unreacted 2,6-diaminopyridine and the solvent was evaporated to obtain a brown-orange solid. A saturated aqueous solution of NaHCO<sub>3</sub> (100 mL) was added to the crude material and the suspension sonicated for 30 minutes. The light brown solid was filtered and washed with water. The sample was dried overnight to obtain 4.66g of **16** (96%). **<sup>1</sup>H NMR** (400 MHz, DMSO-*d*<sub>6</sub>): δ 0.910 (t and t, 6H, -CH<sub>2</sub>-CH<sub>3</sub>), 1.316 (m, 4H, -CH<sub>2</sub>-CH<sub>2</sub>-CH<sub>2</sub>-CH<sub>3</sub>), 1.446 (m, 4H, -CH-(CH<sub>2</sub>)<sub>2</sub>-), 1.713 (m, <sup>3</sup>J = 6 Hz, 1H, -CH-), 4.005 (d, <sup>3</sup>J = 5.6 Hz, 2H, -O-CH<sub>2</sub>-CH-), 5.798 (s, 4H, NH<sub>2</sub>), 6.276 (d, <sup>3</sup>J = 7.2 Hz, 2H, Py-CH<sub>2</sub>[H-5]), 7.382 (d, <sup>3</sup>J = 8 Hz, 2H, Py-CH<sub>2</sub>[H-3] ), 7.441 (t, <sup>3</sup>J = 7.6 Hz, 2H, Py-CH<sub>2</sub>[H-4]), 7.621 (s, 2H, CH(4-6)-Ar), 8.107 (t, 1H, CH(2)-Ar), 10.231 (s, 2H, NH) ppm. **<sup>13</sup>C NMR** (400 MHz, DMSO-*d*<sub>6</sub>): δ 11.535 (-O-CH<sub>2</sub>-CH(CH<sub>2</sub>CH<sub>3</sub>)-CH<sub>2</sub>-CH<sub>2</sub>-CH<sub>2</sub>-CH<sub>3</sub>), 14.531 (-O-CH<sub>2</sub>-CH(CH<sub>2</sub>CH<sub>3</sub>)-CH<sub>2</sub>-CH<sub>2</sub>-CH<sub>2</sub>-CH<sub>3</sub>), 23.093 (-O-CH<sub>2</sub>-CH(CH<sub>2</sub>CH<sub>3</sub>)-CH<sub>2</sub>-CH<sub>2</sub>-CH<sub>2</sub>-CH<sub>3</sub>), 23.918 (-O-CH<sub>2</sub>-CH(CH<sub>2</sub>CH<sub>3</sub>)-CH<sub>2</sub>-CH<sub>2</sub>-CH<sub>2</sub>-CH<sub>3</sub>), 29.023 and 30.514 (-O-CH<sub>2</sub>-CH(CH<sub>2</sub>CH<sub>3</sub>)-CH<sub>2</sub>-CH<sub>2</sub>-CH<sub>2</sub>-CH<sub>3</sub>), 39.228 (-CH-), 71.061 (-O-CH<sub>2</sub>-CH(CH<sub>2</sub>CH<sub>3</sub>)-CH<sub>2</sub>-CH<sub>2</sub>-CH<sub>2</sub>-CH<sub>3</sub>), 102.463 (Py-C3), 104.705 (Py-C5), 117.554 (Ph-C-2), 119.563 (Ph-C-4 and 6), 136.263 (Ph-C-5), 139.547 (Py-C4), 150.855 (C=O), 159.160 and 159.511 (Py-C2-6), 165.124

(Ph-C-1 and 3) ppm. **MS** [M+H<sup>+</sup>] = 476.6. **HRMS** (ESI-TOF) m/z: [M+H]<sup>+</sup> Calcd for C<sub>26</sub>H<sub>32</sub>N<sub>6</sub>O<sub>3</sub>H 477.57; Found 477.2606. **IR**: 790, 1450, 1525, 1624, 1678, 2328, 2362, 2873, 2933, 2954, 3361 cm<sup>-1</sup>. **M.p.** = 83-85°C.

*1,3-bis[[6-bisacrylamid-2-yl]amido]carbonyl]-5-(2-ethylhexyloxy)-benzene*

(monomer 4, **M4**). To a solution of **16** (2 g, 4.19 mmol, FW=476.57, 1 eq) and TEA (1.46 mL, 2.5 eq, 10.475 mmol, FW= 101.19, d=0.726, 1.0599 g) in anhydrous DCM (100 mL), acryloyl chloride (0.749 mL, 9.218 mmol, 2.2 eq, FW=90.51, d=1.114, 0.834 g) dissolved in 10 mL of DCM was added dropwise at 0°C and under a dinitrogen atmosphere. The reaction mixture was left to react overnight at room temperature. The DCM solution was washed with saturated aqueous NaHCO<sub>3</sub> (2 × 100 mL) and water (1 × 100 mL). The organic layer was dried (MgSO<sub>4</sub>), filtered and the solvent evaporated to obtain a caramel like coloured compound, which was dissolved in ethyl acetate and precipitated in cold PE. A light pale brown solid was obtained, which was still not pure. A dry column using silica gel and ethyl acetate: DCM [4:6] was performed to obtain pure monomer 4 (296 mg, 12%). **<sup>1</sup>H NMR** (400 MHz, DMSO-*d*<sub>6</sub>): δ 0.919 (t and t, 6H, -CH<sub>2</sub>-CH<sub>3</sub>), 1.332 (m, 4H, -CH<sub>2</sub>-CH<sub>2</sub>-CH<sub>2</sub>-CH<sub>3</sub>), 1.469 (m, 4H, -CH<sub>2</sub>-(CH<sub>2</sub>)<sub>2</sub>-), 1.753 (m, <sup>3</sup>J = 6 Hz, 1H, -CH-), 4.04 (d, <sup>3</sup>J = 5.6 Hz, 2H, -O-CH<sub>2</sub>-CH-), 5.80 (dd, <sup>2</sup>J = 1.6 Hz, <sup>3</sup>J = 10.2 Hz, 2H, CH<sub>cis</sub>=), 6.33 (dd, <sup>2</sup>J = 2 Hz, <sup>3</sup>J = 17 Hz, 2H, CH<sub>trans</sub>=), 6.66 (dd, <sup>3</sup>J<sub>cis</sub> = 10.4 Hz, <sup>3</sup>J<sub>trans</sub> = 17 Hz, 2H, -CH=), 7.733 (d, <sup>3</sup>J = 1.2 Hz, 2H, Py-CH<sub>2</sub>[H-5]), 7.810 (d, <sup>3</sup>J = 8 Hz, 2H, Py-CH<sub>2</sub>[H-3]), 7.876 (t, <sup>3</sup>J = 7.6 Hz, 2H, Py-CH<sub>2</sub>[H-4]), 7.950 (d, <sup>3</sup>J = 7.6 Hz, 2H, CH(4-6)-Ar), 8.124 (t, 1H, CH(2)-Ar), 10.428 (s, 2H, NH-C<sup>6</sup>), 10.523 (s, 2H, NH-C<sup>2</sup>) ppm. **<sup>13</sup>C NMR** (400 MHz, DMSO-*d*<sub>6</sub>): δ 11.542 (-O-CH<sub>2</sub>-CH(CH<sub>2</sub>CH<sub>3</sub>)-CH<sub>2</sub>-CH<sub>2</sub>-CH<sub>2</sub>-CH<sub>3</sub>), 14.542 (-O-CH<sub>2</sub>-CH(CH<sub>2</sub>CH<sub>3</sub>)-CH<sub>2</sub>-CH<sub>2</sub>-CH<sub>2</sub>-CH<sub>3</sub>), 23.104 (-O-CH<sub>2</sub>-CH(CH<sub>2</sub>CH<sub>3</sub>)-CH<sub>2</sub>-CH<sub>2</sub>-CH<sub>2</sub>-CH<sub>3</sub>), 23.933 (-O-CH<sub>2</sub>-CH(CH<sub>2</sub>CH<sub>3</sub>)-CH<sub>2</sub>-CH<sub>2</sub>-CH<sub>2</sub>-CH<sub>3</sub>), 29.025 and 30.534 (-O-CH<sub>2</sub>-CH(CH<sub>2</sub>CH<sub>3</sub>)-CH<sub>2</sub>-CH<sub>2</sub>-CH<sub>2</sub>-CH<sub>3</sub>), 39.289 (-CH-), 71.170 (-O-CH<sub>2</sub>-CH(CH<sub>2</sub>CH<sub>3</sub>)-CH<sub>2</sub>-CH<sub>2</sub>-CH<sub>2</sub>-CH<sub>3</sub>), 110.837 (Py-C3), 111.660 (Py-C5), 117.732 (Ph-C-2), 120.344 (Ph-C-4 and 6), 128.460 (CH<sub>2</sub>=), 132.078 (-CH=), 136.47 (Ph-C-5), 140.717 (Py-C4), 150.785 and 151.033 (Py-C2-6), 159.450 (Ph-C-1 and 3), 164.293 and 165.552 (C=O) ppm. **MS** [M+H<sup>+</sup>] = 584.7. **HRMS** (ESI-TOF) m/z: [M+H]<sup>+</sup> Calcd for C<sub>32</sub>H<sub>36</sub>N<sub>6</sub>O<sub>3</sub>H 585.67; Found 585.2829. **IR**: 796, 977, 1049, 1238, 1444, 1687, 2358, 2960, 3296, 3518 cm<sup>-1</sup>. **M.p.** = 175-180°C



### 3.2.5 Synthesis of Monomer 5

4-Chloro-2,6-pyridinedicarboxylic acid (**5**)<sup>103b</sup>. i) Chelidamic acid (**1**; 5 g, 27.3 mmol) and  $\text{PCl}_5$  (21.07 g, 0.1 mol, FW=208.24) were stirred and heated at 125°C (reflux) for 4 hours. The solution was then cooled to room temperature and chloroform (200 mL) added and the mixture filtered. The filtrate was cooled to 0°C and MeOH (25mL) was added dropwise. The solvent was removed and the solid recrystallized from hot methanol. The white crystals were filtered and washed with cold methanol to obtain 4-chloro-2,6-dimethylpyridinedicarboxylate (3.65g, 58.2%).  $^1\text{H NMR}$  (400 MHz,  $\text{CDCl}_3$ ):  $\delta$  4.04 (s, 6H,  $-\text{CH}_3$ ), 8.31 (s, 2H, CH-Ar) ppm.  $^{13}\text{C NMR}$  (400 MHz,  $\text{CDCl}_3$ ):  $\delta$  53.51 ( $-\text{CH}_3$ ), 128.33 (CH-Ar), 146.85 ( $-\text{C}-\text{Cl}$ ), 149.45 (C=O), 164.14 (C-Ar) ppm. **MS** [ $\text{M}+\text{H}^+$ ]: 230.1. **IR**: 1198, 1720, 2952, 3083  $\text{cm}^{-1}$ . **M.p.**: 139-141 °C.

ii) A solution of 4-chloro-2,6-dimethylpyridinedicarboxylate (1.19g, 5.18mmol), and NaOH (3g) in water (150mL) was stirred at room temperature for 3 days. The aqueous phase was washed with DCM (1 × 100mL), then the pH lowered with 2M aqueous HCl until formation of a white solid which was collected, washed with cold water, and dried under vacuum (1.01g, quantitative yield).  $^1\text{H NMR}$  (400 MHz,  $\text{DMSO}-d_6$ ):  $\delta$  8.24 (s, 2H, CH-Ar) ppm.  $^{13}\text{C NMR}$  (400 MHz,  $\text{DMSO}-d_6$ ):  $\delta$  128.24 (CH-Ar), 146.28 ( $-\text{C}-\text{Cl}$ ), 151.02(C=O) 165.55 (C-Ar) ppm. **MS** [ $\text{M}+\text{H}^+$ ]: 201.56. **IR**: 678, 900, 1571, 1724, 1809, 2351, 3039, 3367, 3481  $\text{cm}^{-1}$ . **M.p.**: 224-225 °C.

4-piperidine-2,6-pyridinedicarboxylic acid (**12**)<sup>107</sup>. 4-Chloro-2,6-pyridinedicarboxylic acid (**5**, 1 g, 4.96 mmol) was added to 10 mL of a 50% aqueous solution of piperidine. The reaction mixture was heated in a sealed tube at 175°C during a period of 24 h. After 1 day, the solution was left to cool down and the solvent was removed under reduced pressure. A light orange solid was obtained (ca. 1.5 g), which was stirred at room temperature with 100 mL of deionized water and 3 g of sodium hydroxide for 1 day. 4M aqueous 4M was carefully added until an acidic pH was obtained and a white solid precipitated. The solid was filtered and washed with water and then freeze-dried (450 mg, 36.3%).  $^1\text{H NMR}$  (400 MHz,  $\text{DMSO}-d_6$ ):  $\delta$  1.57 (m,  $^3\text{J}= 4.4$  Hz, 4H,  $-\text{CH}_2(3-5)$ -Piperidine), 1.60 (t,  $^3\text{J}= 4.4$  Hz, 2H,  $-\text{CH}_2(4)$ -Piperidine), 3.50 (t,  $^3\text{J}= 5.6$  Hz, 4H,  $-\text{CH}_2(2-6)$ -Piperidine), 7.53 (s,

2H, CH-Ar) ppm.  $^{13}\text{C}$  NMR (400 MHz, DMSO- $d_6$ ):  $\delta$  24.26 ( $-\text{CH}_2(4)$ -Piperidine), 25.29 ( $-\text{CH}_2(3-5)$ -Piperidine), 47.57 ( $-\text{CH}_2(2-6)$ -Piperidine), 110.25 (CH-Py), 147.88 (-C-N), 156.77 (C=O), 165.68 (C-Py) ppm. MS [M+H<sup>+</sup>]: 251. HRMS (ESI-TOF) m/z: [M+H]<sup>+</sup> Calcd for C<sub>12</sub>H<sub>14</sub>N<sub>2</sub>O<sub>4</sub>H 251.25; Found 251.1038. IR: 684, 781, 1637, 1743, 2335, 2868, 3116, 3495, 3591 cm<sup>-1</sup>. M.p.: 254-256 °C.

*2,6-bis[[6-amino-2-yl]amido]carbonyl] 4-piperidine- pyridine (17)*. 4-Piperidine-2,6-pyridinedicarboxylic acid (**12**, 1.9 g, 7.59 mmol, 1 eq) was refluxed with 15 mL of SOCl<sub>2</sub> for 4h at 95°C. The solvent was then evaporated to obtain the corresponding diacid chloride. Without any further purification, the acid dichloride was dissolved in 50 mL of dry THF and added dropwise to a solution of 2,6-diaminopyridine (8.28 g, 0.0759 mol, 10 eq, FW=109.13) and TEA (2.11 mL, 1.536 g, 0.015 mol, FW= 101.19, d=0.726) in anhydrous THF (150 mL) at 0°C and under a dinitrogen atmosphere. The reaction mixture was stirred at room temperature overnight. The next day the precipitate was filtered off and the solvent was evaporated. The dark brown crude product was then washed with water (100mL) and a saturated aqueous solution of NaHCO<sub>3</sub> (100mL). The solid was filtered and sonicated in 150 mL of MeOH, then filtered to obtain the product as a pale brown solid (**17**, 2.5 g, 76.5%).  $^1\text{H}$  NMR (400 MHz, DMSO- $d_6$ ):  $\delta$  1.610 (m, 6H,  $-\text{CH}_2(3-4-5)$ -Piperidine), 3.539 (t, 4H,  $-\text{CH}_2(2-6)$ -Piperidine), 5.949 (s, 4H,  $\text{NH}_2$ ), 6.293 (d,  $^3\text{J}=7.6$  Hz, 2H, Py- $\text{CH}_2$ [H-5]), 7.419 (d,  $^3\text{J}=7.2$  Hz, 2H, Py- $\text{CH}_2$ [H-3]), 7.474 (t,  $^3\text{J}=7.6$  Hz, 2H, Py- $\text{CH}_2$ [H-4]), 7.646 (s, 2H,  $\text{CH}(4-6)$ -Ar), 10.579 (s, 2H,  $\text{NH}$ ) ppm.  $^{13}\text{C}$  NMR (400 MHz, DMSO- $d_6$ ):  $\delta$  24.41 ( $-\text{CH}_2(4)$ -Piperidine), 25.26 ( $-\text{CH}_2(3-5)$ -Piperidine), 47.50 ( $-\text{CH}_2(2-6)$ -Piperidine), 102.07 (Py-CH<sub>2</sub>[C-5]), 104.83 and 139.70 (Py-CH<sub>2</sub>[C-3 and C-4]), 108.49 (Ph-C-3 and 5), 150.05, 150.39, 156.68, 159.27, 162.97 ppm. MS [M+H<sup>+</sup>]: 432.5. HRMS (ESI-TOF) m/z: [M+H]<sup>+</sup> Calcd for C<sub>22</sub>H<sub>24</sub>N<sub>3</sub>O<sub>2</sub>H 433.48; Found 433.2102. IR: 783, 1124, 1458, 1519, 1600, 1674, 2358, 2947, 3196, 3354 cm<sup>-1</sup>. M.p.: 300-304°C.

*2,6-bis[[6-bisacrylamid-2-yl]amido]carbonyl]-4-piperidine-pyridine (monomer 5, M5)*. To a solution of **17** (450 mg, 1.04 mmol, 1 eq.) and triethylamine (0.435 mL, 316 mg, 3.12 mmol, FW= 101.19, d=0.726, 3 eq) in anhydrous DCM (50 mL), 0.211 mL of acryloyl chloride (235 mg, 2.6 mmol, FW=90.51, d=1.114, 2.5 eq) in 10 mL of DCM was added slowly at 0°C and under a dinitrogen atmosphere. The reaction mixture was stirred at room temperature overnight. The next day the

reaction mixture was washed with 50 mL saturated aqueous NaHCO<sub>3</sub> and the organic layer purified by chromatographic column (silica gel, PE:EtOAc/5:5) to obtain monomer 5 (120 mg, 21%). <sup>1</sup>H NMR (400 MHz, CDCl<sub>3</sub>): δ 1.603 (m, 4H, -CH<sub>2</sub>(3-5)-Piperidine), 1.67 (m, 2H, -CH<sub>2</sub>(4)-Piperidine), 3.434 (t, <sup>3</sup>J = 4 Hz, 4H, -CH<sub>2</sub>(2-6)-Piperidine), 5.842 (dd, <sup>2</sup>J = 4.8 Hz, <sup>3</sup>J = 6.8 Hz, 2H, CH<sub>cis</sub>=), 6.533 (d, <sup>3</sup>J = 2 Hz, 2H, Py-CH<sub>2</sub>[H-5]), 6.550 (s, 2H, Py-CH<sub>2</sub>[H-3]), 7.551 (s, 2H, CH(4-6)-Ar), 7.663 (t, <sup>3</sup>J = 8 Hz, 2H, Py-CH<sub>2</sub>[H-4]), 7.924-7.984 (dd & dd, 4H, CH<sub>trans</sub>=), 9.25 (s, 2H, NH-C<sup>6</sup>), 10.20 (s, 2H, NH-C<sup>2</sup>) ppm. <sup>13</sup>C NMR (400 MHz, DMSO-d<sub>6</sub>): δ 24.07 (-CH<sub>2</sub>(4)-Piperidine), 25.06 (-CH<sub>2</sub>(3-5)-Piperidine), 47.14 (-CH<sub>2</sub>(2-6)-Piperidine), 108.05 (Py-CH<sub>2</sub>[C-5]), 110.04 and 140.57 (Py-CH<sub>2</sub>[C-3 and C-4]), 110.49 (Ph-CH<sub>2</sub>[C-3-5]), 128.40 (CH<sub>2</sub>=), 131.18 (CH=), 148.75, 150.21, 151.17, 156.08, 163.75, 165.30 ppm. MS [M+H]<sup>+</sup>: 540.6. HRMS (ESI-TOF) m/z: [M+H]<sup>+</sup> Calcd for C<sub>28</sub>H<sub>28</sub>N<sub>8</sub>O<sub>4</sub>H 541.57; Found 541.2321. IR: 761, 983, 1240, 1442, 1508, 1581, 1683, 2360, 2926, 3273 cm<sup>-1</sup>. M.p.: >340°C.

### 3.2.5 Synthesis of Pentobarbital – MIP1/NIP1

<i>Name</i>	<i>Function</i>	<i>mmol</i>	<i>MIP1</i>	<i>NIP1</i>
<i>1,3-bis[[6-bisacrylamid-2-yl]amido]carbonyl]5-tert-butyl-benzene</i>	functional monomer	1	513 mg	513 mg
<i>Pentobarbital</i>	template	1	226 mg	0.672 mL
<i>EGDMA</i>	crosslinker	20	3.77 mL (3.96 g)	3.77 mL (3.96 g)
<i>2,2'-azobis(2,4-dimethylvaleronitrile) (ABDV)</i>	initiator	1% w/w monomers	52 mg	52 mg
<i>Chloroform</i>	Solvent/porogen		5.6 mL	5.6 mL

The polymer preparation is described in chapter 2. Acetic acid was used in the pre-polymerisation mixture of the control polymer to solubilize the monomer in chloroform.

### 3.3 RESULTS AND DISCUSSION

#### 3.3.1 Job plot

Job plot experiments were performed to confirm the stoichiometry of the complex (1:1) formed between monomer 1 and the different analytes (Figure 23). These experiments confirm the hypothesis that the interaction would be 1:1.

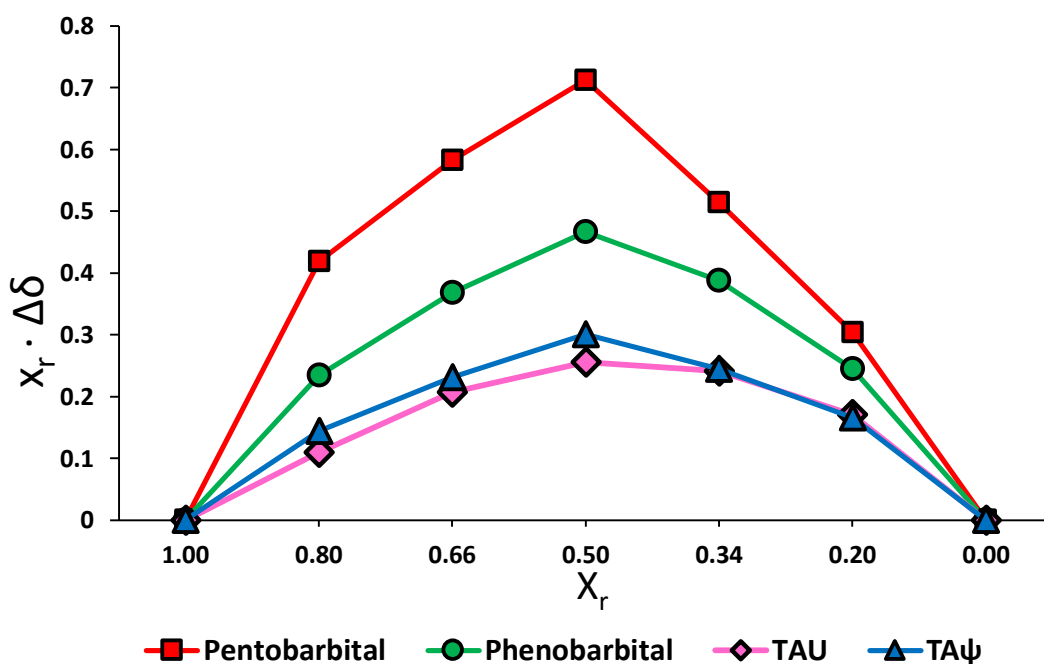


**Figure 23:** Job Plot of monomer 1 with Pentobarbital, Phenobarbital, TAU and TA $\psi$ . The monomer interacts with the analytes in a 1:1 stoichiometric complex. The experiments were made in CDCl<sub>3</sub> using 5mM monomer and template concentration solution.  $X_r$  = molar fraction  $\Delta\delta$  = chemical shift change.

#### 3.3.2 <sup>1</sup>H NMR titrations

<sup>1</sup>H NMR titration studies were performed in order to calculate the binding constants ( $K_a$ ) between the functional monomers and the templates (and related species). All NMR titrations were performed in CDCl<sub>3</sub> or CD<sub>3</sub>CN at 25 °C. To a 0.1 or 1 mM monomer solution an increasing amount of guest was added, as described earlier.

**Table 8:** Monomer M1-template/analyte binding constants value.  $K_a$  ( $M^{-1}$ ) (association constant) and  $\Delta\delta_{max}$  (maximum change in the chemical shift) were calculated by fitting data to a 1:1 binding isotherm using OriginPro 8.5.1.

		$K_a$ ( $M^{-1}$ )	$\Delta\delta_{max}$	mM	solvent
<b>a</b>	Pentobarbital	$80536 \pm 8\%$	$1.63 \pm 0.01$	0.1	$CDCl_3$
<b>b</b>	Phenobarbital	$88602 \pm 12\%$	$1.66 \pm 0.01$	0.1	$CDCl_3$
<b>c</b>	2',3',4'-tri-O-acetyluridine (TAU)	$1288 \pm 2\%$	$1.58 \pm 0.01$	1	$CDCl_3$
<b>d</b>	2',3',4'-tri-O-acetyl Pseudouridine (TA $\psi$ )	$117 \pm 8\%$	$1.87 \pm 0.09$	1	$CDCl_3$
<b>e</b>	Ethylene urea	$12 \pm 19\%$	$6.55 \pm 1.18$	1	$CDCl_3$
<b>f</b>	Phenobarbital	$80 \pm 7.5\%$	$1.63 \pm 0.01$	1	$CD_3CN$

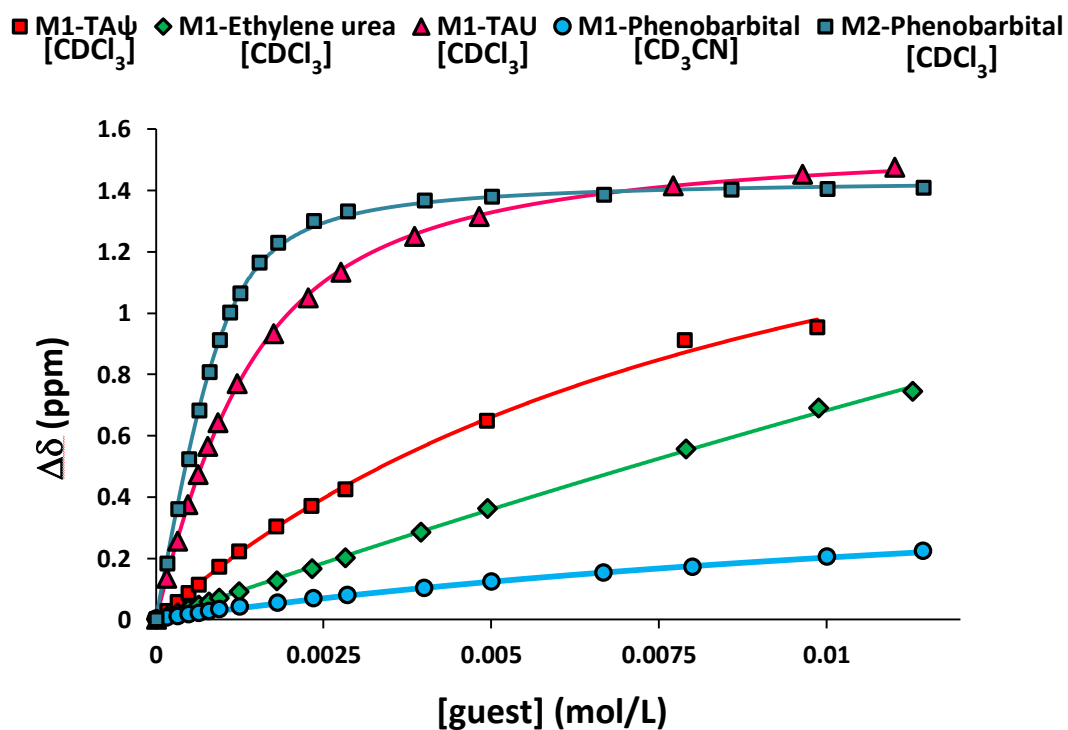


**Figure 24:** Binding Isotherms of monomer 1 and 2 – templates complexes obtained by  $^1H$  NMR titrations studies.

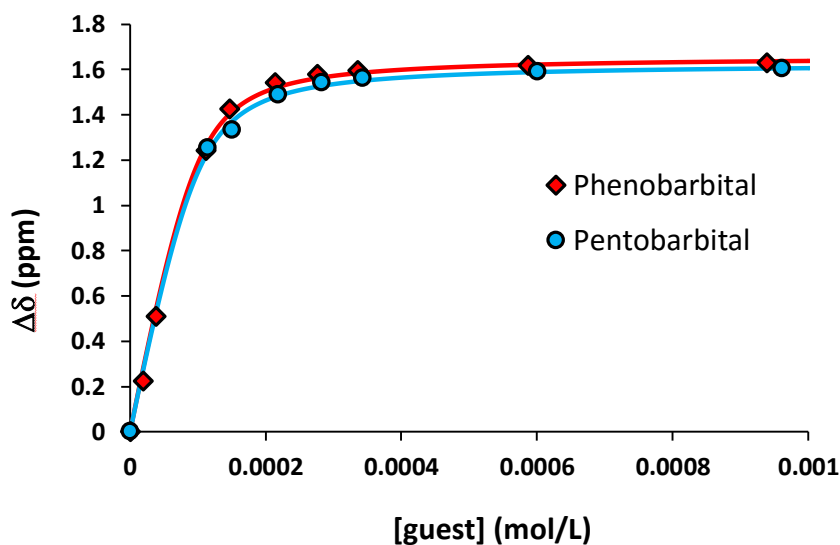


**Figure 25:** Binding Isotherms of monomer 1–barbiturates complexes obtained by  $^1\text{H}$  NMR titrations studies.

As seen in Figure 25, monomer 1 interacts very strongly with both the barbiturate analytes in chloroform. When the solvent used for the titration is more competitive, e.g. acetonitrile, the binding constant decreases by three orders of magnitude (Table 8 and Figure 24). The more polar solvent interferes with the hydrogen bond formation between the monomer cleft and the analyte, resulting in a weaker interaction. M1-barbiturates complexes have the highest association constants, compared to the related species, due to the number of H-bonds interactions formed between the two monomers and the analyte (Table 8). Other analytes, such as TAU or ethylene urea, can still bind to the cleft via the ureido moiety, however the binding strength is far weaker. This behavior is due to the decreased number of H-bonds shared between the host and the guest, the increased ratio of negative secondary interactions versus the positive primary interactions and, also, the  $\text{p}K_a$  of the analyte. The H-bond strength increases with increasing acidity of the H-bond donor. Overall, while monomer 1 is good for the imprinting of barbiturates, as has a high binding constant towards this template and can generate polymers with high selectivity and affinity towards barbiturates, it may also prove promising for the binding of any compound containing an imide moiety.

<sup>1</sup>H NMR titration has a limitation in the measurement of very high association constants; here we have a clear example with monomer 1; the titration for M1 with barbiturates was performed at a concentration of 10<sup>-5</sup> M in order to reach saturation slowly during the titration. A first titration was made using 1 mM solution, but the error observed for the obtained  $K_a$  was too high to ensure reliability in the results. An alternative method would be to use UV or fluorescence titrations, which provide titration data at lower concentrations between 10<sup>-4</sup> and 10<sup>-6</sup> M. Of course, this depends on being able to observe a change in the property being measured.

The association constant for M1 with phenobarbital was calculated for all those hydrogens directly involved in the interaction with the template (Table 9), to show that the entire cleft is involved in complex formation in the pre-polymerisation mixture.

**Table 9:** Association constants of monomer 1 with Phenobarbital.

	$K_a (M^{-1})$	$\Delta\delta_{max}$
<i>1st NH peak</i>	88602 ± 10424	1.66 ± 0.01
<i>2nd NH peak</i>	88876 ± 8022	2.01 ± 0.01
<i>CH peak isophthaloyl 2-H</i>	87456 ± 10438	0.14 ± 0.00
<i>CH peak vinyl group</i>	80738 ± 8909	0.21 ± 0.00

In the pre-polymerisation mixture before the template is added, the cleft's arms can, in principle, move freely, with the need to "spend" energy to organize itself around the template when the latter is added to the solution. Instead, the pyridine nitrogen can create two intramolecular hydrogen bonds with the cleft NH and, thus, pre-organise the uncomplexed cleft (Figure 20, monomer 2 and 5 of Figure 21). Unfortunately the nitrogen creates a primary negative interaction with the carbonyl oxygen of the template, decreasing hugely the binding constant. The overall effect is a drop of  $K_a$  of an order of magnitude ( $K_a = 5530 M^{-1}$ ) (Figure 24, Table 10).

**Table 10:** Association constants of monomer 2 with Phenobarbital.

<i>Monomer 2</i>	
$K_a$ ( $M^{-1}$ )	5530 ± 192
$\Delta\delta_{max}$	1.44 ± 0.01
concentration (mM)	1
temperature ( $^{\circ}C$ )	25

Claramunt *et al.* reported on a similar behaviour,<sup>108</sup> where the binding constant value of an host was affected by the presence of a pyridine ring as the spacer motif. They reported on the synthesis of synthetic receptors for the recognition of biotin, barbital and tolbutamide. In particular, N,N'-bis(6-methylpyridin-2-yl)-1,3-benzenedicarboxamide and 4-chloro-N,N'-bis(6-methylpyridin-2-yl)-2,6-pyridinedicarboxamide, with a benzene and a pyridine ring as the spacer between two methylpyridine arms respectively, were compared in terms of binding constants value towards barbital. The first cleft showed a  $K_a$  of 2442  $M^{-1}$ , while the second had a  $K_a$  of 274  $M^{-1}$ . Once again the carbonyl oxygen was repulsed by the nitrogen on the pyridine ring, affecting the binding between host and guest.

During the NMR titration studies, the peak of the protons involved in the hydrogen bond between the host and the guest shifted downfield when the concentration of the template in the solution increased. When the interaction is strong, the  $\Delta\delta$  reaches a plateau quickly, which is linked to a full saturation of the monomer bonded to the analyte, and the peak becomes broad and flat (Figure 26-27); indeed, the peak tends to disappear when the association constant is very high (Figure 26-a,b). When the binding is not strong, then the peak shape remains similar and visible throughout the titration and the plateau is not obtained (Figure 26-c and 27).



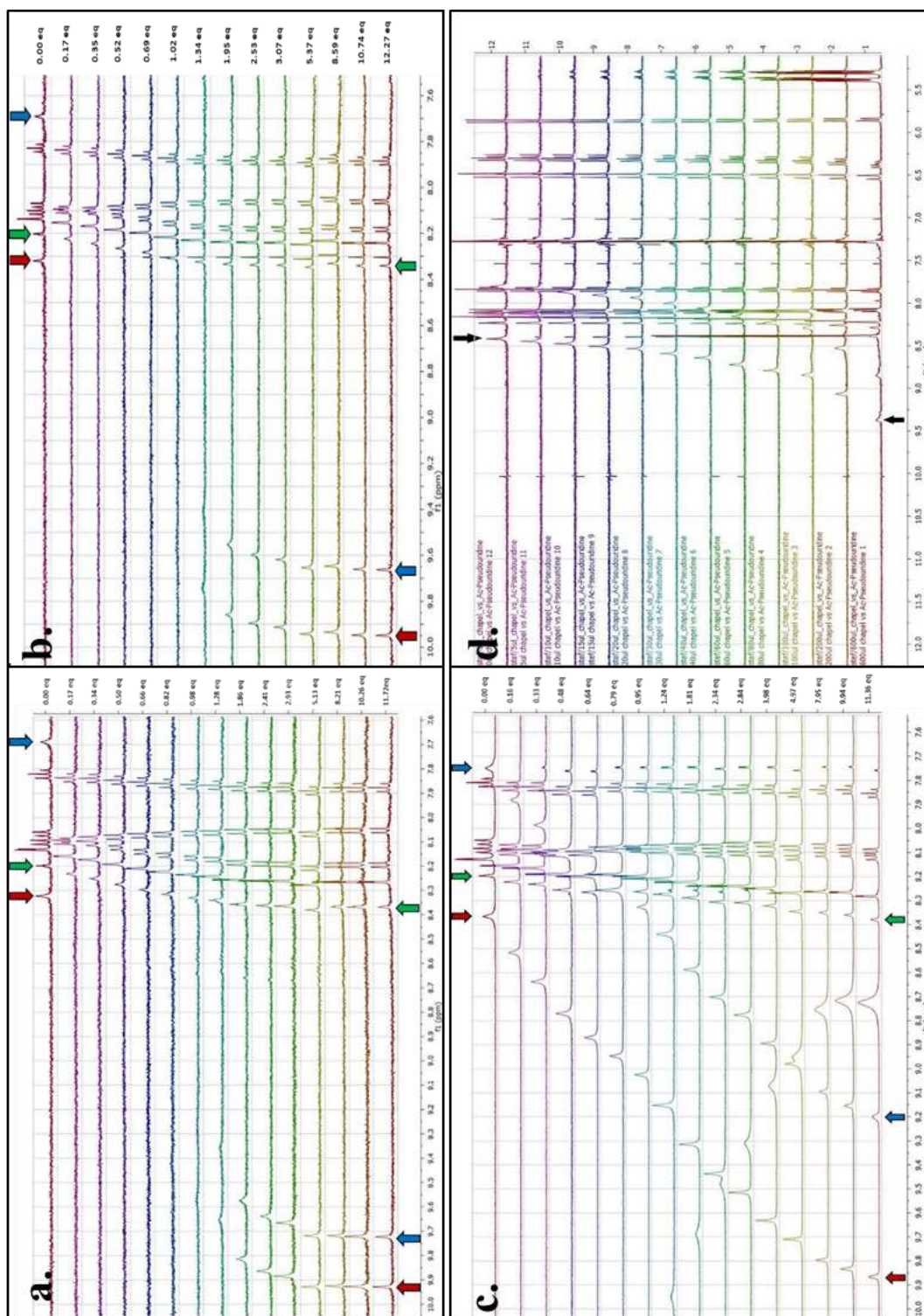


**Figure 26:**  $^1\text{H}$  NMR titrations spectrums. Red and black arrows =  $1^{\text{st}}$  NH of M1, green arrows =  $2^{\text{nd}}$  NH of M1, blue arrows = CH isophthaloyl 2-H. (a) Monomer 1 with Pentobarbital (0.1mM in  $\text{CDCl}_3$ ), (b) Monomer 1 with Phenobarbital (0.1mM in  $\text{CDCl}_3$ ), (c) Monomer 1 with 2',3',4'-Tri-O-acetyluridine (1mM in  $\text{CDCl}_3$ ), (d) Barbiturate cleft with 2',3',4'-Tri-O-acetyl pseudouridine (1mM in  $\text{CDCl}_3$ ).

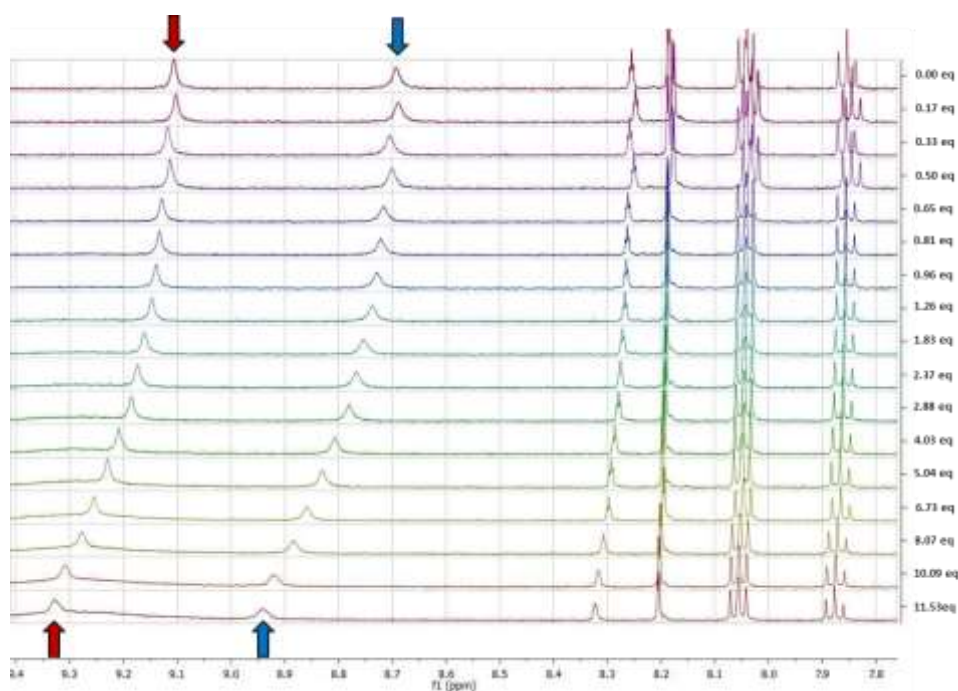


**Figure 27:**  $^1\text{H}$  NMR titration (1mM in  $\text{CD}_3\text{CN}$ ) of Monomer1 with Phenobarbital (f). Red arrow = 1st NH of M1, blue arrow = 2nd NH of M1.

### 3.3.3 Chromatographic evaluation

Chromatographic evaluation of the pentobarbital MIP and NIP was performed in order to study the template/related analyte retention and to determine the selectivity of the polymers (Table 11, Figure 28). Acetonitrile was firstly used as the eluent, but the retention time for the barbiturates was greater than 60 minutes. Other, more competitive solvents were then tested (1-4% AcOH/ $\text{CH}_3\text{CN}$  (v/v), 1% AcOH/MeOH (v/v)), but the barbiturate analytes were still retained strongly by the stationary phase. Finally, we chose to use 1% TFA/ $\text{CH}_3\text{CN}$  (v/v) as the mobile phase. While the template could still not be eluted, the use of a more acidic eluent may have damaged the instrument.

**Table 11:** Selectivity and specificity of template/analytes on MIP1 and NIP1 in 1% TFA/acetonitrile (v/v) as mobile phase. Selectivity  $\alpha(1)=k_1'/k_z'$ ; 1=Pentobarbital, z=structurally related analyte. For analytes with a negative  $k'$ , a fixed value of  $k'=0.1$  was used. <sup>a</sup> SD (standard deviation, n=3). <sup>b</sup> RSD (relative standard deviation)=(SD/x) \*100, x= mean value.

Analyte	Parameter	MIP	NIP	RSD <sup>b</sup> %
Pentobarbital (1)	k'±SD <sup>a</sup>	>90.84±0.00	0.45±0.01	< 2
	α (1)	1.0	1	
	IF	>199.72		
Phenobarbital	k'±SD <sup>a</sup>	>90.84±0.00	0.57±0.01	< 3
	α (1)	1.0	0.8	
	IF	>160.55		
Biotin-NO <sub>2</sub>	k'±SD <sup>a</sup>	0.19±0.00	0.14±0.01	< 10
	α (1)	468.5	3.1	
	IF	1.34		
Uracil	k'±SD <sup>a</sup>	4.90±0.36	2.53±0.11	< 5
	α (1)	18.5	0.2	
	IF	1.94		
Uridine	k'±SD <sup>a</sup>	2.06±0.06	1.22±0.09	< 7
	α (1)	44.2	0.4	
	IF	1.69		
Adenosine	k'±SD <sup>a</sup>	-0.33±0.03	-0.35±0.01	< 9
	α (1)	>908.4	>4.6	
	IF	0.94		
Cytidine	k'±SD <sup>a</sup>	-0.036±0.03	-0.36±0.03	< 10
	α (1)	>908.4	>4.6	
	IF	1.01		
Guanosine	k'±SD <sup>a</sup>	-0.34±0.00	-0.36±0.02	< 7
	α (1)	>908.4	>4.6	
	IF	0.96		
TAU	k'±SD <sup>a</sup>	0.36±0.03	0.14±0.00	< 8
	α (1)	250.8	3.1	
	IF	2.5		
TAG	k'±SD <sup>a</sup>	-0.42±0.04	-0.37±0.02	< 11
	α (1)	>908.4	>4.6	
	IF	1.14		
TAψ	k'±SD <sup>a</sup>	0.12±0.01	0.10±0.01	< 8
	α (1)	741.8	4.5	
	IF	1.21		
5-MeU	k'±SD <sup>a</sup>	2.43±0.15	1.51±0.06	< 7
	α (1)	37.3	0.3	
	IF	1.61		

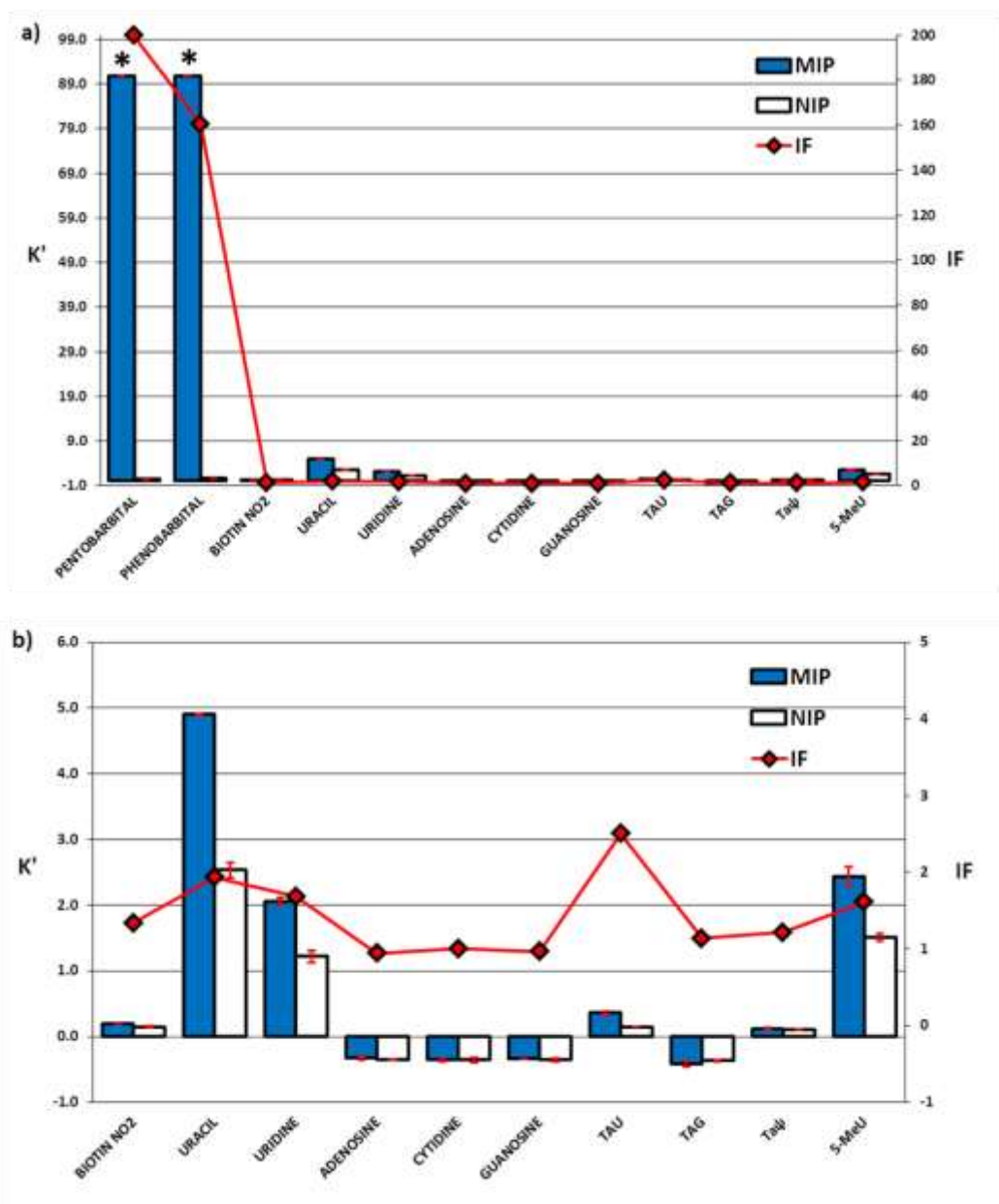


**Figure 28:** Chromatographic evaluation of MIP1 and NIP1 using 1% TFA/acetonitrile (v/v) as eluent. [\*] means greater than, based on a run of 1 hour. a) Complete graph showing  $k'$  and IF for the all tested analytes. b) Close up of the graph reporting  $k'$  and IF of all analytes except for barbiturates.

With an imprinting factor greater than 199 (Table 11), it is clear that there is the imprinting effect shown by the MIP and that the recognition of the template is not linked solely to the polymer or the presence of the functional monomer itself. Also,

there is an evident difference between the retention behaviours of the barbiturates and the structurally similar analytes. Nonetheless, barbiturates naturally create strong hydrogen bonds due to their acidic nature. The recovery of the template was unfortunately impossible, but it is important to underline that the application of this novel MIP is not for chromatographic purposes, but for use in molecularly imprinted solid phase extraction (MISPE) for sample enrichment. In this technique, recovery of the barbiturates can be affected as there is less limitation on the choice of elution solvent.

The polymer showed a cross-selectivity towards phenobarbital (Figure 28, Table 11), which is a positive result if we want to apply the MIP to pre-treatment of human urine samples containing barbiturates in general. It is also important to note the capacity factors for other analytes (Figure 28-b, Table 11). The imide moiety present in these analytes, such as uracil and uridine, together with their similar shape and size, mean that they can still be retained on the MIP with a degree of selectivity. This suggests that the cleft monomer may also be used for the imprinting of other templates, leading to strong and selective MIPs. Titration studies already have already shown the strong interaction of monomer **1** with TAU in chloroform (Table 8).

### **3.3.4 Equilibrium Rebinding Experiments**

Equilibrium rebinding experiments were performed on both MIP1 and NIP1 to evaluate the affinity and, therefore, the performance of the polymers. Acetonitrile was used as the re-binding solvent, which allows the template to bind the imprinted sites having complementary functionalities through hydrogen bonds. Figure 29 shows the binding isotherms for the MIP and the NIP. The difference in the affinities of the imprinted and non-imprinted polymers is visually evident.

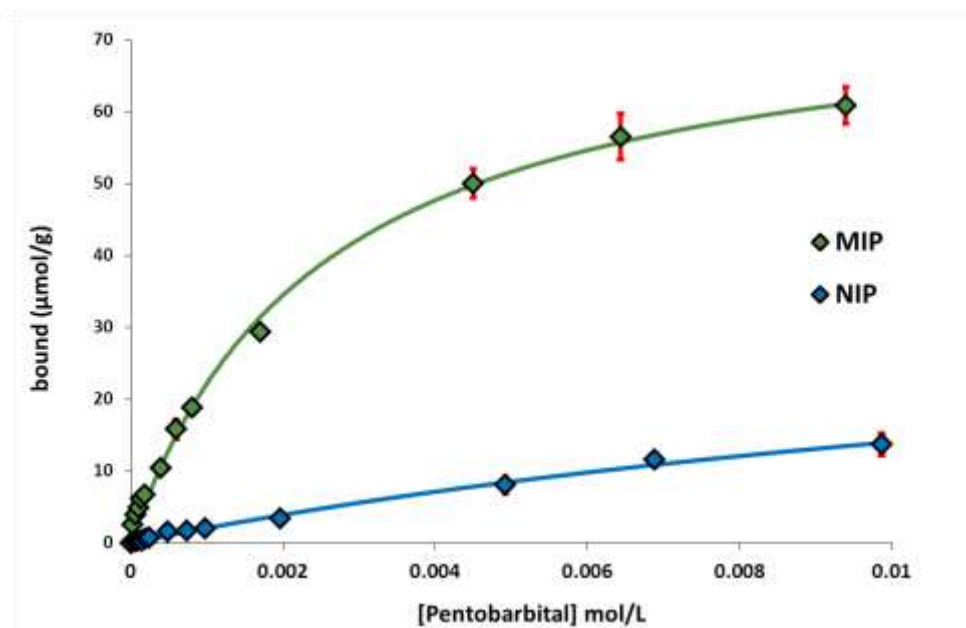


**Figure 29:** Binding isotherms obtained with equilibrium rebinding experiments of MIP1 and NIP1 in acetonitrile. 0-10 mM concentration range of Pentobarbital were used. All experiments were repeated in triplicate. The  $[Pentobarbital]_{free}$  in the supernatant was evaluated with HPLC (Wavelength: 240 nm, Flow rate: 1 mL/min, Injection: 5  $\mu$ L, RSD % < 21, N=3).

The experimental data were fitted using OriginPro 8.5.1 to a Langmuir model (Table 12), as this provided the best fit of the data for each polymer, with an  $R^2$  of 0.99. The Langmuir model takes into consideration a monodisperse population of binding sites. As the imprinting was carried out using stoichiometric non-covalent imprinting and the pre-polymerisation template-functional monomer complex was very strong, this raises the possibility that no free functional monomer was present during the polymerisation, thus decreasing the chance to create non-specific binding sites in the MIP (related to the monomer).

**Table 12:** Binding constants ( $k_a$ ) and number of sites ( $N$ ) of MIP1 and NIP1.

	$k_a$	$N$ ( $\mu$ mol/g)	$R^2$
MIP1	$403 \pm 33$	77	0.99557
NIP1	$54 \pm 13$	40	0.9943

The difference in the binding constants of the MIP1 and NIP1 can be explained by their containing different types of cavities. As the MIP1 was prepared in the presence of the template, high affinity imprinted cavities with specific shape and functionality for pentobarbital were formed. However, in the NIP1, low affinity non-specific cavities were formed with a low  $K_a$ . We reasoned that these non-specific cavities were formed by the incorporation of the cleft in the polymeric matrix during polymerisation. This leaves cleft molecules in cavities which can bind to different analytes, but without the added benefit of shape and size specificity provided by the polymer matrix (as in the case of the MIP1). Thus, the NIP1 interacts non-specifically with many different analytes, not only the template, as the size and shape of these sites does not mirror that of the template. For example, if these cavities are smaller, the template cannot fit in the site. Overall the MIP1 has high affinity binding sites, while the NIP1 has low affinity cavities, showing once again the importance of the imprinting process.

Through the use of a strong host-guest complex during polymerisation, which was achieved with the use of a tailor-made functional monomer that strongly interact with barbiturates, the total yield of imprinted site was of 77  $\mu\text{mol/g}$  (Table 12). This translate in 1/3 of the total template been strongly complexed to the functional monomer during polymerisation allowing the formation of specific binding cavities around the template, having the hydrogen-bond array of the host positioned in the right geometry inside the cavity to later on recognise and re-bind the template..

### 3.3.5 MISPE

Molecularly Imprinted Solid Phase Extraction (MISPE) is a technique widely used for sample enrichment and pre-treatment. Preliminary MISPE experiments using model samples have been performed (Figure 30). We have demonstrated that the MIP can be used as the stationary phase in a SPE cartridge and that an 85% recovery of pentobarbital was possible when an aqueous solution of this barbiturate was loaded onto the cartridge. In this protocol, 1 mL of a 0.1mM aqueous solution of phenobarbital was loaded onto the cartridge, then 1 mL of pure acetonitrile was used for the washing process, and elution was performed in three steps using 1% acetic acid/MeOH v/v (elution #1 = 3 mL and elution #2 = #3 = 1 mL). In the future, we speculate that a single elution may be done using TFA instead of acetic acid.

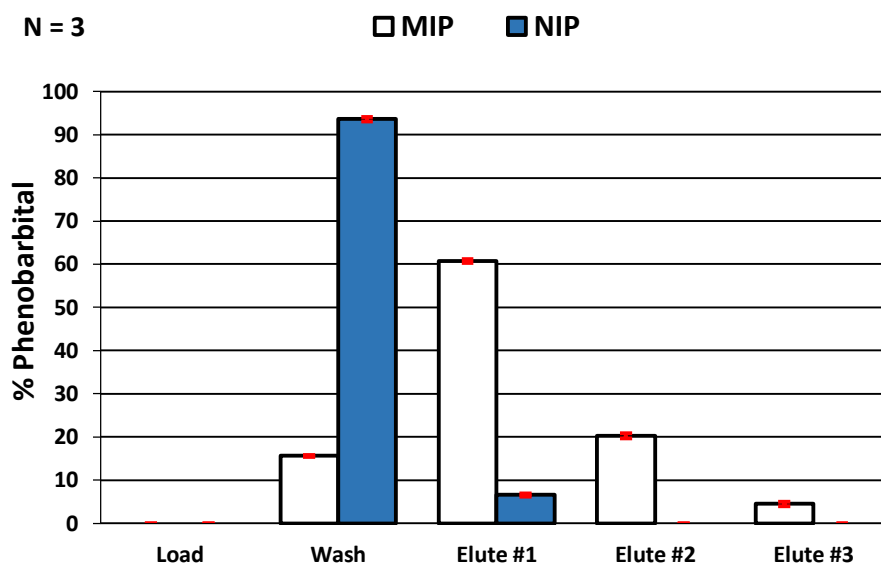


**Figure 30:** Percentage of phenobarbital eluted in each step (load, wash and elution) through MIP1 and the control polymer (NIP1).

The interaction between the template and MIP1 in the final polymer is so strong that even a highly competitive eluent (1% TFA/CH<sub>3</sub>CN v/v) cannot elute the barbiturates in a reasonable time on an HPLC column (Figure 28, Table 11). This can be a drawback if the polymer were to be used in HPLC as a stationary phase. However, this material is far better suited for use in MISPE for human urine sample enrichment. MISPE experiments using human urine spiked with this drugs will be performed in the future on this MIP.

One of the problems that can be faced during a MISPE experiments is the presence of high levels of urea in urine. The competitive interaction of urea with the binding cavities may compromise the experiments and the full recovery of the template. This problem was highlighted when micron-size beads imprinted against barbiturates were used in MISPE with human urine.<sup>109</sup> Here, BAAPy and di-vinyl benzene (DVB) were used as functional monomer and crosslinker respectively. This MISPE was efficient, with a recovery percentage of different barbiturates in urine between 35-65%. Unfortunately a pre-treatment of the sample with a commercially available sorbent to remove firstly urea was necessary. We calculated the binding constant of monomer 1 with both pentobarbital and ethylene urea by means of <sup>1</sup>H NMR titration in chloroform (Table 8). The calculated  $K_a$



values were  $8 \times 10^4$  and  $1 \times 10^1 \text{ M}^{-1}$ , respectively. The huge difference in binding strength should be enough to overcome the competitive behaviour of the different analytes, even if they are present in far higher concentrations than the barbiturate analytes of interest. Future studies will be performed on this polymer.

### 3.4 CONCLUSIONS

Supramolecular binding of barbiturates using a six hydrogen bonding moiety cleft was firstly created by Hamilton.<sup>28, 101</sup> Here we have described the synthesis of a pentobarbital imprinted polymer using the Hamilton-like cleft M1 as the functional monomer (Figure 21). Compared to previously reported barbiturate MIPs (e.g. 2,6-bis(acrylamido)pyridine based MIP showing a capacity factors towards cyclobarbital of 2.64 using 100% methanol as eluent<sup>102</sup>) the novel reported polymer shows higher retention and selectivity towards barbiturates.

Overall, five new clefts were prepared (Figure 21), based on Hamilton's general idea, but only monomer **1** was used for the synthesis of MIPs, as it proved the most convenient in terms of synthesis, starting material cost, solubility and binding strength (Table 8). Monomer **2**, with a pyridine ring as the spacer element, results in weaker binding due to the repulsion generated by the pyridine nitrogen towards the barbiturate carbonyl oxygen (Figure 20).

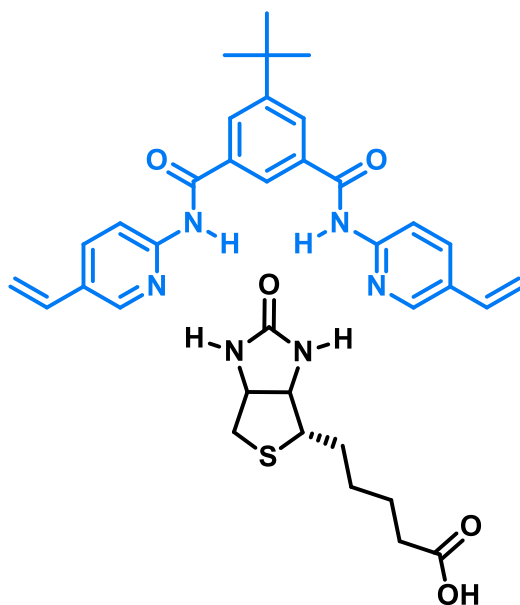
The solubility issue in 0.1M solution of the cleft in chloroform or acetonitrile was overcome by the formation of a template-monomer complex which was so strong that it brought the non-soluble monomer in solution. Pentobarbital was used as the template as phenobarbital could help only partially overcome this solubility issue. Instead the NIP was prepared by adding acetic acid until all monomer was dissolved. Before using acetic acid, different molecules were tested by means of NMR titration (Table 8), in order to find a molecule with low interaction with the cleft that can help the cleft to be solubilized. *Ethylene urea* with a  $K_a$  of  $12 \text{ M}^{-1}$  in chloroform, seemed a suitable choice, but a 0.1 M solution (1:1 ratio) of this compound with the cleft in chloroform was not soluble. 2',3',4'-Tri-*O*-acetyluridine (TAU) was excluded as an alternative template for the NIP, as the

binding constant in chloroform is too high ( $1288 \text{ M}^{-1}$ ) and the structure of the molecules could create binding sites specific for TAU.

We have demonstrated that the use of a tailor made functional monomer for the imprinting of barbiturates can create a MIP with high affinity and selectivity towards the imprinted template. Monomer 1 shows strong interaction with barbiturates, superior to other monomers (BAAPy or MAA) used to imprint this class of drugs. The obtained MIP displays a high Imprinting Factor and can, potentially, be used as an SPE sorbent for the sample enrichments and the facile detection by MS or liquid chromatography of barbiturates. Future studies for this application need to be performed using human urine spiked with barbiturates.

# CHAPTER 4

## *SYNTHETIC AVIDIN-LIKE BIOTIN RECEPTOR*



## 4.1 INTRODUCTION

The idea of using molecularly imprinted polymers instead of natural receptors is extremely challenging, as Nature has, over millennia, created receptors exhibiting strong and selective interactions between biological macromolecules and their ligands. The use of “artificial antibodies” in immunoassays is a revolution in terms of new technologies and cutting cost. Having the opportunity to use a polymeric material, resistant to harsh conditions and reusable is extraordinary.

One of the natural host-guest systems widely used in immunoassays (and other methods) is avidin- and streptavidin-biotin complexation, which has the strongest reported interaction between host and guest.

In the past, the group of Claramunt has reported on the synthesis of a series of artificial receptors for the binding of biotin,<sup>108</sup> which were also tested with other molecules containing a urea moiety (e.g. barbiturates and ethylene urea). Inspired by these artificial receptors, we have designed and synthesised polymerisable versions of such receptors for the molecular imprinting of biotin.

In the area of MIPs, other groups have reported on the approaches towards the synthesis of synthetic avidin mimics.<sup>110</sup> In particular, either 2-acrylamidopyridine or methacrylic acid (MAA), or both, have been used as functional monomers. Unfortunately, only when methacrylic acid was used as the functional monomer did the MIP show selectivity towards biotin. Takeuchi *et al.* have also imprinted biotin using MAA as functional monomer.<sup>111</sup> NMR titration studies were performed and the association constant between MAA and biotin methyl ester in chloroform was shown to be only  $1.55 \cdot 10^2 \text{ M}^{-1}$ . Nonetheless, this interaction is of acceptable strength, although there is room for improvement, if one wishes to use stoichiometric non-covalent imprinting, by creating a stronger monomer-template complex.

Herein we will report on the development of a functional monomer for the binding of biotin and the preparation of an imprinted polymer for biotin recognition showing high affinity and selectivity towards the template.

### 4.1.1 Biotin

Biotin (Figure 31) is a water soluble vitamin, also known variously as Vitamin H, Vitamin B<sub>7</sub> and Coenzyme R, which is present in all living cells and is critical for a number of biological processes (e.g. cell growth, coenzyme for carboxylase enzymes and gluconeogenesis). It is composed of a tetrahydroimidizalone ring and a tetrahydrothiophene ring fused together. A valeric acid substituent is attached to one of the carbon atoms of the latter ring. This chain can be derivatized in order to conjugate biotin to other (macro)molecules. Adding a biotin tag does not alter the biological activity of such molecules (e.g. proteins) and this tagging is used as a tool in biomedical analysis, making use of the specific interaction between biotin and its natural receptors to detect and target biological analytes.

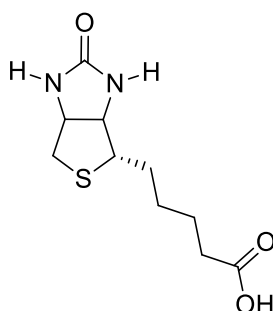


**Figure 31:** *Biotin structure*

Avidin and streptavidin are the natural receptors of biotin. The complex formed between biotin and these proteins is the strongest present in Nature, reported as having a dissociation constant,  $K_d$ , of the order of  $10^{-15}$  M. Avidin comprises four subunits, each one able to bind one molecule of biotin with very high affinity; it is easily purified from chicken egg whites. Streptavidin is also a tetrameric biotin-binding protein that is isolated from *Streptomyces avidinii*.

### 4.1.2 Application for Avidin- and Streptavidin-Biotin probes

The avidin- and streptavidin-biotin system can be used for numerous laboratory methods, where the biotin binding protein is used for the recognition of biotinylated

molecules. These probes are applied in several methods, for instance: *Affinity-based Assays (e.g. ELISA, Western blotting), Protein Detection, Nucleic Acid Detection and Protein Isolation and Enrichment.*

#### 4.1.3 Mimicking biotin natural receptors

MIPs can be a great alternative to avidin and streptavidin: their production is less expensive than their natural counterpart, have a long shelf life greater than 10 years, are easy to store as they don't need special storage condition (e.g. dry environment, low temperature). MIPs are reusable and are resistant to harsh conditions (e.g. temperature, extreme pH, organic solvents). Instead proteins, such as avidin and streptavidin, have a lower shelf life than a MIP and they also need special storage conditions. For example, a protein has a shelf life of a year if it is frozen, of few weeks if it is storage in a fridge, and can only last for few years if the protein is freeze-dried.

Also, MIP synthetic receptors interact with biotin with a readily reversible interaction; thus, they could potentially be used as a tool for protein purification. Biotin and its natural receptor form a very strong interaction that can be almost considered irreversible. This can be a drawback if the avidin-/streptavidin-biotin system is used to purify proteins, as after the interaction of the biotinylated protein with the natural receptor, it is extremely difficult to recuperate the proteins unless harsh conditions, that may denature the protein, are used.

Small-molecule synthetic receptors for biotin have been made previously<sup>108, 112</sup> and a few examples of MIPs selective for biotin have been reported.<sup>110-111, 113</sup> We took inspiration from previous work to create a functional monomer that binds biotin stoichiometrically in a non-covalent manner via hydrogen-bond formation. As mentioned before, the group of Claramunt has made extensive studies about synthetic biotin receptors, and one such example is shown in Figure 32. NMR titration studies were performed in chloroform and binding constants were calculated for complexation between this host molecule and molecules such as biotin ( $K_a = 1000 \text{ M}^{-1}$ ), barbital ( $K_a = 2442 \text{ M}^{-1}$ ) and ethylene urea ( $K_a = 1500 \text{ M}^{-1}$ ).

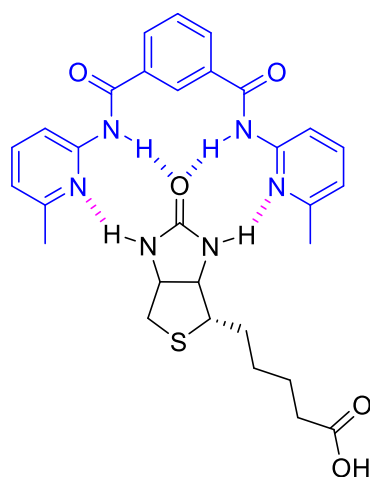


**Figure 32:** Synthetic receptor for biotin previously reported by Claramunt group<sup>108</sup>.

We will report on monomer 6, which is a polymerisable version of the Claramunt host shown above. The interaction between monomer 6 and biotin was  $1221 \text{ M}^{-1}$ , in  $\text{CDCl}_3$ , according to NMR titration studies. The presence of the spacer which connects the two molecules of 2-amidopyridine units is necessary for selective recognition of the template in the polymer, as the presence of 2-acrylamidopyridine alone as a functional monomer led to little, if any, imprinting in the polymeric matrix,<sup>110</sup> as previously reported.

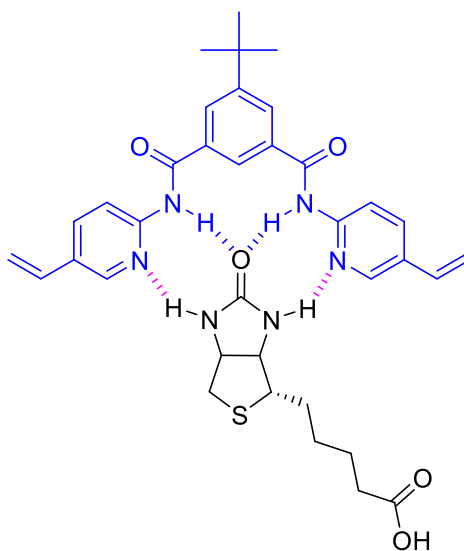
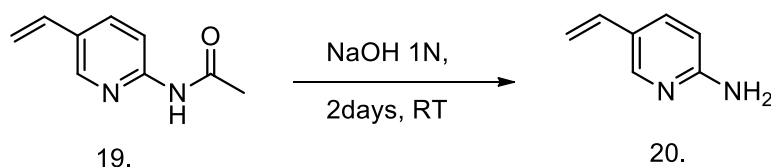


**Figure 33:** Biotin-monomer 6 complex formation. The two molecules interact with a total of four H-bonds.

Biotin methyl ester<sup>110</sup> was used for the binding studies and the imprinting process, as this ester is more soluble in organic solvents, and the free carboxylic moiety may also interfere with the template-monomer complex formation and may lead to polymer limiting the acceptance of biotin derivatives.

## 4.2 EXPERIMENTAL

### 4.2.1 Synthesis of 2-amino-5-vinyl-pyridine (20.)



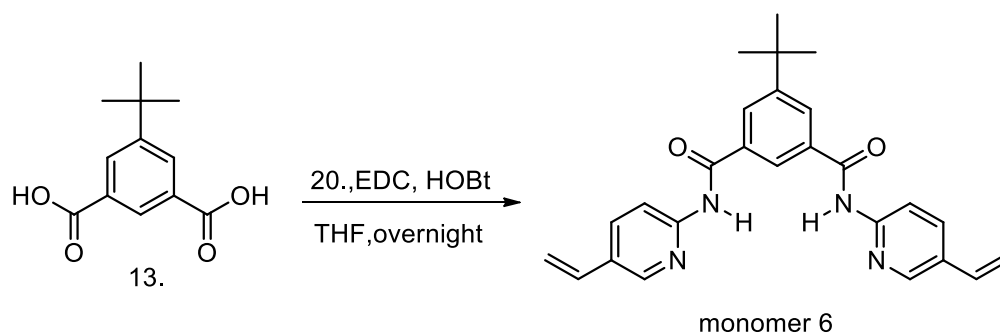
2-acetamido-5-vinylpyridine (**19**, 2 g, 12 mmol, FW = 162.19) was stirred in 100 mL of 1 M aqueous sodium hydroxide for 48 h at room temperature. After this time, the aqueous solution was extracted with dichloromethane (3 × 100 mL). The combined organic layers were dried using magnesium sulphate, which was then filtered off and the filtrate concentrated to dryness under vacuum to obtain a light yellow solid (1.38g, 93%). <sup>1</sup>H NMR (400 MHz, CDCl<sub>3</sub>): δ 4.554 (s, 2H, NH<sub>2</sub>), 5.11 (dd, <sup>2</sup>J = 0.8 Hz, <sup>3</sup>J=8 Hz, 1H, CH<sub>cis</sub> =), 5.56 (dd, <sup>2</sup>J = 0.8 Hz, <sup>3</sup>J=20 Hz, 1H, CH<sub>trans</sub>=), 6.47 (dd, <sup>3</sup>J<sub>cis</sub>= 0.4 Hz, <sup>3</sup>J<sub>trans</sub>= 8 Hz, 1H, -CH=), 6.58 (q, <sup>3</sup>J=6.8 Hz, 1H, -CH<sup>4</sup>), 7.56 (dd, J =2 and 8 Hz, 1H, -CH<sup>3</sup>), 8.05 (d, <sup>3</sup>J =2 Hz, 1H, -CH<sup>6</sup>) ppm. <sup>13</sup>C NMR (400 MHz, CDCl<sub>3</sub>): δ 108.535 (-CH=), 111.294 (=CH<sub>2</sub>), 124.104, 133.427 (-CH<sup>4</sup>), 134.512 (-CH<sup>3</sup>), 147.044 (-CH<sup>6</sup>) 158 ppm. IR: 1001.5, 1420.6, 1598.2, 1622.9, 3122.2, 3295.2, 3447 cm<sup>-1</sup>. M.p. = 106-111 °C.



#### 4.2.2 Synthesis of 1,3-bis[[5-vinylpyrid-2-yl]amido]carbonyl[5-tert-butylbenzene (monomer 6)

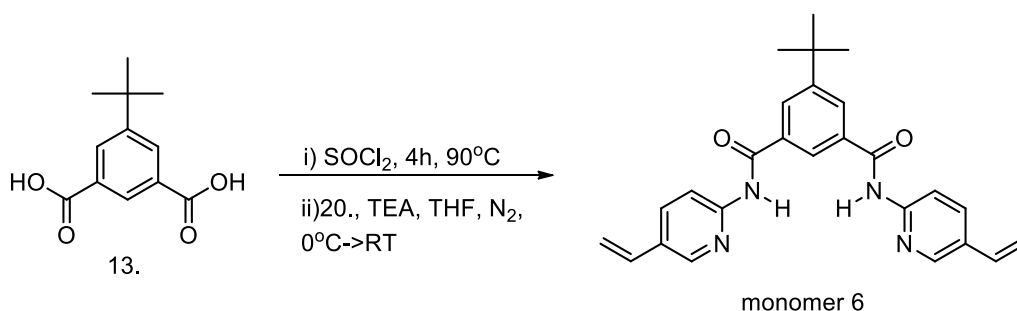
Different protocols for the synthesis of monomer **6** were used, in order to increase the final yield. One of the main issues was the poor reactivity of the 5-substituted aminopyridine, which leads to low yields. The most promising protocol is the third one described below.

##### PROTOCOL 1



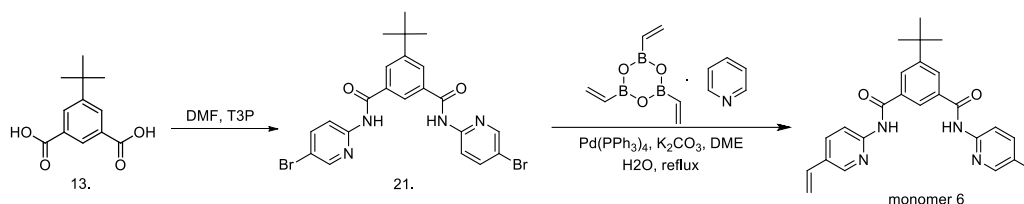
5-*Tert*-butyl isophthalic acid (**13**, 0.46 g, 0.002 mol, 1 eq, FW = 222.24) was stirred at room temperature under a dinitrogen atmosphere with 0.5 g of 2-amino-5-vinylpyridine (**20**, 0.00416 mol, 2 eq, FW = 120.15), EDC (0.88 g, 0.0046 mol, FW = 191.60, 2.2 eq) and HOBT (0.62 g, 0.0046 mol, FW = 135.12, 2.2 eq) in 50 mL of dry THF for 25 hours. The solvent was evaporated the next day and the crude residue dissolved in 70 mL of DCM and washed with brine (2 × 50 mL), NaOH 1N (50 mL) and water (3 × 50 mL). The organic layer was dried (MgSO<sub>4</sub>), filtered and evaporated to obtain a yellow solid, which was purified by column chromatography (silica gel and PE-EtOAc 80% and 50% as eluent). Monomer **6** was obtained as a white solid in 15% yield (130 mg).

##### PROTOCOL 2

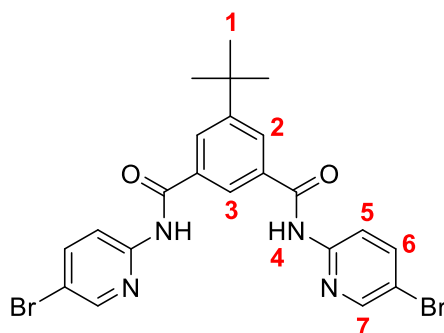


5-*Tert*-butyl isophthalic acid (**13**, 0.550 g, 2.5 mmol, 1 eq, FW = 222.24) was refluxed with 5 mL of  $\text{SOCl}_2$  for 4 hours. The solvent was then evaporated to obtain the corresponding diacid chloride, which was dissolved in 15 mL of dry THF and added dropwise to a solution of 2-amino-5-vinylpyridine (**20**, 0.6 g, 5 mmol, 2 eq, FW = 120.15) and TEA (0.695 mL, 0.5 g, 5 mmol, FW = 101.19, d = 0.726) in anhydrous THF (30 mL) at 0 °C and under a dinitrogen atmosphere. The reaction mixture was stirred at room temperature overnight. The next day the solvent was evaporated and the crude product partitioned between DCM (60 mL) and aqueous saturated  $\text{NaHCO}_3$  (25 mL). The organic layer was then washed with 25 mL of water. The organic layer was dried ( $\text{MgSO}_4$ ), filtered and evaporated to obtain a yellow solid, which was purified by column chromatography (silica gel and 5%, 10% and 20% EtOAc in DCM as eluent). Only 40 mg of monomer **6** were obtained.

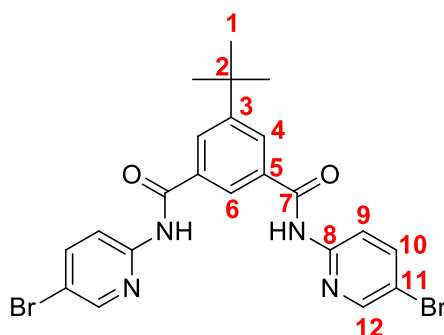
### **PROTOCOL 3**



i) 5-*Tert*-butyl isophthalic acid (**13**, 27.9 mmol, 6.2 g) and 2-amino-5-bromopyridine (63 mmol, 10.73 g) were dissolved in 16.7 mL of DMF. Pyridine (15.74 mL, 82mmol) was added and the mixture left to react for 30 minutes. Then, T3P (50 wt% in DMF, 94.32 mmol, 60 mL) was added dropwise at -20 °C (ice-NaCl bath) after which the reaction was left to stir overnight at room temperature. The next day the solvent was removed and the crude product precipitated in water and filtered. The brown solid was sonicated for 30 minutes in 100 mL 1 N aqueous NaOH (twice) and filtered. The white solid was dried overnight to obtain 5.2 g of **21** (35%)



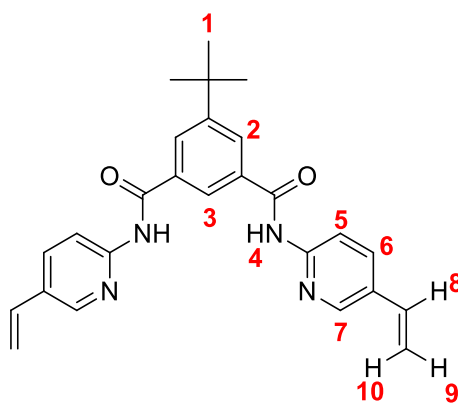
$^1\text{H NMR}$  (400 MHz,  $\text{DMSO-}d_6$ ):  $\delta$  1.389 (s, 9H, tert-butyl- $\text{CH}_3$ , **1**), 8.110 (dd,  $^2J = 2.4$  Hz,  $^3J = 9.2$  Hz, 2H,  $-\text{CH}^4$ , **6**), 8.205 (d,  $^3J = 1.6$  Hz, 2H,  $-\text{CH}^3$ , **5**), 8.248 (d,  $^3J = 8.8$  Hz, 2H,  $-\text{CH}^6$ , **7**), 8.445 (t,  $^3J = 1.6$  Hz, 1H, Ph- $\text{CH-2}$ , **3**), 8.554 (dd,  $^2J = 0.8$  Hz,  $^3J = 2.4$  Hz, 2H, Ph- $\text{CH-4}$  and **6**, **2**), 11.104 (s, 2H, NH, **4**) ppm.



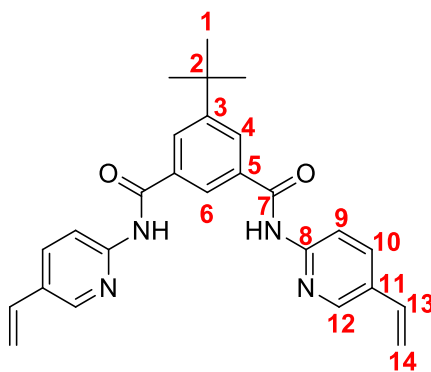
$^{13}\text{C NMR}$  (400 MHz,  $\text{DMSO-}d_6$ ):  $\delta$  31.476 (tert-butyl- $\text{CH}_3$ , **1**), 35.491 (tert-butyl-C, **2**), 114.644 (Py- $\text{CH}_2[\text{C-5}]$ , **11**), 116.624 and 141.331 (Py- $\text{CH}_2[\text{C-3}]$  & Py- $\text{CH}_2[\text{C-4}]$ , **9** & **10**), 125.755 (Ph-C-2, **6**), 129.028 (Ph-C-4 and 6, **4**), 134.273, 149.124 (Py- $\text{CH}_2[\text{C-6}]$ , **12**), 151.723, 152.113, 166.268 ppm.

**MS**  $[\text{M}+\text{H}^+]$ : 533.13. **HRMS** (ESI-TOF)  $m/z$ :  $[\text{M}-\text{H}^+]$  Calcd for  $\text{C}_{22}\text{H}_{20}\text{Br}_2\text{N}_4\text{O}_2$  532.23; Found 531.0032. **IR**: 740, 881, 1091, 1213, 1369, 1499, 1566, 1683, 2962,  $3423\text{ cm}^{-1}$ . **M.p.** = 227-228°C

ii)<sup>114</sup> A stirred solution of **21** (2.9 g, 5.45 mmol, FW = 532.23) in DME under dinitrogen was treated with palladium(0)tetrakis-triphenylphosphine (0.552 mmol, 0.638 g). The reaction mixture was stirred at room temperature for 20 minutes and 2,4,6-trivinylcyclotriboroxane (5.64 mmol, 1.36 g), K<sub>2</sub>CO<sub>3</sub> (11.28 mmol, 1.56 g) and water were added. The reaction mixture was heated under reflux (108 °C) for 2 hours. The reaction mixture was concentrated and the crude product precipitated from water. The crude product was purified by column chromatography (dry column: alumina, PE:EtOAc 7:3) to obtain **M6** (1.13 g, 49%).



<sup>1</sup>H NMR (400 MHz, DMSO-*d*<sub>6</sub>): δ 1.395 (s, 9H, tert-butyl-CH<sub>3</sub>, **1**), 5.34 (dd, <sup>2</sup>J = 2 Hz, <sup>3</sup>J = 11.2 Hz, 2H, CH<sub>cis</sub> =, **9**), 5.93 (dd, <sup>3</sup>J = 18 Hz, 2H, CH<sub>trans</sub> =, **10**), 6.778 (dd, <sup>3</sup>J<sub>cis</sub> = 11.2 Hz, <sup>3</sup>J<sub>trans</sub> = 17.6 Hz, 2H, -CH =, **8**), 8.064 (dd, <sup>2</sup>J = 2.4 Hz, <sup>3</sup>J = 8.8 Hz, 2H, -CH<sup>4</sup>, **6**), 8.20 (d, <sup>3</sup>J = 1.2 Hz, 2H, -CH<sup>3</sup>, **5**), 8.28 (d, <sup>3</sup>J = 8.8 Hz, 2H, -CH<sup>6</sup>, **7**), 8.467 (s, 1H, Ph-CH-2, **3**), 8.493 (d, <sup>3</sup>J = 2.4 Hz, 2H, Ph-CH-4 and 6, **2**), 10.997 (s, 2H, NH, **4**) ppm.



$^{13}\text{C}$  NMR (400 MHz,  $\text{DMSO-}d_6$ ):  $\delta$  31.499 (tert-butyl- $\text{CH}_3$ , **1**), 35.476 (tert-butyl-C, **2**), 114.659 ( $-\text{CH}=\text{}$ , **13**), 115.661 ( $\text{CH}_2=\text{}$ , **14**), 125.525 (Ph-C-2, **6**), 128.913 (Ph-C-4 and 6, **4**), 129.639, 133.509 (Py- $\text{CH}_2$ [C-4], **10**), 134.419 (Py- $\text{CH}_2$ [C-3], **9**), 146.967 (Py- $\text{CH}_2$ [C-6], **12**), 135.420, 152.098, 152.213, 166.115 ppm.

**MS**  $[\text{M}-\text{H}^+]$ : 427. **HRMS** (ESI-TOF)  $m/z$ :  $[\text{M}+\text{H}]^+$  Calcd for  $\text{C}_{26}\text{H}_{26}\text{N}_4\text{O}_2\text{H}$  427.51; Found 427.2128. **IR**: 905.2, 1633.3, 1676.7, 2962.1, 3089.1, 3239.3  $\text{cm}^{-1}$ . **M.p.** = 152-161°C.

#### 4.2.3 Polymer synthesis

<i>Name</i>	<i>Function</i>	<i>mmol</i>	<i>MIP2</i>	<i>NIP2</i>
<i>1,3-bis[[5-vinylpyrid-2-yl]amido]carbonyl-5-tert-butyl-benzene</i>	functional monomer	1	426 mg	426 mg
<i>Biotin-OMe</i>	template	1	258 mg	----
<i>EGDMA</i>	crosslinker	20	3.77 mL (3.96 g)	3.77 mL (3.96 g)
<i>2,2'-azobis(2,4-dimethylvaleronitrile) (ABDV)</i>	initiator		52 mg	52 mg
<i>Chloroform</i>	Solvent/porogen		5.6 mL	5.6 mL

## 4.3 RESULTS AND DISCUSSION

### 4.3.1 Job Plot

A Job plot of the monomer **6**: biotin-OMe complex was made to confirm the 1:1 stoichiometry of the binding interaction. The host and guest do indeed interact in a 1:1 ratio, as predicted, and these NMR studies confirmed our theory (Figure 34).

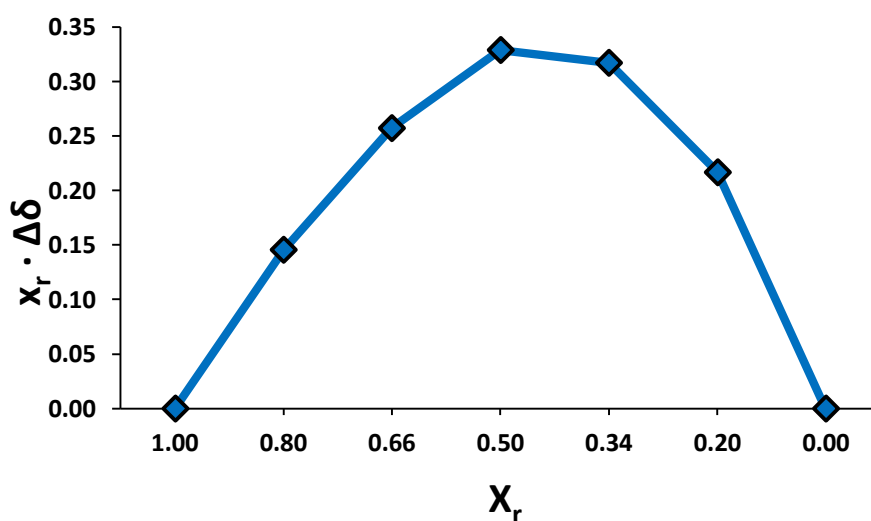


**Figure 34:** Job Plot of monomer **6** with Biotin-OMe. The monomer interact with the analytes in a 1:1 stoichiometric complex. The experiment was made in  $CDCl_3$  using 5mM monomer and template concentration solution.  $X_r$  = molar fraction  $\Delta\delta$  = chemical shift change.

### 4.3.2 $^1H$ NMR titrations

$^1H$  NMR titration studies were performed in  $CDCl_3$  or  $CD_3CN$  at 25°C to study the binding strength of the monomer **6**-template complex in conditions mimicking the pre-polymerisation mixture (Table 13). The methyl ester of biotin<sup>110</sup> was used as the template as it is more soluble in chloroform or acetonitrile than biotin itself and because the free carboxylic group can potentially interact itself with the cleft binding site. The solvent used for the imprinting plays a vital role in the stability of the host-guest complex as the binding constant drop from 1221  $M^{-1}$  to 49  $M^{-1}$  on moving from  $CDCl_3$  to  $CD_3CN$  (Table 13, Figure 35). This data was important to take in consideration when the MIP protocol was prepared. Also TA $\psi$  and phenobarbital were tested with M6, as both have an ureido functionality that is

complementary to the M6. TA $\psi$  forms a reasonably strong 1:1 complex with M6 ( $K_a = 352 \text{ M}^{-1}$ ), while the interaction with phenobarbital is even stronger ( $K_a = 25052 \text{ M}^{-1}$ ). The titration of phenobarbital with M6 was performed using a 0.5mM solution of the template titrated with increasing monomer concentration (Figure 35). At first a 1mM solution was performed, but the experimental error was too high, so the concentration was decreased. This obtained value is still too high in error, so not reliable. Claramunt *et al.* reported an association constant of a similar artificial receptor of  $2442 \text{ M}^{-1}$  with barbital<sup>108</sup>. This latter value seems more realistic. We must remember that a titration needs to be performed in a concentration range that leads to 20-80% complexation so as to avoid saturation.<sup>115</sup> The studies of Claramunt *et al.* also reported that the association constant of the complex of their host with ethylene urea<sup>108</sup> was  $1500 \text{ M}^{-1}$ .

Monomer 6 can be used as a host not only for biotin, but also for barbiturates, and could eventually be used for the imprinting of this class of drugs. Chromatographic studies have showed a strong retention behaviour of the biotin-MIP towards pentobarbital.

**Table 13:** Monomer 6-templates binding constants value.

		$K_a \text{ (M}^{-1}\text{)}$	$\Delta\delta_{max}$	<i>mM</i>	<i>solvent</i>
<b>a</b>	<i>Biotin-Me</i>	1221±15%	2.25±0.08	1	CDCl <sub>3</sub>
<b>b</b>	<i>Phenobarbital</i>	25052±44%	1.40±0.02	0.5	CDCl <sub>3</sub>
<b>c</b>	<i>2',3',4'-tri-O-acetyl Pseudouridine (TA<math>\psi</math>)</i>	352±14%	0.80±0.04	1	CDCl <sub>3</sub>
<b>d</b>	<i>Biotin-Me</i>	49±6%	4.76±0.19	1	CD <sub>3</sub> CN

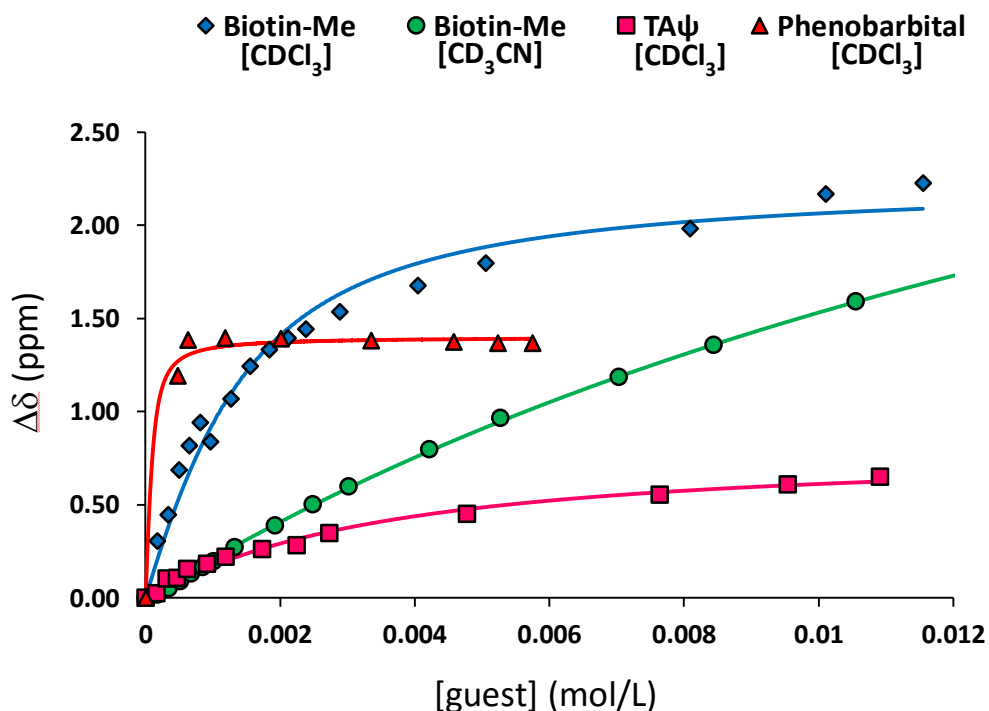


**Figure 35:**  $^1\text{H}$  NMR titration binding isotherms of monomer 6 with different templates. The experiments were performed in chloroform or acetonitrile using 1mM solution of the monomer except for the monomer 6-phenobarbital titration where a 0.5mM solution of Phenobarbital (the “host”) was added an increasing concentration of monomer 6.

### 4.3.3 Chromatographic evaluation

The molecularly imprinted polymer and the control non-imprinted polymer particles (25-50  $\mu\text{m}$ ) were slurry packed into an empty HPLC column to evaluate the specificity and selectivity of these polymers (MIP and NIP). Several analytes, with or without similarity to the imprinted molecule, were passed through the columns, their retention times noted and their retention factors calculated. When pure acetonitrile was used as the eluent, no elution of Biotin-NO<sub>2</sub> was observed within one hour. Thus, a more competitive eluent was used instead (1% acetic acid/acetonitrile [v/v]) (Table 14, Figure 36).

The retention factor for the biotin derivative (Biotin-NO<sub>2</sub>) on MIP2 was 5.3, with poor retention (< 30 seconds) shown on the NIP, leading to an imprinting factor of 10.38 (Table 14). This shows that there is dynamic binding of the biotin species on



the MIP, where the analyte moves freely in the polymer, having access to the imprinted cavities which have been shaped around the template itself. Chromatographic studies prove that the presence of biotin during the polymerisation creates polymeric binding cavities selective towards the template species. Analytes possessing the ureido moiety and a similar or smaller size than the template, e.g. pentobarbital and uracil, were also retained on the MIP. The retention factor for uracil is higher than that for biotin-NO<sub>2</sub>, but the IF smaller, showing that this is not due to a specific binding interaction with the imprinted sites: uracil is a small molecule which can gain easy access and can fit the imprinted cavities, but the interaction is not strictly due to the imprinting process, but is more non-specific in nature, as shown by the retention of the analyte on the NIP. The similar, larger molecules uridine, TAU and 5-MeU are in fact poorly retained on the MIP, despite having similar functionality in their structures.

**Table 14:** Selectivity and specificity of template/analytes on MIP2 and NIP2 in 1% acetic acid/acetonitrile (v/v) as mobile phase. <sup>a</sup> SD (standard deviation, n=3). <sup>b</sup> RSD (relative standard deviation)=(SD/x) \*100, x= mean value.

Analyte	Parameter	MIP	NIP	RSD <sup>b</sup> %
<i>Biotin-NO<sub>2</sub>(I)</i>	k'±SD <sup>a</sup>	<b>5.29±0.05</b>	0.51±0.04	< 7
	α (1)	1	1	
	IF	<b>10.38</b>		
<i>Pentobarbital</i>	k'±SD <sup>a</sup>	<b>11.07±0.04</b>	0.12±0.01	< 7
	α (1)	0.5	4.3	
	IF	<b>92.99</b>		
<i>Phenobarbital</i>	k'±SD <sup>a</sup>	<b>14.80±0.04</b>	0.12±0.01	< 7
	α (1)	0.4	4.3	
	IF	<b>124.30</b>		
<i>Uracil</i>	k'±SD <sup>a</sup>	<b>10.99±0.12</b>	3.34±0.02	< 1
	α (1)	0.5	0.2	
	IF	<b>3.29</b>		
<i>Uridine</i>	k'±SD <sup>a</sup>	1.20±0.07	0.77±0.01	< 6
	α (1)	4.4	0.7	
	IF	1.56		
<i>Adenosine</i>	k'±SD <sup>a</sup>	0.88±0.04	0.81±0.03	< 5
	α (1)	6.0	0.6	
	IF	1.08		
<i>Cytidine</i>	k'±SD <sup>a</sup>	0.99±0.01	0.49±0.04	< 8
	α (1)	5.4	1	
	IF	2.01		
<i>Guanosine</i>	k'±SD <sup>a</sup>	1.15±0.00	0.76±0.00	< 0
	α (1)	4.6	0.7	
	IF	1.53		
<i>TAU</i>	k'±SD <sup>a</sup>	0.33±0.02	0.15±0.01	< 7
	α (1)	16.1	3.3	
	IF	2.16		
<i>TAG</i>	k'±SD <sup>a</sup>	0.25±0.02	0.06±0.00	< 7
	α (1)	21.3	8.9	
	IF	4.35		
<i>TAψ</i>	k'±SD <sup>a</sup>	0.17±0.01	0.06±0.00	< 5
	α (1)	30.5	8.9	
	IF	3.04		
<i>5-MeU</i>	k'±SD <sup>a</sup>	0.84±0.05	0.84±0.08	< 7
	α (1)	6.3	0.6	
	IF	0.99		

Pentobarbital with an imprinting factor of 93 and a retention factor of 11, appears to interact with the MIP in a selective way. The imprinted cavities have the right functionalities, complementary to this molecule's H-bond array, as confirmed by the NMR studies. Also, the nature of pentobarbital is more acidic, which means the formation of stronger H-bond interactions with the binding motif inside the cavities. These results could be used in the future for the development of barbiturate MIPs using monomer 6. As mentioned previously, with MIP1 it was impossible to elute the template in HPLC mode even using a highly competitive and acidic mobile phase, making this polymer unsuitable for chromatographic application. Instead, the use of monomer 6, which is also soluble in chloroform, can lead to the synthesis of a stationary phase for HPLC for the separation of such drugs. On the other hand, as this monomer creates a strong interaction with ethylene urea ( $K_a = 1500 \text{ M}^{-1}$ )<sup>108</sup>, the use of a barbiturate imprinted MIP made with M6, may also lead to cross-reactivity with urea if used in SPE of human urine.

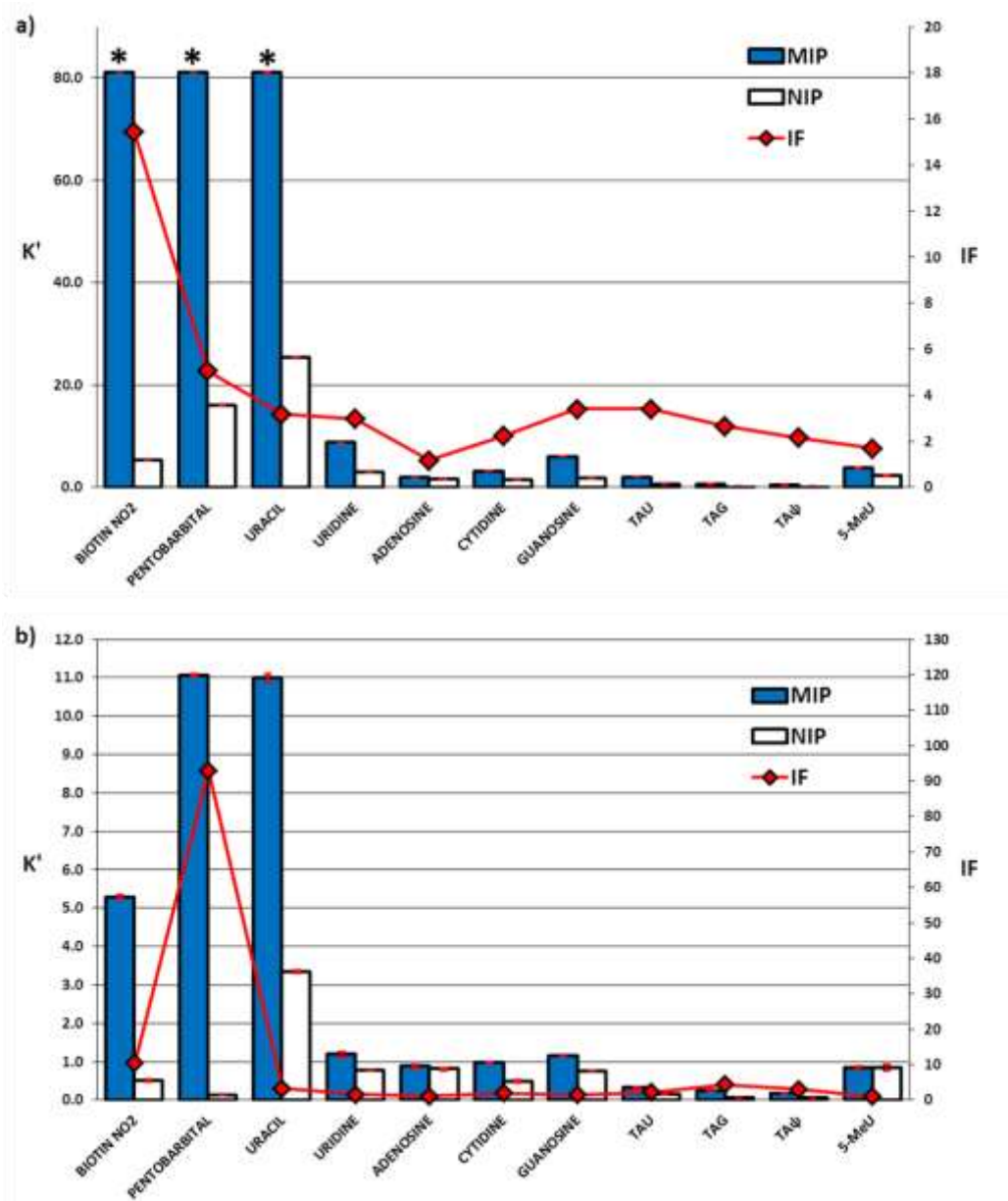


**Figure 36:** Chromatographic evaluation of the Biotin-MIP and NIP using 100% acetonitrile (a) and 1% acetic acid/acetonitrile (v/v) (b) as eluent. [\*] means greater than, based on a run of 1 hour.

When pure acetonitrile was used as the eluent, biotin-NO<sub>2</sub>, pentobarbital and uracil were retained for more than 1 hour. In Figure 36 are shown graphically the results of the chromatographic evaluation of MIP and NIP in each eluent. All analytes differing from the template in terms of H-bond array or shape are non-retained on both the MIP and the NIP.

#### 4.3.4 Equilibrium rebinding experiments

The affinity of the novel polymers towards the template was assessed using equilibrium rebinding experiments. A concentration of 0 – 10 mM biotin-NO<sub>2</sub> in acetonitrile was used to study the quantity of template adsorbed by the polymeric matrices. The affinity constant of the interaction of the template with the polymeric binding cavities and the total number of sites were calculated by fitting the experimental data to the Langmuir model ( $R^2 = 0.99$ ). The supernatant concentration of the free analyte was determined using HPLC using a wavelength of 275 nm and 100% acetonitrile as eluent (Figure 37).

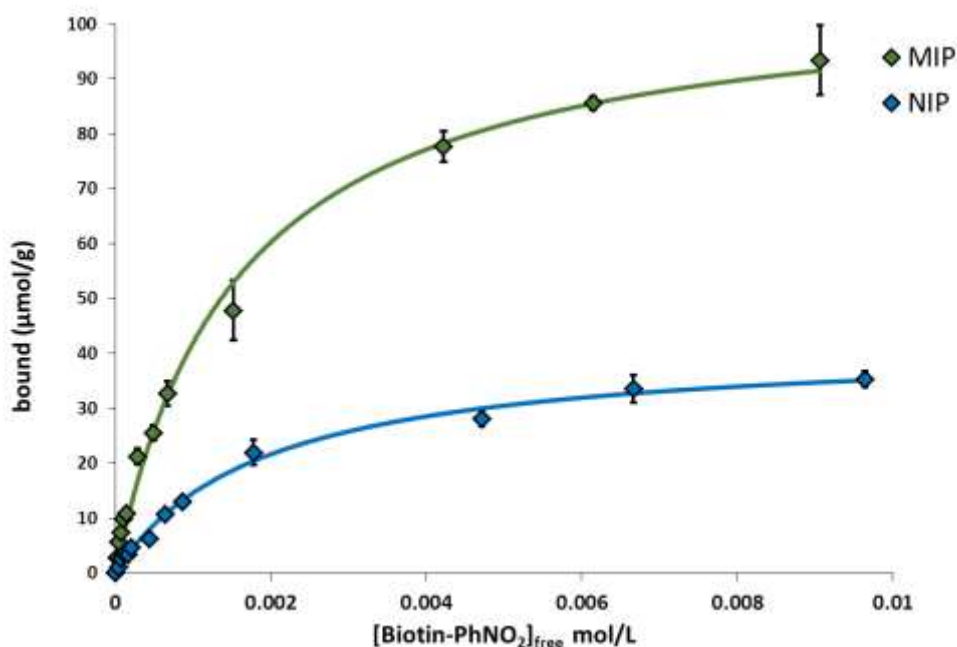


**Figure 37:** Binding isotherms obtained with equilibrium rebinding experiments of MIP2 and NIP2 in acetonitrile. 0-10mM concentration range of Biotin-nitrophenylester were used. The  $[Biotin-nitrophenylester]_{free}$  in the supernatants was evaluated with HPLC (Wavelength: 275 nm, Flow rate: 1mL/min, Injection: 5μL, RSD % < 16, N=3).

**Table 15:** Binding constant ( $k_a$ ) and number of sites ( $N$ ) of MIP2 and NIP2.

	$k_a$	$N$ ( $\mu\text{mol/g}$ )	$R^2$
MIP2	641.03	107.23	0.99343
NIP2	531.9	42	0.99342

The affinities of the binding cavities contained inside the imprinted and non-imprinted polymer are seen to be rather similar. Both polymers show reasonable affinity for the biotin analyte. The difference between the imprinted and non-imprinted polymers appears more due to the actual number of binding cavities present in the materials. Of note is the fact that the number of binding cavities within the imprinted polymer approaches 50% of the theoretical maximum based on the amount of template “given” to the polymerisation.

#### 4.3.5 MISPE

Solid phase extraction using a biotin-imprinted polymer has potential for use in protein purification, where the biotinylated proteins are first retained in the cartridge by the imprinted material and then eluted without the need to use harsh conditions which may compromise the stability of the protein. There are existing technologies which allow for the purification of biotinylated proteins (and other biological macromolecules) without denaturing them, but these can be rather expensive and environmentally sensitive. MIPs offer advantages in terms of cost (far lower) and reusability.

In our preliminary experiments showed in Figure 38, a solution of aqueous 0.1 mM biotin-NO<sub>2</sub> was loaded onto both MIP and NIP (in separate SPE cartridges); the template was retained on both materials. A washing step, using 100% acetonitrile eluted 44% of the template on the MIP2 and 88% on the NIP2, with the remaining analyte eluted with 1% acetic acid/MeOH (v/v). This is a preliminary experiment where 55% of biotin analyte was recuperated. Obviously, optimisation of the SPE method is required to improve this; further, the use of biotinylated macromolecules

as analytes is also necessary in order to prove the possible application of MIP2 in MISPE experiments and protein purification.

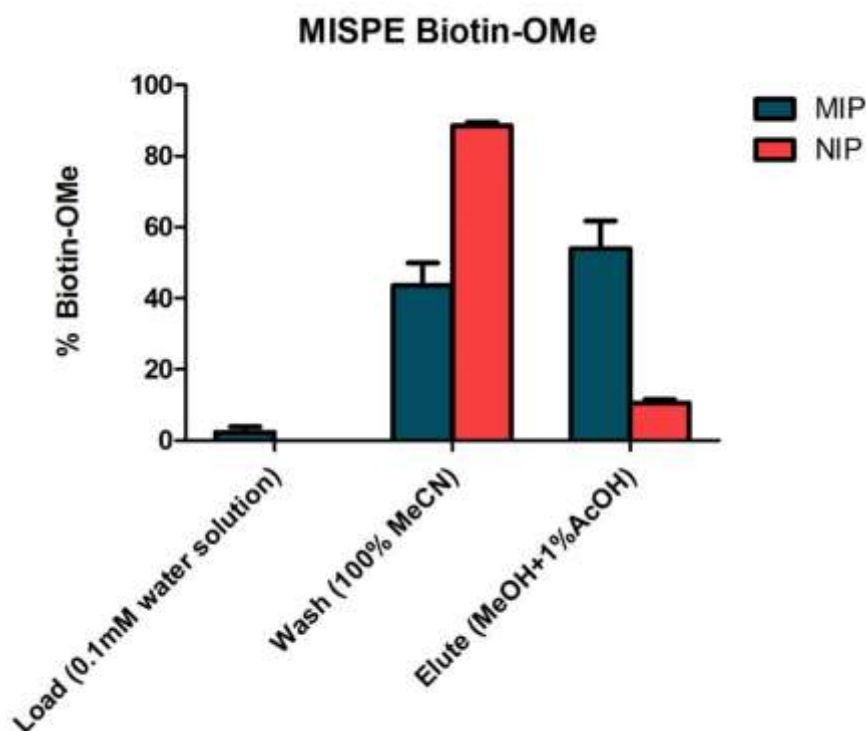


**Figure 38:** Percentage of Biotin eluted in each step (load, wash and elution) through the MIP2 and NIP2.

#### 4.4 CONCLUSIONS

An imprinted polymer for the recognition of biotin is reported. The polymer was prepared using a novel host (monomer 6) for biotin capable of interacting with the ureido functionality of the template via four hydrogen-bonds (Figure 33). The host-guest interaction was studied prior to the synthesis of the polymer using NMR:  $^1\text{H}$  NMR titration and Job plot. By means of these studies, chloroform was chosen as the solvent/porogen, as in this solvent the host-guest complex had a higher association constant (than in acetonitrile) and a 1:1 stoichiometric ratio of template-functional monomer was used, as determined from the Job plot analysis (Figure 34, Table 13).

The biggest challenge here was the synthesis of the new host, as the initial intermediate, 2-amino-5-vinyl pyridine exhibited a low reactivity, causing the

overall yield of monomer to be very low. Three different protocols were developed and the most promising is the two-step reaction protocol where a Suzuki coupling reaction was used to introduce the polymerisable double bond to the host cleft.

Monomer 6 has some good characteristics: great solubility in chloroform, a solvent often used in non-covalent imprinting, and it is a good host for several different analyte classes (barbiturates, pseudouridine and uridine). Later, we will report on the use of monomer 6 for the imprinting of pseudouridine, a urinary biomarker used in post-treatment diagnosis of colorectal cancer and which has also been proposed as a biomarker for other human disease states such as heart failure.<sup>116</sup>

The work presented in this chapter concerning the polymeric receptors represents preliminary studies which give us an idea of the potential of this material. It has been shown to be more selective and specific toward biotin compared to previously reported biotin-MIPs, where MAA and 2-acrylamidopyridine were used as functional monomers.<sup>110</sup>

MIP 2 was made in monolithic form, where the binding cavities are positioned on all surfaces of the polymeric particles. It is unclear at present whether this MIP format and morphology will be the best for the application of the MIP as a synthetic avidin, as biotin will be only the recognition part of macromolecules. Future work should focus on affinity experiments using biotinylated macromolecules: adsorption-desorption kinetics of a small biotin molecule are quick as it moves freely inside the porous material and easily reaches the imprinted cavities. Instead a macromolecule has a more limited access to the binding sites, as size may be a limitation. If a macromolecule, e.g. biotinylated protein cannot move inside the porous material due to its size, it will not interact with the imprinted cavities and there will be no specific binding. “Pull down” experiments will be performed on MIP2 using biotinylated macromolecules. If the experiment is of limited or no success, other polymeric morphologies, as thin film or beads, will be studied. As show in Figure 39, ideally all binding cavities on the MIP will be on the surface of the material, making them more accessible to potential biotinylated substrates.



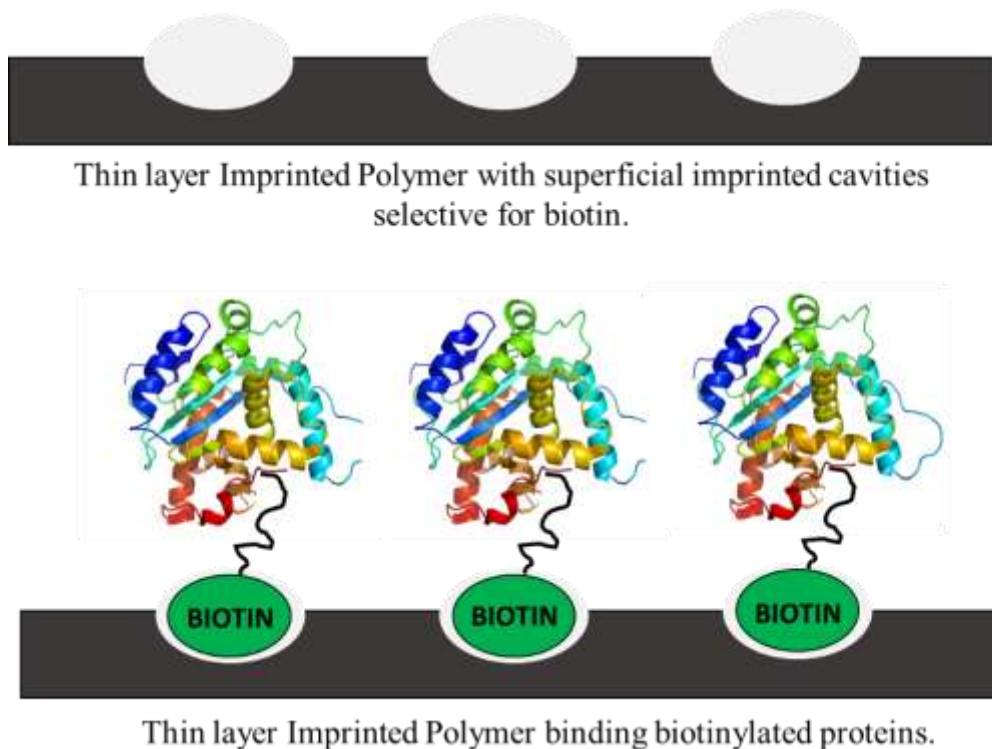
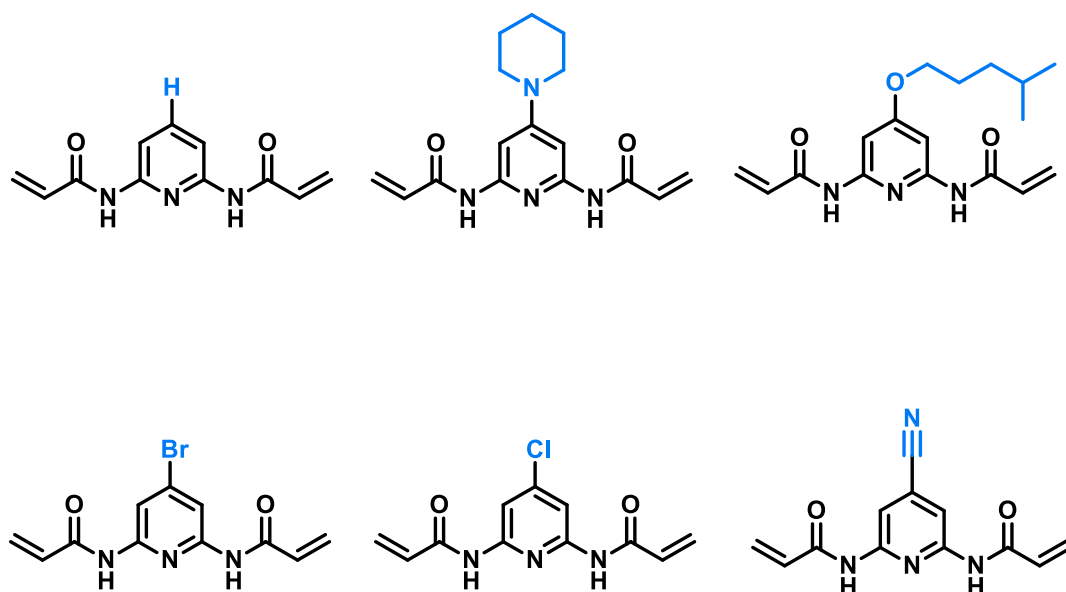


**Figure 39:** *Highly schematic representation of a thin layer Imprinted Polymer for the binding of biotinylated macromolecules.*

# CHAPTER 5

## *4-SUBSTITUTED-2,6-BIS(ACRYLAMIDO)PYRIDINES*



## 5.1 INTRODUCTION

### 5.1.1 The imide structural motif

The imide functionality is a common motif present in a large number of small molecules of pharmaceutical interest, such as 5-fluorouracil and aminoglutethimide, shown in Figure 40. Typical commercially available functional monomers used for the imprinting of these molecules with an A-D-A (acceptor-donor-acceptor) motif are methacrylic acid (MAA) and acrylamide (AA), examples of this being the non-covalent imprinting of phenytoin<sup>117</sup> and 5-methyluridine.<sup>118</sup>

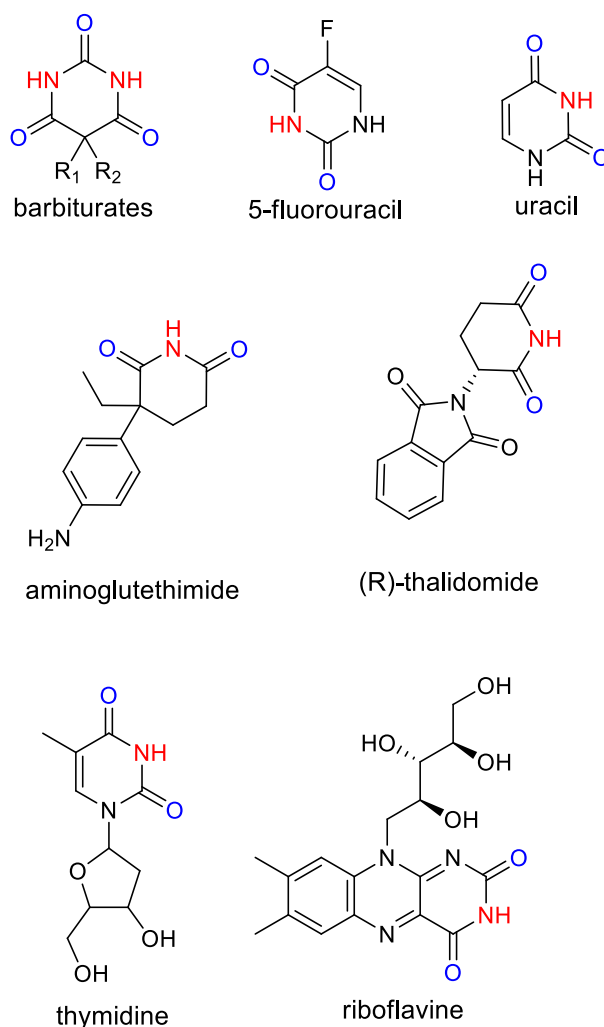


**Figure 40:** Structures of molecules previously imprinted using BAAPy as the functional monomer. The recognition part of the compounds is the imide moiety. Hydrogen bond donors are in red, while hydrogen bond acceptors are in blue.

However both functional monomers need to be used in excess in order to successfully imprint these molecules, as the functional monomer-template complex is not strong enough to create a stoichiometric interaction. Takeuchi<sup>27</sup> was the first to use this functional monomer for the stoichiometric non-covalent imprinting of imide-based molecules. This monomer has a donor-acceptor-donor (D-A-D) moiety complementary to the imido motif (A-D-A) (figure 41) and was first used for the imprinting of barbiturates.<sup>102</sup>

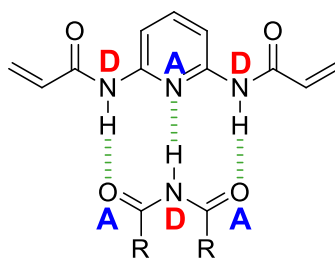


**Figure 41:** BAAPy-template *H*-bonds interactions

Inspiration for the use of this monomer came from the supramolecular studies of Hamilton,<sup>101</sup> who has reported extensively on the development of artificial receptors for barbiturates. The novel functional monomer was a 2,6-*bis*(acrylamido)pyridine (BAAPy), which can interact with any imido moiety via three hydrogen-bonds. It has been demonstrated that BAAPy can be used to create MIPs with high selectivity towards several different templates containing an imido motif in their structure, as demonstrated by the wide use of BAAPy in the years since its introduction to the field by Takeuchi's group. BAAPy interacts with such template molecules with an association constant of the order of 500 – 1000 M<sup>-1</sup> (in chloroform), an interaction strong enough to ensure stoichiometric complexation of the template in the pre-polymerisation mixture, leading to the eventual formation of high affinity binding cavities in the imprinted polymer.

Takeuchi himself has used BAAPy for the imprinting of 5-fluorouracil<sup>119</sup> (5-FU), an antitumor active compound; the functional monomer and template were used in a 1:1 ratio in the preparation of the MIP, obtaining a polymer selective towards 5-FU.

Recently BAAPy was used for the enantiomeric resolution of the breast cancer drug aminoglutethimide<sup>120</sup> and the enantioselective controlled release of (R)-thalidomide<sup>121</sup>. Other examples of stoichiometric imprinting using this functional monomer are the imprinting of thymidine,<sup>122</sup> phenytoin,<sup>117</sup> uridine<sup>95</sup> and riboflavin<sup>35, 61</sup>.

It is evident that BAAPy has a great potential for use with such templates, due to the easy synthesis in a high yield, starting from cheap materials, and the stoichiometric interaction with imide-based templates, which leads to the creation of MIPs with good selectivity in apolar solvents that are also useful for application to aqueous-based samples.

### 5.1.2 Enhancing the properties of BAAPy?

Manesiotis *et al.* reported on the synthesis of novel 6-substituted-2,4-bis(acrylamido)pyrimidines<sup>123</sup> for the recognition of imide containing compounds. In particular, 2,4-bis(acrylamido)-6-piperidinopyrimidine showed in Figure 42 was used in the imprinting of 1-benzyluracil (BU).

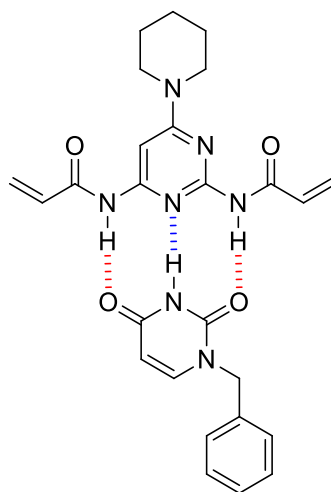


**Figure 42:** 2,4-bis(acrylamido)-6-piperidinopyrimidine and 1-benzyluracil complex previously reported by Manesiotis<sup>123</sup>.

This novel imide receptor creates an improved MIP compared to a traditional BAAPy-based MIP. Unfortunately the  $K_a$  of 2,4-bis(acrylamido)-6-piperidinopyrimidine complex with BU, determined by means of NMR titration ( $K_a = 596 \pm 85 \text{ M}^{-1}$ ), was lower than that of the BAAPY-BU complex ( $K_a = 757 \pm 85$

$M^{-1}$ ), due to the dimerization of former monomer in solution (Figure 43). The enhanced behaviour is due by the presence of an electron-donating group in position 6 of the pyrimidine ring, which increases the basicity of N3 due to the mesomeric effect of the piperidine on the pyrimidine ring; this renders N3 a stronger H-bond acceptor due to its increased basicity (compared to the unsubstituted pyrimidine).

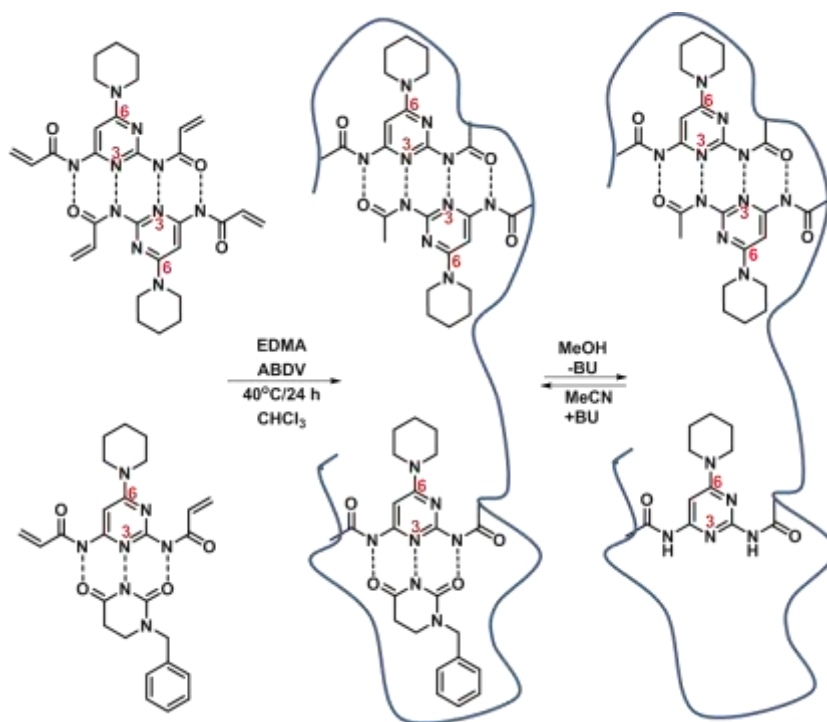


**Figure 43:** Modified scheme showing modes of 2,4-bis(acrylamido)-6-piperidinopyrimidine incorporation in the imprinting of 1-benzyluracil (BU)<sup>123</sup>.

Based on previous studies, we decided to synthesise novel BAAPys, by similarly varying the functionality at the four-position of the pyridine ring.

Electron-withdrawing groups, such as Br, Cl and CN, should decrease the  $pK_a$  of the ring nitrogen, making the nitrogen less basic. Hence, its ability as a hydrogen bond acceptor should be lessened. On the other hand, electron-donating groups, such as an alkoxy group, should increase the  $pK_a$  of the ring nitrogen, making it a better hydrogen bond acceptor.

BAAPy does not engage in homo-dimer formation, and so it is possible to study the host-guest complex formation using NMR titration techniques, without the need to consider other types of complexation, which is not the case with the analogous pyrimidine-based monomers.

As mentioned, based on the nature of the substituents at the 4-position the ring nitrogen of BAAPy should have either increased or decreased basicity, thus modifying the binding strength of the monomer with the imide motif of any putative template (Figure 44).

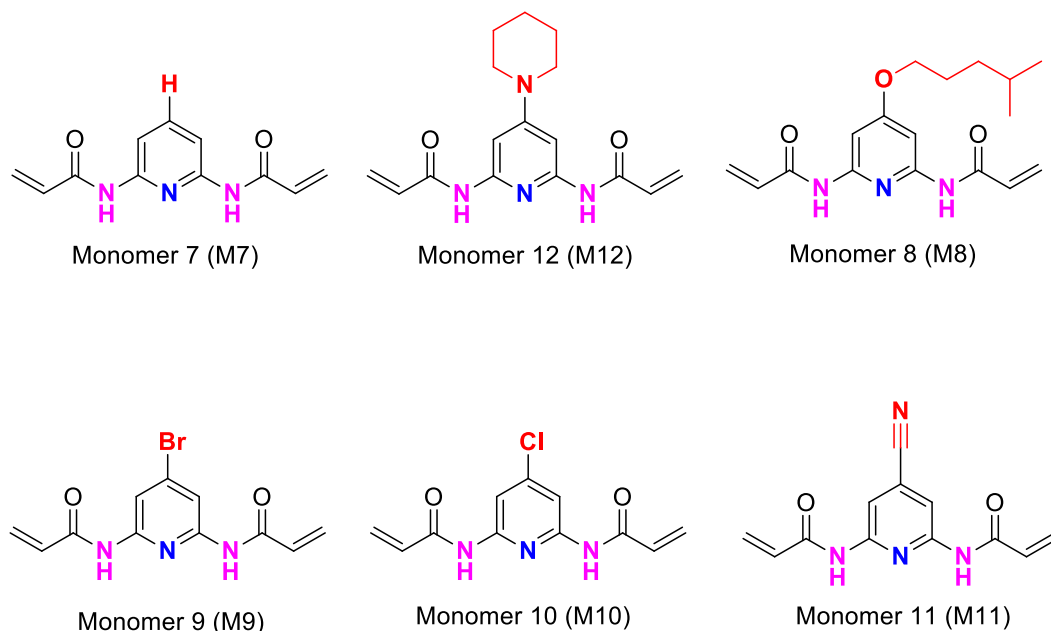


**Figure 44:** Novel 4-substituted BAAPy functional monomers. Six different groups in four-position (red). Hydrogen-bond donor (pink) and hydrogen-bond acceptor (blue).

Nonetheless, the substituted group can have an inductive and/or mesomeric effect that affects not only the basicity of ring nitrogen, but also the acidity of the amido NHs at the 2- and 6-positions; thus, the ability of the substituted BAAPys to bind to a template will be a balance between these effects.

Halogens (Br and Cl), and the cyano group were chosen as the electron withdrawing functionalities, with the 3-methylbutoxy and piperidino groups serving as the electron-donating groups. Here we report on the synthesis of these 4-substituted-2,6-bis(acrylamido)pyridines (Figure 44) and the evaluation of their ability to form complexes with Tegafur, a model guest/template, by means of  $^1\text{H}$  NMR titrations. All monomers are seen to perform in accordance with the increase of their ring nitrogen basicity, which is related to the mesomeric effect of the substituent at the 4-position.

## 5.2 EXPERIMENTAL

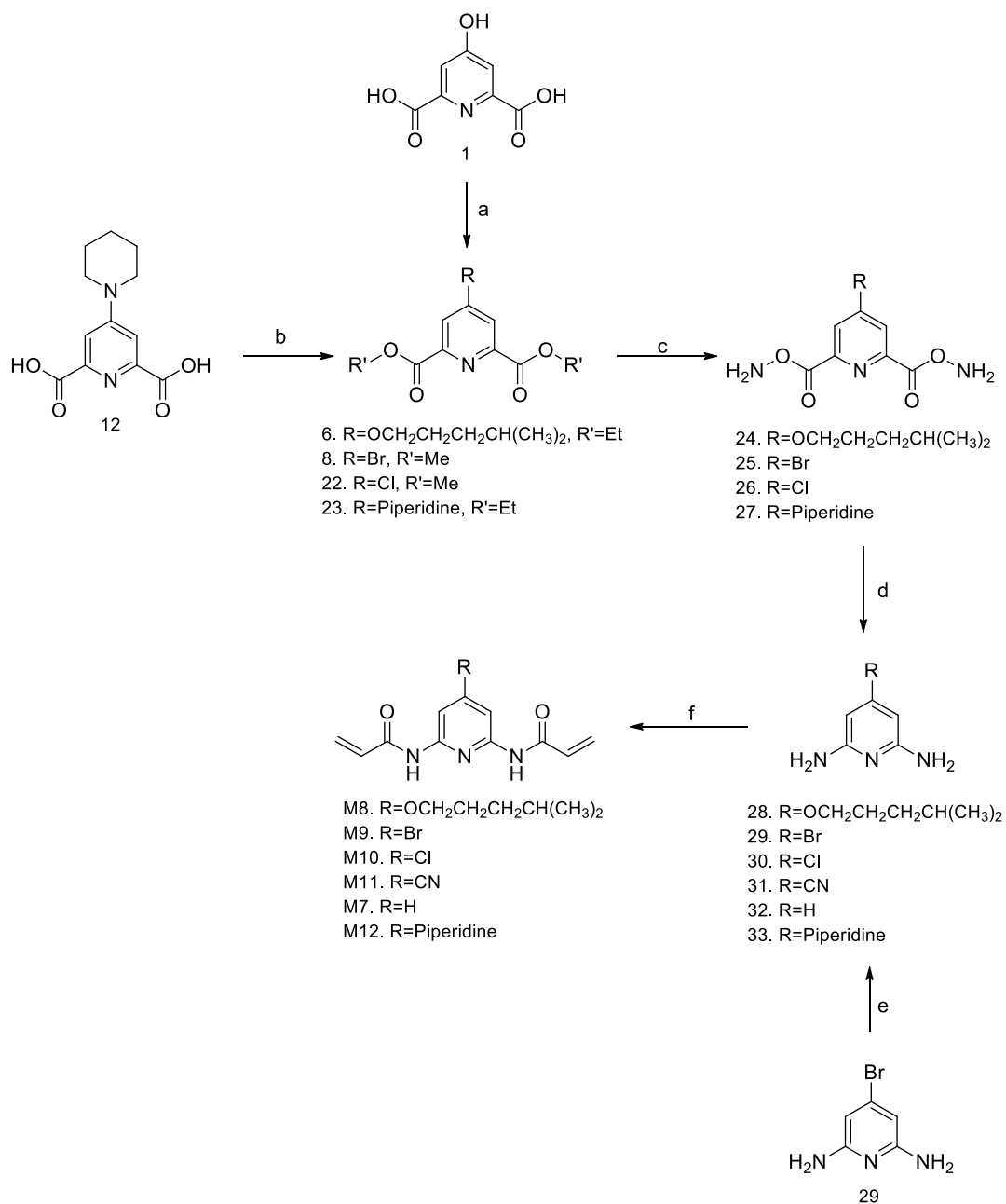


**Figure 45:** Scheme of monomers 7-12 synthesis. **a.** i)  $PBr_5$ ,  $130^\circ C$ , 4h; ii)  $MeOH$ ,  $0^\circ C$ ; **b.**  $EtOH$ ,  $H_2SO_4$ , 7 h, reflux; **c.**  $NH_3$  7N in  $MeOH$ , 3h, RT; **d.**  $KOH$  5M,  $Br_2$ ,  $90^\circ C$ , 5h; **e.** i) 50% aqueous solution piperidine,  $175^\circ C$ , 24 h; ii)  $CuCN$ ,  $DMF$ , sealed tube,  $190^\circ C$ , 3h; **f.**  $THF$  or  $DCM$ ,  $TEA$ ,  $CH_2=CHCOCl$ ,  $N_2$ ,  $0^\circ C \rightarrow RT$ , overnight.



### 5.2.1 Synthesis of 2,6-bis(acrylamido)pyridine (monomer 7)

To a solution of 2,6-diaminopyridine (**32**, 2 g, 0.018 mol), triethylamine (0.055 mol, 7.66 mL) and anhydrous DCM (150 mL), 3.72 mL of acryloyl chloride (0.0458 mol) dissolved in 15 mL of DCM was added slowly in an ice bath and under a dinitrogen atmosphere. The reaction mixture was stirred at room temperature overnight. The next day water was added to quench any unreacted acryloyl chloride. The organic layer was then extracted with saturated aqueous sodium bicarbonate (2 × 100 mL) and brine (100 mL). The organic layer was collected and dried over MgSO<sub>4</sub>, filtered and the filtrate evaporated. The residue was then purified by column chromatography (6:4, PE-ethyl acetate). The monomer was precipitated into PE from DCM. The white crystals were filtered and washed with PE (1.73g, 45%). **<sup>1</sup>H NMR** (400 MHz, DMSO-*d*<sub>6</sub>): δ 5.79 (dd, <sup>2</sup>J = 2 Hz, <sup>3</sup>J=10.2 Hz, 2H, -CH<sub>cis</sub>=), 6.31 (dd, <sup>2</sup>J = 2 Hz, <sup>3</sup>J=17 Hz, 2H, -CH<sub>trans</sub>=), 6.65 (dd, <sup>3</sup>J<sub>cis</sub>= 10 Hz, <sup>3</sup>J<sub>trans</sub>= 17.2 Hz, 2H, CH=), 7.79 (dd, <sup>3</sup>J=6.8, 2.4 Hz, 1H, CH-Ar), 7.87 (d, <sup>3</sup>J=7.2 Hz, 2H, CH-Ar), 10.31 (s, 2H, NH) ppm. **<sup>13</sup>C NMR** (400 MHz, CDCl<sub>3</sub>): δ 110.20 (CH-Ar), 128.86 (CH<sub>2</sub>=), 130.87 (CH=), 141.02 (C-H), 149.55 (C=O), 163.58 (C=N) ppm. **MS** [M+H<sup>+</sup>]: 218.2. **HRMS** (ESI-TOF) m/z: [M+H]<sup>+</sup> Calcd for C<sub>11</sub>H<sub>11</sub>N<sub>3</sub>O<sub>2</sub>H 218.22; Found 218.0934. **IR**: 694.7, 979, 1313, 1584, 1677, 3325 cm<sup>-1</sup>. **M.p.** = 115-118°C.

### 5.2.2 Synthesis of 4-(3-methyl-butoxy)-2,6-bis(acrylamido)pyridine (monomer 8)

4-(3-methyl-butoxy)-2,6-pyridinediamide (**24**). Diethyl 4-(3-methyl-butoxy)-2,6-pyridinedicarboxylate (**6**, 11.92 g, 0.038 mol) was stirred with MeOH (10 mL) and a saturated solution of ammonia in MeOH (7 M, 50 mL) for 4.5 hours at room temperature. The solvent was removed under reduced pressure to give the corresponding diamide as a white powder (9.39g, 99%). **<sup>1</sup>H NMR** (400 MHz, DMSO-*d*<sub>6</sub>): δ 0.94 (d, <sup>3</sup>J = 6.0 Hz, 6H, -CH-CH<sub>3</sub>), 1.66 (q, <sup>3</sup>J = 6.4 Hz, 2H, -O-CH<sub>2</sub>-CH<sub>2</sub>-CH-), 1.79 (m, <sup>3</sup>J = 7.2 Hz, 1H, -CH-), 4.22 (t, <sup>3</sup>J = 6.8 Hz, 2H, -O-CH<sub>2</sub>-CH<sub>2</sub>-CH-), 7.65 (s, 2H, CH-Ar), 7.70-8.84 (s, 4H, NH<sub>2</sub>) ppm. **<sup>13</sup>C NMR** (400 MHz, DMSO-*d*<sub>6</sub>): δ 22.92 (-CH-CH<sub>3</sub>), 25.11(-CH-), 37.45 (-O-CH<sub>2</sub>-CH<sub>2</sub>-CH-), 67.53 (-O-CH<sub>2</sub>-CH<sub>2</sub>-CH-), 110.67 (CH-Ar), 151.69 (C-O), 165.82 (C=O), 167.63 (C=N) ppm. **MS** [M+H<sup>+</sup>]: 252.2. **HRMS** (ESI-TOF) m/z: [M+H]<sup>+</sup> Calcd for

$C_{12}H_{17}N_3O_3H$  252.28; Found 252.1349. **IR**: 1030.5, 1661.5, 3422.3  $cm^{-1}$ . **M.p.**: 220-245 °C.

4-(3-methyl-butoxy)-2,6-pyridinediamina (**28**)<sup>124</sup>. 4-(3-methyl-butoxy)-2,6-pyridinediamide (**24**, 5 g, 0.02 mol) was added to an aqueous solution of potassium hydroxide (5 M, 50 mL) and bromine (0.05 mol, 2.55 mL). The resulting reaction mixture was heated to 90°C for 5 hours. After cooling down, the solution was filtered and the filtrate extracted with DCM (4 × 100mL). The organic phase was dried over  $MgSO_4$  and the solvent evaporated under reduced pressure to give **5** as a copper-coloured solid (610 mg, 15%). **<sup>1</sup>H NMR** (400 MHz,  $DMSO-d_6$ ):  $\delta$  0.90 (d,  $^3J=6.4$  Hz, 6H, -CH-CH<sub>3</sub>), 1.54 (q,  $^3J=6.8$  Hz, 2H, -O-CH<sub>2</sub>-CH<sub>2</sub>-CH-), 1.71 (m,  $^3J=7.4$  Hz, 1H, -CH-), 3.85 (t,  $^3J=6.8$  Hz, 2H, -O-CH<sub>2</sub>-CH<sub>2</sub>-CH-), 5.25 (s, 2H, CH-Ar), 5.22 (s, 4H, NH<sub>2</sub>) ppm. **<sup>13</sup>C NMR** (400 MHz,  $DMSO-d_6$ ):  $\delta$  23.32 (-CH-CH<sub>3</sub>), 25.53(-CH-), 38.25 (-O-CH<sub>2</sub>-CH<sub>2</sub>-CH-), 65.81 (-O-CH<sub>2</sub>-CH<sub>2</sub>-CH-), 83.02 (CH-Ar), 160.86 (C-O), 168.16 (C=N) ppm. **MS** [M+H<sup>+</sup>]: 196.2. **HRMS** (ESI-TOF) m/z: [M+H]<sup>+</sup> Calcd for  $C_{10}H_{17}N_3OH$  196.26; Found 196.1456. **IR**: 1187, 1578, 3438  $cm^{-1}$ . **M.p.**: 136-139°C.

4-(3-methyl-butoxy)-2,6-bis(acrylamido)pyridine (**monomer 8**). To a solution of 4-(3-methyl-butoxy)-2,6-pyridinediamine (**28**, 350 mg, 1.8 mmol), triethylamine (6.3 mmol, 0.88 mL) in anhydrous DCM (60 mL), 0.44 mL of acryloyl chloride (5.4 mol, 0.5 g) dissolved in 10 mL of DCM was added slowly in an ice bath and under a dinitrogen atmosphere. The solution was stirred overnight at room temperature. The reaction mixture was then extracted with water (60 mL) and saturated sodium bicarbonate (2 × 60 mL). The organic layer was collected and dried over  $MgSO_4$ . The compound was purified column chromatography (PE and ethyl acetate, 7:3) using a small amount of DCM to solubilize the crude. A brown-red oil was obtained, which was crystallized from a mixture of DCM and PE. White ivory crystals were formed (100 mg, 18.30%). **<sup>1</sup>H NMR** (400 MHz,  $DMSO-d_6$ ):  $\delta$  0.94 (d,  $^3J=6.8$  Hz, 6H, -CH-CH<sub>3</sub>), 1.64 (q,  $^3J=6.4$  Hz, 2H, -O-CH<sub>2</sub>-CH<sub>2</sub>-CH-), 1.77 (m,  $^3J=6.8$  Hz, 1H, -CH-), 4.07 (t,  $^3J=6.4$  Hz, 2H, -O-CH<sub>2</sub>-CH<sub>2</sub>-CH-), 5.78 (dd,  $^2J=2$  Hz,  $^3J=10.2$  Hz, 2H, -CH<sub>cis</sub>=), 6.29 (dd,  $^2J=2$  Hz,  $^3J=16$  Hz, 2H, -CH<sub>trans</sub>=), 6.64 (dd,  $^3J_{cis}=10.4$  Hz,  $^3J_{trans}=16.8$  Hz, 2H, CH=), 7.54(s, 2H, CH-Ar), 10.23 (s, 2H, NH) ppm. **<sup>13</sup>C NMR** (400 MHz,  $DMSO-d_6$ ):  $\delta$  23.31 (-CH-CH<sub>3</sub>), 25.49 (-CH-), 37.92 (-

O-CH<sub>2</sub>-CH<sub>2</sub>-CH-), 67.22 (-O-CH<sub>2</sub>-CH<sub>2</sub>-CH-), 97.31 (CH-Ar), 128.76 (CH<sub>2</sub>=), 132.50 (CH=), 152.34 (C-O), 164.76 (C=O), 168.29 (C=N) ppm. **MS** [M+H<sup>+</sup>]: 303.4 **IR**: 720, 745, 978, 1210, 1309, 1429, 1575, 1614, 1669, 2957, 3234 cm<sup>-1</sup>. **M.p.**: 98-100 °C.

### 5.2.3 Synthesis of 4-Bromo-2,6-bis(acrylamido)pyridine (monomer 9)

*4-bromo-2,6-dimethylpyridinedicarboxylate (22)*. Chelidamic acid (**1**, 3.12 g, 17 mmol) and phosphorous pentabromide (25 g, 58 mmol) were stirred and heated at 135°C for 4 hours. After 4 hours the solution was cooled to room temperature and chloroform (250 mL) was added and the mixture filtered. The filtrate was cooled to 0°C and MeOH (15 mL) was added drop wise. The solvent was removed under reduced pressure and the crude recrystallized from DCM. The white soft crystals were filtered and washed with cold MeOH and PE (3.48 g, 74.7%). **<sup>1</sup>H NMR** (400 MHz, CDCl<sub>3</sub>): δ 4.04 (s, 6H, -CH<sub>3</sub>), 8.46 (s, 2H, CH-Ar) ppm. **<sup>13</sup>C NMR** (400 MHz, CDCl<sub>3</sub>): δ 53.82 (-CH<sub>3</sub>), 131.64 (CH-Ar), 135.45 (-C-Br), 149.42 (C=O), 164.34 (C-Ar) ppm. **MS** [M+H<sup>+</sup>]: 274.0. **IR**: 1194, 1716, 2952, 3077 cm<sup>-1</sup>. **M.p.**: 164-167°C.

*4-Bromo-2,6-pyridinediamide (25)*. Dimethyl 4-bromo-2,6-pyridinedicarboxylate (**22**, 2 g, 7.3 mmol) was stirred with MeOH (20 mL) and a saturated solution of ammonia in MeOH (7 M, 30 mL) for 4 hours at room temperature. The solvent was removed under reduced pressure to give the corresponding diamide as a white powder (1.7 g, 95.5%). **<sup>1</sup>H NMR** (300 MHz, DMSO-*d*<sub>6</sub>): δ 7.85-8.90 (s, 4H, NH<sub>2</sub>), 8.30 (s, 2H, CH-Ar) ppm. **<sup>13</sup>C NMR** (300 MHz, DMSO-*d*<sub>6</sub>): δ 127.56 (CH-Ar), 135.50 (-C-Br), 151.03 (C=O), 164.65 (C-Ar) ppm. **MS** [M+H<sup>+</sup>]: 246.1. **IR**: 630, 788, 902, 1556, 1649, 3130, 3361 cm<sup>-1</sup>. **M.p.**: 304-307°C.

*4-Bromo-2,6-pyridinediamine (29)*. 4-Bromo-2,6-pyridinediamide (**25**, 1.5 g, 6.15 mmol) was added to an aqueous solution of potassium hydroxide (5 M, 16 mL) and bromine (0.016 mol, 0.82 mL). The resulting reaction mixture was heated to 90°C for 5 hours. After 5 hours the reaction mixture was cooled down in ice, and a precipitate was formed. After filtration, the filtrate was extracted with ethyl acetate (3 × 50 mL). The combined organic layers were dried over magnesium sulphate and evaporated to give a light orange solid (350 mg, 22.5%). **<sup>1</sup>H NMR** (400 MHz,

DMSO- $d_6$ ):  $\delta$  5.66 (s, 4H, NH<sub>2</sub>), 5.78 (s, 2H, CH-Ar), ppm. <sup>13</sup>C NMR (400 MHz, DMSO- $d_6$ ):  $\delta$  98.22 (CH-Ar), 133.35 (-C-Br), 160.60 (C-Ar) ppm. MS [M+H<sup>+</sup>]: 188. IR: 1554, 1624, 2720, 3319, 3408 cm<sup>-1</sup>. M.p.: 125-127 °C.

*4-Bromo-2,6-bis(acrylamido)pyridine (monomer 9)*. To a solution of 4-Bromo-2,6-pyridinediamine (**29**, 0.32 g, 1.7 mmol), triethylamine (5.95 mol, 0.83 mL) and anhydrous DCM (60 mL), 0.42 mL of acryloyl chloride (5.1 mmol) dissolved in 10 mL of DCM was added slowly in an ice bath and under a dinitrogen atmosphere. The mixture was stirred overnight at room temperature. The monomer was obtained as a solid insoluble in the reaction mixture, which was filtered and washed with water and a saturated aqueous solution of sodium bicarbonate (170 mg, 34%). <sup>1</sup>H NMR (400 MHz, DMSO- $d_6$ ):  $\delta$  5.82 (dd, <sup>2</sup>J = 2 Hz, <sup>3</sup>J = 10 Hz, 2H, -CH<sub>cis</sub>=), 6.33 (dd, <sup>2</sup>J = 1.6 Hz, <sup>3</sup>J = 17.2 Hz, 2H, -CH<sub>trans</sub>=), 6.65 (dd, <sup>3</sup>J<sub>cis</sub> = 10 Hz, <sup>3</sup>J<sub>trans</sub> = 17.2 Hz, 2H, CH=), 8.12 (s, 2H, CH-Ar), 10.56 (s, 2H, NH) ppm. <sup>13</sup>C NMR (400 MHz, DMSO- $d_6$ ):  $\delta$  112.99 (CH-Ar), 129.41 (CH<sub>2</sub>=), 132.14 (CH=), 134.93 (C-Br), 152.17 (C=O), 165.01 (C=N) ppm. MS [M+H<sup>+</sup>]: 298. HRMS (ESI-TOF) m/z: [M]<sup>+</sup> Calcd for C<sub>11</sub>H<sub>10</sub>BrN<sub>3</sub>O<sub>2</sub> 296.12; Found 296.0035. IR: 701.9, 978.1, 1310, 1568, 1627, 1679, 3265 cm<sup>-1</sup>. M.p.: 225-228 °C.

#### 5.2.4 Synthesis of 4-Chloro-2,6-bis(acrylamido)pyridine (monomer 10)

*4-Chloro-2,6-pyridinediamide (26)*. Dimethyl 4-Chloro-2,6-pyridinedicarboxylate (**5a**, 2 g, 8.71 mmol) was stirred with MeOH (30 mL) and a saturated solution of ammonia in MeOH (7 M, 25 mL) for 5 hours at room temperature. The solvent was removed under reduced pressure to give the corresponding diamide as a white powder (1.66g, 95%). <sup>1</sup>H NMR (300 MHz, DMSO- $d_6$ ):  $\delta$  7.87-8.916 (s, 4H, NH<sub>2</sub>), 8.169 (s, 2H, CH-Ar) ppm. <sup>13</sup>C NMR (300 MHz, DMSO- $d_6$ ):  $\delta$  124.58 (CH-Ar), 146.53 (-C-Cl), 151.44 (C=O), 164.69 (C-Ar) ppm. MS [M+H<sup>+</sup>]: 200.1. IR: 1423, 1668, 3243, 3398 cm<sup>-1</sup>. M.p.: 315-328 °C.

*4-Chloro-2,6-pyridinediamine (30)*. 4-Chloro-2,6-pyridinediamide (**26**, 1.5g, 7.5mmol) was added to an aqueous solution of potassium hydroxide (5 M, 19 mL) and bromine (0.0195 mol, 1 mL). The resulting reaction mixture was heated to 90°C for 5 hours. After 5 hours the reaction mixture was cooled down in ice and a

precipitate formed. After filtration, the filtrate was extracted with ethyl acetate (3 x 50 mL). The organic layers were dried over magnesium sulfate and evaporated to give a light brown solid (650 mg, 60%).  $^1\text{H NMR}$  (300 MHz, DMSO- $d_6$ ):  $\delta$  5.63 (s, 2H, CH-Ar), 5.67 (s, 4H, NH<sub>2</sub>) ppm.  $^{13}\text{C NMR}$  (300 MHz, DMSO- $d_6$ ):  $\delta$  94.97 (CH-Ar), 143.81 (-C-Cl), 160.34 (C-Ar) ppm. **MS** [M+CH<sub>3</sub>CN]: 185.1. **IR**: 1558, 1617, 3168, 3309, 3420 cm<sup>-1</sup>. **M.p.**: 100-102 °C.

*4-Chloro-2,6-bis(acrylamido)pyridine (monomer 10)*. To a solution of 4-Chloro-2,6-pyridinediamine (**30**, 0.55 g, 3.83 mmol), triethylamine (0.0115 mol, 1.6 mL) and anhydrous DCM (100 mL), 0.78 mL of acryloyl chloride (0.0096 mol) diluted in 10 mL of DCM were added slowly in an ice bath and under a dinitrogen atmosphere. The solution was stirred overnight at room temperature. Thereafter, the solvent was removed by under vacuum and a pale yellow solid was obtained, which was then washed with brine (100 mL), saturated aqueous sodium bicarbonate (100 mL) and water. The yellow solid was freeze-dried overnight to obtain 740 mg of product (77% yield).  $^1\text{H NMR}$  (400 MHz, DMSO- $d_6$ ):  $\delta$  5.83 (dd,  $^2\text{J} = 1.6$  Hz,  $^3\text{J} = 10.2$  Hz, 2H, -CH<sub>cis</sub>=), 6.34 (dd,  $^2\text{J} = 1.6$  Hz,  $^3\text{J} = 16.8$  Hz, 2H, -CH<sub>trans</sub>=), 6.65 (dd,  $^3\text{J}_{\text{cis}} = 10$  Hz,  $^3\text{J}_{\text{trans}} = 17$  Hz, 2H, CH=), 7.98 (s, 2H, CH-Ar), 10.58 (s, 2H, NH) ppm.  $^{13}\text{C NMR}$  (400 MHz, DMSO- $d_6$ ):  $\delta$  110.10 (CH-Ar), 129.49 (CH<sub>2</sub>=), 132.10 (CH=), 145.93 (C-Cl), 152.24 (C=O), 165.03 (C=N) ppm. **MS** [M+H<sup>+</sup>]: 252.2. **HRMS** (ESI-TOF) m/z: [M+H]<sup>+</sup> Calcd for C<sub>11</sub>H<sub>10</sub>ClN<sub>3</sub>O<sub>2</sub>H 252.67; Found 252.0549. **IR**: 690.7, 977.8, 1311, 1569, 1623, 1679, 3265 cm<sup>-1</sup>. **M.p.**: 221-223 °C.

### 5.2.5 Synthesis of 4-Cyano-2,6-bis(acrylamido)pyridine (monomer 11)

*4-Cyano-2,6-pyridinediamina (31)*<sup>125</sup>. A mixture of 2,6-diamino-4-bromopyridine (**29**, 1 g, 0.0053 mol) and copper (I) cyanide (0.992 g, 0.011 mol) in 10 mL DMF was heated in a sealed tube at 190 °C for 3 hours. The resulting mixture was stirred for 2 hours in a mixture of 10% aqueous ammonium chloride (50 mL) and ethyl acetate (80 mL). The phases were separated and the aqueous phase extracted with ethyl acetate (80 mL). The organic phases were combined and washed with brine (100 mL), dried over magnesium sulfate, filtered and the filtrate evaporated. The solid residue was dissolved in hot ethyl acetate and petrol ether was added until crystallization began. The mixture was cooled to room temperature and the yellowish crystals were collected by filtration (160 mg, 22%).  $^1\text{H NMR}$  (400 MHz,

DMSO-*d*<sub>6</sub>):  $\delta$  5.83 (s, 2H, CH-Ar), 5.95 (s, 4H, NH<sub>2</sub>) ppm. <sup>13</sup>C NMR (400 MHz, DMSO-*d*<sub>6</sub>):  $\delta$  96.97 (CH-Ar), 119.33 (-CN), 121.30 (-C-Br), 160.35 (C-Ar) ppm. MS [M+H<sup>+</sup>]: 134.1 IR: 623, 1429, 1554, 1643, 2233, 3184, 3361, 3448 cm<sup>-1</sup>. M.p. = 199-202 °C.

*4-Cyano-2,6-bis(acrylamido)pyridine (monomer 11)*. To a solution of 4-Cyano-2,6-pyridinediamine (**31**, 150 mg, 1.12 mmol), triethylamine (3.92 mmol, 0.546 mL) and anhydrous THF (6 mL), acryloyl chloride (3.35 mmol, 0.27 mL) dissolved in THF was added slowly in an ice bath and under a dinitrogen atmosphere. The mixture was stirred overnight at room temperature. The solvent was evaporated to lead to a brown solid, which was purified by column chromatography using first ether and then ethyl acetate as eluent (50 mg, 18%). <sup>1</sup>H NMR (400 MHz, DMSO-*d*<sub>6</sub>):  $\delta$  5.83 (dd, <sup>2</sup>J = 2 Hz, <sup>3</sup>J = 9.6 Hz, 2H, -CH<sub>cis</sub>=), 6.36 (dd, <sup>2</sup>J = 2 Hz, <sup>3</sup>J = 17 Hz, 2H, -CH<sub>trans</sub>=), 6.67 (dd, <sup>3</sup>J<sub>cis</sub> = 10.4 Hz, <sup>3</sup>J<sub>trans</sub> = 17 Hz, 2H, CH=), 8.17 (s, 2H, CH-Ar), 10.77 (s, 2H, NH) ppm. <sup>13</sup>C NMR (400 MHz, DMSO-*d*<sub>6</sub>):  $\delta$  117.96 (-CN) 111.97(CH-Ar), 129.84 (CH<sub>2</sub>=), 131.89 (CH=), 123.26 (C-CN), 152.26 (C=O), 165.16 (C=N) ppm. MS [M+H<sup>+</sup>]: 242.2. IR: 792, 1411, 1567, 1668, 1705, 2242, 2423, 3340, 3390 cm<sup>-1</sup>.

### 5.2.6 Synthesis of 4- Piperidino-2,6-bis(acrylamido)pyridine (monomer 12)

*4- piperidino -2,6-pyridinediamine (33)*. 2,6-diamino-4-bromopyridine (**29**, 476 mg, 0.0025 mol) was reacted with 10 mL 50% (v/v) aqueous piperidine in a sealed tube, at 155°C, for 24 hours. The next day the reaction mixture was evaporated and the solid washed with water to remove the remaining piperidine. 100 mg of dry crude was recuperated. Compound 33 was purified by column chromatography using 20:80, MeOH/EtOAc as eluent. 50 mg (10%) of pure product was obtained, as a light brown solid. <sup>1</sup>H NMR (400 MHz, DMSO-*d*<sub>6</sub>):  $\delta$  1.52 (m, 6H, -CH<sub>2</sub>(3,4,5)-Piperidine), 3.11 (d, 6H, -CH<sub>2</sub>(2,6)-Piperidine), 4.98 (s, 4H, NH<sub>2</sub>), 5.23 (s, 2H, CH<sub>2</sub>-Py) ppm. <sup>13</sup>C NMR (400MHz, DMSO-*d*<sub>6</sub>):  $\delta$  24.78 (-CH<sub>2</sub>(4)-Piperidine), 25.38 (-CH<sub>2</sub>(3-5)-Piperidine), 39.48 (-CH<sub>2</sub>(2-6)-Piperidine), 82.51 (CH-Py), 158.64 (C4-N), 160.07 (C2,6-Py) ppm. MS [M+H<sup>+</sup>]: 192.3. IR: 785, 977, 1118, 1446, 1546, 1627, 2358, 2808, 2920, 3184, 3369, 3433 cm<sup>-1</sup>. M.p.: 130-132 °C.

4- Piperidino-2,6-bis(acrylamido)pyridine (**monomer 12**). To a solution of 4-piperidino -2,6-pyridinediamine (**33**, 25 mg, 0.13 mmol, 1 eq), triethylamine (0.32 mmol, 45.3  $\mu$ L, 2.5 eq,  $d = 0.726$ ) and anhydrous DCM (5 mL), acryloyl chloride (0.28 mmol, 23.2  $\mu$ L, 2.2 eq,  $d = 1.114$ ) dissolved in 2 mL of DCM was added slowly in an ice bath and under a dinitrogen atmosphere. The mixture was stirred overnight at room temperature. The mixture reaction was washed with a saturated aqueous solution of  $\text{NaHCO}_3$  ( $2 \times 10$  mL) and water (10 mL). The organic layer was dried over  $\text{MgSO}_4$ , filtered and the filtrate evaporated to obtain a light brown solid (10 mg, 25%).  $^1\text{H NMR}$  (400 MHz,  $\text{DMSO-}d_6$ ):  $\delta$  1.59 (m, 6H,  $-\text{CH}_2(3,4,5)$ -Piperidine), 3.33 (d, 6H,  $-\text{CH}_2(2,6)$ -Piperidine), 5.75 (dd,  $^3J=12$  Hz, 2H,  $-\text{CH}_{cis}=\text{)$ , 6.26 (dd,  $^3J=4$  Hz, 2H,  $-\text{CH}_{trans}=\text{)$ , 6.64 (dd,  $^3J_{cis}=12$  Hz,  $^3J_{trans}=16$  Hz, 2H,  $\text{CH}=\text{)$ , 7.49 (s, 2H,  $\text{CH}_2\text{-Py}$ ), 9.96 (s, 2H, NH) ppm.  $^{13}\text{C NMR}$  (400MHz,  $\text{DMSO-}d_6$ ):  $\delta$  24.52 ( $-\text{CH}_2(4)$ -Piperidine), 25.26 ( $-\text{CH}_2(3-5)$ -Piperidine), 47.78 ( $-\text{CH}_2(2-6)$ -Piperidine), 95.10 ( $\text{CH-Py}$ ), 127.83 ( $\text{CH}=\text{)$ , 132.45 ( $\text{CH}_2=\text{)$ , 151.73 ( $\text{C}=\text{O}$ ), 158.08 ( $\text{C4-N}$ ), 164.20 ( $\text{C2,6-Py}$ ) ppm. **MS** [ $\text{M}+\text{H}^+$ ]: 301. **IR**: 790, 983, 1193, 1436, 1556, 1670, 2360, 2854, 2927, 3292  $\text{cm}^{-1}$ . **M.p.**: 129-139°C.

### 5.2.7 Synthesis of monomer 12 intermediate

A previous attempt to synthesise monomer 12 was made. Unfortunately, the Hofmann rearrangement was unsuccessful with compound 27, as the reactivity of the amido group drops in accordance with the electron-donating properties of the 4-substituent of the pyridine ring. Hence, compound 27 was hydrolysed to a diacid before conversion to an amine could be attempted. Different attempts were made, using different protocols (e.g. Hofmann rearrangement in MeOH), but all were unsuccessful. We then decided to synthesise monomer 12 using another route.

4-Piperidino-2,6-diethylpyridinedicarboxylate (**23**). 4-Piperidino-2,6-pyridinedicarboxylic acid (**12**, 450 mg, 1.8 mmol) was suspended in absolute ethanol (30 mL) and sulfuric acid (0.5 mL) was carefully added at room temperature with vigorous stirring. The mixture was refluxed for 7 hours at 130 °C and the solvent then evaporated. The viscous residue was made basic (pH 8) using a saturated aqueous solution of  $\text{NaHCO}_3$  (50 mL) and the aqueous solution was

extracted with DCM. The organic phase was then dried over MgSO<sub>4</sub>, filtered and filtrate evaporated to give the diester (270 mg, 49%). **<sup>1</sup>H NMR** (400 MHz, DMSO-*d*<sub>6</sub>): δ 1.31 (t, <sup>3</sup>J= 7.2 Hz, 6H, O-CH<sub>2</sub>-CH<sub>3</sub>), 1.57 (m, 4H, -CH<sub>2</sub>-), 1.59 (t, 2H, -CH<sub>2</sub>-), 3.45 (t, 4H, N-CH<sub>2</sub>-), 4.33 (q, <sup>3</sup>J= 7.2 Hz, 4H, O-CH<sub>2</sub>-CH<sub>3</sub>), 7.52 (s, 2H, CH-Ar) ppm. **<sup>13</sup>C NMR** (400MHz, CDCl<sub>3</sub>): δ 14.29 (-CH<sub>2</sub>-CH<sub>3</sub>), 24.26 (-CH<sub>2</sub>(4)-Piperidine), 25.22 (-CH<sub>2</sub>(3-5)-Piperidine), 47.35 (-CH<sub>2</sub>(2-6)-Piperidine), 62.23 (O-CH<sub>2</sub>-CH<sub>3</sub>), 111.42 (CH-Ar), 149.38 (C-N), 156.05 (C=O), 165.97 (C-Py). **MS** [M+H<sup>+</sup>]: 306.4. **HRMS** (ESI-TOF) m/z: [M+H]<sup>+</sup> Calcd for C<sub>16</sub>H<sub>22</sub>N<sub>2</sub>O<sub>4</sub>H 307.36; Found 307.1662. **IR**: 690,781, 1274, 1639, 1749, 2872, 2945, 3122 cm<sup>-1</sup>. **m.p.**: 102-106 °C.

*4-Piperidino-2,6-pyridinediamide* (27). 4-Piperidin0-2,6-diethylpyridinedicarboxylate (23, 250 mg, 0.82 mmol) was stirred in a saturated methanolic solution of ammonia (8 mL) for 3 hours at room temperature. The solvent was evaporated and the product obtained as a white powder in quantitative yield. **<sup>1</sup>H NMR** (400 MHz, DMSO-*d*<sub>6</sub>): δ 1.57 (m, <sup>3</sup>J= 4.4 Hz, 4H, -CH<sub>2</sub>-), 1.62 (t, <sup>3</sup>J= 4.4 Hz, 2H, -CH<sub>2</sub>-), 3.45 (t, <sup>3</sup>J= 5.2 Hz, 4H, N-CH<sub>2</sub>-), 7.51 (s, 2H, CH-Ar), 7.53-8.72 (s, 4H, NH<sub>2</sub>) ppm. **<sup>13</sup>C NMR** (400MHz, DMSO-*d*<sub>6</sub>): δ 24.43 (-CH<sub>2</sub>(4)-Piperidine), 25.18 (-CH<sub>2</sub>(3-5)-Piperidine), 47.41 (-CH<sub>2</sub>(2-6)-Piperidine), 107.64 (CH-Ar), 150.66 (C-N), 156.66 (C=O), 166.74 (C-Py). **MS** [M+H<sup>+</sup>]: 249. **HRMS** (ESI-TOF) m/z: [M+H]<sup>+</sup> Calcd for C<sub>12</sub>H<sub>16</sub>N<sub>4</sub>O<sub>2</sub>H 249.28; Found 249.1363. **IR**: 719, 995, 1423, 1577, 1666, 2366, 2933, 3142, 3290, 3456 cm<sup>-1</sup>. **m.p.** = 292-294 °C.

## 5.3 RESULTS AND DISCUSSION

### 5.3.1 Job plot

We assumed that the 4-substituted BAAPys will create a 1:1 complex with tegafur in solution, as it is well accepted and documented that BAAPy binds mono-imido-based compounds with a 1:1 ratio.<sup>61, 119</sup> Also, all NMR titrations perfectly fit the 1:1 binding isotherm (R = 0.99). However, Job plots of monomer 8 and 10 were performed to reinforce this assumption (Figure 46).



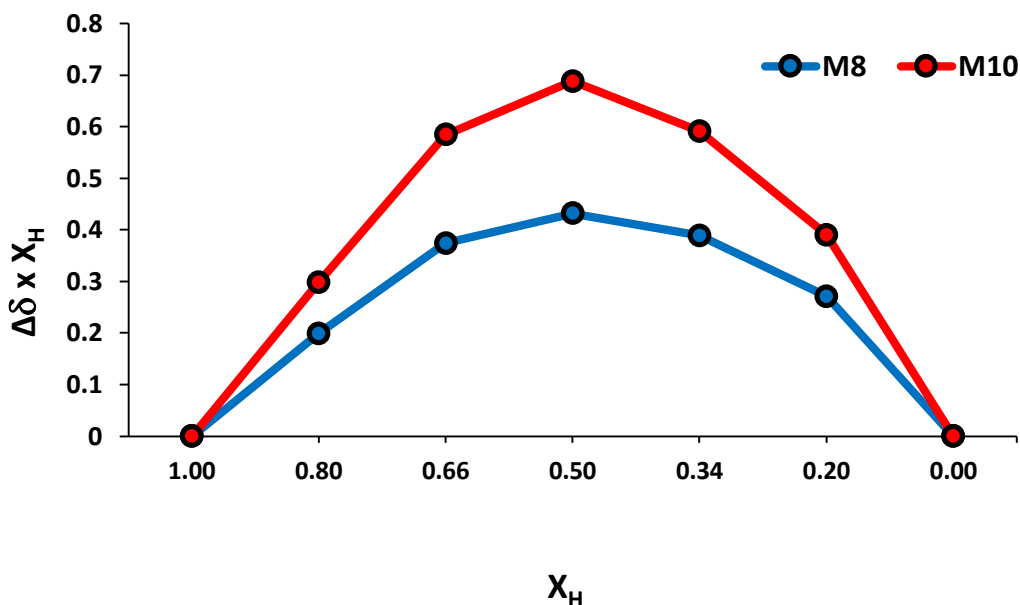
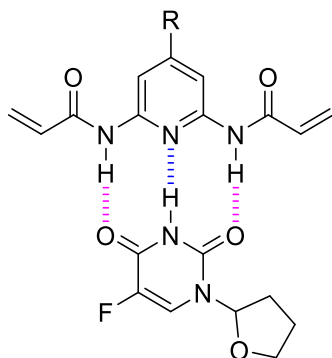


Figure 46: Job plot experiments of Tegafur with monomer 8 and 10.

### 5.3.2 $^1\text{NMR}$ titrations

The 4-substituted-2,6-bis(acrylamido)pyridines were synthesised as potential substitutes for BAAPy in the imprinting of imide-containing target molecules. We wanted to investigate the effect on basicity/H-bond acceptor ability of such molecules on varying the substituent at this position on the ring. While there will also be a concurrent effect on the acidity of the amide protons at the 2- and 6-positions, we reasoned that the change in basicity of the ring nitrogen would be the main driver for differences between the new, potential monomers. The predicted acidity and basicity of the D-A-D array of monomers 7-12 were calculated (predicted values, Table 18), and the main change was in the basicity of the pyridine nitrogen, rather than on the amide protons' acidity. Hence, the conclusion was that the binding constant strength will be mainly affected by the changes in the nitrogen basicity.



**Figure 47:** 4-substituted 2,6-bis(acrylamido)pyridines - Tegafur complex. The D-A-D motif of the functional monomer binds the complementary A-D-A motif of Tegafur with three H-bonds.

To this end,  $^1\text{H}$  NMR titrations were performed, using  $\text{CDCl}_3$  as the solvent and a temperature of  $25^\circ\text{C}$ . An increasing amount of the guest, Tegafur (Figure 47), was added to either a 1 mM or 0.1 mM solution of the respective monomers and the results are presented in Table 16.

**Table 16:** Binding constants for association of monomers 7-11 with Tegafur.  $K_a$  ( $M^{-1}$ ) (association constant) and  $\Delta\delta_{\text{max}}$  (maximum change in the chemical shift) were calculated using OriginPro 8.5.1.

monomer	$K_a$ ( $M^{-1}$ )	$\Delta\delta_{\text{max}}$	mM	solvent
monomer 11 ( $R=\text{CN}$ )	$661 \pm 2\%$	$2.58 \pm 0.02$	1	$\text{CDCl}_3$
monomer 10 ( $R=\text{Cl}$ )	$898 \pm 3\%$	$2.50 \pm 0.02$	1	$\text{CDCl}_3$
monomer 9 ( $R=\text{Br}$ )	$844 \pm 2\%$	$2.58 \pm 0.02$	1	$\text{CDCl}_3$
monomer 7 ( $R=\text{H}$ )	$732 \pm 5\%$	$2.52 \pm 0.03$	1	$\text{CDCl}_3$
monomer 8 ( $R=\text{OAlk}$ )	$1673 \pm 3\%$	$2.46 \pm 0.04$	0.1	$\text{CDCl}_3$
monomer 12 ( $R=\text{NR}_2$ )	$3481 \pm 7\%$	$2.53 \pm 0.06$	0.1	$\text{CDCl}_3$

The experimental data for monomers 7-12 were fitted to the expected 1:1 isotherm curve, leading to a very good fit ( $R^2 = 0.99$ ) (Figure 48-49). Monomers 8 and 12 show an increased association constant (Table 16), in comparison to BAAPy, which reflects the mesomeric effect of the electron-donating groups on the pyridine ring

nitrogen basicity. The  $pK_a$  of the ring nitrogen in both M8 and M12 increases relative to BAAPy, enhancing its hydrogen bond accepting properties and the strength of their association with Tegafur.

Monomers 9 and 10 show lower  $pK_a$  values (of the ring-nitrogen) than BAAPy, due to the electron-withdrawing properties of halogen substituents. However M9 and M10 exhibit an association constant slightly higher than BAAPy which we attribute to the increased acidity of the two amido protons which enhances their hydrogen-bond donating abilities. The predicted  $pK_a$  of the amido protons of M9 (R = Br) and M10 (R = Cl) are 12.1, while the predicted  $pK_a$  of BAAPy amido protons are 12.2. The acidity slightly increases, enough to be able to observe a small enhancement in the binding constants of these two novel monomers.

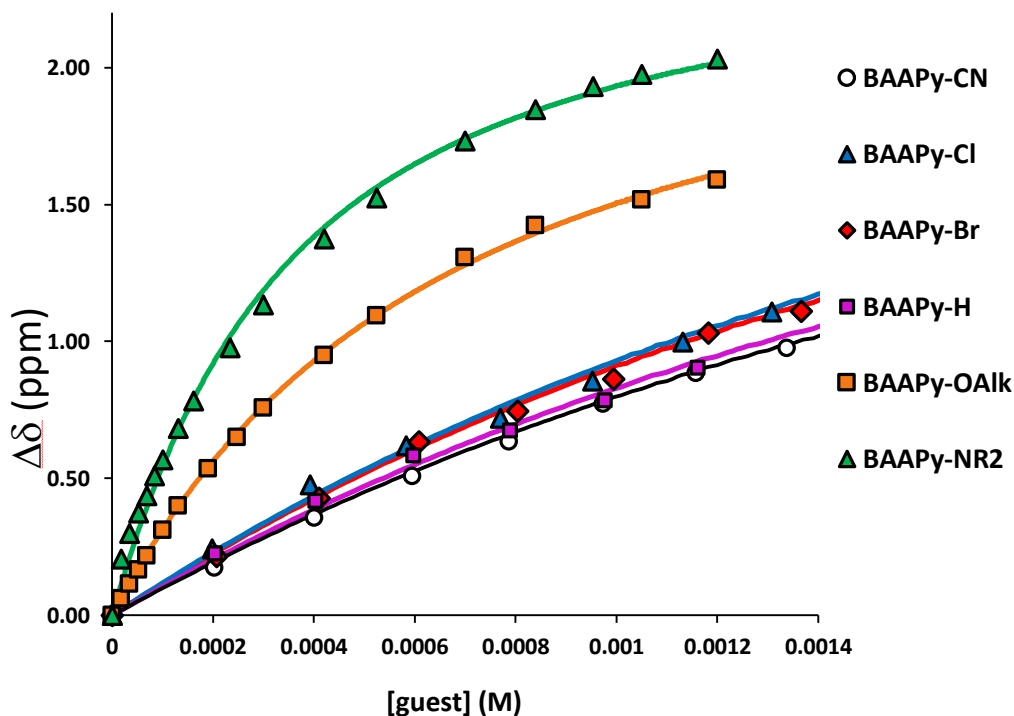


**Figure 48:** Binding isotherms of monomers 7, 8, 9, 10, 11 and 12 with Tegafur obtained by  $^1H$  NMR titrations studies.

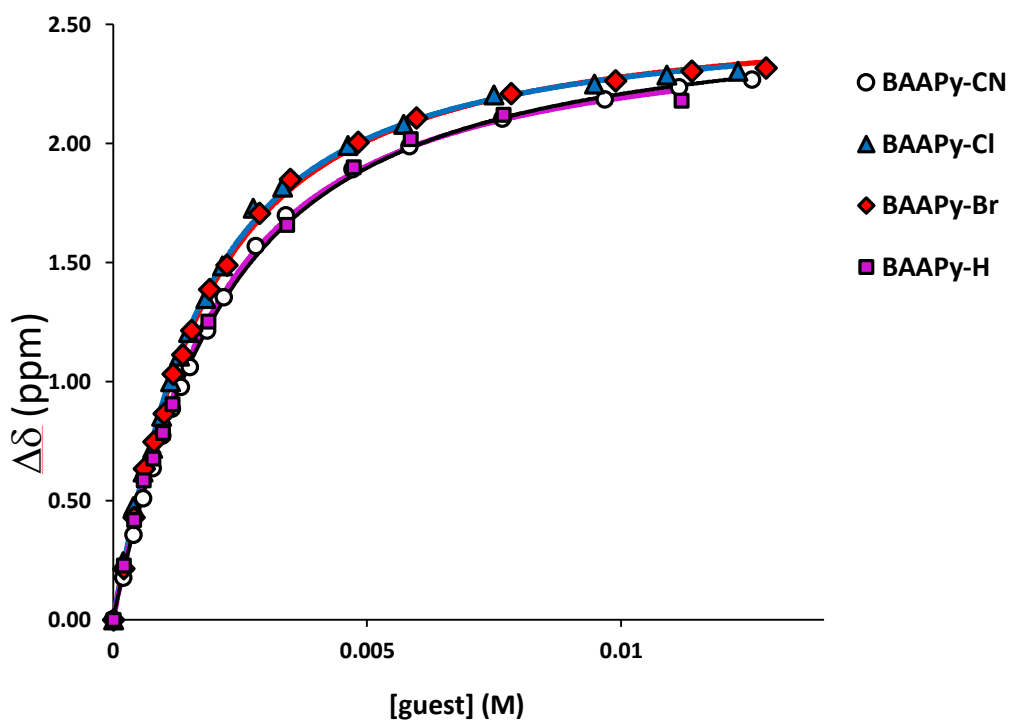


**Figure 49:** Binding isotherms for monomers 7, 9, 10 and 11 with Tegafur obtained by  $^1\text{H}$  NMR titrations studies.

### 5.3.3 Inductive and mesomeric effects of substituents

As can be seen, there is an obvious correlation between the nature of the substituent at the 4-position and the association of the monomer with the model guest, Tegafur. The behaviour of each functional monomer is linked to the changes in the acidity and basicity of the hydrogen bond donors (HBD) and hydrogen bond acceptor (HBA), respectively. As we know, the strength of an HBD and an HBA are directly proportional to the acidity and basicity of the functionalities.<sup>126</sup> The *inductive* (I) effect (or polarisation effect) and *mesomeric* (M) effects (or resonance effect) of the functional group in four position plays an important role in changing the acidity and basicity of the D-A-D (donor-acceptor-donor) motif.

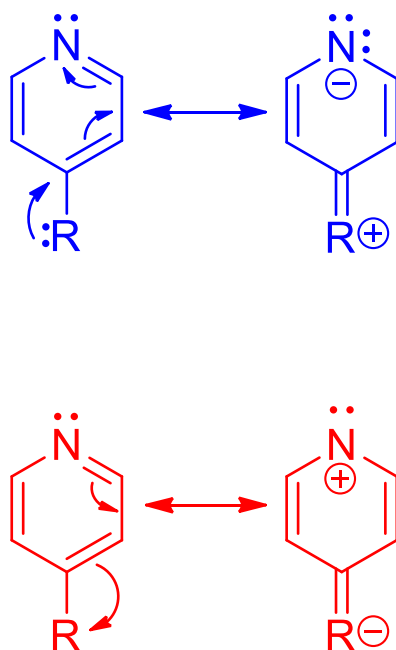


**Figure 50:** Selected resonance structures of pyridine substituted with electron donating (blue) and electron withdrawing (red) substituent<sup>127</sup>.

The inductive effect is the polarization of the electron density of a  $\sigma$  bond caused by the electronegativity of a nearby atom. The electron displacement through covalent bonds caused by the presence of a functional group with electron-donating or electron-accepting properties determines the polarity of the molecule, which in turn affects the chemical properties of the latter. The mesomeric effect is the redistribution of electrons which takes place in unsaturated and especially in conjugated systems via their  $\pi$ -orbitals. Positive and negative inductive and mesomeric effects can affect the acidity and basicity of the modified BAAPy. Such effects are summarized by the Hammett equation. The Hammett Equation<sup>128</sup> describes the straight line correlation between change of acidity of benzoic acid and the substituent in para or meta position to the acid.  $\sigma$  is the substituent constant, which measure the total polar effect extended by substituent X (relative to no substituent) on the reaction centre. ( $\sigma = -(\text{pK}_a - \text{pK}_a(\text{H}))$ ).

The equation describes the linear free energy relationship relating equilibrium constants (or reactions rates) to only two parameters – a substituent constant ( $\sigma$ ) and the equilibrium constant (or reaction constant,  $\rho$ ).

$$\log \left( \frac{k}{k_H} \right) = \rho \cdot \sigma \quad \text{or} \quad \log \left( \frac{K}{K_H} \right) = \rho \cdot \sigma$$

Log of the ratio of either the reaction rate constant or the equilibrium constant.

$\rho$  = reaction constant.  
Proportionality constant between log of k (or K) values and  $\sigma$ .

$\sigma$  = substituent constant. A measure of the total polar effect exerted by substituent X (relative to no substituent) on the reaction centre.

$$\sigma = -(pK_a - pK_a(H)).$$

**Figure 51:** The Hammett Equation<sup>128</sup>

**Table 17:** Experimental association constants for monomers 7-12 and para-substituent constants ( $\sigma$ ) from the Hammett Equation<sup>128</sup>.  $K_a(R)$  = association constant 4-substituted BAAPY.  $K_a(H)$  = association constant BAAPY.

monomer	$K_a (M^{-1})$	$\sigma$	$K_a(R)/K_a(H)$	$\log [K_a(R)/K_a(H)]$
monomer 11 (R=CN)	661 $\pm$ 2%	0.66	0.90301	-0.04431
monomer 10 (R=Cl)	898 $\pm$ 3%	0.23	1.22678	0.08877
monomer 9 (R=Br)	844 $\pm$ 2%	0.23	1.15301	0.06183
monomer 7 (R=H)	732 $\pm$ 5%	0	1.00000	0.00000
monomer 8 (R=OAlk)	1673 $\pm$ 3%	-0.27	2.28552	0.35898
monomer 12 (R=NR <sub>2</sub> )	3481 $\pm$ 7%	-0.83	4.75546	0.67719

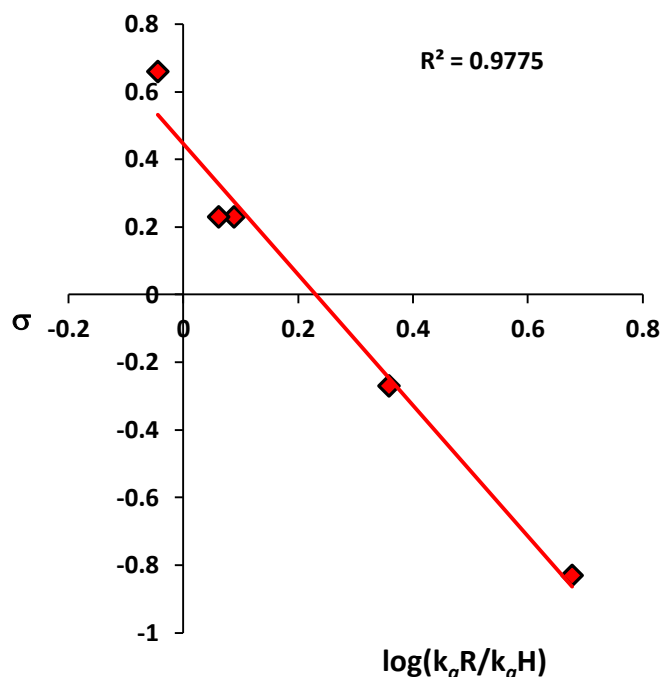


**Figure 52:** Correlation between  $\sigma$  (para-substituent constants  $\sigma$  from the Hammett Equation) and the association constants of monomer 7-12. The Para substituents constants  $\sigma$  were plotted with  $\log k_aR/k_aH$  ( $R^2=0.97$ ).  $k_aR$  = association constant of 4-substituted BAAPY.  $k_aH$  = association constant of BAAPy.  $\sigma = -(pK_a - pK_a(H))$ .

**Table 18:** Predicted  $pK_a$  values for the ring nitrogen in monomers 7-12.  $pK_a$  calculated at <https://epoch.uky.edu/ace/public/pKa.jsp>.

monomer	$K_a$ ( $M^{-1}$ )	$pK_a$
monomer 11 ( $R=CN$ )	$661 \pm 2\%$	-1.2
monomer 10 ( $R=Cl$ )	$898 \pm 3\%$	1.9
monomer 9 ( $R=Br$ )	$844 \pm 2\%$	1.8
monomer 7 ( $R=H$ )	$732 \pm 5\%$	2.9
monomer 8 ( $R=OAlk$ )	$1673 \pm 3\%$	4.4
monomer 12 ( $R=NR_2$ )	$3481 \pm 7\%$	6.7

### 5.3.3.1 The substituent effect

#### *Cyano substituent*

A strong electron-withdrawing group, such as the cyano group, has a negative I and a negative M effect. The resonance decreases the electron density at the ortho- and para-positions and the polarization effects lead to a pull of electron density away from the ring nitrogen. Hence, the cooperative behaviour of these two negative effects causes a huge decrease in the ring nitrogen basicity (predicted  $pK_a = -1.2$ ), which consequently becomes a weak HBA, as demonstrated by the decreased binding strength ( $K_a = 661 \pm 2\% \text{ M}^{-1}$ ) of monomer 11. These effects should also slightly increase the HBD acidity, but eventually this effect is swamped by the huge effect that the cyano group has on the ring nitrogen basicity.

#### *Halogen substituents*

Monomers 9 and 10, with either a *bromo-* or *chloro-* atom at the 4-position, respectively, exhibit an increased binding constant compared to BAAPy. Halogens are electronegative and hence give a negative I effect. However, they also release electrons by delocalization (a positive M effect) of a lone pair. The negative I effect of the halogen atoms decreases the basicity of the pyridine ring nitrogen (table 18). Nonetheless the -I effect of the halogens is also responsible for the increased acidity of the HBD group in meta-position accordingly to the Hammett Equation<sup>128</sup>. Halogens also give a positive M effect, as they are resonance donating (a +M effect causes a drop in acidity by decreasing the polarity of the acid): halogens donate an ion pair into the ring increasing the electron density on the ring. However the positive M effect on the pyridine system is negligible compared with the negative I effect.<sup>129</sup> Overall, the presence of the halogen atom enhances the association constant of the respective monomers towards the complementary guest. The effect is stronger with increasing electronegativity of the atom. The 4-halogenated BAAPy monomers therefore bind more strongly compared to BAAPy itself.

#### *Alkoxy substituent*

The alkoxy substituent pushes electron density towards the ring nitrogen. A +M effect can cause a drop in the HBD acidity, but from the Hammett Equation<sup>128</sup> the alkoxy group has a positive effect in increasing the acidity in the HBD at the meta-



position (positions 2- and 6-). Also, the predicted  $pK_a$  value of the amide protons of monomer 8 (R=OAlk) is 12.10, while the  $pK_a$  of BAAPy amide protons is 12.2. The basicity of M8 is also enhanced, as the predicted  $pK_a$  value of the nitrogen ( $pK_a = 4.4$ ) is increased relative to BAAPy. Therefore, the overall effect of this substituent is an enhancement of the binding constant with Tegafur.

It should be noted that in initial experiments, the isotherm obtained for M8-Tegafur complexation was sigmoidal, suggesting the presence of some kind of pre-assembly event preventing the guest from interacting with the host. This caused a drop in binding constant value, which was  $651 \text{ M}^{-1}$  for this particular event. The experiment was repeated using scrupulously anhydrous condition. A fresh bottle of  $\text{CDCl}_3$  was used and the template and monomer dried under vacuum and stored under a dinitrogen atmosphere prior to the experiment. These conditions prevent the isotherm from being sigmoidal and the experimental data were fitted to a Langmuir model isotherm to obtain the reported  $K_a$  of  $1673 \text{ M}^{-1}$  ( $R^2 = 0.99$ ). This demonstrates the importance of using anhydrous conditions in such titrations, as the presence of water molecules can perhaps interact with the monomer in the early stage of the complex formation and mask the true nature of the host-guest interaction.

#### *Amino substituent*

A non-aromatic secondary amine was chosen as the most electron-donating group. In particular piperidine was introduced on four-position of BAAPy. The positive mesomeric effect of such a strong electron-donating group, increases the basicity of the pyridine ring nitrogen ( $pK_a = 6.7$ ), making it a stronger HBA. The predicted  $pK_a$  of the amide protons of M12 is 12.2, the same as BAAPy. Thus, the acidity and so the HBD strength of M12 remains unchanged. Hence piperidine has only a positive effect on the D-A-D motif of the functional monomer, enhancing its association constant 4.7 times. Overall these effects cause an increase in the association constant of monomer 12 ( $k_a = 3481 \text{ M}^{-1}$ ) compared to the non-substituted BAAPy. Thus monomer 12 is a great candidate to substitute BAAPy in Molecular Imprinting.

### 5.3.4 Synthesis and overall yields

5 novel functional monomers were synthesised in 4-5 synthetic steps. The overall yield was unfortunately quite low compared to BAAPy, which is easily prepared in one synthetic step starting from a really cheap material as 2,6-diamino-pyridine. Now, monomer 8 and 12 are the only functional monomers with a real improvement in terms of binding constant, as predicted in the beginning, but a question about the worthiness of making them arises.

**Table 19:** Total yield of monomer 7-12

<i>monomer</i>	$K_a (M^{-1})$	Yield (%)
<i>monomer 11 (R=CN)</i>	661 ± 2%	0.6
<i>monomer 10 (R=Cl)</i>	898 ± 3%	25.5
<i>monomer 9 (R=Br)</i>	844 ± 2%	5.5
<i>monomer 7 (R=H)</i>	732 ± 5%	45
<i>monomer 8 (R=OAlk)</i>	1673 ± 3%	1.7
<i>monomer 12 (R=NR<sub>2</sub>)</i>	3481 ± 7%	0.4

However monomer 12 can be made in only two synthetic step if instead of preparing 2,6-diamino-4-bromopyridine (29), the latter compound is bought. Compound 29 is quite expensive, but allows us to produce M12 in only a two-step reaction. Nonetheless, monomer 12 yield can be improved. Its yield was quite low due to the lack of time which didn't allow for improvement of the synthetic protocol.

Thus, even if BAAPy is a common functional monomer used in imprinting due to its overall cost and easy synthesis, M12 can still substitute BAAPy, as it can be made easily (two synthetic step) and its yield can be improved.

## 5.4 CONCLUSIONS

Five 4-substituted-2,6-*bis*(acrylamido)pyridine functional monomers for the stoichiometric non-covalent imprinting of imide-containing targets were designed and synthesised in order to study the effect of the substituted group on the binding constant strength. The substituted groups were chosen based on their electron donating/withdrawing characteristics. The association constants between the functional monomers and Tegafur were determined via NMR titration in deuterated chloroform. There is a linear correlation between the mesomeric and inductive effect of the substituent on ring nitrogen and the changes in its basicity. An increase in binding constant for the chloro- and bromo-substituted BAAPy monomers was observed, due to the negative inductive effect that both the chloro- and bromo-atoms have on the pyridine ring. This leads to a drop in the basicity on the ring nitrogen, but an enhancement of the acidity of two amido protons at the meta-position. The overall effect was an improvement in the binding of monomers 9 and 10  $K_a$  compared to BAAPy.

Monomer 11, with a cyano functionality, instead exhibited  $K_a$  lower than BAAPy, probably due by the cooperative effect of  $-I$  and  $-M$  effect, which explain both the strong decrease in ring nitrogen basicity and acidity of the HBDs.

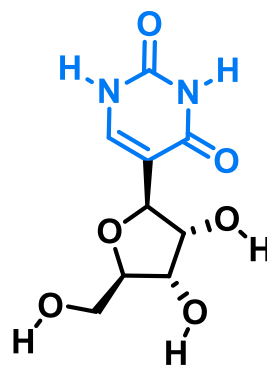
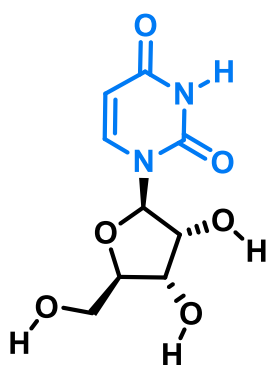
Monomers 8 and 12 have a strong electron-donating group at the 4-position, which increases the ring nitrogen basicity by pushing electron towards it via the mesomeric effect. This translates in an increase of their association constant towards Tegafur, in comparison to BAAPy.

We have proven that BAAPy can be modified and that the D-A-D motif is sensitive to substituents added to the pyridine ring. Monomer 12 is the most valuable, as the  $K_a$  is 4.7 times bigger ( $K_a = 3481 \text{ M}^{-1}$ ) than the association constant of BAAPy ( $K_a = 732 \text{ M}^{-1}$ ) towards Tegafur. Unfortunately the overall yield was poor (0.4%), due to the lack of time which prevented me from revisiting the synthetic process and improving the final yield. For my thesis, it was enough to have few mg of material to be able to study the supramolecular interaction with a selected guest. In the future the final yield will be improved, in order to be able to use this functional monomer for imprinting. Regarding the other novel functional monomers, they won't be used for Imprinting, as no massive improvement of  $K_a$  was observed to justify four or five synthetic steps.

It is interesting to observe how hydrogen bonds strengths are subjected to changes due to electron-density modifications on a molecule. Further modelling investigation will be made to study the interactions of the modified BAAPys with a specific guest in solution.

# CHAPTER 6

## *EVALUATION OF MOLECULARLY IMPRINTED POLYMERS USING “DUMMY” TEMPLATES FOR NUCLEOSIDE RECOGNITION*



## 6.1 INTRODUCTION

The following project was developed in collaboration with the group of Prof. Luigi Agrofoglio at the Université d'Orléans, France.

Nucleosides and nucleotides are the structural components of nucleic acids. Rapid metabolic turnover of nucleic acids due by health problems, leads to an increased concentration of naturally modified nucleosides in human bodily fluids. Hence, these products of the degradation of nucleic acid are potential disease biomarkers<sup>130</sup>. The challenge in the imprinting of nucleosides such as uridine and pseudouridine lies in the limited solubility of these templates in organic solvents, such as chloroform or acetonitrile. It is of vital importance for successful imprinting based on hydrogen bond interactions between template and functional monomer, to use low polar solvents which do not destroy the H-bond interaction which drive the imprinting process.

Previously the imprinting of riboflavin<sup>61</sup> has been reported using the “dummy” template method, as this vitamin exhibits very low solubility in organic solvents. Hence, riboflavin tetraesters (methyl, ethyl and propyl) were used to create imprinted materials targeting this vitamin and allowing the use of chloroform as the solvent/porogen. As the tetraesters have a different dimensions, size exclusion behaviour was observed on the MIPs, but overall the riboflavin methyl tetraester gave the more selective MIP towards the target, riboflavin. Lakka *et al.*<sup>131</sup> have also reported on the use of tri-*O*-acetyladenosine as a dummy template for the imprinting of adenosine.

A “dummy template” is a molecule, similar to the selected target, which is used during the imprinting process as it has, for example, greater solubility, is less toxic or is less expensive of the molecule that we wish to recognise. Using this method, we prepared dummy templates for both uridine and pseudouridine.

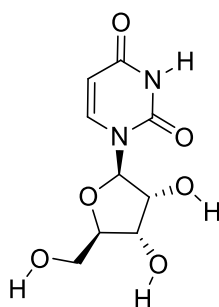
Firstly, we focused on the synthesis of MIPs using three different uridine triesters (methyl, ethyl and propyl) as a model to discover which triester would be the most suitable candidate in our subsequent attempts to imprint pseudouridine, which is a rather expensive molecule. Herein, I will report on the synthesis and solution

binding studies of both uridine and pseudouridine trimer ester dummy templates with different functional monomers; these experiments were performed prior to the preparation of the imprinted polymers for the recognition of these nucleosides.

### 6.1.1 Uridine and Pseudouridine

#### Uridine

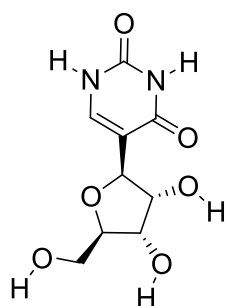
Uridine is a nucleoside comprising a uracil attached to a ribose ring. Uridine itself is of little pharmacological, pharmaceutical or environmental interest. The part of the molecule targeted for recognition is the imido motif, which is complementary to the DAD moiety of BAAPy. Uridine was chosen as a model system, in order to define the ideal conditions for the imprinting of pseudouridine, which is a putative, urinary cancer biomarker. Uridine is an inexpensive molecule, with a similar H-bonding moiety to that of pseudouridine. As previously reported, a size exclusion behaviour directly linked to the size of the template, i.e. the type of ester group, can be observed<sup>95</sup>. Hence, we predicted that the trimethyl ester of the nucleoside would be the most promising dummy template. However, three different uridine esters were synthesised and then used as dummy templates to imprint uridine, with the aim to improve our knowledge on this particular system such that it could be transferred to the imprinting of pseudouridine.



Uridine

#### Pseudouridine

Pseudouridine (5-β-D-ribofuranosyluracil,  $\psi$ )<sup>132</sup> is a modified nucleoside derived from ongoing RNA metabolism<sup>130b</sup>. It is formed by an enzyme called pseudouridine synthase which post-transcriptionally isomerizes specific uridine residues in RNA.<sup>133</sup>



Pseudouridine

As the concentrations of modified urinary nucleosides such as pseudouridine in biological fluids are linked to RNA breakdown, they may be used as a diagnostic tool in various disease states, especially cancers, such as leukaemia, breast cancer, colorectal cancer, bladder cancer and hepatocellular carcinoma.<sup>134</sup> Nucleoside levels in urine do not depend on the age, gender, habits or genetic picture of the patient,<sup>135</sup> such as other cancer biomarkers like proteins, making it simpler to develop a diagnostic test.

### 6.1.2 Colorectal cancer (CRC)

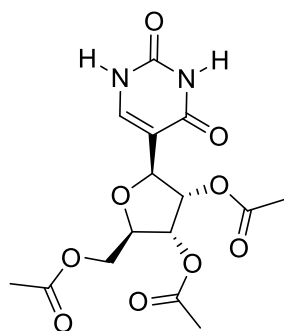
Over the past decade a steady increase in CRC and CRC-related mortality has been observed in Europe. Traditional methods for screening of cancer rely mostly on cell morphology using microscopy and cell staining, which requires primarily invasive methods to gather and process the tissue. More recent techniques use immunoassays (e.g. ELISA) to detect cancer biomarkers and these are carried out in hospital laboratories.<sup>136</sup> However, even if they are very sensitive and selective, they can be time consuming and expensive. Our focus is the development of easy, cheaper, faster and more sensitive diagnostic tests. Here we present the development of a MIP as the recognition element of a biosensor to be used directly on urine for the detection of pseudouridine.

### 6.1.3 Dummy templates

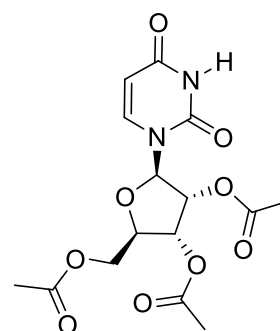
Pseudouridine and uridine are not soluble in those solvents normally used in imprinting, such as chloroform and acetonitrile. The use of more polar solvents in the pre-polymerization mixture, to solubilise the target, can lead to fewer and



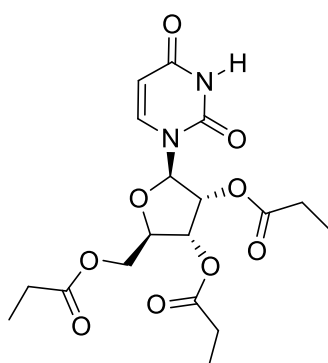
weaker imprinted binding sites because the polar solvent can interfere in the formation of host-guest complex as it is governed by non-covalent interactions such as hydrogen bonds. Pseudouridine and uridine triesters were therefore used as “dummy template”<sup>137</sup> for the preparation of MIPs. All these esters have good solubility in chloroform making them suitable for an imprinting process based on H-bond interactions.



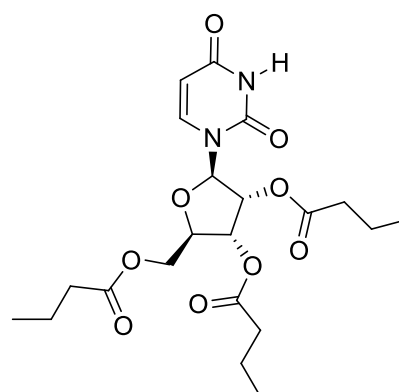
2',3',4'-Tri-O-acetylpseudouridine



2',3',4'-Tri-O-acetyluridine



2',3',4'-Tri-O-propionyluridine



2',3',4'-Tri-O-butyryluridine

**Figure 53:** Chemical structure of the esters of Uridine and Pseudouridine.

#### 6.1.4 The functional monomers

Both uridine and pseudouridine have an imide moiety. The ADA motif can share three hydrogen-bonds with a functional monomer such as BAAPy in a stoichiometric non-covalent imprinting protocol. Hence, BAAPy was selected as the functional monomer for the imprinting of uridine and pseudouridine. However,

the pseudouridine structure is a bit more complex, as it has four, rather than three, possible hydrogen bonding sites.

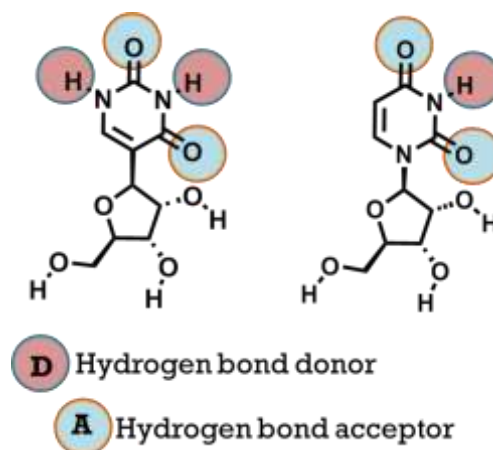


**Figure 54:** Pseudouridine and uridine hydrogen bond donor (in red) and hydrogen bond acceptor (in blue).

Monomers 1 and 6 are also interesting clefs to be used for the imprinting of pseudouridine. NMR titration studies were performed in order to calculate the association of each of the monomer-template complexes in deuterated chloroform. The obtained binding constants were observed to be in line with the ratio between the primary positive hydrogen-bonded interactions and secondary electrostatic repulsive interactions between the template and the monomers; overall, all monomers showed an acceptable binding strength. Acrylamide was also used as a functional monomer to demonstrate how the selectivity of a MIP towards the imprinted template can be improved by the use of tailor-made functional monomers used in a stoichiometric manner instead of a commercially available monomer.

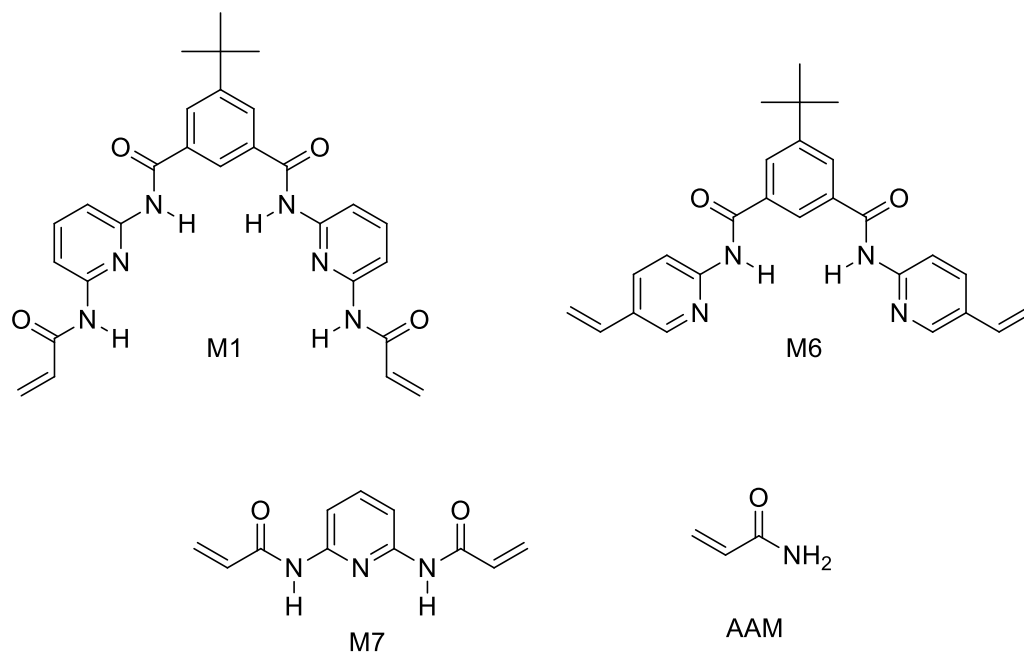


**Figure 55:** Functional monomers used for the imprinting of pseudouridine.

## 6.2 EXPERIMENTAL

### 6.2.1 Synthesis of 2',3',4'-Tri-*O*-acetylpsseudouridine<sup>94</sup>

Pseudouridine (732 mg, 3 mmol, FW = 244.2) was stirred in dry pyridine (6 mL) and acetic anhydride (0.983 mL, 1.061 g, 10.5 mmol, FW = 102.09, d = 1.08) at 20 °C for 25 hours under a dinitrogen atmosphere. The next day the reaction mixture was concentrated and the residue dissolved in 75 mL of DCM. The organic layer was extracted with saturated aqueous NaHCO<sub>3</sub> (2 × 50 mL) and water (2 × 50 mL). The organic layer was dried (MgSO<sub>4</sub>), filtered and co-evaporated with toluene to obtain a white solid. The crude material was purified by column chromatography (silica gel, 3% methanol in DCM) to give 2',3',4'-Tri-*O*-acetylpsseudouridine as a white solid (690 mg).

The water layers (200 mL) were then concentrated by rotary evaporation (water bath of 50 °C) to a 50 mL volume, which was extracted with DCM (3 × 100 mL). The organic layers were evaporated to obtain a further 240 mg of pure triacetylated pseudouridine (total yield 930 mg, 84%). <sup>1</sup>H NMR (400 MHz, CDCl<sub>3</sub>): δ 2.086, 2.103 and 2.116 (s, 9H, C(O)CH<sub>3</sub>), 4.280 (m, J=Hz, 2H, 5'-H), 4.370 (m, J=Hz, 1H, 4'-H), 4.879 and 4.891 (d, J= Hz, 1H, 1'-H), 5.277 (t, J=Hz, 1H, 3'-H), 5.378 (t, J=Hz, 1 H, 2'-H), 7.541 and 7.543 (d, J=Hz, 1 H, 6-H) ppm. <sup>13</sup>C NMR (400 MHz, CDCl<sub>3</sub>): δ 20.59, 20.70 and 20.90 (C(O)CH<sub>3</sub>), 63.67 (C-5'), 71.29 (C-3'), 74.07 (C-

2'), 77.52 (C-1'), 78.49 (C-4'), 111.49, 139.38 (C-6), 152.48, 162.81, 169.82, 169.91, 171.10 ppm. **MS** [M+Na<sup>+</sup>]: 393. **HRMS** (ESI-TOF) m/z: [M+H]<sup>+</sup> Calcd for C<sub>15</sub>H<sub>18</sub>N<sub>2</sub>O<sub>9</sub>H 371.31; Found 371.108. **IR**: 715, 988, 1227, 1508, 1675, 1723, 2962, 3225 cm<sup>-1</sup>. **M.p.** = 133-135°C.

### 6.2.2 Synthesis of 2',3',4'-Tri-*O*-propionyluridine<sup>94</sup>

Uridine (1 g, 4.1 mmol, FW = 244.2) was stirred in dry pyridine (5 mL) and propionic anhydride (1.83 mL, 1.86 g, 14.3 mmol, FW = 130.14, d = 1.015) at 20 °C for 25 hours under a dinitrogen atmosphere. The next day the reaction mixture was concentrated and the residue dissolved in 100 mL of DCM. The organic layer was extracted with saturated aqueous NaHCO<sub>3</sub> (1 × 50 mL). The aqueous layer was then washed with DCM (2 × 50 mL) and the combined organic layers dried (MgSO<sub>4</sub>), filtered and co-evaporated with toluene to obtain a pale yellow oil. The tripropionylated uridine was dried under vacuum at 50 °C overnight to eliminate any traces of pyridine and propionic acid. Yield = quantitative

**<sup>1</sup>H NMR** (400 MHz, DMSO-*d*<sub>6</sub>): δ 0.970-1.071 (9H, C(O)CH<sub>2</sub>CH<sub>3</sub>), 2.309–2.388 (6H, C(O)CH<sub>2</sub>CH<sub>3</sub>), 4.215–4.338 (3H, 4'-H, 5'-H<sub>a</sub> and 5'-H<sub>b</sub>), 5.354 (t, J=5.2Hz, 1H, 2'-H), 5.463 (t, J=5.2Hz, 1H, 3'-H), 5.719 (dd, J=7.8 and 2Hz, 1H, 5-H), 5.881 (d, J=4.8Hz, 1H, 1'-H), 7.710 (d, J=8.0Hz, 1 H, 6-H), 11.457 (s, 1 H, NH) ppm. **<sup>1</sup>H NMR** (400 MHz, CDCl<sub>3</sub>): δ 1.171 (m, J=7.2Hz, 9H, C(O)CH<sub>2</sub>CH<sub>3</sub>), 2.292–2.603 (6H, C(O)CH<sub>2</sub>CH<sub>3</sub>), 4.313–4.420 (3H, 4'-H, 5'-H<sub>a</sub> and 5'-H<sub>b</sub>), 5.328-5.365 (2H, 2'-H and 3'-H), 5.789 (dd, J=8.2 and 2.4Hz, 1H, 5-H), 6.067 (dd, J=3.2 and 2.4Hz, 1H, 1'-H), 7.417 (d, J=8.4Hz, 1 H, 6-H), 8.717 (s, 1 H, NH) ppm. **<sup>13</sup>C NMR** (400 MHz, CDCl<sub>3</sub>) δ 8.824 and 8.985 (C(O)CH<sub>2</sub>CH<sub>3</sub>), 27.116, 27.238 and 27.452 (C(O)CH<sub>2</sub>CH<sub>3</sub>), 63.117 (C-5'), 70.145 and 72.691 (C-2' and C-3'), 80.155 (C-4'), 87.190 (C-1'), 103.378 (C-5), 139.188 (C-6), 150.039, 162.496, 173.133, 173.607 ppm. **MS** [M+Na<sup>+</sup>]: 435; **MS** [M+CH<sub>3</sub>CN Na<sup>+</sup>]: 476; **MS** [M-C<sub>4</sub>H<sub>4</sub>N<sub>2</sub>O<sub>2</sub> / uracil]: 301. **HRMS** (ESI-TOF) m/z: [M+H]<sup>+</sup> Calcd for C<sub>18</sub>H<sub>24</sub>N<sub>2</sub>O<sub>9</sub>H 413.39; Found 413.1554. **IR**: 1165, 1267, 1685, 1740, 2945, 2984, 3067, 3204 cm<sup>-1</sup>.

### 6.2.3 Synthesis of 2',3',4'-Tri-*O*-butyryluridine<sup>94</sup>

Uridine (1 g, 4.1 mmol, FW = 244.2) was stirred in dry pyridine (5 mL) and butyric anhydride (2.34 mL, 2.26 g, 14.3 mmol, FW = 158.19, d =0.967) at 20 °C for 25

hours under a dinitrogen atmosphere. The next day the reaction mixture was concentrated and the residue dissolved in 100 mL of DCM. The organic layer was extracted with saturated aqueous NaHCO<sub>3</sub> (1 × 50 mL). The aqueous layer was washed with DCM (2 × 50 mL) and the combined organic layers dried (MgSO<sub>4</sub>), filtered and evaporated with toluene to yield a yellow oil. The tributylated uridine was dried under vacuum at 50 °C overnight to eliminate any traces of pyridine and butyric acid. Yield = quantitative. **<sup>1</sup>H NMR** (400 MHz, DMSO-*d*<sub>6</sub>): δ 0.847-0.919 (9H, C(O)CH<sub>2</sub>CH<sub>2</sub>CH<sub>3</sub>), 1.466-1.605 (6H, C(O)CH<sub>2</sub>CH<sub>2</sub>CH<sub>3</sub>), 2.240-2.406 (6H, C(O)CH<sub>2</sub>CH<sub>2</sub>CH<sub>3</sub>), 4.226–4.356 (3H, 4'-H, 5'-H<sub>a</sub> and 5'-H<sub>b</sub>), 5.352 (t, J=5.6Hz, 1H, 2'-H), 5.475 (t, J=5.2Hz, 1H, 3'-H), 5.719 (dd, J=8.4 and 2.4Hz, 1H, 5-H), 5.882 (d, J=5.2Hz, 1H, 1'-H), 7.713 (d, J=8.0Hz, 1 H, 6-H), 11.464 (s, 1 H, NH) ppm. **<sup>1</sup>H NMR** (400 MHz, CDCl<sub>3</sub>): δ 0.968 (q, J=7.2Hz, 9H, C(O)CH<sub>2</sub>CH<sub>2</sub>CH<sub>3</sub>), 1.666 (m, J=7.6Hz, 6H, C(O)CH<sub>2</sub>CH<sub>2</sub>CH<sub>3</sub>), 2.261-2.439 (6H, C(O)CH<sub>2</sub>CH<sub>2</sub>CH<sub>3</sub>), 4.309–4.416 (3H, 4'-H, 5'-H<sub>a</sub> and 5'-H<sub>b</sub>), 5.330-5.341 (2H, 2'-H and 3'-H), 5.792 (dd, J=8.2 and 2.0Hz, 1H, 5-H), 6.073 (dd, J=3.4 and 2.0Hz, 1H, 1'-H), 7.425 (d, J=8.4Hz, 1 H, 6-H), 9.152 (s, 1 H, NH) ppm. **<sup>13</sup>C NMR** (400 MHz, CDCl<sub>3</sub>): δ 13.535, 13.611 and 13.650 (C(O)CH<sub>2</sub>CH<sub>2</sub>CH<sub>3</sub>), 18.154 and 18.291 (C(O)CH<sub>2</sub>CH<sub>2</sub>CH<sub>3</sub>), 35.566, 35.703 and 35.963 (C(O)CH<sub>2</sub>CH<sub>2</sub>CH<sub>3</sub>), 63.026 (C-5'), 70.084 and 72.630 (C-2' and C-3'), 80.239 (C-4'), 87.213 (C-1'), 103.355 (C-5), 139.242 (C-6), 150.139, 162.802, 172.299, 172.812 ppm. **MS** [M+Na<sup>+</sup>]:518. **MS** [M+CH<sub>3</sub>CN Na<sup>+</sup>]:477. **MS** [M-C<sub>4</sub>H<sub>4</sub>N<sub>2</sub>O<sub>2</sub> / uracil]: 343. **HRMS** (ESI-TOF) m/z: [M+H]<sup>+</sup> Calcd for C<sub>21</sub>H<sub>30</sub>N<sub>2</sub>O<sub>9</sub>H 455.47; Found 455.202. **IR**: 1165, 1249, 1690, 1741, 2877.7, 2966, 3066 cm<sup>-1</sup>.

#### **6.2.4 Polymer formulations**

The molar ratio of template/monomer/cross-linker (EGDMA) was 1:1:20. However for polymers imprinted with the commercial functional monomer (acrylamide), the molar ratio of template/monomer/cross-linker (EGDMA) was 1:2:20. All polymers were prepared using chloroform as the porogen, except for the MIP/NIP 9 prepared using monomer 1 and TAψ as functional monomer and template respectively. Due to the lack of solubility of monomer 1 in chloroform and acetonitrile, a mixture of 1,4-dioxane/THF (1:3 v/v) was used as the solvent/porogen.

**Table 20:** Formulations of imprinted and non-imprinted polymers.

<i>Polymer</i>	<i>Template (g)</i>	<i>Monomer (g)</i>	<i>EGDMA (mL)</i>	<i>ABDV (g)</i>	<i>Solvent (mL)</i>
<b><i>MIP 3</i></b>	TA $\psi$ (0.185)	Acrylamide (0.071)	1.880	0.02	CHCl <sub>3</sub> (2.8)
<b><i>MIP 7</i></b>	TA $\psi$ (0.185)	M7 (0.109)	1.880	0.02	CHCl <sub>3</sub> (2.8)
<b><i>MIP 8</i></b>	TA $\psi$ (0.185)	M6 (0.213)	1.880	0.02	CHCl <sub>3</sub> (2.8)
<b><i>MIP 9</i></b>	TA $\psi$ (0.185)	M1 (0.138)	1.880	0.02	1,4-dioxane / THF (1.5 / 0.5)
<b><i>NIP 3</i></b>	-	Acrylamide (0.071)	1.880	0.02	CHCl <sub>3</sub> (2.8)
<b><i>NIP 7</i></b>	-	M7 (0.109)	1.880	0.02	CHCl <sub>3</sub> (2.8)
<b><i>NIP 8</i></b>	-	M6 (0.213)	1.880	0.02	CHCl <sub>3</sub> (2.8)
<b><i>NIP 9</i></b>	-	M1 (0.138)	1.880	0.02	1,4-dioxane / THF (1.5 / 0.5)
<b><i>MIP 10</i></b>	TAU (0.37)	M7 (0.217)	3.772	0.04	CHCl <sub>3</sub> (5.6)
<b><i>MIP 11</i></b>	TPU (0.412)	M7 (0.217)	3.772	0.04	CHCl <sub>3</sub> (5.6)
<b><i>MIP 12</i></b>	TBU (0.454)	M7 (0.217)	3.772	0.04	CHCl <sub>3</sub> (5.6)
<b><i>NIP 10</i></b>	-	M7 (0.217)	3.772	0.04	CHCl <sub>3</sub> (5.6)
<b><i>NIP 11</i></b>	-	M7 (0.217)	3.772	0.04	CHCl <sub>3</sub> (5.6)
<b><i>NIP 12</i></b>	-	M7 (0.217)	3.772	0.04	CHCl <sub>3</sub> (5.6)

## 6.3 RESULTS AND DISCUSSION

### 6.3.1 Job plot

As BAAPy can, theoretically, form a 1:2 (guest:host) complex with triacetylated pseudouridine as shown in Figure 56, a Job plot was made.

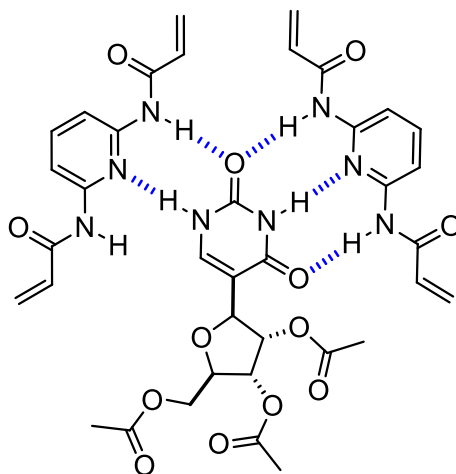


**Figure 56:** Potential 1:2 binding ration of Pseudouridine with monomer 7.

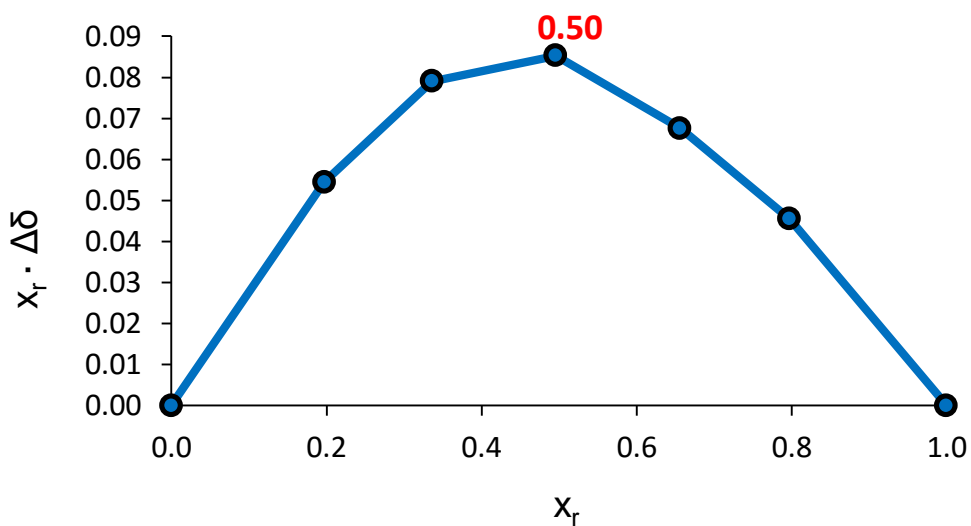


**Figure 57:** Job Plot of monomer 7 with Pseudouridine.

As can be seen from the Job plot in Figure 57, monomer 7 interact with pseudouridine with a 1:1 interaction.

### 6.3.2 <sup>1</sup>H NMR titration

**Table 21:** Monomer 1,6 and 7 – Tegafur complexes binding constants value.

	$K_a (M^{-1})$	$\Delta\delta_{max}$
Monomer 6	352 ± 49	0.80 ± 0.04
Monomer 7	211 ± 4	2.27 ± 0.02
Monomer 1	117 ± 10	1.87 ± 0.09

The association constants between 2',3',4'-Tri-*O*-acetylpsseudouridine and the different functional monomers were determined using NMR titrations, by adding an increasing amount of the template to a 1mM chloroform solution of each of the monomers. Monomer 6 creates the strongest interaction with TAψ, compared to monomers 1 and 7. M6 interacts with the template with four primary hydrogen bonds while M7 can only share three H-bonds with the imido motif of the template, making M6 a better functional monomer. However M1, which should be the strongest, providing a five hydrogen bond interaction with pseudouridine, is the weakest of the three. Hence, the primary hydrogen-bond interactions are not the only ones to play an important role in the binding strength; the secondary electrostatic interactions can interfere with the association process. In figure 58 are shown the positive hydrogen-bond primary interactions and secondary electrostatic repulsive interactions that occur in the host-guest complexation process. Overall, monomer 6 is the strongest, as demonstrated also by the final MIP 8 performance.



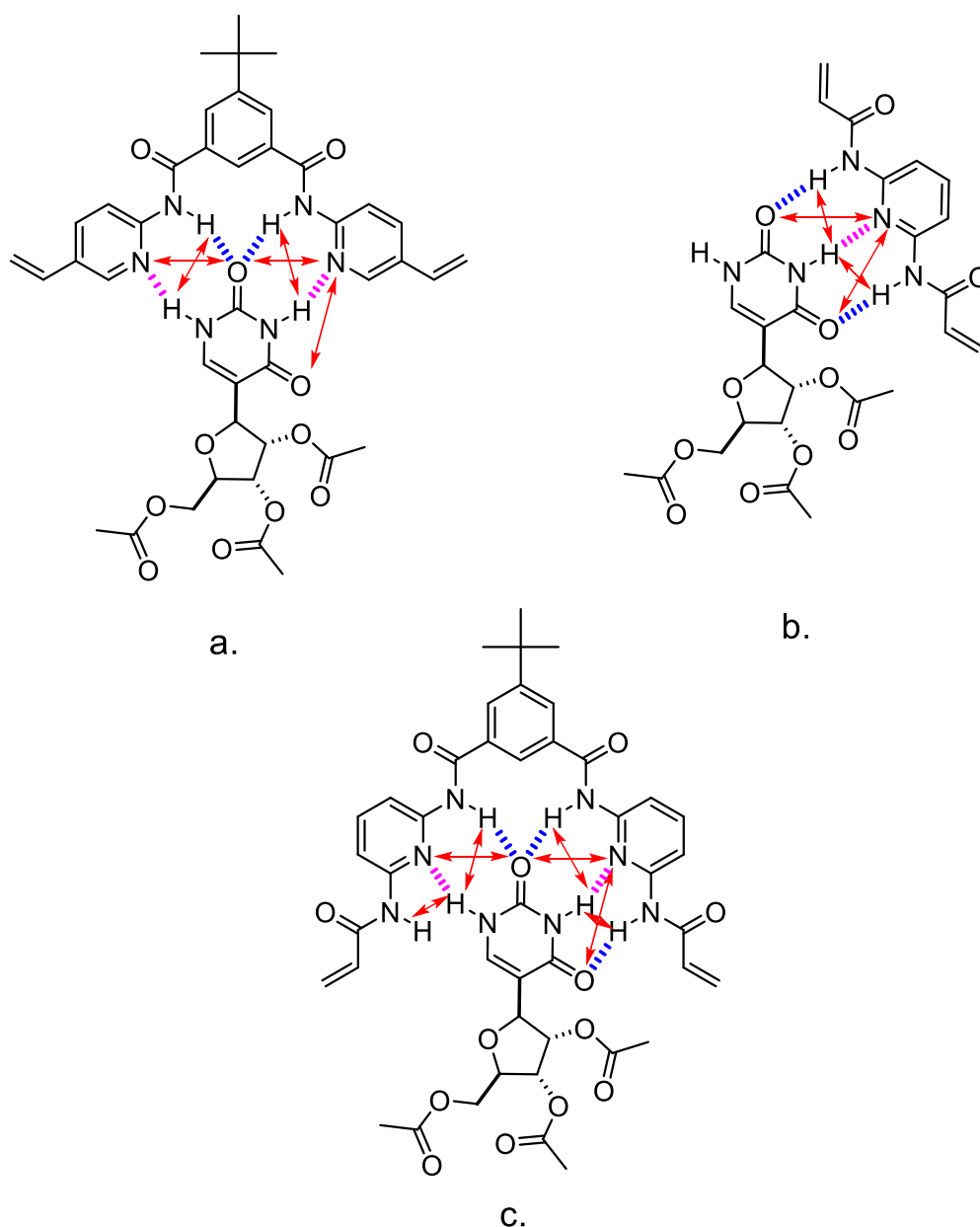


**Figure 58:** Primary positive hydrogen-bonded interactions (blue and pink) and secondary electrostatic repulsive interactions (red arrow): a) monomer 6 with four positive interactions and five negative interactions; b) monomer 7 with three positive interactions and four negative interactions; c) monomer 1 with five positive interactions and seven negative interactions.

Monomer 1 is potentially the strongest binder, but shares seven secondary electrostatic repulsive interactions with the template, destabilising the complex.

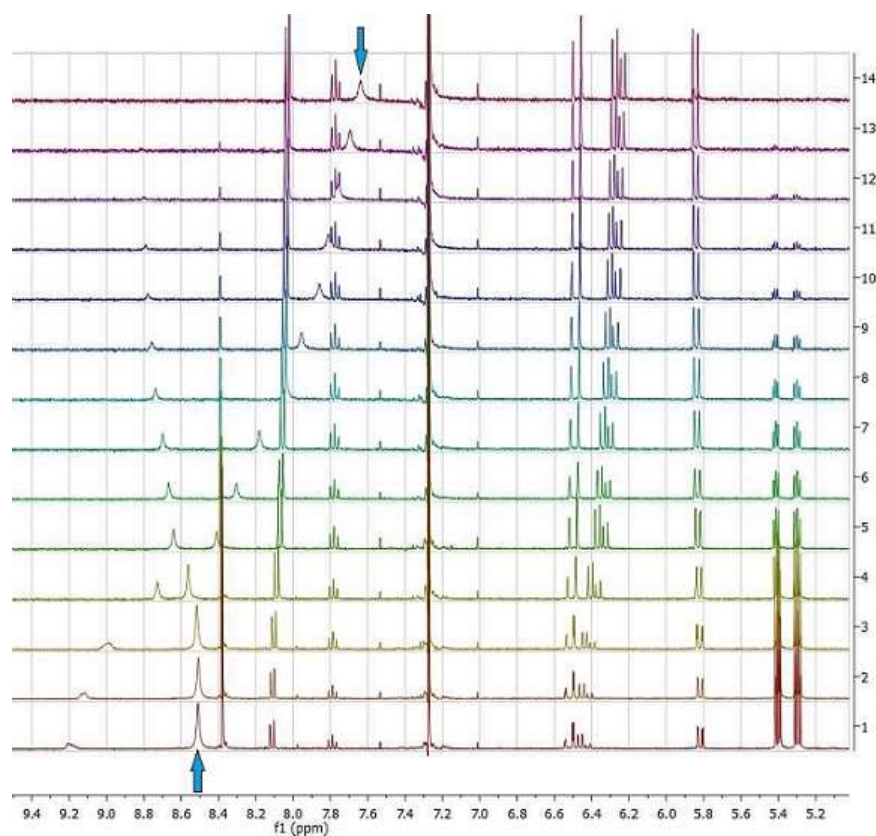


**Figure 59:** <sup>1</sup>H NMR titration of BAAPy with 2',3',4'-Tri-O-acetylpsudouridine

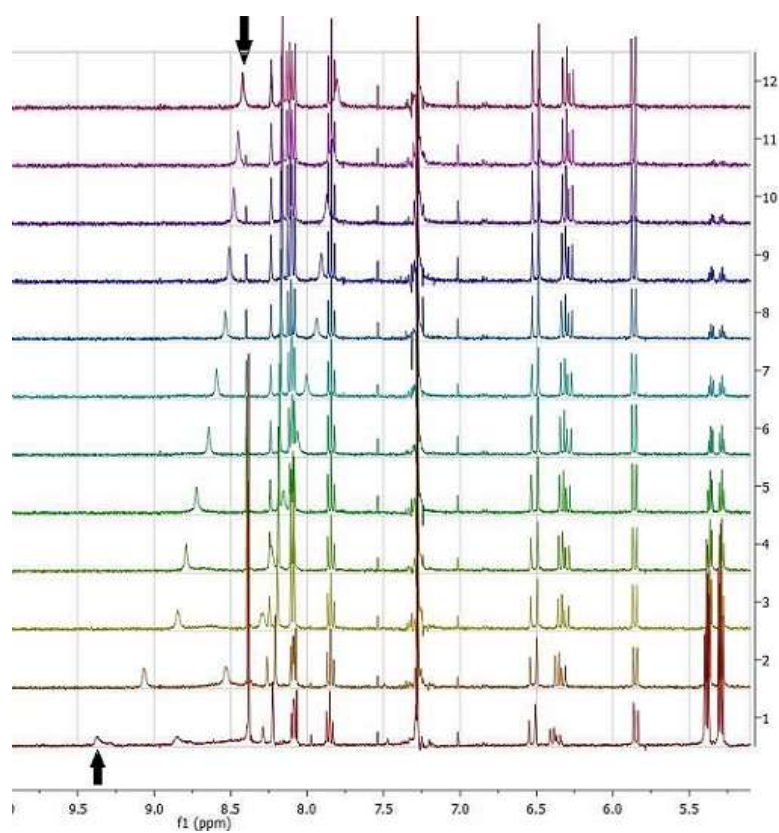


**Figure 60:** <sup>1</sup>H NMR titration of monomer 1 with 2',3',4'-Tri-O-acetylpsudouridine

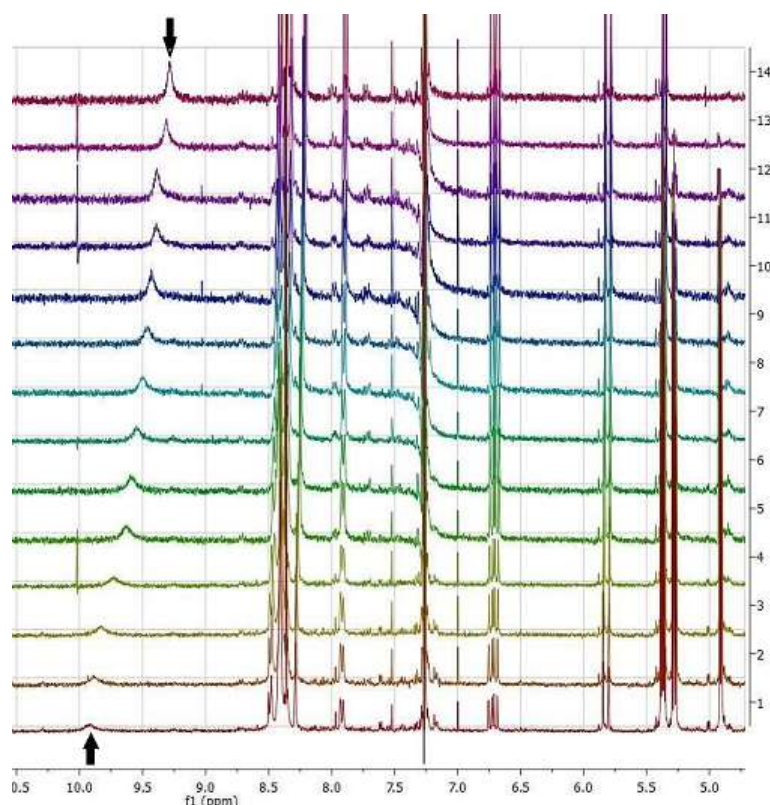


Figure 61:  $^1\text{H}$  NMR titration of monomer 6 with 2',3',4'-Tri-O-acetylpsudouridine

### 6.3.3 MIPs/NIPs evaluation

HPLC analysis, frontal chromatography and MISPE experiments were performed on all polymers by Dr. Aleksandra Krstulja of the Université d'Orléans, France.

#### *HPLC ANALYSIS*

##### Uridine-MIP

The evaluation of imprinted polymers for the recognition of uridine and their control polymers was performed in 1% acetic acid/acetonitrile in order to compare the analytical parameters of retention ( $k'$ ), specificity (IF) and selectivity ( $\alpha$ ). Overall, all MIPs were shown to be specific towards uridine and the uridine esters used as dummy templates, compared to the non-imprinted polymers, with IF values of 7-12 using uridine as the analyte. The best performing polymer was MIP 8, prepared by using TAU as template. There was also evidence for a size exclusion

effect<sup>35</sup> with this polymers, though not as pronounced as the case with riboflavin imprinting,<sup>61</sup> making the MIP with the smaller binding cavities the more specific and selective of the MIPs towards uridine. Nonetheless each of the MIPs 10-12 are more selective towards their own dummy templates, due to the imprinted cavities been shaped around different the different uridine triesters.

#### Pseudouridine-MIP

The evaluation of imprinted polymers for the recognition of pseudouridine and their control polymers was performed in 1% acetic acid/acetonitrile (v/v) in order to compare the analytical parameters of retention ( $k'$ ), specificity (IF) and selectivity ( $\alpha$ ). In this solvent, the retention time on MIPs 7 and 8 towards  $\psi$  as was greater than 40 minutes and no retention factor could be calculate; hence, they are the best performing MIP, supporting the NMR titration studies for the corresponding functional monomers. However MIP 9 was made in a different solvent (dioxane and THF), which is more polar. Hence is not possible to fairly compare MIP 7 and 8 with MIP 9. All NIPs showed poor retention of  $\psi$  apart from NIP 9 which show a slight retention of the template, dropping the IF of the MIP 9 to 4, compared to an IF for MIPs 7 and 8 that is greater than 29. Cross-selectivity towards similar nucleoside, such as uridine, was observed on MIP 7-9; this is to be expected due to the A-D-A motif of uridine being complementary to the motifs found in the binding functional monomers. Each MIP prepared is more specific towards the imprinted template and target species than the corresponding NIP. The retention factor for  $\psi$  on MIP 3, prepared using a commercially available monomer was low (MIP 3  $k'$ = 4.25), demonstrating once again the importance of designed monomers for a stoichiometric imprinting. All non-imprinted polymers have a similar behaviour towards TA $\psi$ , with the exception of MIP 3, where the  $t_R$  towards the dummy template is higher than  $\psi$ .

**Table 22:** Selectivity and specificity of template/analytes on MIPs and NIPs imprinted with TA $\psi$  in 1% acetic acid/acetonitrile (v/v) as mobile phase. <sup>a</sup> SD (standard deviation, n=3). <sup>b</sup> RSD (relative standard deviation)=(SD/x) \*100, x= mean value. \* Elution time > 40 min, N/D (non-determinate).

Polymer	Parameter	TA $\psi$ (7)	$\psi$	Uridine	5-MeU	Cytidine	Guanosine	Adenosine	RSD <sup>b</sup> %
<b>MIP 3</b>	k' $\pm$ SD <sup>a</sup>	18.27 $\pm$ 0.8	4.25 $\pm$ 0.05	1.52 $\pm$ 0.2	1.32 $\pm$ 0.05	2.47 $\pm$ 0.04	4.82 $\pm$ 0.3	3.11 $\pm$ 0.2	<10
	$\alpha$ ( $\psi$ )	0	1	3	3	1	1	3	
	IF	18	2	1	1	1	1	1	
<b>NIP 3</b>	k' $\pm$ SD <sup>a</sup>	0.99 $\pm$ 0.05	2.62 $\pm$ 0.03	1.35 $\pm$ 0.04	1.1 $\pm$ 0.02	2.88 $\pm$ 0.07	4.68 $\pm$ 0.08	1.72 $\pm$ 0.5	<6
	$\alpha$ ( $\psi$ )	3	1	2	2	1	1	2	
<b>MIP 7</b>	k' $\pm$ SD <sup>a</sup>	>40*	>40	32.78 $\pm$ 0.5	16.99 $\pm$ 0.8	8.45 $\pm$ 0.7	2.17 $\pm$ 0.04	1.3 $\pm$ 0.03	<5
	$\alpha$ ( $\psi$ )	N/D	N/D	N/D	N/D	N/D	N/D	N/D	
	IF	~91	~29	20	10	2	2	2	
<b>NIP 7</b>	k' $\pm$ SD <sup>a</sup>	0.44 $\pm$ 0.2	1.36 $\pm$ 0.05	1.63 $\pm$ 0.25	1.68 $\pm$ 0.5	1.7 $\pm$ 0.7	0.49 $\pm$ 0.8	0.83 $\pm$ 0.6	<6
	$\alpha$ ( $\psi$ )	3	1	1	1	1	2	2	
<b>MIP 8</b>	k' $\pm$ SD <sup>a</sup>	>40	>40	>40	13.91 $\pm$ 0.7	9.31 $\pm$ 0.07	7.55 $\pm$ 0.25	5.07 $\pm$ 0.03	<5
	$\alpha$ ( $\psi$ )	N/D	N/D	N/D	N/D	N/D	N/D	N/D	
	IF	~65	~39	~6	1	4	5	3	
<b>NIP 8</b>	k' $\pm$ SD <sup>a</sup>	0.62 $\pm$ 0.08	1.62 $\pm$ 0.09	17.32 $\pm$ 0.5	13.18 $\pm$ 0.4	1.7 $\pm$ 0.2	1.49 $\pm$ 0.06	1.13 $\pm$ 0.4	<6
	$\alpha$ ( $\psi$ )	5	1	10	14	12	14	19	
<b>MIP 9</b>	k' $\pm$ SD <sup>a</sup>	21.09 $\pm$ 0.08	19.79 $\pm$ 0.3	16.05 $\pm$ 0.5	13.12 $\pm$ 0.4	4.18 $\pm$ 0.2	5.14 $\pm$ 0.8	6.83 $\pm$ 0.5	<5
	$\alpha$ ( $\psi$ )	N/D	N/D	N/D	N/D	N/D	N/D	N/D	
	IF	21	4	3	2	2	2	1	
<b>NIP 9</b>	k' $\pm$ SD <sup>a</sup>	1.08 $\pm$ 0.01	6.78 $\pm$ 0.5	4.26 $\pm$ 0.03	4.21 $\pm$ 0.04	1.25 $\pm$ 0.06	2.52 $\pm$ 0.09	2.10 $\pm$ 0.04	<8
	$\alpha$ ( $\psi$ )	2	1	3	4	4	8	15	

### *BINDING SITE DISTRIBUTION AND AFFINITY*

In order to characterise the binding site affinity and capacity of the synthesised polymers, frontal chromatography was performed on each imprinted or non-imprinted polymer with its corresponding template analogue. The binding of each template analogue on its polymer was described using a Freundlich (FI) model, which accounts for surface heterogeneity. The model used relies on calculations based on isothermal (25 °C) equilibrium adsorption kinetics. From each step, the corresponding amount of the bound analyte (Q) was calculated and plotted against the corresponding concentration of template used, in order to produce binding isotherms.

MIPs 10-12 showed affinity towards their template, while the affinity is lost on the NIP. MIP 3 has a similar affinity towards TA $\psi$  to their control non-imprinted polymer, showing the lower performance of polymers made using non-stoichiometric imprinting. MIPs 7-9 have instead binding sites with high affinities towards TA $\psi$ , while NIPs 7-9 do not. MIP 8 overall has the higher binding capacity and affinity, in agreement with the findings of the titration studies. Hence, MIP 8 was selected for further studies and monomer 6 will be used in future work for the development of sensor selective towards pseudouridine.

### *MOLECULARLY IMPRINTED SOLID PHASE EXTRACTION*

Because of its good behaviour in HPLC chromatographic evaluation and its apparent higher number of imprinted sites, MIP 8 was evaluated as an SPE sorbent for the extraction of pseudouridine from synthetic urine. Synthetic urine was used in order to mimic real samples and to observe the influence of the complex matrix on the polymer's recognition capabilities. Thus, a mixture of pseudouridine with its close analogues uridine, 5-MeU and 5-fluoro-uracil (5-FU), which might be found in the urine of CRC patients, was used for this experiment.

#### *Protocol (from Dr. Aleksandra Krstulja)*

Following the initial conditioning step using 3 mL of methanol and 3 mL of water, 1 mL of a mixture pseudouridine and its analogues (5  $\mu\text{g mL}^{-1}$  each) was loaded on the polymer. Then, a 1 mL aqueous wash was performed in order to remove the buffer salts present in the synthetic urine. A subsequent “molecular recognition”

step was included in the extraction protocol, as a second wash with 1 mL of MeCN, aiming to maximize the existing polymer selectivity for a pseudouridine and eliminate as much as possible any non-specific interactions with the close analogues in the mixture. Finally, the polymers were eluted using a mixture of methanol containing 10% formic acid.

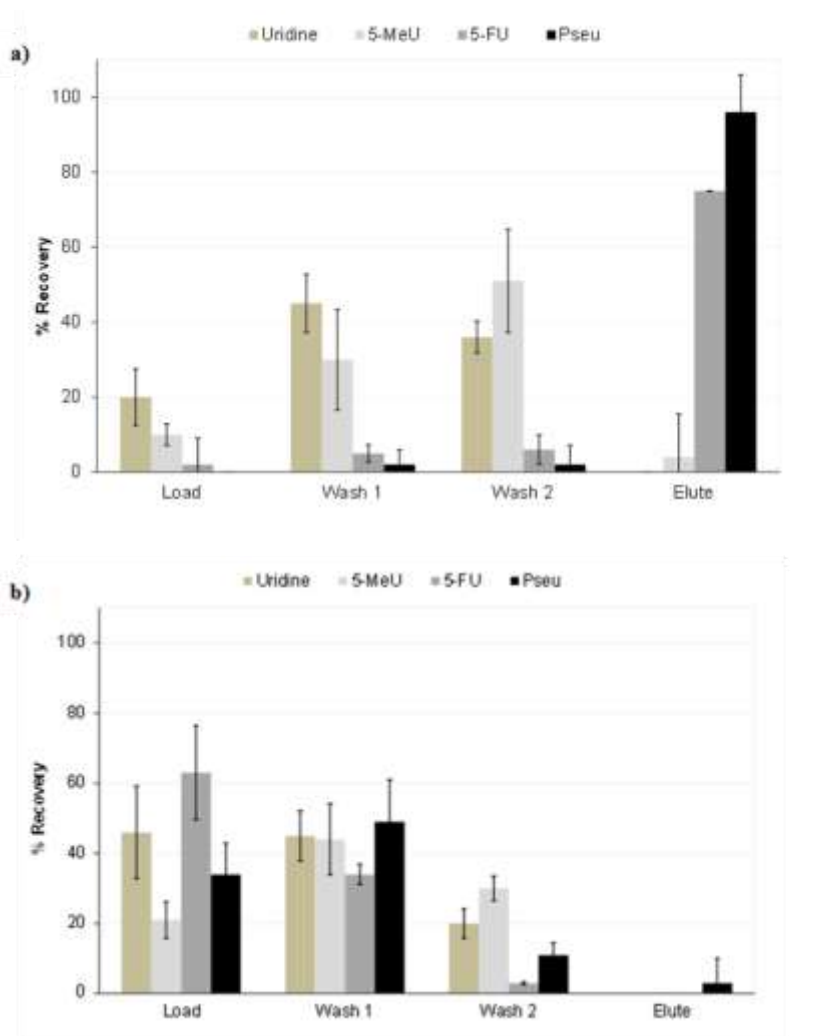


**Figure 62:** MISPE experiment for MIP 8 (a) and NIP 8 (b). Percentage of analytes eluted in each step (load, wash and elution) through the MIP and the control polymer (NIP). Uridine, 5-methyl-uridine (5-MeU), 5-fluoro-uracil (5-FU) and pseudouridine were used as analytes. Experimental data obtained from Aleksandra Krstulja.

Almost 100% of pseudouridine was recovered from the synthetic urine, together with 75% of 5-FU, which is an anticancer drug that can be found in the urine of patients. No recovery was observed on the NIP 8. Hence the use of monomer 6 was

vital to create an imprinted polymer with a great performance for the evaluation of a cancer biomarker in human fluid with a non-invasive method. These are preliminary results that will be applied to real patient urine in the future.

## **6.4 CONCLUSIONS**

For non-covalent imprinting, the characteristics of the solvent/porogen used during the polymerisation are vital. To maintain the driving binding force responsible for the imprinting, aprotic solvents, such as chloroform, acetonitrile and tetrahydrofuran, need to be used. Unfortunately, the template to be imprinted is not always soluble in such systems, as is the case with nucleosides. We successfully overcame this issue by using nucleoside triesters as “dummy” templates to imprint uridine and pseudouridine.

Pseudouridine was imprinted using tailor-made functional monomers previously prepared for the stoichiometric non-covalent imprinting of biotin and barbiturates. These novel functional monomers, due to their high number of hydrogen-bond functionality, can be applied successfully to different systems, as demonstrated by the imprinting of pseudouridine.

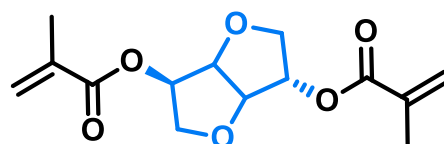
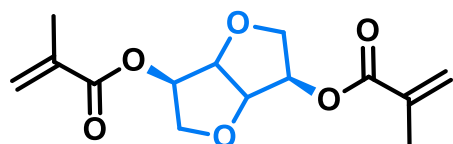
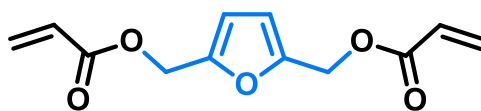
The pre-polymerisation studies, such as NMR titrations, can provide information about the likely characteristics of a MIP before its fabrication, allowing us to design more selective materials. Monomers 1, 6 and 7 were titrated with TA $\psi$  in order to evaluate their potential in imprinting this molecule. Monomer 6 showed the highest association constant, which translated to the creation of the best  $\psi$ -binding polymer. A size exclusion behaviour of the uridine esters MIP was also observed, which is in agreement with previous finding, underlying the importance of the dummy template’s size to create cavities that more perfectly accommodate and bind the template.

Another observation can also be made about the difference between MIPs made using a stoichiometric non-covalent method, which apply tailor-made functional monomers, and the use of a commercially available monomer, such as methacrylates. MIPs 7-9 were superior in performance to MIP 3, which once more supports this theory.



# CHAPTER 7

## *BIO-SUSTAINABLE CROSS-LINKERS FOR MOLECULAR IMPRINTING*



## 7.1 INTRODUCTION

### 7.1.1 The role of the Cross-linker

It is a general idea that the formation of binding sites during the imprinting process is driven mainly by the nature of the functional monomer-template complex. This complex can be affected by the solvent polarity and can be estimated the performance of the imprinted polymers by means of spectroscopic techniques, such as NMR studies. In non-covalent imprinting, the strength of the template-functional monomer complex is an indication of the future MIP selectivity and affinity towards the template. However the cross-linker also plays an important role in the polymer performance and various groups have previously investigated the effect of the crosslinking agent.<sup>36b, 138</sup> The stoichiometry and chemical reactivity, the degree of cross-linkage, the stability of crosslinker-template interaction, the crosslinker-template interaction and the distance between the crosslinking points may all influence the template recognition and the selectivity of the final imprinted polymer. The crosslinking agent is the component that “freezes” the functional monomer-template complex inside the matrix, creating around it a cavity with the right shape and size, and with the right spatial arrangement of the functional groups, that can later accommodate and recognise the template during the rebinding event. The crosslinker nature and concentration in the pre-polymerisation matrix can lead to a more rigid or flexible matrix. Extensive early studies showed that EGDMA in a 70-95% is one of the more efficient crosslinkers and leads to polymers with higher selectivity.<sup>36b</sup> Lower crosslinker concentration can create a flexible, gel-like polymeric matrix, which shows lower selectivity towards the template, as the complex is not strongly fixed inside the polymer. On the other hand, a polymer with a high degree of cross-linkage, may not allow the template to move freely in the porous material and to reach the binding cavities. The crosslinker can also play an important role in the design of a MIP, as it can interact with the functional monomer and the template in the pre-polymerisation mixture through hydrogen bonding and other non-covalent interactions. An example of this has been shown in the Molecular Dynamic Simulations studies performed on EGDMA- and TRIM-crosslinked MAA copolymers selective for (S)-propranolol<sup>138a</sup> with the results supported by NMR titration experiments. It was demonstrated that the crosslinkers’

ester groups can interact with the hydrogen bond donors of both MAA and the template.

In order to find a greener alternative to EGDMA, herein we will report on the synthesis of three acrylate- and methacrylate-based crosslinking monomers (figure 63) prepared by esterification of isosorbide (1,4:3,6-dianhydrosorbitol), isomannide (1,4:3,6-dianhydromannitol) and 2,5-bis(hydroxymethyl)furan. In order to verify the influence of the crosslinkers, the BAAPy-TAU system was used as a model to prepare the novel MIPs.<sup>95</sup>

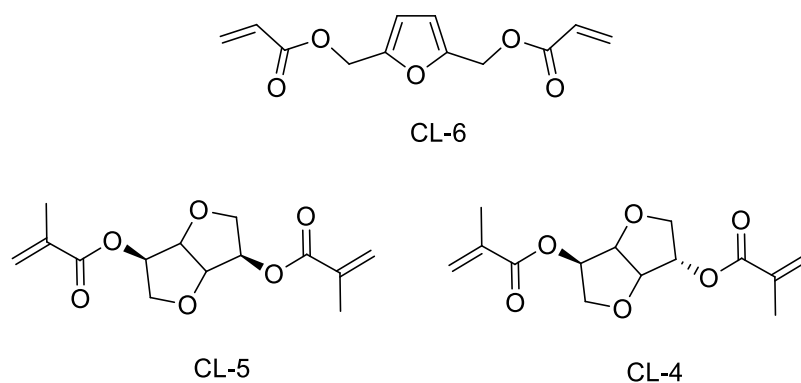


**Figure 63:** CL-6. 2,5-Bis(hydroxymethyl)furan-diacrylate; CL-5. isomannide-dimethacrylate; CL-4. isosorbide-dimethacrylate.

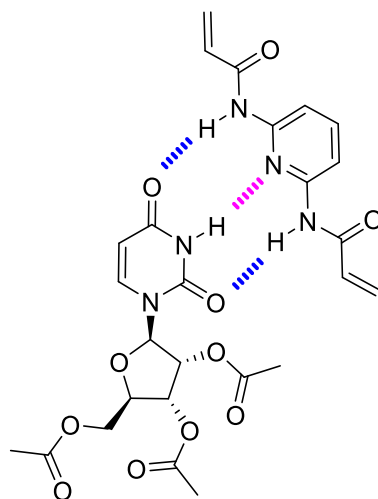


**Figure 64:** BAAPy and 2',3',4'-tri-O-acetyluridine interaction in the pre-polymerization mixture. Three hydrogen bonds are shared between host (DAD) and guest (ADA).

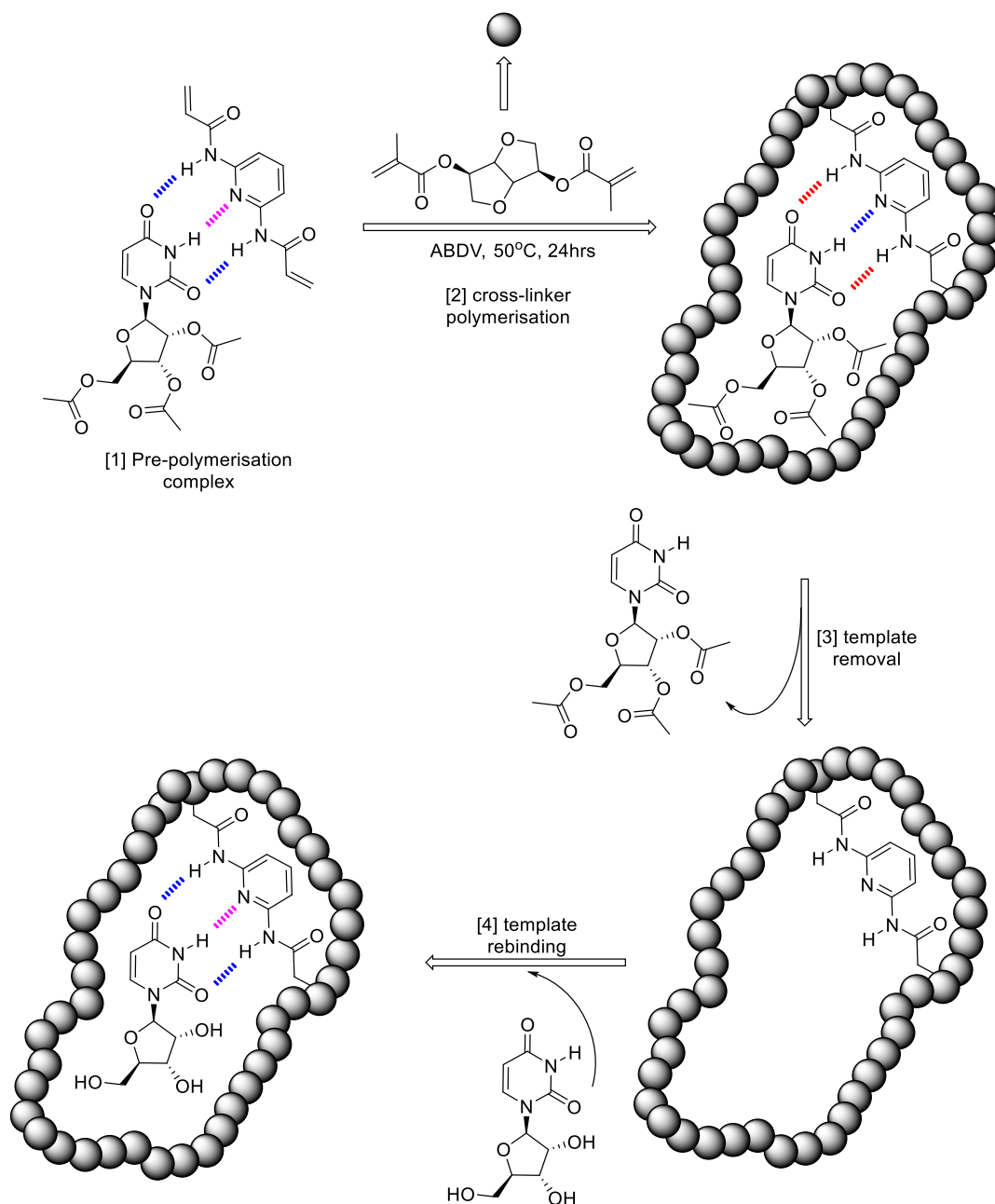


**Figure 65:** MIP5 preparation scheme.

### 7.1.2 Biomass as renewable resources

In recent years there has been an increased demand for using greener sources to create chemicals and to make materials bio-sustainable.<sup>139</sup> Biomass is an inexpensive renewable resource, which can reduce the environmental impact of the industrial production of fuels, chemicals and materials in general. Biomass can

substitute dangerous and more toxic chemicals, making them bio-friendly for the environment and, overall, sustainable.<sup>140</sup>

Isomannide, isosorbide and bis(hydroxymethyl)furan (BHF) are molecules obtained from such natural resources. Isomannide and isosorbide are anhydrous sugars derived from *starch extracted from cereals*.<sup>141</sup> HMF is instead produced from cellulose and hemicellulose, which represent the larger part of woody biomass (55% to 80%). Hence, while isomannide and isosorbide are still interrupting the food chain, HMF production does not, enhancing its green credentials. There is a growing push to increase the number of future bio-refineries to use non-food sources as renewable resources.<sup>140</sup>

*“Biomass is defined as any organic material from plants or animals. Biomass can be produced by farming, land management and forestry sectors and used for renewable energy generation.” [Farming Future].*

*“Biomass is biological material derived from living, or recently living organisms. In the context of biomass for energy this is often used to mean plant based material, but biomass can equally apply to both animal and vegetable derived material.” [BIOMASS Energy Centre]*

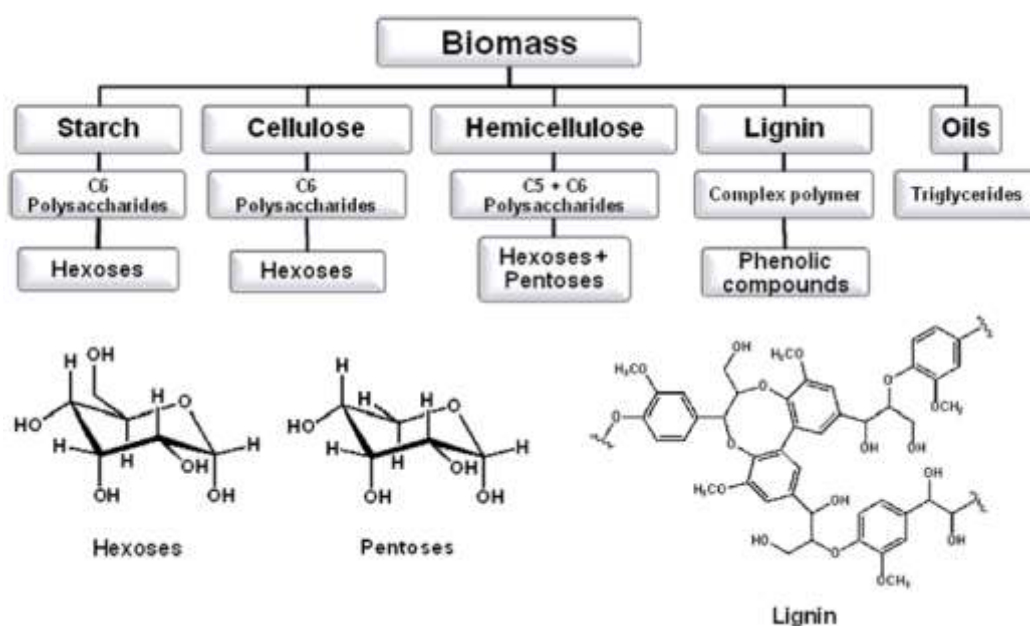
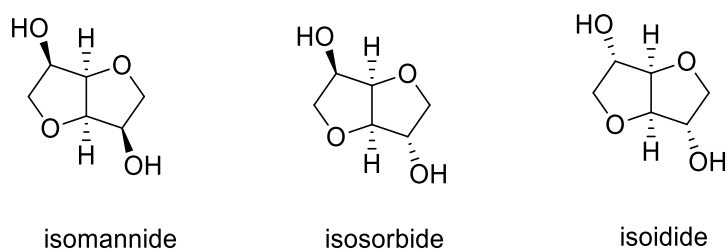


Figure 66: Main biomass components<sup>141</sup>

### 7.1.2 Isomannide, isosorbide and isoidide

The anhydrous sugars isomannide, isosorbide (and isoidide) (Figure 67) are isomers derived from *starch extracted from cereals*, which is first degraded into D-glucose and D-mannose by an enzymatic process (Figure 68). The two sugars are then hydrogenated to give D-sorbitol and D-mannitol. Sorbitol and mannitol are subsequently dehydrated to obtain isosorbide (1,4:3,6-dianhydrosorbitol) and isomannide (1,4:3,6-dianhydromannitol).



**Figure 67:** The structures of isomannide, isosorbide and isoidide.

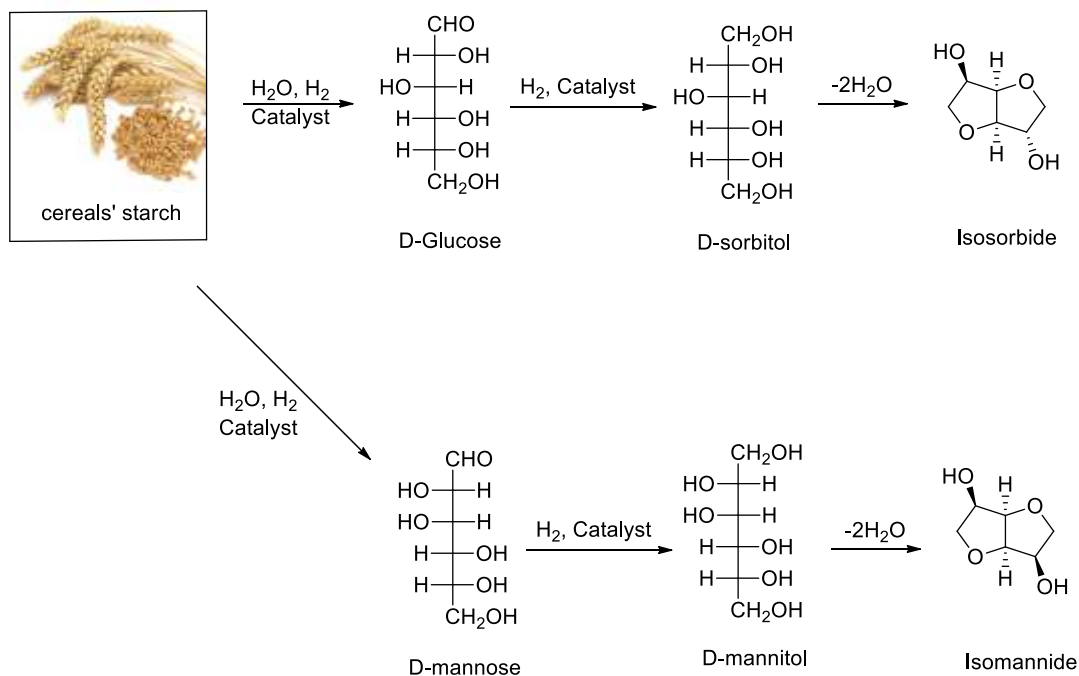


**Figure 68:** The preparation of isosorbide and isomannide from cereals starch.

Unfortunately isoidide is produced from L-idose (Figure 69), which rarely exists in nature and cannot be extracted from vegetable biomass.

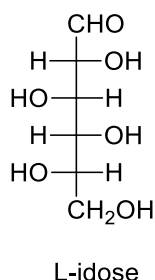


Figure 69: L-idose structure.

### 7.1.3 2,5-Bis(hydroxymethyl)furan

5-hydroxymethylfurfural (HMF) is produced from cellulose and hemicellulose, which represent the larger part of woody biomass (55% to 80%), as shown in Figure 70 and 71. Cellulose and hemicellulose are generally hydrolysed into monomeric sugar units which can then be dehydrated to form HMF. HMF can be readily reduced to obtain 2,5-bis(hydroxymethyl)furan (BHF), which can then be used to obtain a crosslinking monomer.

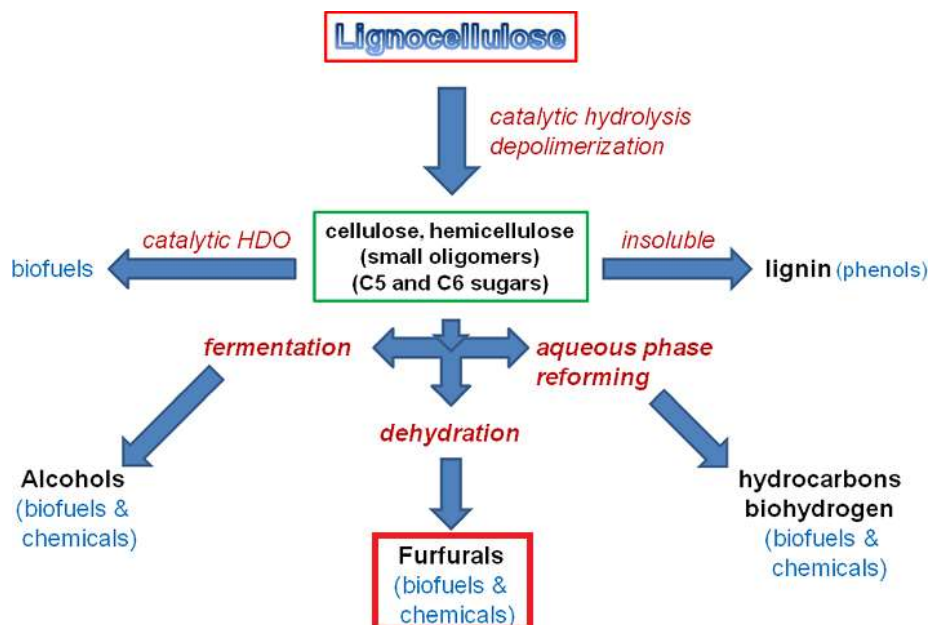
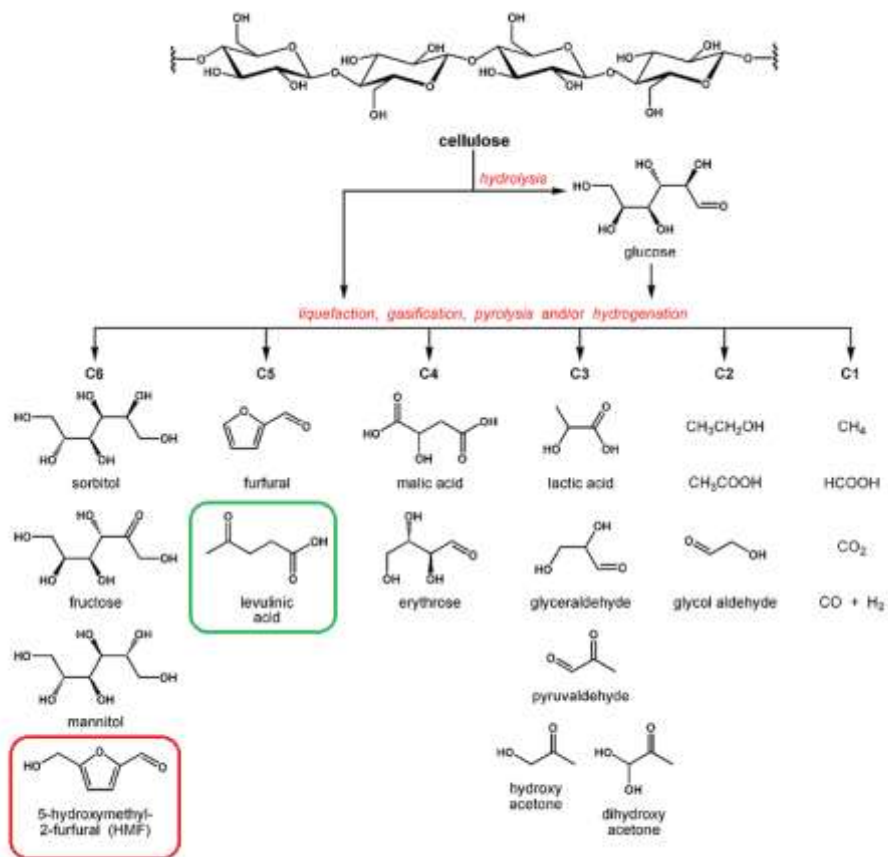


Figure 70: Products obtained from the treatment of lignocellulose obtained from biomass<sup>141</sup>.



**Figure 71:** Products obtained from the treatment of lignocellulose obtained from biomass<sup>141</sup>.



## 7.2 EXPERIMENTAL

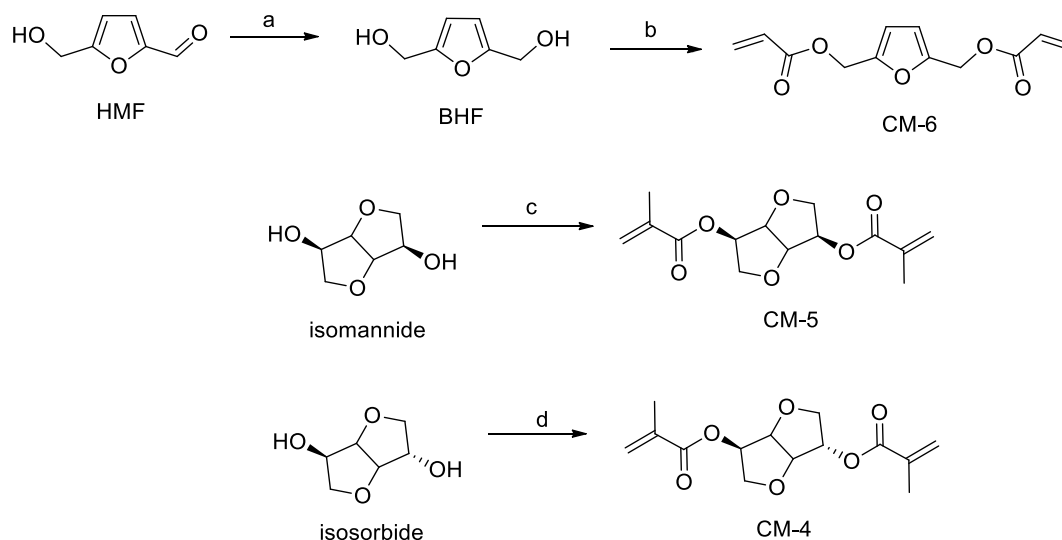


**Figure 72:** Cross-linkers reaction scheme. a) i. HMF, THF and  $\text{NaBH}_4$ ,  $0^\circ\text{C}$ , ii. HCl 2N,  $0^\circ\text{C}$ ; b) BHF, TEA, DCM,  $\text{CH}_2=\text{CHCOCl}$ ,  $0^\circ\text{C} \rightarrow \text{RT}$ ,  $\text{N}_2$ ; c) Isomannide, NaOH 5M,  $\text{CH}_2=\text{C}(\text{CH}_3)\text{COCl}$ ,  $0^\circ\text{C} \rightarrow \text{RT}$ ; d) Isosorbide, NaOH 5M,  $\text{CH}_2=\text{C}(\text{CH}_3)\text{COCl}$ ,  $0^\circ\text{C} \rightarrow \text{RT}$ .

7.2.1 Synthesis of 2,5-bis(hydroxymethyl)furan [BHF]<sup>142</sup>

In a 200 mL Schlenk flask, 5-hydroxymethylfurfural (HMF) (5 g, 40 mmol) was dissolved in dehydrated tetrahydrofuran (15 mL) and kept at  $0^\circ\text{C}$  in an ice bath. Sodium borohydride (3 g, 79.3 mmol) was added to the flask slowly over 10 minutes and then the reaction mixture was neutralized with HCl (2 N). In total, 40 mL of HCl 2N was added and the precipitate formed filtered off before an extraction was performed. The water layer was extracted again with ethyl acetate ( $3 \times 40$  mL). The organic phase was dried with  $\text{MgSO}_4$ , filtered and the filtrate placed in the refrigerator to allow the product to recrystallize. The product was obtained as white crystals (4.4 g, 88.0%).  **$^1\text{H NMR}$**  (400 MHz,  $\text{DMSO-d}_6$ ):  $\delta$  4.349 (d,  $^3\text{J} = 6\text{Hz}$ , 4H,  $\text{CH}_2$ ), 5.156 (t,  $^3\text{J} = 6\text{Hz}$ , 2H, OH), 6.181 (s, 2H, furan) ppm.  **$^{13}\text{C NMR}$**  (400 MHz,  $\text{DMSO-d}_6$ ):  $\delta$  56.275 ( $\text{CH}_2$ ), 107.953 (CH furan), 155.203 (C furan) ppm. **MS** [ $\text{M}+\text{H}^+$ ]: 152.1. **IR**: 810.8, 1001.0, 1453.1, 1678.6, 2877.5, 2943.7, 3218.2  $\text{cm}^{-1}$ . **M.p.**:  $65\text{--}75^\circ\text{C}$ .

**7.2.2 Synthesis of 2,5-bis(hydroxymethyl)furan-diacrylate (CM-6)**

5g of BHF (0.04 mol, 1 eq) and TEA (13.94 mL, 0.1 mol, 2.5 eq) were solubilized in 150 mL of dry DCM. Acryloyl chloride (7.15 mL, 0.088 mol, 2.2 eq) dissolved in 10 mL of DCM was then added dropwise at 0 °C under a dinitrogen atmosphere. The reaction mixture was left to stir overnight at RT and the next day the DCM solution was washed with water (150 mL), saturated aqueous NaHCO<sub>3</sub> (2 × 150 mL), aqueous NaOH 1M (150 mL) and brine (150 mL). The organic layer was dry (MgSO<sub>4</sub>), filtered and evaporated. A silica-plug was performed on the oil (DCM) and a pale yellow oil was obtained (8.9g, 80%). **<sup>1</sup>H NMR** (400 MHz, DMSO-*d*<sub>6</sub>): δ 5.144 (s, 4H, CH<sub>2</sub>), 5.974 (dd, <sup>2</sup>J = 2 Hz, <sup>3</sup>J=10 Hz, 2H, CH<sub>cis</sub> =), 6.207 (dd, <sup>3</sup>J<sub>cis</sub>= 10.4 Hz, <sup>3</sup>J<sub>trans</sub>= 17.2 Hz, 2H, -CH=), 6.358 (dd, <sup>3</sup>J<sub>cis</sub>= 1.6 Hz, <sup>3</sup>J<sub>trans</sub>= 17.6 Hz, 2H, CH<sub>trans</sub>=), 6.552 (s, 2H, furan) ppm. **<sup>13</sup>C NMR** (400 MHz, DMSO-*d*<sub>6</sub>): δ 58.279 (CH<sub>2</sub>), 112.556 (CH furan), 128.423 (-CH=), 132.843 (=CH<sub>2</sub>), 150.523 (C furan), 165.603 (C=O) ppm. **MS** [M+Na<sup>+</sup>]: 259.144. **HRMS** (ESI-TOF) m/z: [M+Na]<sup>+</sup> Calcd for C<sub>12</sub>H<sub>12</sub>O<sub>5</sub>Na 259.21; Found 259. **IR**: 812.0, 1152.7, 1453.6, 1716.2, 2873.7, 2930.0, 2980.2 cm<sup>-1</sup>.

**7.2.3 Synthesis of isomannide-dimethacrylate (CM-5)<sup>143</sup>**

Isomannide (8 g, 0.0547 mol, 1 eq) was dissolved in 80 mL of NaOH 5M. 12.6 mL of methacryloyl chloride (0.120 mol, 2.2 eq) were added drop wise at 0 °C. Note that the addition needs to be very slow in order to avoid polymerisation occurring during the reaction. After addition, the aqueous phase was extracted with ether (3 × 100 mL) and the combined organic layers were dried (MgSO<sub>4</sub>) and filtered. The solvent was evaporated to obtain a white solid (2.9g, 19%). **<sup>1</sup>H NMR** (400 MHz, DMSO-*d*<sub>6</sub>): δ 1.89 (s, 6H, CH<sub>3</sub>), 3.72 (dd, <sup>2</sup>J = 6.4 Hz, <sup>3</sup>J=9.2 Hz, 2H), 3.98 (dd, <sup>2</sup>J = 6.4 Hz, <sup>3</sup>J=9.2 Hz, 2H) 4.67 (m, 2H, CH<sub>cis</sub> =), 5.07 (m, 2H, CH<sub>trans</sub>=), 5.73 (m, 2H), 6.07 (m, 2H) ppm. **<sup>13</sup>C NMR** (400 MHz, DMSO-*d*<sub>6</sub>): δ 18.513 (CH<sub>3</sub>), 70.456 (C), 74.232 (C), 80.476 (C), 126.882 (=CH<sub>2</sub>), 135.969 (-CH=), 166.429 (C=O) ppm. **MS** [M+H<sup>+</sup>]: 283.2043. **HRMS** (ESI-TOF) m/z: [M+H]<sup>+</sup> Calcd for C<sub>14</sub>H<sub>19</sub>O<sub>6</sub>H 283.29; Found 283.1189. **IR**: 1093.0, 1296.7, 1637.7, 1716.2, 2873.7, 2930.0, 2980.2 cm<sup>-1</sup>. **M.p.:** 67-69°C.

### 7.2.4 Synthesis of isosorbide-dimethacrylate (CM-4)

Isosorbide (16 g, 0.109 mol, 1 eq) was dissolved in 160 mL of NaOH 5M. 26.7 mL of methacryloylchloride (0.27 mol, 2.5 eq) were added dropwise at 0°C (the addition needs to be very slow in order to avoid polymerisation). After addition the water phases was extracted with ether (3 × 200 mL) and the organic layers combined, dried (MgSO<sub>4</sub>) and filtered. The solvent was evaporated to obtain a crude oil (15g, impure). The crude material was stirred at room temperature in 200 mL of deionized water for 5 days. After 5 days, 150 mL of DCM were added. The organic layer was washed with 50 mL of NaOH 1M and 70 mL of saturated bicarbonate solution to remove the impurity. The solution was dried (MgSO<sub>4</sub>), filtered and the solvent evaporated to obtain a light yellow oil (7mL, 23%). **<sup>1</sup>H NMR** (400 MHz, DMSO-*d*<sub>6</sub>): δ 1.88 and 1.90 (s, 6H, CH<sub>3</sub>), 3.86 (m, 4H), 4.46 (d, J=4.8 Hz, 1H, **5a-d**), 4.84 (t, J=4.84 Hz, 1H), 5.13 (d, J=2.8 Hz, 1H), 5.18 (dd, <sup>2</sup>J = 5.6 Hz, <sup>3</sup>J=10 Hz, 1H), 5.72 (d, J=1.6 Hz, 2H), 6.05 (d, J=6.4 Hz, 2H) ppm. **<sup>13</sup>C NMR (400 MHz, DMSO-*d*<sub>6</sub>)**: δ 18.519 (CH<sub>3</sub>), 70.891 and 72.879 (C), 74.550 (C), 78.481 (C), 81.027 (CH<sub>3</sub>), 86.019 (C), 126.708 and 127.048 (=CH<sub>2</sub>), 136.045 (-CH=), 166.338 (C=O) ppm. **MS [M+H<sup>+</sup>]**: 283.1406. **HRMS** (ESI-TOF) m/z: [M+H]<sup>+</sup> Calcd for C<sub>14</sub>H<sub>19</sub>O<sub>6</sub>H 283.29; Found 283.1190. **IR**: 1017.5, 1159.6, 1451.4, 1633.9, 1718.0, 2879.7, 2957.8, 2988.5 cm<sup>-1</sup>.

### 7.2.5 Polymer formulations

**Table 23:** MIPs 4-6 and NIPs 4-6 formulation.

	2',3',5'-tri-O-acetyl-uridine (mass/mmol)	BAAPy (mass/mmol)	Crosslinker (mass/mmol)	ABDV (mass/mmol)	CHCl <sub>3</sub> (volume)
MIP 4	185.2 mg/0.5	108.6 mg/0.5	<b>3</b> (2.82 g/10)	29 mg/0.12	2.8 mL
NIP 4	-----	108.6 mg/0.5	<b>3</b> (2.82 g/10)	29 mg/0.12	2.8 mL
MIP 5	185.2 mg/0.5	108.6 mg/0.5	<b>2</b> (2.82 g/10)	29 mg/0.12	2.8 mL
NIP 5	-----	108.6 mg/0.5	<b>2</b> (2.82 g/10)	29 mg/0.12	2.8 mL
MIP 6	185.2 mg/0.5	108.6 mg/0.5	<b>1</b> (2.36 g/10)	25 mg/0.10	2.8 mL
NIP 6	-----	108.6 mg/0.5	<b>1</b> (2.36 g/10)	25 mg/0.10	2.8 mL

## 7.3 RESULTS AND DISCUSSION

### 7.3.1 Synthesis

All crosslinking monomers were obtained by esterification of the hydroxyl groups of isosorbide (1,4:3,6-dianhydrosorbitol), isomannide (1,4:3,6-dianhydromannitol) and 2,5-*bis*(hydroxymethyl)furan with either acryloyl chloride or methacryloyl chloride.

The three crosslinkers are highly reactive, and can auto-polymerise even under mild conditions (RT overnight). Hence, none of them was dried under vacuum, as they polymerised under this condition. All crosslinkers were stored in the freezer with sulfur to inhibit polymerisation. The overall yield of CM-4 and CM-5 was low, as a Schotten–Baumann protocol was used to avoid the formation of an impurity which is present in the commercial methacryloyl chloride (MAACl) and proved otherwise impossible to remove. As previously reported<sup>144</sup> the highest concentration impurity that can be found in a fresh bottle of commercially available MAACl is the dimerization product **3**. (Figure 73) which can be found to be as much as 10-15% of the total product. Even the storage of MAACl at -20°C can lead to the formation of this impurity. Compound **3** can then react again and create other dimerization product (Figure 73), but the major impurity is **3**. Several reactions and protocols using different fresh bottles of MAACl were performed, however the same impurity identify by <sup>1</sup>H NMR was always present in different crosslinkers, even after purification.

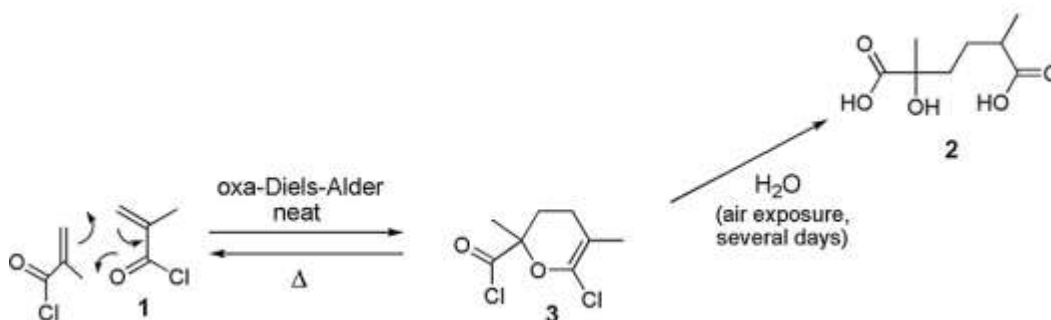


**Figure 73:** MAACl's impurity (**3**)<sup>144</sup>

In CM-4 the impurity was removed only after prolonged exposure on air and water, while in CM-5, as it is a solid, the crosslinker was obtained pure after extraction. Several attempts were made in order to synthesize 2,5-bis(hydroxymethyl)furan-dimethacrylate, but the impurity was consistently present (figure 74).

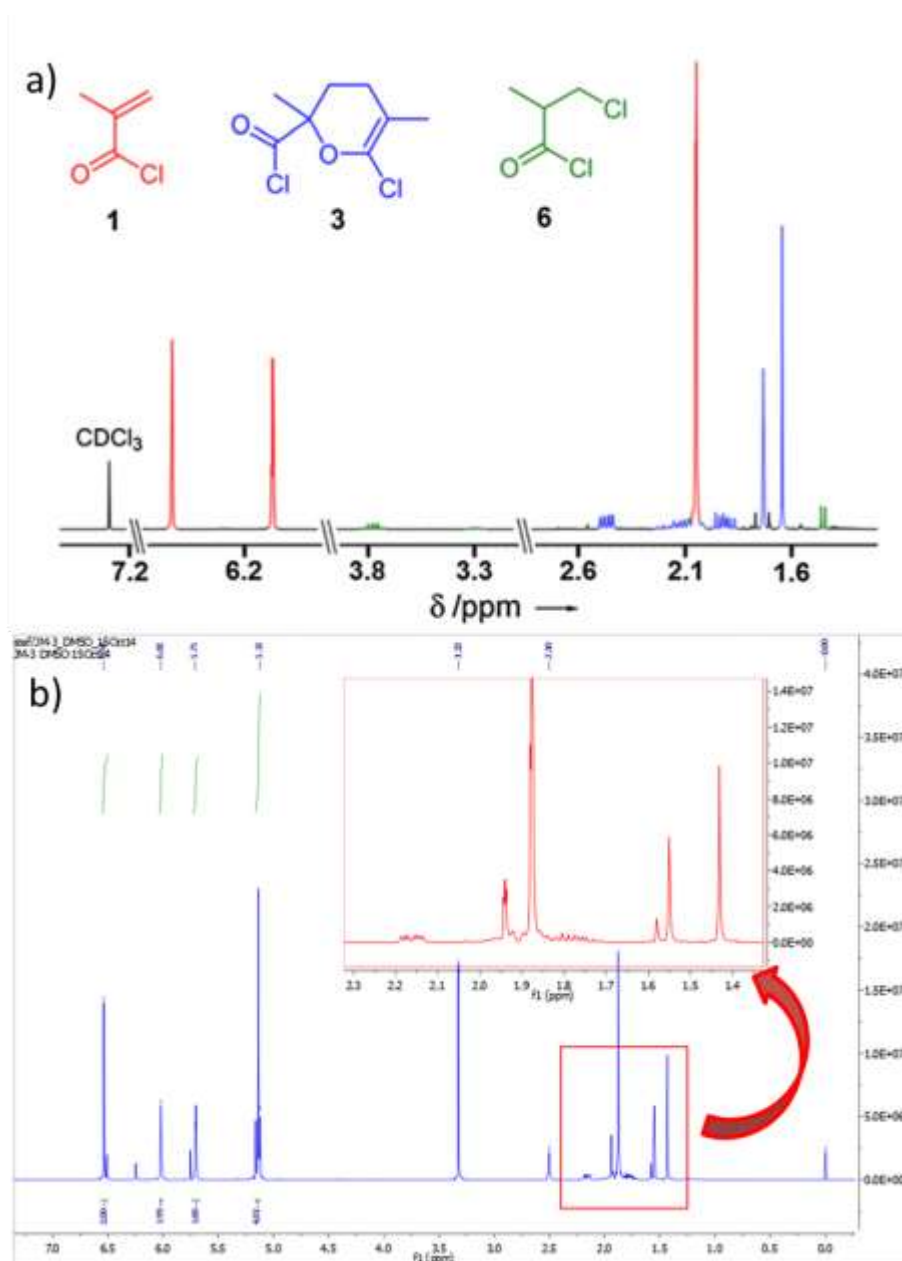


**Figure 74:** a)  $^1\text{H}$  NMR of MAACl's impurities<sup>144</sup>; b)  $^1\text{H}$  NMR of bis(hydroxymethyl)furan-dimethacrylate showing the MAACl impurity 3 presents in the upfield area (red box).

### 7.3.2 Chromatographic evaluation

#### *MIP selectivity in organic mobile phase*

Chromatographic evaluation of the polymers was performed in order to obtain imprinting characteristic of our material in terms of retention behaviour ( $k'$ ) Imprinting Factor (IR) and selectivity ( $\alpha$ ). 1% acetic acid/acetonitrile (v/v) was used as eluent, which is a fairly polar solvent, in order to have retention times  $t_R$  for the analytes lower than one hour. In Figure 75-76 and Table 24 are shown the  $k'$ ,  $\alpha$  and IF values for the template and related molecules on MIPs 4-6 and NIPs 4-6.

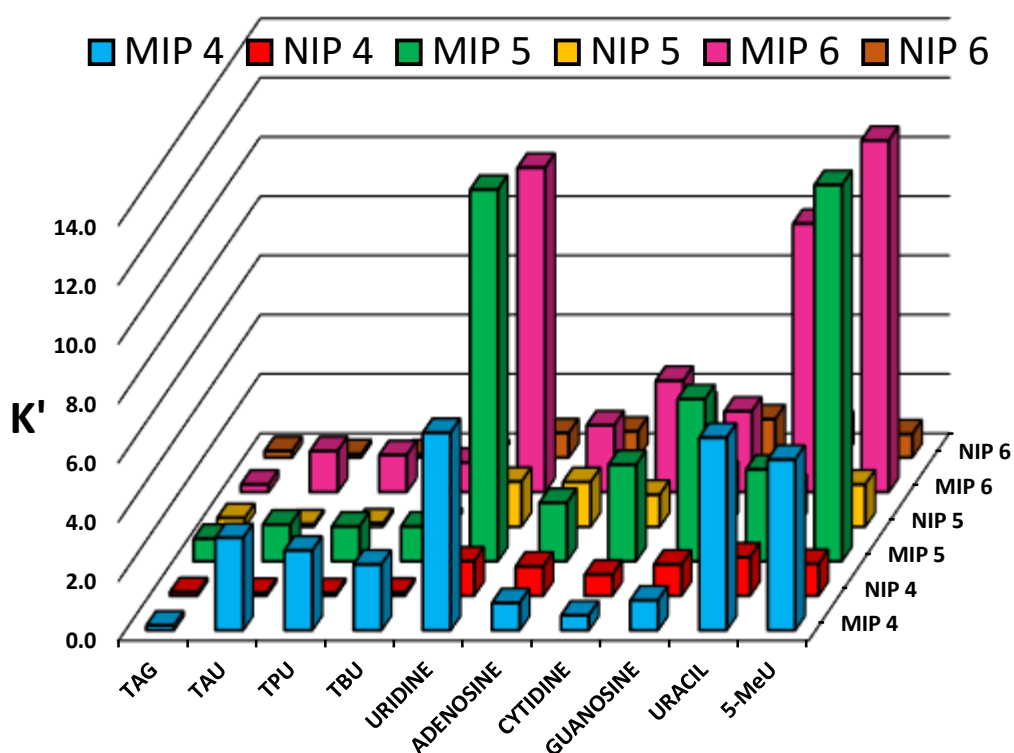


**Figure 75:** Chromatographic evaluation of MIP 4-6 and NIP 4-6 using 1% acetic acid/acetonitrile (v/v) as eluent.  $K'$  = retention factor.

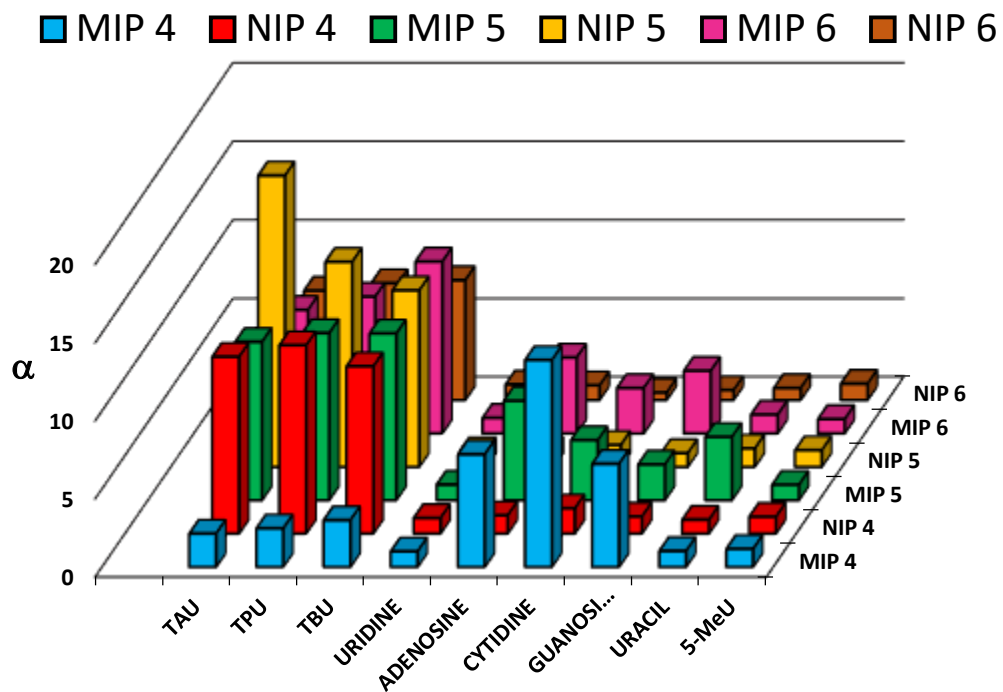


**Figure 76:** Selectivity ( $\alpha$ ) of the target and related nucleoside for MIPs 4-6 and NIPs 4-6 in 1% acetic acid/acetonitrile (v/v).

**Table 24:** Selectivity and specificity of template/analytes on imprinted polymers MIP 4, MIP 5, MIP 6 and control polymers NIP 4, NIP 5, NIP 6 in 1% acetic acid/acetonitrile (v/v) as mobile phase. SD (standard deviation, n=3). <sup>b</sup> RSD (relative standard deviation)=(SD/x) \*100, x= mean value.

Polymer	Parameter	Uridine (7)	Uracil	5-MeU	Cytidine	Adenosine	Guanosine	TAG	TAU	TPU	TBU	RSD <sup>b</sup> %
<b>MIP 4</b>	K <sup>±</sup> SD <sup>a</sup>	6.7±0.02	6.5±0.03	5.7±0.04	0.5±0.02	0.9±0.04	1.0±0.04	0.2±0.02	3.1±0.03	2.7±0.01	2.2±0.04	<10
	α (7)	1.0	1.0	1.2	13.3	7.2	6.6	41.5	2.1	2.5	3.0	
	IF	6	5	5	1	1	1	1	30	28	21	
<b>NIP 4</b>	K <sup>±</sup> SD <sup>a</sup>	1.2±0.06	1.3±0.04	1.3±0.04	0.7±0.04	1.0±0.03	1.1±0.03	0.1±0.01	0.1±0.01	0.1±0.01	0.1±0.01	<10
	α (7)	1.0	0.9	1.1	1.6	1.2	1.1	9.2	11.3	12.1	10.7	
	IF	8	2	9	3	1	3	3	15	10	9	
<b>MIP 5</b>	K <sup>±</sup> SD <sup>a</sup>	12.5±0.03	3.1±0.06	12.7±0.04	3.3±0.04	2.0±0.00	5.5±0.03	0.8±0.03	1.2±0.03	1.2±0.03	1.2±0.01	<4
	α (7)	1.0	4.1	1.0	3.9	6.4	2.3	16.6	10.2	10.7	10.7	
	IF	8	2	9	3	1	3	3	15	10	9	
<b>NIP 5</b>	K <sup>±</sup> SD <sup>a</sup>	1.5±0.02	1.3±0.04	1.4±0.03	1.1±0.04	1.5±0.01	1.7±0.09	0.3±0.03	0.1±0.00	0.1±0.01	0.1±0.01	<7
	α (7)	1.0	1.2	1.1	1.4	1.0	0.9	5.2	18.6	13.1	11.3	
	IF	13	8	15	2	3	2	1	12	11	9	
<b>MIP 6</b>	K <sup>±</sup> SD <sup>a</sup>	10.9±0.02	9.0±0.03	11.9±0.05	3.8±0.18	2.3±0.04	2.7±0.03	0.3±0.01	1.4±0.03	1.2±0.01	1.0±0.01	<5
	α (7)	1.0	1.2	0.9	2.9	4.9	4.0	42.9	7.9	8.8	11.0	
	IF	13	8	15	2	3	2	1	12	11	9	
<b>NIP 6</b>	K <sup>±</sup> SD <sup>a</sup>	0.8±0.02	1.1±0.09	0.8±0.05	1.7±0.04	0.9±0.02	1.3±0.07	0.2±0.02	0.1±0.01	0.1±0.01	0.1±0.01	<10
	α (7)	1.0	0.8	1.0	0.5	0.9	0.6	3.8	7.0	7.5	7.7	
	IF	13	8	15	2	3	2	1	12	11	9	



All imprinted polymers show selectivity towards uridine, uracil and 5-MeU, as expected, while the control polymers do not retain these analytes. Hence, the selectivity of the polymers is due to specific binding cavities shaped around the template during polymerisation. The different nature of the cross-linkers does not affect enormously the selectivity of the materials towards uridine, although uridine has a greater retention on EGDMA-based MIPs when analysed by chromatography using the same solvent system.<sup>95</sup> However, here we want to understand if, using a different cross-linker, MIPs with high selectivity can be still made, avoiding the need to use an oil-derived methacrylate (from ethylene glycol) as the cross-linking agent. TAU, TPU and TBU are less retained compared to uridine, in line with a previously reported study on a similar MIP<sup>95</sup>, however the imprinting is present (IF = 9 - 30).

A nucleoside has hydroxyl groups on the  $\beta$ -D-ribofuranose moiety which can, potentially, create hydrogen bonds with the carboxylic groups of the crosslinkers.

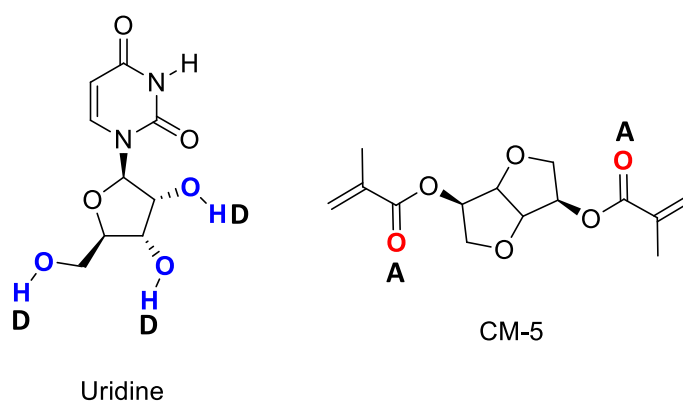


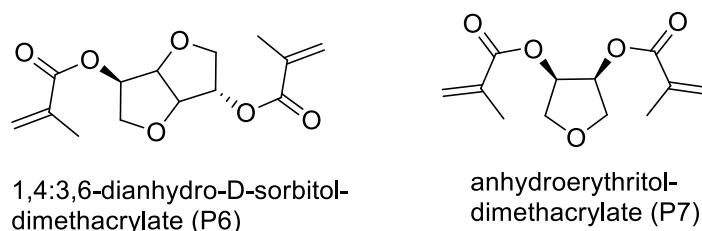
**Figure 77:** Uridine structure with a three hydrogen bond donors on the  $\beta$ -D-ribofuranose (blue). Crosslinker CM-5 with two hydrogen bond acceptors (red).

As all polymers made with the same system have a higher retention time towards the nucleoside compared to the nucleoside esters used as dummy template, it is evident that the template-crosslinker interaction must play a role in determining the retention behaviour. The imprinting on the material was successfully obtained for the template, as the IF values for the uridine esters on MIP 4-6 were between 9 and 30, regardless the  $t_R$  value. The size exclusion behaviour previously reported using different esters of the uridine was observed on this polymers too, as TAU, the

smaller analyte, has the longer retention time between all esters in all MIPs. However, the previous EGDMA-based polymers show a better selectivity.

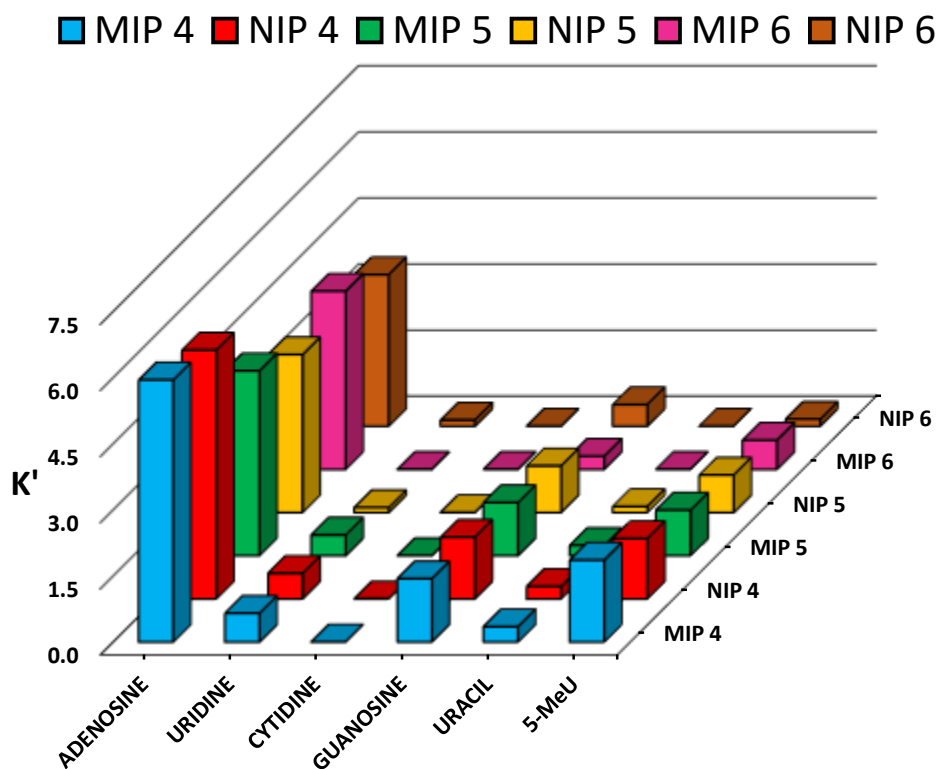
MIP 4 and 5 are based on a similar crosslinkers which are stereoisomers. The different three-dimensional orientation of their functional groups in space creates similar functional material, with a slightly different selective behaviour. CM-4, with an endo-exo configuration, and CM-5, with an endo-endo configuration, create a slightly different 3D network. CM-5, with an endo-endo configuration, has a behaviour similar to CM-6, suggesting the formation of a similar morphology of the polymer.

The crosslinkers should be small and flexible to accommodate itself around the template and create specific cavities. Their accurate adjustment around the template is very important. Wulff reported previously on MIPs prepared using anhydroerythritol-dimethacrylate (P7) and 1,4:3,6-dianhydro-D-sorbitol-dimethacrylate (P6)<sup>36b</sup> (figure 77).



**Figure 78:** *anhydroerythritol-dimethacrylate (P7) and 1,4:3,6-dianhydro-D-sorbitol-dimethacrylate (P6) structure previously reported by Wulff<sup>36b</sup>.*

Both polymers showed a lower selectivity towards the imprinted template compared to an EGDMA-based polymer (P4).<sup>36b</sup> The inner surface area of P7 and P4 were similar. However, P7 had a longer distance between the crosslinking points decreasing the selectivity. P6 was the one with the lower inner surface area, resulting in the lower selectivity between the three polymers.

*Effect of water content in retention*

**Figure 79:** Retention factor ( $k'$ ) of the target and related nucleoside for MIPs 4-6 and NIPs 4-6 in 100% water.

The selectivity of the MIPs is totally lost using 100% water as eluent (Figure 79); the hydrogen bond interactions between analytes and polymer are completely destroyed by a polar solvent as water, meaning that the predominant interaction between polymer and analytes is driven only by hydrophobic interaction. We have previously reported a similar behaviour for related MIPs.<sup>95</sup>

**Table 25:** Selectivity and specificity of template/analytes on imprinted polymers MIP 4, MIP 5, MIP 6 and control polymers NIP 4, NIP 5, NIP 6 in 100% water as mobile phase.

<sup>a</sup> SD (standard deviation, n=3). <sup>b</sup> RSD (relative standard deviation)=(SD/x) \*100, x= mean value.

Polymer	Parameter	Uridine (7)	Uracil	5-MeU	Cytidine	Adenosine	Guanosine	RSD <sup>b</sup> %
MIP 4	k'±SD <sup>a</sup>	0.7±0.02	0.3±0.01	1.9±0.03	0.0±0.04	6.0±0.01	1.4±0.04	<4
	α (7)	1.0	1.9	0.4	-15.6	0.1	0.5	
	IF	1	1	1	0	1	1	
NIP 4	k'±SD <sup>a</sup>	0.6±0.04	0.3±0.03	1.4±0.02	-0.1±0.02	5.6±0.03	1.4±0.00	<10
	α (7)	1.0	2.1	0.4	-6.0	0.1	0.4	
	IF	4	2	1	2	1	1	
MIP 5	k'±SD <sup>a</sup>	0.5±0.01	0.2±0.02	1.0±0.02	-0.1±0.01	4.2±0.03	1.2±0.02	<10
	α (7)	1.0	2	0.4	-3.9	0.1	0.4	
	IF	4	2	1	2	1	1	
NIP 5	k'±SD <sup>a</sup>	0.1±0.01	0.1±0.01	0.9±0.06	-0.1±0.03	3.6±0.02	1.1±0.03	<10
	α (7)	1.0	0.8	0.1	-2.1	0.0	0.1	
	IF	1	0	4	1	1	1	
MIP 6	k'±SD <sup>a</sup>	-0.2±0.00	0.0±0.01	0.7±0.02	-0.3±0.02	4.0±0.03	0.3±0.02	<5
	α (7)	1.0	5.9	-0.2	0.6	0.0	-0.5	
	IF	-1	0	4	1	1	1	
NIP 6	k'±SD <sup>a</sup>	0.1±0.01	-0.3±0.01	0.2±0.01	-0.3±0.02	3.4±0.05	0.5±0.04	<9
	α (7)	1.0	-0.4	0.9	-0.5	0.0	0.3	

### 7.3.3 Equilibrium rebinding

Determination of the binding site distributions and binding affinities for MIPs 4-6 and their control polymers was performed using equilibrium rebinding experiments. TAU solution was prepared in 1% acetic acid in acetonitrile, using a concentration range of 0 - 10mM. The experimental data obtained were fitted to a Langmuir model, which was the most suitable for this fitting, giving R<sup>2</sup> values > 0.98. In Figure 80 are shown the isotherms obtained from these experiments. The difference between the imprinted and non-imprinted polymers is evident, in terms of both the number and affinity of the polymeric binding cavities. The dummy template model is once again shown to work and the use of different crosslinkers appears not to affect the formation of cavities with high affinities towards the template.

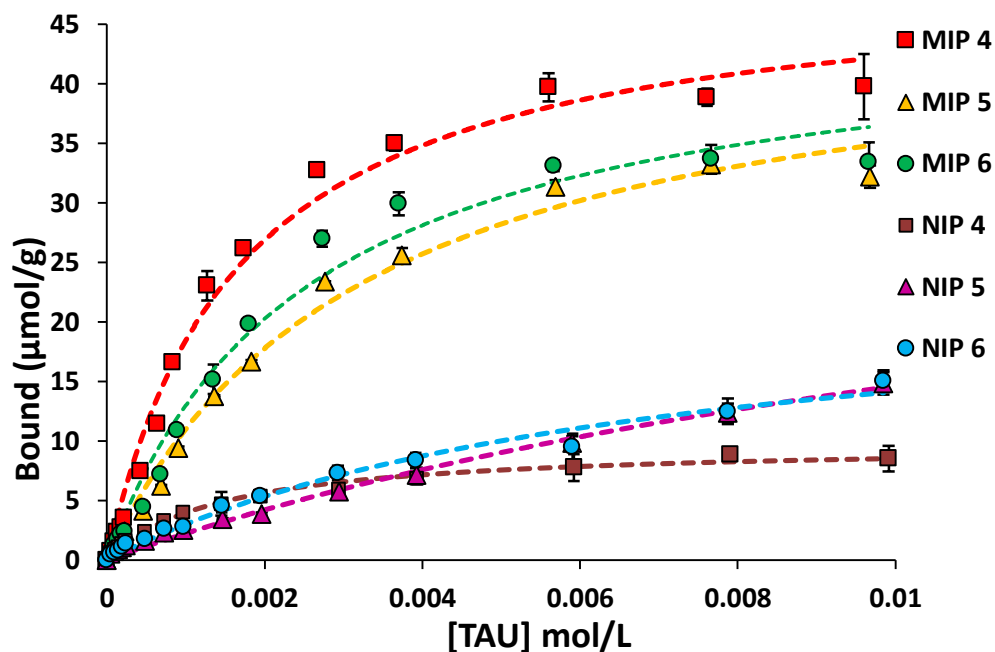


**Figure 80:** Binding isotherms obtained with equilibrium rebinding experiments of MIPs 4-6 and NIPs 4-6 in acetonitrile. The  $[TAU]_{free}$  in the supernatant was evaluated with HPLC (Wavelength: 260 nm, Flow rate: 1 mL/min, Injection: 5  $\mu$ L, RSD % < 21, N=3).

A complete comparison with previously imprinted polymers for the recognition of uridine is not possible, as the binding site distributions and affinities were obtained from frontal chromatography experiments using a different, lower template concentration (0 – 1 mM) range. In this case, the Freundlich model was used to calculate binding site distributions and affinities, as a non-saturated curve was obtained<sup>95</sup>. We tried to fit the experimental data with a Freundlich model, but the  $R^2$  was < 0.8. The fitting of the data to a bi-Langmuir model gave instead two distributions of binding cavities with the same affinity! Hence, the simple Langmuir fitting provides the best model for these materials under the conditions applied.

**Table 26:** Binding constants ( $k_a$ ) and number of sites ( $N$ ) of MIPs 4-6 and NIPs 4-6.

	$k_a$	$N$	$R^2$
MIP 4	$0.595 \cdot 10^3$	49.4	0.9876
NIP 4	$0.647 \cdot 10^3$	10.0	0.9891
MIP 5	$0.299 \cdot 10^3$	47.4	0.9899
NIP 5	$0.061 \cdot 10^3$	38.4	0.9892
MIP 6	$0.395 \cdot 10^3$	45.9	0.9817
NIP 6	$0.142 \cdot 10^3$	24.1	0.9840

All MIPs show high binding sites and affinity towards the template, while the control polymers have, overall, fewer binding sites with a lower affinity, except for NIP 4. Hence, we have confirmed the successful preparation of imprinted polymers that selectively bind uridine while using greener crosslinkers.

## 7.4 CONCLUSIONS

In this chapter, we have reported on the preparation of crosslinkers from renewable resources, as an alternative to ethylene glycol dimethacrylate (EGDMA), to reduce the use of petroleum-based materials, which are more toxic and limited resources. Biomass and the bio-refinery concept are becoming vital to produce greener compounds to be used as the base of new materials. The crosslinkers were used to prepare molecularly imprinted polymers selective towards uridine, as a model compound, to compare them to previously reported MIPs prepared with the widely used EGDMA. We successfully managed to prepare three different MIPs and characterise them in terms of binding capacity, affinity and selectivity. Overall, all MIPs perform well, even if the selectivity towards uridine and similar analytes drops slightly compared to the EGDMA-based MIPs. This research has shown the possibility to substitute traditional oil-based crosslinkers with more sustainable materials, which goes alongside the worries that oil resources will shortly finish on our planet and the need for new, more sustainable molecules to be used instead. The overall behaviour of the polymers made with the renewable crosslinkers is beyond our expectation. The ability of the crosslinker to accommodate the template in the polymeric matrix and create good binding cavities, along with their effect on the flexibility and porosity of the polymer, affects the overall performance of the

polymer to recognise the template. These novel MIPs can retain the imprinted template and the selectivity towards the target, uridine, and related analyte is good. Even if the EGDMA system is one of the more efficient and well-established cross-linking agents in MIP technology, the use of greener cross-linkers can add value to the field in terms of sustainability and environmentally-friendly approach.

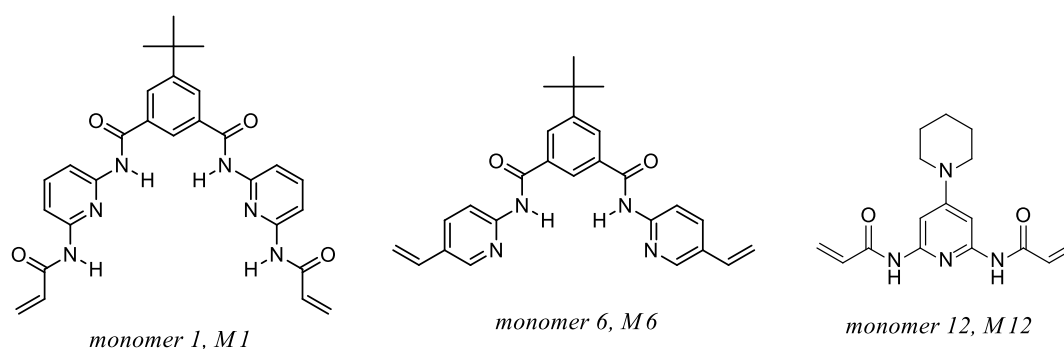
# CHAPTER 8

## *CONCLUSION and FUTURE PERSPECTIVES*



It is a common knowledge in molecular imprinting that it is possible to predict the performance of an imprinted polymer prior to the actual creation of the polymer itself.<sup>145</sup> Also, it is been accepted by the scientific community that an appreciation for the template-functional monomer system can facilitate this prediction and allow for the design of more efficient imprinted polymers.<sup>20-21</sup> This project was based on the development of building blocks capable of creating stoichiometric pre-polymerisation complex which can lead to the creation of better-performing MIPs. Starting from the design and synthesis of novel functional monomers, we then studied the template-functional monomer complex strength to help in predicting the behaviour of the final MIPs.

Tailor-engineered functional monomers can certainly add value to the molecular imprinting field. Overall monomers 1 and 6 are promising candidates to be introduced as basic functional monomers in molecular imprinting, as both may be synthesised in less than two synthetic steps, with relatively acceptable yields. Monomer 12 is also a great candidate for the imprinting of small, imido-group containing molecules. However, the yield and the extended synthetic pathway are, perhaps, not cost-effective in this case. Therefore, M12 can be perhaps used when only small quantities of functional monomer are needed, such as when the MIP acts as the recognition element of a sensor. If a more efficient synthetic route can be found to M12, then it would become a useful weapon in the MIP functional monomer arsenal.



Bio-friendly cross-linkers, synthesized from biomass derived compounds, were also developed during my work. The cross-linker represents the vast majority of most MIP formulations. Many questions have been raised about the limited and

dwindling fossil fuel resources on our planet and the need to recycle material for environmental benefit; hence, the decision to use renewables-based cross-linkers to substitute classic cross-linkers, such as EGDMA, in imprinting. The cross-linkers help to define shape and size of the binding cavities in the polymer. The rigidity and the three-dimensional organisation of the binding motif of the functional monomer are defined by the percentage of the cross-linker in the material and by the nature of the cross-linkers. The biomass-derived cross-linking monomers that were tested give to the novel MIPs selectivity and affinity towards the imprinted template. The higher retention for the nucleoside compared to the acetylated one used as the dummy template, can perhaps be linked to hydrogen bonds shared between the ester carbonyl groups of the cross-linker and the hydroxyl groups of the uridine sugar. The obtained results were extremely promising and open a new door for bio-renewable imprinted polymers. Given the vast number of bio-renewable molecules, there are many potential new cross-linkers molecules to study and explore, to create different, but still efficient, imprinted polymers with high affinity and selectivity towards their templates.

Barbiturates are “old fashioned” drugs that are used less frequently than in the past, due to their addictive properties. However, they can still be present in drug “cocktails” and they are still in use for a limited number of therapeutic and clinical purposes. Different polymerisable clefts were designed and prepared for their imprinting, aiming at improving the solubility of these functional monomers in an organic solvent (e.g. chloroform or acetonitrile) and at the pre-organisation of the cleft in solution prior to the addition of the template. None of the clefts were very soluble in such solvents; however, they were soluble in the presence of the template, such as pentobarbital. Monomer 1 was finally selected for the imprinting of barbiturates, due to the short synthetic route, the good yield obtained and its strong association with both pentobarbital ( $K_a = 80536 \text{ M}^{-1}$ ) and phenobarbital ( $K_a = 88602 \text{ M}^{-1}$ ), as determined by NMR titration experiments in deuterated chloroform. Monomer 1 shares six hydrogen bonds with pentobarbital, creating very strong complex. Other analytes with similar complementary arrays to this cleft were also tested by means of NMR titration studies. TAU ( $1288 \text{ M}^{-1}$ ) and TA $\psi$  ( $117 \text{ M}^{-1}$ ) both create complexes, albeit weaker ones, with M1 by sharing three and four hydrogen

bonds, respectively, with this monomer; this points to the possibility of using M1 to prepare MIPs selective towards these templates too.

MIP1 has a great potential for sample enrichment and should be tested with human urine spiked with barbiturates in order to fully understand a potential SPE application of this material. As previously stated, the abuse of barbiturates is generally linked to the abuse of other drugs and they can be consumed in a drug “cocktail”, in combination with other drugs.<sup>100</sup> Therefore, there can be difficulties in the analysis of human urine with MS or HPLC, as the sample tested is extremely complex. Sample enrichment using MIP1 can allow the pre-concentration and clean-up of a large volume of human sample into smaller volumes of solvent to be later tested, with no presence of other analytes which can cause problem in the drug’s evaluation. This material will be cheap and reusable, which are two great characteristics for cutting manufacturing and laboratory costs. Another potential application of this MIP can be its use as a real drug. We mentioned before the preparation of the first melittin-MIP nanoparticles<sup>46</sup> (NPs) to remove this venom from mice that have been poisoned with it. Potentially, barbiturate-MIP nanoparticles can be also used as drug-like material to be introduced in the bloodstream in case of barbiturates overdose, which can lead to coma or even death. However, the use of monomer 1 as the functional monomer for NP preparation can be challenging due to its lack of solubility. Alternatively, monomer 6 can be used for this purpose, as it binds strongly to barbiturates (phenobarbital-M6 complex  $K_a = 25052 \text{ M}^{-1}$ ), as reported for similar synthetic receptors selective towards barbital<sup>108</sup>.

A “plastic avidin” receptor was also developed to be used in biomedical assays, e.g. to purify proteins, for the pull-down of interacting proteins from cell lysates or arraying proteins on arrays.<sup>146</sup> During my PhD, I developed this polymer only in the monolith format and it was tested using biotin-nitrophenyl ester as the analyte, which is a small UV-active molecule. The recognition of biotinylated macromolecules on MIP2 will be tested by others in the near future. Firstly, a preliminary Dot Blot experiment will be performed, to observe any reduction in the quantity of a biotinylated-macromolecule after exposure of an aqueous solution to both the MIP and NIP. Should this first experiment prove successful, further experiments on more complex systems, e.g. cell lysates, will be performed using

MIP2. These biological experiments will inform on whether, regardless of their size, macromolecules can move inside the porous material and reach the biotin-imprinted cavities. However, the microporous internal structure of the MIP2 particles may potentially prevent functionalised macromolecules from reaching the imprinted-cavities, causing a loss of recognition towards such analytes. Hence, in the future, different MIP morphologies, such as thin layer or surface-grafted beads, may be used for the preparation of MIPs using the designed monomer. The idea here would be to create the biotin binding cavities on the surface of the material, avoiding the need for the macromolecular analytes to reach the inside of the imprinted material. Such thin-film imprinted layers could then be used as surfaces where immunoassays can be performed. Alternatively, imprinted beads or NPs can be immobilised on a surface or used in cartridge for protein purification and pull-down experiments for sample enrichment. Polymers prepared from the designed monomer 6 are perhaps the most exciting and promising of those made, as it can potentially be used in a number of different applications, cutting the disadvantages linked to the use of the biotin natural receptors avidin and streptavidin.

I have been also working in collaboration with researchers at the Université d'Orléans (France) on the imprinting of nucleosides. One of the challenges for the imprinting of nucleosides is their lack of solubility in apolar solvents. The non-covalent imprinting process is based on interactions such as hydrogen bonds, which are destroyed by polar solvents, such as water, alcohols, etc. To be able to have a reasonable selectivity and specificity toward nucleoside of diagnostic interest, non-covalent imprinting should be performed in organic solvent, such as chloroform. The use of a dummy template, where the polar hydroxyl groups of the nucleoside's sugar were acylated, made the polymerisation in chloroform possible, resulting in MIPs selective and specific towards (i) uridine and (ii) pseudouridine. This latter modified nucleoside is produced physiologically by the breakdown of genetic material. An increased concentration of this nucleoside in human bodily fluids can be linked to various types of cancer, making pseudouridine a cancer biomarker and giving information about the stage of the cancer during tumour treatment. The possibility to use a non-invasive, cheap and quick technique to evaluate the presence and concentration of this biomarker in patients is very attractive in cancer therapy. MIPs were developed using different functional monomers. A

commercially available functional monomer, acrylamide, was also used to demonstrate the superior performance of tailor-made functional monomer. MIP3 has a small selectivity towards  $\psi$ , while MIP8, made with monomer 6, which stoichiometrically binds  $\psi$  via four hydrogen bonds, performs the best. Hence, the demonstration of how new synthetic functional monomers can perform better than commercially available ones, making the work surrounding their creation worthwhile. Pre-polymerisation studies also showed that monomer 6 was the best candidate to be used for the imprinting of pseudouridine. Once again, performing host-guest studies on the pre-polymerisation complex is demonstrated to be a precious tool in the design of imprinted polymers. Future work will include the use of monomer 6 for the synthesis of MIPs as the recognition element of sensor for the evaluation of pseudouridine in human fluids.

A series of 4-substituted-2,6-*bis*(acrylamido)pyridines were synthesised in order to study the effect of a single substituent on the pyridine ring on the binding performance of the monomers. Overall an improvement was observed on the novel monomers. Nonetheless need to be considered if it is worth the effort to follow a long synthetic protocol (4-5 synthetic steps for each monomer). However, monomer 12 can be a great candidate to be used when small quantity of functional monomer are required, as it shows a good improvement in binding constant straight ( $K_a = 3481 \pm 7\% \text{ M}^{-1}$ ) compare to BAAPy ( $K_a = 732 \pm 5\% \text{ M}^{-1}$ ) towards tegafur. M12 was obtained in a small yield, due to the lack of time which didn't allow me to improve the synthetic protocol. I am confident that the yield can be increased, making this monomer a great candidate for the preparation of imprinted polymers. The obtained results are interesting on a supramolecular chemistry point of view showing how hydrogen bonds are affected by the increased or decreased acidity and basicity of HBD and HBA.

In conclusion, the main aim of my PhD was to prepare novel functional monomers and cross-linkers for the creation of MIPs more selective and specific than polymers made using commercially available functional monomers. The use of commercially available functional monomers is convenient, as no synthetic effort is expended on them. However, these functional monomers are not always the best candidates for non-covalent imprinting, as the binding constant between host and guest in the pre-

polymerisation mixture needs to be in a range of  $5 \cdot 10^2 - 10^7 \text{ M}^{-1}$ .<sup>22</sup> This generally translates to the use of an excess of functional monomers in the pre-polymerisation solution, which causes the formation of non-specific, non-imprinted yet functional binding cavities in the MIP. The synthetic effort in creating new monomers has been shown to be worth it, as the novel MIPs show a great performance. Equilibrium binding studies showed the mono-dispersity of the cavities in this MIPs, as a mono-Langmuir model was used to calculate the binding cavities affinities. Such mono-dispersity is ideal and can be obtained when stoichiometric non-covalent imprinting is used. Also, the rebinding studies showed that the total yields of high selective cavities in the MIPs, calculated from the original quantity of template used during polymerisation, are 36% and 50% for MIP1 and MIP2 respectively. This is a great result, which underlined again the importance of a strong binding between host and guest during polymerisation. We were hoping to have an even bigger imprinted cavities yield. However there is a possibility for some of the template molecules to be trapped inside the polymer and for some binding cavities to be un-accessible due to the high crosslinked matrix.

It is clear that this project has contributed to the molecular imprinting field. The variety of new monomers that has been developed during this research are intended to be introduced as 'basic' building blocks for future imprinted polymers. A little synthetic effort can lead to a greater synthetic receptor, which can perhaps substitute natural ones, bringing many great advantages.

## BIBLIOGRAPHY

1. Wulff, G.; Sarhan, A., Macromolecular Colloquium. *Angewandte Chemie International Edition in English* 1972, 11 (4), 334-342.
2. Takagishi, T.; Klotz, I. M. Macromolecule-small molecule interactions; introduction of additional binding sites in polyethyleneimine by disulfide cross-linkages *Biopolymers* Volume 11, Issue 2 *Biopolymers* [Online], 1972, p. 483-491. <http://onlinelibrary.wiley.com/doi/10.1002/bip.1972.360110213/abstract> (accessed 01).
3. Polyakov, M. V., Zhur. Fiz. Khim. 1931.
4. Dickey, F. H., The Preparation of Specific Adsorbents. *Proceedings of the National Academy of Sciences* 1949, 35 (5), 227-229.
5. (a) Pauling, L.; Campbell, D. H., THE PRODUCTION OF ANTIBODIES IN VITRO. *Science* 1942, 95 (2469), 440-1; (b) Pauling, L.; Campbell, D. H., THE MANUFACTURE OF ANTIBODIES IN VITRO. *The Journal of Experimental Medicine* 1942, 76 (2), 211-220.
6. Haldeman, R. G.; Emmett, P. H., Specific Adsorption of Alkyl Orange Dyes on Silica Gel. *The Journal of Physical Chemistry* 1955, 59 (10), 1039-1043.
7. Dickey, F. H., Specific Adsorption. *The Journal of Physical Chemistry* 1955, 59 (8), 695-707.
8. Curti, R.; Colombo, U., CHROMATOGRAPHY OF STEREOISOMERS WITH "TAILOR MADE" COMPOUNDS. *Journal of the American Chemical Society* 1952, 74 (15), 3961-3961.
9. Beckett, A. H.; Anderson, P., A Method for the Determination of the Configuration of Organic Molecules using 'Stereo-selective Adsorbents'. *Nature* 1957, 179 (4569), 1074-1075.
10. Patrikeev V., S. Z., Maksimova G., Some biological properties of specifically formed silica. *Doklady Akademii Nauk SSSR*: 1962; Vol. 146, pp 707-709.
11. Alexander, C.; Andersson, H. S.; Andersson, L. I.; Ansell, R. J.; Kirsch, N.; Nicholls, I. A.; O'Mahony, J.; Whitcombe, M. J., Molecular imprinting science and technology: a survey of the literature for the years up to and including 2003. *J. Mol. Recognit.* 2006, 19, 106-180.
12. Cowie, J. M. G.; Arrighi, V., *Polymers : Chemistry and Physics of Modern Materials*, Third Edition. 3 ed.; CRC Press: Hoboken, 2007. <http://kentuk.ebib.com/patron/FullRecord.aspx?p=1449424>.
13. Hodge, P., Entropically Driven Ring-Opening Polymerization of Strainless Organic Macrocycles. *Chemical Reviews* 2014, 114 (4), 2278-2312.
14. Wulff, G., Selective binding to polymers via covalent bonds - the construction of chiral cavities as specific receptor-sites. *Pure And Applied Chemistry* 1982, 54 (11), 2093-2102.
15. Awino, J. K.; Zhao, Y., Water-Soluble Molecularly Imprinted Nanoparticles (MINPs) with Tailored, Functionalized, Modifiable Binding Pockets. *Chemistry – A European Journal* 2015, 21 (2), 655-661.
16. Stephenson-Brown, A.; Acton, A. L.; Preece, J. A.; Fossey, J. S.; Mendes, P. M., Selective glycoprotein detection through covalent templating and allosteric click-imprinting. *Chemical Science* 2015, 6 (9), 5114-5119.
17. Sellergren, B.; Andersson, L., Molecular recognition in macroporous polymers prepared by a substrate analog imprinting strategy. *The Journal of Organic Chemistry* 1990, 55 (10), 3381-3383.
18. Whitcombe, M. J.; Rodriguez, M. E.; Villar, P.; Vulfson, E. N., A New Method for the Introduction of Recognition Site Functionality into Polymers Prepared by Molecular

- Imprinting: Synthesis and Characterization of Polymeric Receptors for Cholesterol. *Journal of the American Chemical Society* 1995, **117** (27), 7105-7111.
19. Taguchi, H.; Sunayama, H.; Takano, E.; Kitayama, Y.; Takeuchi, T., Preparation of molecularly imprinted polymers for the recognition of proteins via the generation of peptide-fragment binding sites by semi-covalent imprinting and enzymatic digestion. *Analyst* 2015, **140** (5), 1448-1452.
20. Arshady, R.; Mosbach, K., Synthesis of substrate-selective polymers by host-guest polymerization. *Die Makromolekulare Chemie* 1981, **182** (2), 687-692.
21. (a) Sellergren, B.; Lepistö, M.; Mosbach, K., Highly enantioselective and substrate-selective polymers obtained by molecular imprinting utilizing noncovalent interactions. NMR and chromatographic studies on the nature of recognition. *Journal of the American Chemical Society* 1988, **110** (17), 5853-5860; (b) Karlsson, B. r. C. G.; O'Mahony, J.; Karlsson, J. G.; Bengtsson, H.; Eriksson, L. A.; Nicholls, I. A., Structure and Dynamics of Monomer-Template Complexation: An Explanation for Molecularly Imprinted Polymer Recognition Site Heterogeneity. *Journal of the American Chemical Society* 2009, **131** (37), 13297-13304; (c) Karim, K.; Breton, F.; Rouillon, R.; Piletska, E. V.; Guerreiro, A.; Chianella, I.; Piletsky, S. A., How to find effective functional monomers for effective molecularly imprinted polymers? *Advanced Drug Delivery Reviews* 2005, **57** (12), 1795-1808.
22. Wulff, G.; Biffis, A., Chapter 4 - Molecular imprinting with covalent or stoichiometric non-covalent interactions. In *Techniques and Instrumentation in Analytical Chemistry*, Börje, S., Ed. Elsevier: 2001; Vol. Volume 23, pp 71-111.
23. Fujii, Y.; Matsutani, K.; Kikuchi, K., Formation of a specific co-ordination cavity for a chiral amino acid by template synthesis of a polymer Schiff base cobalt(III) complex. *Journal of the Chemical Society, Chemical Communications* 1985, (7), 415-417.
24. Lian, H.; Hu, Y.; Li, G., Novel metal-ion-mediated, complex-imprinted solid-phase microextraction fiber for the selective recognition of thiabendazole in citrus and soil samples. *Journal of Separation Science* 2014, **37** (1-2), 106-113.
25. Sellergren, B., Chapter 5 - The non-covalent approach to molecular imprinting. In *Techniques and Instrumentation in Analytical Chemistry*, Börje, S., Ed. Elsevier: 2001; Vol. Volume 23, pp 113-184.
26. Wulff, G.; Gross, T.; Schönfeld, R., Enzyme Models Based on Molecularly Imprinted Polymers with Strong Esterase Activity. *Angewandte Chemie International Edition in English* 1997, **36** (18), 1962-1964.
27. Tanabe, K.; Takeuchi, T.; Matsui, J.; Ikebukuro, K.; Yano, K.; Karube, I., Recognition of barbiturates in molecularly imprinted copolymers using multiple hydrogen bonding. *Journal of the Chemical Society, Chemical Communications* 1995, (22), 2303-2304.
28. Chang, S. K.; Van Engen, D.; Fan, E.; Hamilton, A. D., Hydrogen bonding and molecular recognition: synthetic, complexation, and structural studies on barbiturate binding to an artificial receptor. *Journal of the American Chemical Society* 1991, **113** (20), 7640-7645.
29. Asanuma, H.; Kakazu, M.; Shibata, M.; Hishiya, T., Molecularly imprinted polymer of [small beta]-cyclodextrin for the efficient recognition of cholesterol. *Chemical Communications* 1997, (20), 1971-1972.
30. Steinke, J. H. G.; Dunkin, I. R.; Sherrington, D. C., A simple polymerisable carboxylic acid receptor: 2-acrylamido pyridine. *TrAC Trends in Analytical Chemistry* 1999, **18** (3), 159-164.
31. Spivak, D.; Shea, K. J., Molecular Imprinting of Carboxylic Acids Employing Novel Functional Macroporous Polymers. *The Journal of Organic Chemistry* 1999, **64** (13), 4627-4634.



32. Castro, B.; Whitcombe, M. J.; Vulfson, E. N.; Vazquez-Duhalt, R.; Bárzana, E., Molecular imprinting for the selective adsorption of organosulphur compounds present in fuels. *Analytica Chimica Acta* 2001, **435** (1), 83-90.
33. Hall, A. J.; Achilli, L.; Manesiotis, P.; Quaglia, M.; De Lorenzi, E.; Sellergren, B., A Substructure Approach toward Polymeric Receptors Targeting Dihydrofolate Reductase Inhibitors. 2. Molecularly Imprinted Polymers against Z-l-Glutamic Acid Showing Affinity for Larger Molecules. *The Journal of Organic Chemistry* 2003, **68** (23), 9132-9135.
34. (a) Rathbone, D. L.; Ge, Y., Selectivity of response in fluorescent polymers imprinted with N1-benzylidene pyridine-2-carboxamidrazones. *Analytica Chimica Acta* 2001, **435** (1), 129-136; (b) Zhang, H.; Verboom, W.; Reinhoudt, D. N., 9-(Guanidinomethyl)-10-vinylanthracene: a suitable fluorescent monomer for MIPs. *Tetrahedron Letters* 2001, **42** (26), 4413-4416.
35. Manesiotis, P.; Hall, A. J.; Courtois, J.; Irgum, K.; Sellergren, B., An Artificial Riboflavin Receptor Prepared by a Template Analogue Imprinting Strategy. *Angewandte Chemie International Edition*: 2005; Vol. 44, pp 3902-3906.
36. (a) Wulff, G.; Kemmerer, R.; J., V.; Poll, H., Chirality of vinyl-polymers - the preparation of chiral cavities in synthetic-polymers. *Nouveau Journal de Chimie-New Journal of Chemistry* 1982, **6**, 681-687; (b) Wulff, G.; Vietmeier, J.; Poll, H.-G., Enzyme-analogue built polymers, 22. Influence of the nature of the crosslinking agent on the performance of imprinted polymers in racemic resolution. *Die Makromolekulare Chemie* 1987, **188** (4), 731-740.
37. Sarhan, A.; Wulff, G., Enzyme-analogue built polymers, 13. On the introduction of amino- and boronic acid groups into chiral polymer cavities. *Die Makromolekulare Chemie* 1982, **183** (1), 85-92.
38. Sellergren, B.; Hall, A. J., Chapter 2 - Fundamental aspects on the synthesis and characterisation of imprinted network polymers. In *Techniques and Instrumentation in Analytical Chemistry*, Börje, S., Ed. Elsevier: 2001; Vol. Volume 23, pp 21-57.
39. Sellergren, B.; Hall, A. J., Molecularly Imprinted Polymers. In *Supramolecular Chemistry*, John Wiley & Sons, Ltd: 2012.
40. Švec, F.; Fréchet, J. M. J., Chapter 2 - Rigid Macroporous Organic Polymer Monoliths Prepared by Free Radical Polymerization. In *Journal of Chromatography Library*, František Švec, T. B. T. a. Z. D., Ed. Elsevier: 2003; Vol. Volume 67, pp 19-50.
41. Mayes, A. G., Chapter 12 - Polymerisation techniques for the formation of imprinted beads. In *Techniques and Instrumentation in Analytical Chemistry*, Börje, S., Ed. Elsevier: 2001; Vol. Volume 23, pp 305-324.
42. Flores, A.; Cunliffe, D.; Whitcombe, M. J.; Vulfson, E. N., Imprinted polymers prepared by aqueous suspension polymerization. *Journal of Applied Polymer Science* 2000, **77** (8), 1841-1850.
43. Barrett, K. E. J., *Dispersion polymerization in organic media*. Wiley-Interscience: 1975.
44. Székely, G.; Valtcheva, I. B.; Kim, J. F.; Livingston, A. G., Molecularly imprinted organic solvent nanofiltration membranes – Revealing molecular recognition and solute rejection behaviour. *Reactive and Functional Polymers* 2015, **86**, 215-224.
45. Hoshino, Y.; Kodama, T.; Okahata, Y.; Shea, K. J., Peptide Imprinted Polymer Nanoparticles: A Plastic Antibody. *Journal of the American Chemical Society* 2008, **130** (46), 15242-15243.
46. Hoshino, Y.; Koide, H.; Urakami, T.; Kanazawa, H.; Kodama, T.; Oku, N.; Shea, K. J., Recognition, Neutralization, and Clearance of Target Peptides in the Bloodstream of Living Mice by Molecularly Imprinted Polymer Nanoparticles: A Plastic Antibody. *Journal of the American Chemical Society* 2010, **132** (19), 6644-6645.

47. Taguchi, Y.; Takano, E.; Takeuchi, T., SPR Sensing of Bisphenol A Using Molecularly Imprinted Nanoparticles Immobilized on Slab Optical Waveguide with Consecutive Parallel Au and Ag Deposition Bands Coexistent with Bisphenol A-Immobilized Au Nanoparticles. *Langmuir* 2012, 28 (17), 7083-7088.
48. (a) Nematollahzadeh, A.; Sun, W.; Aureliano, C. S. A.; Lütkemeyer, D.; Stute, J.; Abdekhodaie, M. J.; Shojaei, A.; Sellergren, B., High-Capacity Hierarchically Imprinted Polymer Beads for Protein Recognition and Capture. *Angewandte Chemie International Edition* 2011, 50 (2), 495-498; (b) Titirici, M. M.; Sellergren, B., Peptide recognition via hierarchical imprinting. *Analytical & Bioanalytical Chemistry* 2004, 378 (8), 1913-1921.
49. Urraca, J. L.; Aureliano, C. S. A.; Schillinger, E.; Esselmann, H.; Wiltfang, J.; Sellergren, B., Polymeric Complements to the Alzheimer's Disease Biomarker  $\beta$ -Amyloid Isoforms A $\beta$ 1-40 and A $\beta$ 1-42 for Blood Serum Analysis under Denaturing Conditions. *Journal of the American Chemical Society* 2011, 133 (24), 9220-9223.
50. Kugimiya, A.; Matsui, J.; Takeuchi, T., Sialic acid-imprinted polymers using noncovalent interactions. *Materials Science and Engineering: C* 1997, 4 (4), 263-266.
51. (a) Kempe, M.; Mosbach, K., Separation of amino acids, peptides and proteins on molecularly imprinted stationary phases. *Journal of Chromatography A* 1995, 691 (1-2), 317-323; (b) Sellergren, B.; Shea, K. J., Origin of peak asymmetry and the effect of temperature on solute retention in enantiomer separations on imprinted chiral stationary phases. *Journal of Chromatography A* 1995, 690 (1), 29-39; (c) Szabelski, P.; Kaczmarski, K.; Cavazzini, A.; Chen, Y. B.; Sellergren, B.; Guiochon, G., Energetic heterogeneity of the surface of a molecularly imprinted polymer studied by high-performance liquid chromatography. *Journal of Chromatography A* 2002, 964 (1-2), 99-111.
52. Nicholls, I. A.; Ramström, O.; Mosbach, K., Insights into the role of the hydrogen bond and hydrophobic effect on recognition in molecularly imprinted polymer synthetic peptide receptor mimics. *Journal of Chromatography A* 1995, 691 (1-2), 349-353.
53. Tong, D.; Heényi, C.; Bikádi, Z.; Gao, J.-P.; Hjertén, S., Some studies of the chromatographic properties of gels ('Artificial antibodies/receptors') for selective adsorption of proteins. *Chromatographia: 2001; Vol. 54*, pp 7-14.
54. Haginaka, J.; Takehira, H.; Hosoya, K.; Tanaka, N., Molecularly imprinted uniform-sized polymer-based stationary phase for naproxen: Comparison of molecular recognition ability of the molecularly imprinted polymers prepared by thermal and redox polymerization techniques. *Journal of Chromatography A* 1998, 816 (2), 113-121.
55. Haginaka, J.; Sanbe, H.; Takehira, H., Uniform-sized molecularly imprinted polymer for (S)-ibuprofen: Retention properties in aqueous mobile phases. *Journal of Chromatography A* 1999, 857 (1-2), 117-125.
56. Valero-Navarro, Á.; Gómez-Romero, M.; Fernández-Sánchez, J. F.; Cormack, P. A. G.; Segura-Carretero, A.; Fernández-Gutiérrez, A., Synthesis of caffeic acid molecularly imprinted polymer microspheres and high-performance liquid chromatography evaluation of their sorption properties. *Journal of Chromatography A* 2011, 1218 (41), 7289-7296.
57. Xia, Y.; McGuffey, J. E.; Bhattacharyya, S.; Sellergren, B.; Yilmaz, E.; Wang, L.; Bernert, J. T., Analysis of the Tobacco-Specific Nitrosamine 4-(Methylnitrosamino)-1-(3-pyridyl)-1-butanol in Urine by Extraction on a Molecularly Imprinted Polymer Column and Liquid Chromatography/Atmospheric Pressure Ionization Tandem Mass Spectrometry. *Analytical Chemistry* 2005, 77 (23), 7639-7645.
58. Theodoridis, G.; Manesiotis, P., Selective solid-phase extraction sorbent for caffeine made by molecular imprinting. *Journal of Chromatography A* 2002, 948 (1-2), 163-169.

59. Turiel, E.; Martín-Esteban, A.; Fernández, P.; Pérez-Conde, C.; Cámara, C., Molecular Recognition in a Propazine-imprinted Polymer and Its Application to the Determination of Triazines in Environmental Samples. *Analytical Chemistry* 2001, **73** (21), 5133-5141.
60. Narayanaswamy, P.; Shinde, S.; Sulc, R.; Kraut, R.; Staples, G.; Thiam, C. H.; Grimm, R.; Sellergren, B.; Torta, F.; Wenk, M. R., Lipidomic "Deep Profiling": An Enhanced Workflow to Reveal New Molecular Species of Signaling Lipids. *Analytical Chemistry* 2014, **86** (6), 3043-3047.
61. Manesiotis, P.; Borrelli, C.; Aureliano, C. S. A.; Svensson, C.; Sellergren, B., Water-compatible imprinted polymers for selective depletion of riboflavine from beverages. *Journal of Materials Chemistry* 2009, **19** (34), 6185-6193.
62. Le Noir, M.; Lepeuple, A.-S.; Guieysse, B.; Mattiasson, B., Selective removal of 17 $\beta$ -estradiol at trace concentration using a molecularly imprinted polymer. *Water Research* 2007, **41** (12), 2825-2831.
63. (a) Levi, R.; McNiven, S.; Piletsky, S. A.; Cheong, S.-H.; Yano, K.; Karube, I., Optical Detection of Chloramphenicol Using Molecularly Imprinted Polymers. *Analytical Chemistry* 1997, **69** (11), 2017-2021; (b) McNiven, S.; Kato, M.; Levi, R.; Yano, K.; Karube, I., Chloramphenicol sensor based on an in situ imprinted polymer. *Analytica Chimica Acta* 1998, **365** (1-3), 69-74.
64. (a) Kröger, S.; Turner, A. P. F.; Mosbach, K.; Haupt, K., Imprinted Polymer-Based Sensor System for Herbicides Using Differential-Pulse Voltammetry on Screen-Printed Electrodes. *Analytical Chemistry* 1999, **71** (17), 3698-3702; (b) Schollhorn, B.; Maurice, C.; Flohic, G.; Limoges, B., Competitive assay of 2,4-dichlorophenoxyacetic acid using a polymer imprinted with an electrochemically active tracer closely related to the analyte. *Analyst* 2000, **125** (4), 665-667.
65. Surugiu, I.; Svitel, J.; Ye, L.; Haupt, K.; Danielsson, B., Development of a Flow Injection Capillary Chemiluminescent ELISA Using an Imprinted Polymer Instead of the Antibody. *Analytical Chemistry* 2001, **73** (17), 4388-4392.
66. Baggiani, C.; Anfossi, L.; Giovannoli, C., MIP-based immunoassays: State of the Art, limitations and Perspectives. In *Molecular Imprinting*, 2013; Vol. 1, p 41.
67. Dickert, F.; Hayden, O.; Lieberzeit, P.; Palfinger, C.; Pickert, D.; Wolff, U.; Scholl, G., Borderline applications of QCM-devices: synthetic antibodies for analytes in both nm- and  $\mu$ m-dimensions. *Sensors and Actuators B: Chemical* 2003, **95** (1-3), 20-24.
68. Dickert, F. L.; Lieberzeit, P.; Tortschanoff, M., Molecular imprints as artificial antibodies — a new generation of chemical sensors. *Sensors and Actuators B: Chemical* 2000, **65** (1-3), 186-189.
69. Fu, Y.; Finklea, H. O., Quartz Crystal Microbalance Sensor for Organic Vapor Detection Based on Molecularly Imprinted Polymers. *Analytical Chemistry* 2003, **75** (20), 5387-5393.
70. Suriyanarayanan, S.; Nawaz, H.; Ndizeye, N.; Nicholls, I., Hierarchical Thin Film Architectures for Enhanced Sensor Performance: Liquid Crystal-Mediated Electrochemical Synthesis of Nanostructured Imprinted Polymer Films for the Selective Recognition of Bupivacaine. *Biosensors* 2014, **4** (2), 90.
71. Gao, S.; Wang, W.; Wang, B., Building Fluorescent Sensors for Carbohydrates Using Template-Directed Polymerizations. *Bioorganic Chemistry* 2001, **29** (5), 308-320.
72. Turkewitsch, P.; Wandelt, B.; Darling, G. D.; Powell, W. S., Fluorescent Functional Recognition Sites through Molecular Imprinting. A Polymer-Based Fluorescent Chemosensor for Aqueous cAMP. *Analytical Chemistry* 1998, **70** (10), 2025-2030.

73. Matsui, J.; Kubo, H.; Takeuchi, T., Molecularly Imprinted Fluorescent-Shift Receptors Prepared with 2-(Trifluoromethyl)acrylic Acid. *Analytical Chemistry* 2000, **72** (14), 3286-3290.
74. (a) Kugimiya, A.; Takeuchi, T., Surface plasmon resonance sensor using molecularly imprinted polymer for detection of sialic acid. *Biosensors and Bioelectronics* 2001, **16** (9–12), 1059-1062; (b) Raitman, O. A.; Arslanov, V. V.; Pogorelova, S. P.; Kharitonov, A. B., Molecularly Imprinted Polymer Matrices for Analysis of the Cofactor NADH: A Surface Plasmon Resonance Study. *Doklady Physical Chemistry*: 2003; Vol. 392, pp 256-258.
75. (a) Kriz, D.; Mosbach, K., Competitive amperometric morphine sensor based on an agarose immobilised molecularly imprinted polymer. *Analytica Chimica Acta* 1995, **300** (1–3), 71-75; (b) Blanco-López, M. C.; Lobo-Castañón, M.-J.; Miranda-Ordieres, A. J.; Tuñón-Blanco, P., Voltammetric response of diclofenac-molecularly imprinted film modified carbon electrodes. *Analytical & Bioanalytical Chemistry* 2003, **377** (2), 257-261.
76. (a) Lahav, M.; Kharitonov, A. B.; Katz, O.; Kunitake, T.; Willner, I., Tailored Chemosensors for Chloroaromatic Acids Using Molecular Imprinted TiO<sub>2</sub> Thin Films on Ion-Sensitive Field-Effect Transistors. *Analytical Chemistry* 2000, **73** (3), 720-723; (b) Lahav, M.; Kharitonov, A. B.; Willner, I., Imprinting of Chiral Molecular Recognition Sites in Thin TiO<sub>2</sub> Films Associated with Field-Effect Transistors: Novel Functionalized Devices for Chiroselective and Chiro-specific Analyses. *Chemistry – A European Journal*: 2001; Vol. 7, pp 3992-3997.
77. Surugiu, I.; Danielsson, B.; Ye, L.; Mosbach, K.; Haupt, K., Chemiluminescence Imaging ELISA Using an Imprinted Polymer as the Recognition Element Instead of an Antibody. *Analytical Chemistry* 2001, **73** (3), 487-491.
78. Jakusch, M.; Janotta, M.; Mizaikoff, B.; Mosbach, K.; Haupt, K., Molecularly Imprinted Polymers and Infrared Evanescent Wave Spectroscopy. A Chemical Sensors Approach. *Analytical Chemistry* 1999, **71** (20), 4786-4791.
79. (a) Guo, Y.; Kang, L.; Chen, S.; Li, X., High performance surface-enhanced Raman scattering from molecular imprinting polymer capsulated silver spheres. *Physical Chemistry Chemical Physics* 2015, **17** (33), 21343-21347; (b) Kamra, T.; Zhou, T.; Montelius, L.; Schnadt, J.; Ye, L., Implementation of Molecularly Imprinted Polymer Beads for Surface Enhanced Raman Detection. *Analytical Chemistry* 2015, **87** (10), 5056-5061.
80. Damen, J.; Neckers, D. C., Stereoselective syntheses via a photochemical template effect. *Journal of the American Chemical Society* 1980, **102** (9), 3265-3267.
81. Yu, Y.; Ye, L.; Haupt, K.; Mosbach, K., Formation of a Class of Enzyme Inhibitors (Drugs), Including a Chiral Compound, by Using Imprinted Polymers or Biomolecules as Molecular-Scale Reaction Vessels. *Angewandte Chemie*: 2002; Vol. 114, pp 4639-4643.
82. Kirsch, N.; Hedin-Dahlström, J.; Henschel, H.; Whitcombe, M. J.; Wikman, S.; Nicholls, I. A., Molecularly imprinted polymer catalysis of a Diels-Alder reaction. *Journal of Molecular Catalysis B: Enzymatic* 2009, **58** (1–4), 110-117.
83. Hedin-Dahlström, J.; Rosengren-Holmberg, J. P.; Legrand, S.; Wikman, S.; Nicholls, I. A., A Class II Aldolase Mimic. *The Journal of Organic Chemistry* 2006, **71** (13), 4845-4853.
84. Polborn, K.; Severin, K., Biomimetic Catalysis with Immobilised Organometallic Ruthenium Complexes: Substrate- and Regioselective Transfer Hydrogenation of Ketones. *Chemistry – A European Journal*: 2000; Vol. 6, pp 4604-4611.
85. Cammidge, A. N.; Baines, N. J.; Bellingham, R. K., Synthesis of heterogeneous palladium catalyst assemblies by molecular imprinting. *Chemical Communications* 2001, (24), 2588-2589.

86. Alvarez-Lorenzo, C.; Yañez, F.; Barreiro-Iglesias, R.; Concheiro, A., Imprinted soft contact lenses as norfloxacin delivery systems. *Journal of Controlled Release* 2006, **113** (3), 236-244.
87. Suedee, R.; Jantarat, C.; Lindner, W.; Viernstein, H.; Songkro, S.; Srichana, T., Development of a pH-responsive drug delivery system for enantioselective-controlled delivery of racemic drugs. *Journal of Controlled Release* 2010, **142** (1), 122-131.
88. Cutivet, A.; Schembri, C.; Kovensky, J.; Haupt, K., Molecularly Imprinted Microgels as Enzyme Inhibitors. *Journal of the American Chemical Society* 2009, **131** (41), 14699-14702.
89. Sellergren, B.; Wieschemeyer, J.; Boos, K.-S.; Seidel, D., Imprinted Polymers for Selective Adsorption of Cholesterol from Gastrointestinal Fluids. *Chemistry of Materials* 1998, **10** (12), 4037-4046.
90. Huval, C. C.; Bailey, M. J.; Braunlin, W. H.; Holmes-Farley, S. R.; Mandeville, W. H.; Petersen, J. S.; Polomoscanik, S. C.; Sacchiro, R. J.; Chen, X.; Dhal, P. K., Novel Cholesterol Lowering Polymeric Drugs Obtained by Molecular Imprinting. *Macromolecules* 2001, **34** (6), 1548-1550.
91. Cristallini, C.; Ciardelli, G.; Barbani, N.; Giusti, P., Acrylonitrile-Acrylic Acid Copolymer Membrane Imprinted with Uric Acid for Clinical Uses. *Macromolecular Bioscience*: 2004; Vol. 4, pp 31-38.
92. Hoeben, F. J. M.; Jonkheijm, P.; Meijer, E. W.; Schenning, A. P. H. J., About Supramolecular Assemblies of  $\pi$ -Conjugated Systems. *Chemical Reviews* 2005, **105** (4), 1491-1546.
93. Prins, L. J.; Reinhoudt, D. N.; Timmerman, P., Noncovalent Synthesis Using Hydrogen Bonding. *Angewandte Chemie International Edition* 2001, **40** (13), 2382-2426.
94. Winqvist, A.; Strömberg, R., Investigation on Condensing Agents for Phosphinate Ester Formation with Nucleoside 5'-Hydroxyl Functions. *European Journal of Organic Chemistry* 2008, **2008** (10), 1705-1714.
95. Krstulja, A.; Lettieri, S.; Hall, A.; Delépée, R.; Favetta, P.; Agrofoglio, L., Evaluation of molecularly imprinted polymers using 2',3',5'-tri-O-acyluridines as templates for pyrimidine nucleoside recognition. *Anal Bioanal Chem* 2014, **406** (25), 6275-6284.
96. Yano, K.; Tanabe, K.; Takeuchi, T.; Matsui, J.; Ikebukuro, K.; Karube, I., Molecularly imprinted polymers which mimic multiple hydrogen bonds between nucleotide bases. *Analytica Chimica Acta* 1998, **363** (2-3), 111-117.
97. Rebek, J.; Askew, B.; Killoran, M.; Nemeth, D.; Lin, F. T., Convergent functional groups. 3. A molecular cleft recognizes substrates of complementary size, shape, and functionality. *Journal of the American Chemical Society* 1987, **109** (8), 2426-2431.
98. López-Muñoz, F.; Ucha-Udabe, R.; Alamo, C., The history of barbiturates a century after their clinical introduction. *Neuropsychiatr Dis Treat* 2005, **1** (4), 329-343.
99. Orbán, P. T., Barbiturate abuse. *Journal of Medical Ethics* 1976, **2** (2), 63-67.
100. Shabir, G. A.; Bradshaw, T. K.; Arain, S. A.; Shar, G. Q., A NEW VALIDATED METHOD FOR THE SIMULTANEOUS DETERMINATION OF A SERIES OF EIGHT BARBITURATES BY RP-HPLC. *Journal of Liquid Chromatography & Related Technologies* 2010, **33** (1), 61-71.
101. Chang, S. K.; Hamilton, A. D., Molecular recognition of biologically interesting substrates: synthesis of an artificial receptor for barbiturates employing six hydrogen bonds. *Journal of the American Chemical Society* 1988, **110** (4), 1318-1319.
102. Kubo, H.; Nariai, H.; Takeuchi, T., Multiple hydrogen bonding-based fluorescent imprinted polymers for cyclobarbitol prepared with 2,6-bis(acrylamido)pyridine. *Chemical Communications* 2003, (22), 2792-2793.

103. (a) Chauvin, A.-S.; Comby, S.; Song, B.; Vandevyver, C. D. B.; Bünzli, J.-C. G. A Versatile Ditopic Ligand System for Sensitizing the Luminescence of Bimetallic Lanthanide Bio-Imaging Probes

Chemistry - A European Journal Volume 14, Issue 6 *Chemistry - A European Journal* [Online], 2008, p. 1726-1739. <http://onlinelibrary.wiley.com/doi/10.1002/chem.200701357/abstract> (accessed 18);

(b) Gassner, A.-L.; Duhot, C. I.; G. Bünzli, J.-C.; Chauvin, A.-S., Remarkable Tuning of the Photophysical Properties of Bifunctional Lanthanide tris(Dipicolinates) and its Consequence on the Design of Bioprobes. *Inorganic Chemistry* 2008, 47 (17), 7802-7812.

104. Busto, E.; González-Álvarez, A.; Gotor-Fernández, V.; Alfonso, I.; Gotor, V., Optically active macrocyclic hexaazapyridinophanes decorated at the periphery: synthesis and applications in the NMR enantiodiscrimination of carboxylic acids. *Tetrahedron* 2010, 66 (32), 6070-6077.

105. van Oijen, A. H.; Huck, N. P. M.; Kruijtzter, J. A. W.; Erkelens, C.; van Boom, J. H.; Liskamp, R. M. J., Syntheses of Amino Acid Based Phosphodiester Linkage-Containing Cryptands as well as Diphosphorylated Macrocycles. *The Journal of Organic Chemistry* 1994, 59 (9), 2399-2408.

106. Xu, Y.-X.; Zhao, X.; Jiang, X.-K.; Li, Z.-T., Organic nanotubes assembled from isophthalamides and their application as templates to fabricate Pt nanotubes. *Chemical Communications* 2009, (28), 4212-4214.

107. Bhattacharya, S.; Snehathatha, K.; George, S. K., Synthesis of Some Copper(II)-Chelating (Dialkylamino)pyridine Amphiphiles and Evaluation of Their Esterolytic Capacities in Cationic Micellar Media. *The Journal of Organic Chemistry* 1998, 63 (1), 27-35.

108. Claramunt, R. M.; Herranz, F.; Santa María, M. D.; Pinilla, E.; Torres, M. R.; Elguero, J., Molecular recognition of biotin, barbital and tolbutamide with new synthetic receptors. *Tetrahedron* 2005, 61 (21), 5089-5100.

109. Beltran, A.; Borrull, F.; Cormack, P. A. G.; Marcé, R. M., Molecularly imprinted polymer with high-fidelity binding sites for the selective extraction of barbiturates from human urine. *Journal of Chromatography A* 2011, 1218 (29), 4612-4618.

110. Wiklander, J.; Karlsson, B. C. G.; Aastrup, T.; Nicholls, I. A., Towards a synthetic avidin mimic. *Analytical & Bioanalytical Chemistry* 2011, 400 (5), 1397-1404.

111. Takeuchi, T.; Dobashi, A.; Kimura, K., Molecular Imprinting of Biotin Derivatives and Its Application to Competitive Binding Assay Using Nonisotopic Labeled Ligands. *Analytical Chemistry* 2000, 72 (11), 2418-2422.

112. Herranz, F.; Santa María, M. D.; Claramunt, R. M., Molecular Recognition: Improved Binding of Biotin Derivatives with Synthetic Receptors. *The Journal of Organic Chemistry* 2006, 71 (8), 2944-2951.

113. Piletska, E.; Piletsky, S.; Karim, K.; Terpetschnig, E.; Turner, A., Biotin-specific synthetic receptors prepared using molecular imprinting. *Analytica Chimica Acta* 2004, 504 (1), 179-183.

114. Cottineau, B.; O'Shea, D. F., Carbolithiation of vinyl pyridines as a route to 7-azaindoles. *Tetrahedron Letters* 2005, 46 (11), 1935-1938.

115. Claramunt, R. M.; Herranz, F.; María, M. D. S.; Jaime, C.; Federico, M. d.; Elguero, J., Towards the design of host-guest complexes: biotin and urea derivatives versus artificial receptors. *Biosensors and Bioelectronics* 2004, 20 (6), 1242-1249.

116. Dunn, W.; Broadhurst, D.; Deepak, S.; Buch, M.; McDowell, G.; Spasic, I.; Ellis, D.; Brooks, N.; Kell, D.; Neyses, L., Serum metabolomics reveals many novel metabolic markers of heart failure, including pseudouridine and 2-oxoglutarate. *Metabolomics* 2007, 3 (4), 413-426.

117. Lanza, F.; Hall, A. J.; Sellergren, B.; Bereczki, A.; Horvai, G.; Bayoudh, S.; Cormack, P. A. G.; Sherrington, D. C., Development of a semiautomated procedure for the synthesis and evaluation of molecularly imprinted polymers applied to the search for functional monomers for phenytoin and nifedipine. *Analytica Chimica Acta* 2001, **435** (1), 91-106.
118. Jégourel, D.; Delépée, R.; Breton, F.; Rolland, A.; Vidal, R.; Agrofoglio, L. A., Molecularly imprinted polymer of 5-methyluridine for solid-phase extraction of pyrimidine nucleoside cancer markers in urine. *Bioorganic & Medicinal Chemistry* 2008, **16** (19), 8932-8939.
119. Kugimiya, A.; Mukawa, T.; Takeuchi, T., Synthesis of 5-fluorouracil-imprinted polymers with multiple hydrogen bonding interactions. *Analyst* 2001, **126** (6), 772-774.
120. Kadirvel, P.; Azenha, M.; Schillinger, E.; Halhalli, M. R.; Silva, A. F.; Sellergren, B., Recognitive nano-thin-film composite beads for the enantiomeric resolution of the metastatic breast cancer drug aminoglutethimide. *Journal of Chromatography A* 2014, **1358**, 93-101.
121. Suksuwan, A.; Lomlim, L.; Rungrotmongkol, T.; Nakpheng, T.; Dickert, F. L.; Suedee, R., The composite nanomaterials containing (R)-thalidomide-molecularly imprinted polymers as a recognition system for enantioselective-controlled release and targeted drug delivery. *Journal of Applied Polymer Science* 2015, **132** (18), n/a-n/a.
122. Li, B.; Tang, L.; Qiang, L.; Chen, K., Novel polymer nanowires with triple hydrogen-bonding sites fabricated by metallogel template polymerization and their adsorption of thymidine. *Soft Matter* 2011, **7** (3), 963-969.
123. Manesiotis, P.; Hall, A. J.; Sellergren, B., Improved Imide Receptors by Imprinting Using Pyrimidine-Based Fluorescent Reporter Monomers. *The Journal of Organic Chemistry* 2005, **70** (7), 2729-2738.
124. Braxmeier, T.; Demarcus, M.; Fessmann, T.; McAteer, S.; Kilburn, J. D., Identification of Sequence Selective Receptors for Peptides with a Carboxylic Acid Terminus. *Chemistry – A European Journal* 2001, **7** (9), 1889-1898.
125. Haap, W. H., Paul Kitas, Eric A. Kuhn, Bernd Mohr, Peter Wessel, Hans Peter 2008.
126. Abraham, M. H.; Gola, J. M. R.; Cometto-Muñiz, J. E.; Acree, W. E., Hydrogen Bonding between Solutes in Solvents Octan-1-ol and Water. *The Journal of organic chemistry* 2010, **75** (22), 7651-7658.
127. Palusiak, M., Substituent effect in para substituted Cr(CO)<sub>5</sub>-pyridine complexes. *Journal of Organometallic Chemistry* 2007, **692** (18), 3866-3873.
128. Hammett, L. P., The Effect of Structure upon the Reactions of Organic Compounds. Benzene Derivatives. *Journal of the American Chemical Society* 1937, **59** (1), 96-103.
129. Grandberg, I. I.; Faizova, G. K.; Kost, A. N., Comparative basicities of substituted pyridines and electronegativity series for substituents in the pyridine series. *Chem Heterocycl Compd* 1967, **2** (4), 421-425.
130. (a) Borek, E.; Baliga, B. S.; Gehrke, C. W.; Kuo, C. W.; Belman, S.; Troll, W.; Waalkes, T. P., High turnover rate of transfer RNA in tumor tissue. *Cancer research* 1977, **37** (9), 3362-6; (b) Limbach, P. A.; Crain, P. F.; McCloskey, J. A., Summary: the modified nucleosides of RNA. *Nucleic Acids Research* 1994, **22** (12), 2183-2196.
131. Lakka, A.; Tsakalof, A., Molecular Imprinting of Tri-O-Acetyladenosine for the Synthetic Imitation of an ATP-Binding Cleft in Protein Kinases. *ChemPlusChem* 2013, **78** (8), 808-815.
132. Cohn, W. E., Pseudouridine, a carbon-carbon linked ribonucleoside in ribonucleic acids: isolation, structure, and chemical characteristics. *The Journal of biological chemistry* 1960, **235**, 1488-98.

133. Cortese, R.; Kammen, H. O.; Spengler, S. J.; Ames, B. N., Biosynthesis of pseudouridine in transfer ribonucleic acid. *The Journal of biological chemistry* 1974, **249** (4), 1103-8.
134. (a) Zambonin, C. G.; Aresta, A.; Palmisano, F.; Specchia, G.; Liso, V., Liquid chromatographic determination of urinary 5-methyl-2'-deoxycytidine and pseudouridine as potential biological markers for leukaemia. *Journal of Pharmaceutical and Biomedical Analysis* 1999, **21** (5), 1045-1051; (b) Rasmuson, T.; Bjork, G. R., Urinary excretion of pseudouridine and prognosis of patients with malignant lymphoma. *Acta Oncol* 1995, **34** (1), 61-7; (c) Zheng, Y.; Xu, G.; Yang, J.; Zhao, X.; Pang, T.; Kong, H., Determination of urinary nucleosides by direct injection and coupled-column high-performance liquid chromatography. *Journal of Chromatography B* 2005, **819** (1), 85-90; (d) Yang, J.; Xu, G.; Zheng, Y.; Kong, H.; Pang, T.; Lv, S.; Yang, Q., Diagnosis of liver cancer using HPLC-based metabonomics avoiding false-positive result from hepatitis and hepatocirrhosis diseases. *Journal of Chromatography B* 2004, **813** (1-2), 59-65.
135. Liebich, H. M.; Müller-Hagedorn, S.; Bacher, M.; Scheel-Walter, H. G.; Lu, X.; Frickenschmidt, A.; Kammerer, B.; Kim, K. R.; Gérard, H., Age-dependence of urinary normal and modified nucleosides in childhood as determined by reversed-phase high-performance liquid chromatography. *Journal of Chromatography B* 2005, **814** (2), 275-283.
136. Ishiwata, S.; Itoh, K.; Yamaguchi, T.; Ishida, N.; Mizugaki, M., Comparison of Serum and Urinary Levels of Modified Nucleoside, 1-Methyladenosine, in Cancer Patients Using a Monoclonal Antibody-Based Inhibition ELISA. *The Tohoku Journal of Experimental Medicine* 1995, **176** (1), 61-68.
137. Manesiotis, P.; Hall, A. J.; Courtois, J.; Irgum, K.; Sellergren, B., An Artificial Riboflavin Receptor Prepared by a Template Analogue Imprinting Strategy. *Angewandte Chemie International Edition* 2005, **44** (25), 3902-3906.
138. (a) Shoravi, S.; Olsson, G.; Karlsson, B.; Nicholls, I., On the Influence of Crosslinker on Template Complexation in Molecularly Imprinted Polymers: A Computational Study of Prepolymerization Mixture Events with Correlations to Template-Polymer Recognition Behavior and NMR Spectroscopic Studies. *International Journal of Molecular Sciences* 2014, **15** (6), 10622; (b) Olsson, G. D.; Karlsson, B. C. G.; Schillinger, E.; Sellergren, B.; Nicholls, I. A., Theoretical Studies of 17- $\beta$ -Estradiol-Imprinted Prepolymerization Mixtures: Insights Concerning the Roles of Cross-Linking and Functional Monomers in Template Complexation and Polymerization. *Industrial & Engineering Chemistry Research* 2013, **52** (39), 13965-13970.
139. Liu, S., Woody biomass: Niche position as a source of sustainable renewable chemicals and energy and kinetics of hot-water extraction/hydrolysis. *Biotechnology Advances* 2010, **28** (5), 563-582.
140. Vilela, C.; Sousa, A. F.; Fonseca, A. C.; Serra, A. C.; Coelho, J. F. J.; Freire, C. S. R.; Silvestre, A. J. D., The quest for sustainable polyesters - insights into the future. *Polymer Chemistry* 2014, **5** (9), 3119-3141.
141. Donate, P., Green synthesis from biomass. *Chemical and Biological Technologies in Agriculture* 2014, **1** (1), 4.
142. Zeng, C.; Seino, H.; Ren, J.; Hatanaka, K.; Yoshie, N., Bio-Based Furan Polymers with Self-Healing Ability. *Macromolecules* 2013, **46** (5), 1794-1802.
143. Haworth, W. N.; Gregory, H.; Wiggins, L. F., 95. Some derivatives of simple carbohydrates containing unsaturated substituents. *Journal of the Chemical Society (Resumed)* 1946, (0), 488-491.
144. Warneke, J.; Wang, Z.; Zeller, M.; Leibfritz, D.; Plaumann, M.; Azov, V. A., Methacryloyl chloride dimers: from structure elucidation to a manifold of chemical transformations. *Tetrahedron* 2014, **70** (37), 6515-6521.



145. (a) Golker, K.; Karlsson, B.; Rosengren, A.; Nicholls, I., A Functional Monomer Is Not Enough: Principal Component Analysis of the Influence of Template Complexation in Pre-Polymerization Mixtures on Imprinted Polymer Recognition and Morphology. *International Journal of Molecular Sciences* 2014, *15* (11), 20572; (b) Golker, K.; Karlsson, B. C. G.; Wiklander, J. G.; Rosengren, A. M.; Nicholls, I. A., Hydrogen bond diversity in the pre-polymerization stage contributes to morphology and MIP-template recognition – MAA versus MMA. *European Polymer Journal* 2015, *66*, 558-568.
146. Kay, B. K.; Thai, S.; Volgina, V. V., High-throughput Biotinylation of Proteins. *Methods in molecular biology (Clifton, N.J.)* 2009, *498*, 185-196.